2017

RESEARCH PRODUCTIVITY 2017

ABSTRACT BOOK

Library Information Services, CIIT-Lahore
Defence Road Off Raiwind Road, Lahore
+92 42 111 001 007, library.ciitlahore.edu.pk

Table of Contents

Preface:

CIIT is not only providing quality education, but also producing the valued research publications. Due to this research work, the CIIT got its better ranking in Pakistan and Higher Education Commission declared CIIT at top ranking among Pakistani Universities. The credit goes to the researchers of CIIT, who, as usual, produced lots of papers in the year 2017. For this accomplishment, the contribution of researchers of CIIT Lahore is also extraordinary. They produced 396 journal papers during the year 2017. The compilation in your hands consists of the papers which published during the year 2017 and at CIIT platform. We only included journal papers for this anthology. The purpose of this compilation is to record the research work of our faculty members and also to facilitate the users to get all the research papers of all departments in one binding. Apart from the record, I am also sure that this compilation will provide the guidelines to new researchers of CIIT and to the researchers of other institutes, as well. I am very much thankful to worthy Director CIIT-Lahore Dr. Qaiser Abbas and Dr. Robbina Farooq, Convener Library Affairs Committee, they not only provided the guidelines, but also encourage us to prepare this compilation in appropriate form. I am also very much thankful to ORIC, which provided the data to compile this report. Without this help, it was very difficult to prepare this collection of research articles.

With Regards

Muhammad Tariq Incharge

Library Information Services

CIIT Lahore

February, 2018

SUMMARY

Departments	Journal Papers
Department of Management Sciences	26
Department of Chemical Engineering	34
Department of Mathematics	79
Department of Electrical Engineering	15
Department of Computer Sciences	43
IRCBM	82
Department of Statistics	08
Department of Physics	90
Department of Humanites	11
Department of Chemistry	06
Non-Academics	06
Total	396

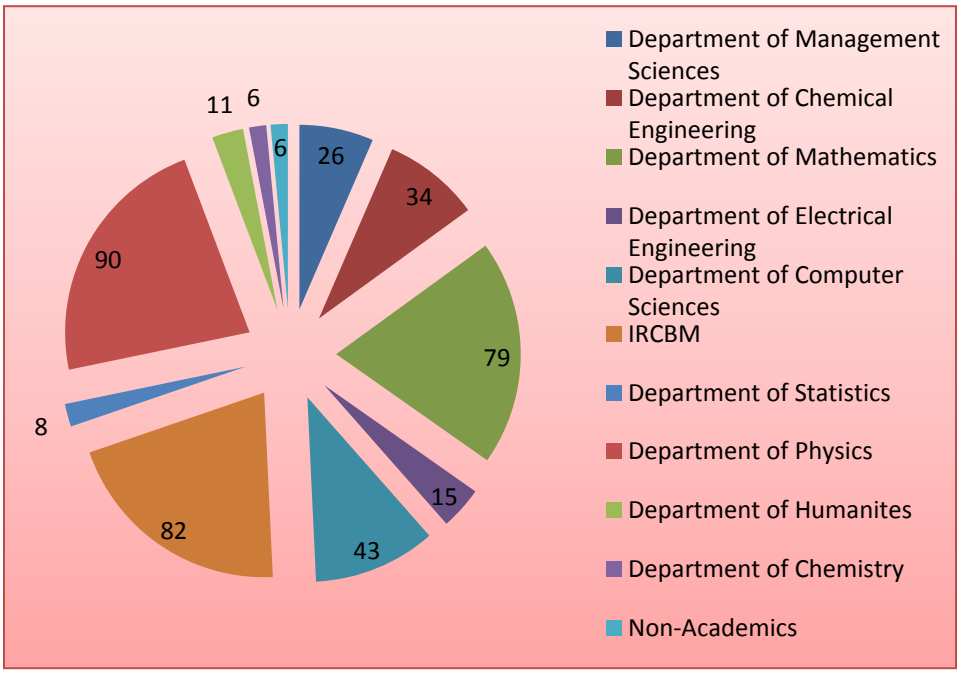

DEPARTMENT OF MANAGEMENT SCIENCES

Journal Papers

1. Hussain, M., Rehman, F., Bibi, I., Khalid, S., & Khalid, S. (2017). IMPACT OF FARMER FIELD SCHOOL APPROACH ON THE COMPETENCY OF THE FARMERS. ***JAPS, Journal of Animal and Plant Sciences*****,** ***27*****(3), 991-995.**

ABSTRACT:

The present study was conducted in the Lahore district to analyze the impact of Farmer Field School (FFS) approach on the competency of the farmers. The population for the study was consisted of both the registered and non-registered farmers under the FFS approach in the public sector in Lahore district. A sample was drawn from the entire population of twenty four FFSs of Lahore district, by using simple random sampling technique. Out of twenty four, eight FFSs were selected randomly and from each FFS eight registered farmers was interviewed, thus the total sample size of registered farmers was sixty four. The non-registered farmers (non-member farmers) were also interviewed to make the research result more authenticated. Thus the number of non-registered farmers was also sixty four. Hence the total sample frame was 128 farmers. The data were collected with the help of a pre-tested and validated interview schedule especially designed for this purpose. The data were analyzed by using computer software Statistical Package for Social Sciences (SPSS). Analysis of the data shows that the farmers' competency in the conduction of agricultural activities land preparation and direct sowing were top in rank order in member and non-members' farmers. While on the other hand member farmers' competency in controlling harmful insects was at the bottom in rank order, however, non-members had lowest competency in conduction of Agro Ecosystem Analysis (AESA) activity. T-test clearly indicates that all aspects of competency in undertaking the agricultural activities had significant difference in favour of member farmers. It means member farmers had more competency in agriculture as compared to non-member farmers

Web URL: http://www.thejaps.org.pk/docs/v-27-03/37.pdf

2. Bibi, I., Sultan, A., Kamal, S., Nouren, S., Safa, Y., Jalani, K., ... & Rehman, F. (2017). Extraction and quantification of phenolic compounds from Prunus armeniaca seed and their role in biotransformation of xenobiotic compounds. ***Korean Journal of Chemical Engineering*****, *34*(2), 392-399**.

ABSTRACT:

The current research project has been devoted to isolating new low cost and eco-friendly phenolic compounds from fruit seeds, peels and vegetables to reduce the atmospheric pollution. Natural phenolic compounds were extracted from different fruit seeds and agriculture waste: P. armeniaca, P. persica, P. domestica and Triticum aesativum. The total phenolic content was quantified, and the maximum value (1 mL extract having 1,933 µg) was found in P. armeniaca seed extract. Phytochemical screening showed that P. armeniaca seeds contain higher amount of alkaloid, tannins, saponins and flavonoid. P. armeniaca seeds enhanced the biotransformation of reactive yellow dye up to 69.89% with maximum laccase (322.45 IU/mL) production. Biodegradation of reactive yellow was only 23.34% without natural redox mediator at sixth day of incubation. Use of P. armeniaca seed stimulators resulted in maximum laccase activity (894.4 IU/mL) with 99.5% rate of removal. UV-Vis, HPLC & FTIR analysis confirmed the transformation of parent dye into various new products. Phytotoxicity study indicated 0% germination index of Avena sativa seeds with reactive yellow, whereas 83% germination index having 100% seed germination while 83% root elongation with treated sample. Thus, the study revealed that the natural phenolic compounds could serve as high potential redox mediators for enhanced laccase-mediated decolorization of reactive yellow dye.

Web URL: ***https://link.springer.com/content/pdf/10.1007/s11814-016-0275-3.pdf***

3. Bibi, I., Nazar, N., Iqbal, M., Kamal, S., Nawaz, H., Nouren, S., ... & Rehman, F. (2017). Green and eco-friendly synthesis of cobalt-oxide nanoparticle: Characterization and photo-catalytic activity. ***Advanced Powder Technology*****.**

ABSTRACT:

Cobalt-oxide nanoparticles (NPs) were fabricated using *Punica granatum* peel extract from cobalt nitrate hexahydrate at low temperature. The synthesized cobalt-oxide NPs were

characterized using X-ray powder diffraction, scanning electron microscopy, energy-dispersive X-ray, atomic force microscopy, fourier transform infrared spectroscopy and UV-visible techniques. The cobalt-oxide NPs were in highly uniform shape and size was in the size of 40–80 nm. Photo-catalytic activity (PCA) of the synthesized NPs was evaluated by degrading Remazol Brilliant Orange 3R (RBO 3R) dye and a degradation of 78.45% was achieved (dye conc. 150 mg/L) using 0.5 g cobalt-oxide NPs for 50 min irradiation time. In view of eco-benign and cost-effective nature, the present investigation revealed that *P. granatum* could be used for the synthesis of cobalt-oxide NPs for photo-catalytic applications.

Web URL: ***http://www.sciencedirect.com/science/article/pii/S0921883117302121***

4. Hussain, G., Hussain, G., Wan Ismail, W. K., Wan Ismail, W. K., Javed, M., & Javed, M. (2017). Comparability of leadership constructs from the Malaysian and Pakistani perspectives. *Cross Cultural & Strategic Management*, *24*(4), 617-644.

ABSTRACT:

Purpose

The purpose of this paper is to compare the applicability of transformational leadership and substitutes-for-leadership theories in Malaysia's and Pakistan's work settings.

Design/methodology/approach

This study employed a survey-based approach using professional employees in both countries as respondents. In total, 215 responses to a web-based survey in Malaysia and 523 responses to a survey administered using personal methods in Pakistan were used for the analysis.

Findings

The results revealed that Malaysia's leaders were rated high on the dimensions of transformational and transactional leadership. The transformational leadership dimensions produced desirable effects on subordinates' outcomes in both samples, but the contingent punishment dimension of transactional leadership produced especially undesirable effects

on subordinates' outcomes. Substitutes for leadership also independently affected subordinates' outcomes and produced similar effects on subordinates' outcomes in both samples. In general, the effects in the Malaysian sample are larger than those in the Pakistani sample.

Research limitations/implications

The results suggest that the transformational leadership style is effective in both cultures, but the transactional leadership style is culturally contingent. While leaders in collectivist cultures like Malaysia and Pakistan should practice more transformational leadership than transactional leadership, leaders in Pakistan should be particularly careful while practicing transactional leadership because of the society's high level of collectivism and moderately high-power distance orientation.

Practical implications

The results suggest that the transformational leadership style is effective in both cultures, but the transactional leadership style is culturally contingent. While leaders in collectivist cultures like Malaysia and Pakistan should practice more transformational leadership than transactional leadership, leaders in Pakistan should be particularly careful while practicing transactional leadership because of the society's low power distance orientation.

Originality/value

Since this study is the first to compare the applicability of western theories in collectivist cultures that differ significantly in their power distance orientation, it contributes meaningfully to the cross-culture leadership field.

Web URL: ***http://www.emeraldinsight.com/doi/full/10.1108/CCSM-11-2015-0158***

5. Javed, M., Rashid, M. A., & Hussain, G. (2017). Well-governed responsibility spurs performance. ***Journal of Cleaner Production*****,** ***166*****, 1059-1073.**

ABSTRACT:

The mixed and inconsistent findings on the relationship between corporate social responsibility and organizational performance (CSR-OP) have exposed the universal approach as weak. Scholars have argued that not all CSR initiatives (including environment) all the time can be rewarded and have suggested the use of moderating variables to control the ambiguity surrounding CSR-OP relationship. Researchers viewed strong corporate governance (CG) as an important condition for reaping CSR benefits.

This study tests the direct effect of aggregate and segregated CSR on organizations' financial and non-financial performance. Moreover, it also investigates the moderating effects of corporate governance on the relationship between CSR and organizational financial and non-financial performance. Data in this study were collected from managers of public listed companies in Pakistan's manufacturing sector, and 179 valid responses were analyzed. Structural model results regarding the direct effects of aggregated and segregated CSR reveal that CSR significantly and positively influences organizational financial and non-financial performance. However, CSR is a better predictor of non-financial performance like reputation. Employees are observed as the most influential stakeholder in leveraging performance and the environment as the least influential stakeholder in Pakistan. Stakeholders' perspective of CSR creates a win-win for organizations and their disparate stakeholders.

The findings reveal that corporate governance significantly and positively influences both organizations' financial and non-financial performance but CG has a stronger influence on financial part. Moreover, moderation results reflected that strong CG strengthens the CSR-performance link and vice versa. So organizations need to have strong governance for optimizing CSR benefits. This study contributes to contingency perspective of CSR-performance relationship.

Web URL: ***https://www.sciencedirect.com/science/article/pii/S095965261731733X***

6. Zahid Mahmood, H., Abbas, K., & Fatima, M. (2017). Islamic microfinance and household welfare nexus: empirical investigation from Pakistan. ***Journal of Global Entrepreneurship Research*****, *7*(1), 18.**

ABSTRACT:

Many approaches and tools have been utilized throughout the globe by public and private sector organizations to curtail the deprivations and enhance welfare of the poor. Islamic Microfinance is one of them and is rapidly getting popular in Muslims as well as non-Muslims majority population countries. This study was conducted to gauge the impact of Islamic microfinance on the household welfare of the target clients by observing its impact on health, education, income, expenditures and assets of the poor who took loan from Islamic Microfinance institutions (IMFIs). Study is based on primary data and assessment was made rendering pre and post project approach by employing paired sample *t*-test and Regressionanalysis as statistical tools. Respondents were selected from three microfinance institutions, namely Akhuwat Foundation, Farz Foundation and NAYMET. Results delineate statistically significant differences in Pre and Post borrowing scenarios in the welfare indicators of the target households. It has been observed that borrowing from Islamic Microfinance institutions has not only significantly raised monthly income; expenditures on food, education and health; and incremented households' assetsbut also surprisingly raised borrowed amount of loan which negatively affected income. This requires some further investigation and it is recommended that practitioners and policy makers must keep IMF on its top agenda to enhanceliving standards of the poor in developing countries.

Web URL: ***https://journal-jger.springeropen.com/articles/10.1186/s40497-017-0075-1***

7. Iftikhar, S., & Mahmood, H. Z. (2017). Spatial distribution of agricultural resources and food security: A case of Punjab Pakistan. *Cogent Food & Agriculture*, *3*(1), 1357265.

ABSTRACT:

Agriculture is Pakistan's most vital sector and backbone of the economy, whose productivity depends upon several agricultural and natural resources. 19.8% of GDP of Pakistan's economy is come from the agriculture sector and it employs 42.3% of the total work force. There are several agricultural resources which enhance the food production and helps in efficient production. Different regions of Pakistan have different type and amount of resources, these agricultural resources include land, water, livestock, agricultural credit, agricultural machinery,

fertilizers and farm workers. The purpose of this study is to provide geographical intensity, district wise mapping of Punjab province of Pakistan. These maps illustrated the spatial distribution of districts in terms of crucial agricultural stocks which are important for higher food security. Then further econometric analysis is used to see the impact of various agricultural resources on food security. The study concluded that in overall availability of agricultural resources, Muzzafargarh, Sahiwal and Vehari districts are having abundance agricultural resources. With the increase in agricultural resources, more food will be produced which leads to increase the level of food security. Empirical investigation shows that Gini of Operational Farm Holding, Irrigated Area and Agricultural Machinery (Tractors) are significantly affecting the food security. The regression coefficients will direct the policy makers about what is the optimal combination of resources in terms of their importance for the food security, commercial importance of these input variables and assist them to prioritize their district wise spending using the geographical representations.

Web URL: ***http://www.tandfonline.com/doi/pdf/10.1080/23311932.2017.1357265***

8. Khaliq, I. H., Mahmood, H. Z., Malik, S., Jan, M. J., & Zameer, A. (2017). Exploring Switching Factors for Mobile Number Portability: A Survey.

ABSTRACT:

Pakistan's mobile phone market is one of the world's fastest growing markets with a subscriber base of 137 million users. Competition in the country's telecommunication industry is dominated by four players and customer demand is high. In addition, Pakistan is the first country in South Asia to have implemented Mobile Number Portability (MNP) in March 2007. MNP is a facility that allows mobile subscribers to switch between service providers without changing their existing phone numbers. Mobile phone service provider's selection may be influenced by various factors. Therefore, this research was undertaken to explore factors affecting MNP and to determine which factors were most influential in the selection of mobile phone service providers in a developing economy like Pakistan. Moreover, the study also probed into differences in customer perceptions between prepaid and post-paid customers. This exploratory study is based on primary data collected from 300 customers using services of

different cellular companies who had experienced MNP facility. Factor analysis was carried out on obtained data and reliability of the resultant scale was verified to achieve the objectives of the study. The outcome of this research provided a concise framework of the various dimensions of customer choice. Contrary to previous researches, the result of this study indicated that infrastructural services, customer relationships, call quality and promotional packages were the most important factors affecting MNP. However, price of services was found less important factor in selection of telecommunication service providers. This study also showed that pre-paid and post-paid customers can be significantly different for many value-added services and promotional tools

Web URL: ***http://www.ciitlahore.edu.pk/Papers/Abstracts/555-8587009754911680543.pdf***

9. Husnain, M. I. U., Khan, M., & Mahmood, H. Z. (2017). An assessment of public and private benefits of organic farming in Pakistan. ***JAPS: Journal of Animal & Plant Sciences*****,** ***27*****(3).**

ABSTRACT:

Despite the acknowledged advantages of organic farming, questions remain about its productivity differential and financial viability to its counterpart conventional farming. We test this claim in Pakistan, by comparing the productivity and profitability of organic and conventional farms that grow two major crops, wheat and rice, based on primary data collected from 444 (220 organic & 224 conventional) farms located in three districts of Punjab province. We find that growing organic crops is at least as profitable as conventional crops despite their low yields due to lower input costs and higher commodity prices. The Benefit Cost Ratio is also higher for organic crops which suggest that farmers can get higher profits by moving from conventional to organic crops. Overall, input costs are 20% and 10% lower in organic wheat and rice farms relative to their conventional counterparts. Soil nutrient tests show that organic farms tend to better conserve soil fertility and system stability than conventional farms. Based on these private and public benefits, we argue that organic agriculture should be encouraged to ensure sustainable agricultural practices in Pakistan. Farmers' tentative adoption of commercial organic farming will largely depend on how demand for organically farmed food continues to grow.

Web URL:

http://web.a.ebscohost.com/abstract?direct=true&profile=ehost&scope=site&authtype=crawler&jrnl=10187081&AN=124122324&h=%2fapMBvnnuJtiZdHSNiBHUPx9eCyH14CGiXgLJKH5HCczJKrA%2fbvW0k%2bz28EYy%2bpC8NBHrYzt%2b6PcJUelsPsQQQ%3d%3d&crl=c&resultNs=AdminWebAuth&resultLocal=ErrCrlNotAuth&crlhashurl=login.aspx%3fdirect%3dtrue%26profile%3dehost%26scope%3dsite%26authtype%3dcrawler%26jrnl%3d10187081%26AN%3d124122324

10. Khan, M., Mahmood, H. Z., Abbas, G., & Damalas, C. A. (2017). Agroforestry Systems as Alternative Land-Use Options in the Arid Zone of Thal, Pakistan. *Small-scale Forestry*, *16*(4), 553-569.

ABSTRACT:

Agroforestry offers unique opportunities for increasing biodiversity, preventing land degradation, and alleviating poverty, particularly in developing countries, but factors explaining the adoption by farmers are not well understood. A survey of 524 farm households was conducted in Bhakkar district of Punjab, Pakistan to study factors that determine the adoption of agroforestry on the sand dunes in the resource-deficient region of Thal. Two types of agroforestry systems were studied: intercropping and border cropping (also known as boundary or perimeter planting). Both agroforestry systems included irrigated cultivation of the timber trees *Eucalyptus camaldulensis* (local name: sufeda) and *Tamarix aphylla* (local name: sars) with wheat, chickpeas (*Cicer arietinum*) (local name: chana) or cluster beans (*Cyamous tetragocalobe*) (local name: guars). The majority of the farmers was in favour of intercropping and border cropping. Most farmers reported the protection of nearby crops from dust storms as the most important positive perception about both agroforestry systems. Age, education, and farm to market distance were significant determinants of agroforestry adoption. Older and less-educated farmers, with farms closer to markets were less likely to adopt tree planting or border cropping in Thal. In general, the agroforestry systems examined were more likely to be adopted by farmers who can wait 3–4 years for harvesting crop outputs, but not by poorer farmers who are totally dependent on subsistence agriculture and cannot afford the high initial cost of agroforestry establishment, nor can they wait for crop

output for extended periods. Furthermore, the adoption of both agroforestry systems was more likely in remote marginal areas than in areas close to markets. To increase agroforestry adoption rates, government policies should strengthen farmers' knowledge of every stage of agroforestry through extension services, focusing particularly among the prime prospects, i.e. farmers who will be most likely to adopt agroforestry. Once the prime prospects have adopted it, the older, less-educated, and poor farmers of the rural population can be also focused on to motivate adoption.

Web URL: ***https://link.springer.com/article/10.1007/s11842-017-9372-3***

11. Iftikhar, S., & Mahmood, H. Z. (2017). Ranking and relationship of agricultural credit with food security: A district level analysis. *Cogent Food & Agriculture*, *3*(1), 1333242.

ABSTRACT:

Agriculture sector is back bone of agrarian economies and it is the primary source of food in these economies like Pakistan. Current situation of Pakistan's economy highlighted that agriculture sector contributes the 19.8% share to GDP and provides 42.3% of the total work force. There is a lot of empirical work which focus on consistent expansion of agriculture output. Food production in agricultural economy require bundle of resources but credit is one of the factor which help in risk aversion and risk Management. The one of the major problem faced by the farmers is the shortage of credit availability. Therefore, this study has been devised to observe the impact of institutional and non-institutional agricultural credit on the level of food security in the districts of Punjab province of Pakistan. In this regard multiple linear regression models are rendered to quantify the relationship between food security (i.e. Food Insecure Population, Food Availability, Food Access and Food Absorption) and Agricultural Credit (i.e. Overall Agricultural Credit, Institutional Agricultural Credit and Non-Institutional Agricultural Credit). The study find that Institutional Agricultural Credit is significantly helping in combating food insecurity while Non-Institutional Agricultural Credit shows unexpected results. Therefore it is strongly recommended to cates institutional credit to reduce food insecurity issues in the country.

Web URL: **http://www.tandfonline.com/doi/pdf/10.1080/23311932.2017.1333242**

12. Riaz, A., & Mahmood, H. Z. (2017). Cross-Level Relationship of Implemented High Performance Work System and Employee Service Outcomes: The Mediating Role of Affective Commitment. ***Pakistan Journal of Commerce & Social Sciences*****, *11*(1).**

ABSTRACT:

This study examines cross-level relationship between implemented high performance work system (HPWS) and employee service related behaviors along with the mediating effects of employees' affective commitment between this relationship. Although, research studies have confirmed the positive linkage between high performance work system (HPWS) and firm performance. Previous studies were criticized for being management-centric with insights mostly from manufacturing and Western context. Using multilevel approach, this research examines the relationship of bank branch managers' implemented HPWS with (i) employees' service performance and their (ii) service oriented organizational citizenship behavior (OCB) with a particular focus on studying affective commitment as a mediator. For the purpose of this study, data from branch managers of 323 bank branches operating in Punjab, Pakistan and their 1369 front line employees were used. Hierarchical linear modeling (HLM) was applied to test crosslevel hypotheses of this study. Study results revealed that implemented HPWS was significantly related with employees' service performance and their service related discretionary behavior. Further, affective commitment partially mediated both the direct relationships between implemented HPWS and employees' service related behaviors. Empirical findings of this study implied that effectively implemented HPWS by branch managers has the potential to influence affective commitment level of front line employees which further influence their customers service related behaviors. This study contributes by highlighting the potential influence of branch managers' implemented HPWS on service related behaviors of employees.

Web URL: **https://www.researchgate.net/profile/Amir_Riaz/publication/316878818_Cross-Level_Relationship_of_Implemented_High_Performance_Work_System_and_Employee_Service_Outcomes_The_Mediating_Role_of_Affective_Commitment/links/59158527a6fdcc963e82f72e/Cross-Level-Relationship-of-Implemented-High-Performance-Work-System-and-Employee-Service-Outcomes-The-Mediating-Role-of-Affective-Commitment.pdf**

13. Ahmed, I., Shaukat, M. Z., Usman, A., Nawaz, M. M., & Nazir, M. S. (2017). Occupational health and safety issues in the informal economic segment of Pakistan: a survey of construction sites. *International journal of occupational safety and ergonomics*, 1-11.

ABSTRACT:

This research covers the current status of occupational health and safety (OHS)-related practices in the informal construction segment of Pakistan. Data were collected, through interviews, from 316 construction sites employing 3577 workers. The results of the study reveal that both employers and workers lack knowledge of OHS laws/standards and no practices of this nature are enacted at these construction sites. Alarmingly, work-related accidents, whenever they happen, are not given due attention and there is no formal injury-report system. The informal construction industry employs a huge portion of the informal workforce, and lack of OHS happens at tremendous human cost. These research findings may thus play their role in strengthening the case for reforms in the sector. This study, if properly utilized, may also enable employers of the sector by increasing their knowledge about OHS practices and, as a result, trying to offer safer environments for their workers.

Web URL: ***http://www.tandfonline.com/doi/abs/10.1080/10803548.2017.1366145***

14. Akhter, W., Pappas, V., & Khan, S. U. (2017). A comparison of Islamic and conventional insurance demand: Worldwide evidence during the Global Financial Crisis. *Research in International Business and Finance*, *42*, 1401-1412.

ABSTRACT:

In this paper we compare the Islamic insurance industry (Takaful) to the conventional insurance across 14 countries over the 2005–2014 period. Our methodology relies on panel regressions and accounts for the periods during and post the global financial crisis (GFC). Specifically, we investigate: i) the difference in the insurance demand dynamics of the two insurance types; ii) if Islamic insurance demand has been boosted in the period that followed the crisis. To allow for cross-country heterogeneities we form sub-samples of high/low insurance regions and ASEAN/Middle East. We find Islamic and conventional insurance demand to be negatively affected by GDP/capita, albeit the Islamic showing a greater resilience during crisis. A negative

link between conventional insurance and saving rate shows that conventional saving products work as substitutes to conventional insurance. Higher average income is positively (negatively) related to Islamic insurance demand in the Middle East (ASEAN), a finding plausibly related to the different practices relating to Islamic finance in the two regions.

Web URL: ***https://www.sciencedirect.com/science/article/pii/S0275531916304871***

15. Akhtar, B., Akhter, W. & Shahbaz, M. (2017). Determinants of deposits and conventional and Islamic banking, empirical evidence from an emerging economy. ***International Journal of Emerging Markets 12(2).***

ABSTRACT:

The main objective of present study is to examine the impact of selected macroeconomic variables on deposits of both conventional and Islamic banks in Pakistan. Six years quarterly data i.e. 2006 to 2011 was obtained from 30 banks consist of 25 conventional and 5 islamic banks. Both short-run and long-run relationship among these variables were examined using bounds testing approach of the Autoregressive-Distributed Lag (ARDL), to find cointegration and error correction framework. Results of this study reveal that variables such as interest rate of conventional banks, profit of Islamic banks, consumer price index, money supply and base lending rate have different impact on both conventional and Islamic bank deposits. Depositors of both conventional and Islamic banks are sensitive to the returns received on the deposits. Any boost in interest rate increases the deposits of conventional banks and decreases the deposits of Islamic banks. The study shows that an important element to attract the depositors towards the Islamic banks is religious factor. This paper has important implications for Islamic banks to offer more competitive rates of profit with respect to the interest rate of conventional banks in order to collect more deposits

Web URL: ***http://www.emeraldinsight.com/doi/pdfplus/10.1108/IJoEM-04-2015-0059***

16. Akhter, W., & Khan, S. U. (2017). Determinants of Takāful and conventional insurance demand: A regional analysis. ***Cogent Economics & Finance*****, *5*(1), 1291150.**

ABSTRACT:

In this study, we focused on analysing and differentiating the determinants of conventional insurance and *Takāful* demand across ASEAN and Middle East Regions. We used panel data econometrics on a sample of 14 Asian countries having both conventional insurance and *Takāful* over the period 2005–2014. We applied fixed and random effect regression models to assess the impact of macroeconomic and demographic factors on conventional insurance and *Takāful* demand. Income and financial sector were found to have significant positive impact on insurance demand across all regions. On the other hand, dependency ratio was found to be negatively affecting *Takāful* demand across all regions while inflation shows positive impact. Urbanization was found to be significant positive impact on both conventional insurance and *Takāful* demand. Financial sector development positively triggers the insurance and *Takāful* demand across ASEAN region, while it triggers conventional insurance demand only in Middle East Region. Education shows negative impact on *Takāful* demand across both regions while it shows positive impact on insurance demand in Middle East. The study recognises the key role of urbanization and education in creating awareness to enhance *Takāful* demand in large populated countries of ASEAN and South Asia.

Web URL: ***http://www.tandfonline.com/doi/full/10.1080/23322039.2017.1291150***

17. Rahman, K. U., Akhter, W., & Khan, S. U. (2017). Factors affecting employee job satisfaction: A comparative study of conventional and Islamic insurance. *Cogent Business & Management*, *4*(1), 1273082.

ABSTRACT:

This paper attempts to investigate the factors that affect job satisfaction of sales agents from Islamic (Hereafter; *Takāful*) and conventional insurance of Pakistan using Herzberg two-factor motivation theory. Using multi-stage stratified random sampling, we received a total of 318 usable responses (185 from family *Takāful* and 133 from life insurance). A multiple regression and hierarchal regression model including 11 hygiene–motivational factors were used to examine job satisfaction in the presence of moderating factor *Shari'ah* perception. The outcomes regarding Herzberg two-factor theory were entirely distinctive between those two direct sales groups with the presence of moderating variable *Shari'ah* perception. Without

moderating the effect of *Shari'ah* perception, family *Takāful* and conventional life insurance full-time direct sales agents demonstrated that hygiene factors and motivational factors were both more effective indicators of job satisfaction in Pakistani context. While checking the moderating effect in the presence of moderating variable *Shari'ah* perception, family *Takāful* sales agents are satisfied with hygiene factors where the motivators are not significantly affected by *Shari'ah* perception. On the other hand, conventional life insurance sales agents have no concern with *Shari'ah*perception.

Web URL: ***http://www.tandfonline.com/doi/full/10.1080/23311975.2016.1273082***

18. Zaman, Q. U., Hassan, M. K., Akhter, W., & Meraj, M. A. (2017). From interest tax shield to dividend tax shield: A corporate financing policy for equitable and sustainable wealth creation. *Pacific-Basin Finance Journal*.

ABSTRACT:

This study critically analyzes debt-incentivized corporate tax and financing policy and provides an Islamic perspective to this important tax deductibility debate. This study advocates that the corporate tax incentive to debt (interest tax shield) be abolished and shifted to equity (dividend tax shield). Later, we use the implications of our proposed taxation policy to reframe the firm financing model and modify M & M's firm valuation model. We use a scenario-based simulation technique and conduct various policy experiments to assess the impact of conventional and proposed tax regimes on levered and zero-levered firms and their values. We find that aligning corporate financing policy with the fundamentals of Islamic finance helps restrain corporate indebtedness and promote profit and loss sharing. According to our proposed model, firms have a reduced cost of financing, tend to be more stable, and are value oriented, especially when they avoid debt to the maximum extent. We further propose that an optimal dividend payout ratio may lead to aggregate equilibrium amongst cost of financing, firm value, and corporate tax contribution to the economy. This study provides new contributions to the discipline of Islamic corporate finance.

Web URL: ***http://www.sciencedirect.com/science/article/pii/S0927538X17300343***

19. Ali, I., Akhter, W., & Ashraf, N. (2017). Impact of Muslim Holy Days on Asian stock markets: An empirical evidence. *Cogent Economics & Finance*, *5*(1), 1311096.

ABSTRACT:

This study investigated the impact of Muslim Holy Days on daily stock returns of Asian financial markets for a period of 2001–2014. These markets include Pakistan, Bahrain, Saudi Arabia, and Turkey. The study has tried to isolate the effect of Gregorian calendar anomalies from Muslim Holy Days to certify that the documented effect is actually a result of Muslim Holy Days rather than Gregorian calendar anomalies. Pooled fixed/random effect Panel Regression is used to check the underlined effect. The results reveal that Eid-ul-Fitr is the only Holy day, which has significant positive effect on stock returns of Asian markets, while all other Holy Days have no effect. Friday is the only Gregorian calendar anomaly, which exists in Asian markets. These results provide support to the fact that both Islamic and Gregorian calendar anomalies exist in Asian markets.

Web URL: **http://www.tandfonline.com/doi/full/10.1080/23322039.2017.1311096**

20. Khan, S., & Akhter, W. (2017). Service quality and the moderating effect of Shari'ah perception on client satisfaction: A comparison of islamic and conventional microfinance in Pakistan. *Cogent Economics & Finance*, *5*(1), 1315206.

ABSTRACT:

Microfinance is an emerging concept which is improving the socioeconomic status of customers. This study assesses customer satisfaction of clients of Islamic and conventional microfinance providers using a sample of 578 clients i.e. 289 from each side. Akhuwat and Kashf (Islamic microfinance) and RCDS and DAMEN (conventional microfinance) are selected. The correlation, regression, ANOVA, and interaction tests are used for testing the relationship of *Shari'ah* perception as moderator between service quality and client satisfaction. The results indicate that *Shari'ah* perception acts as a strong moderator in case of Islamic microfinance whereas it is a weak moderator in case of conventional microfinance. The study concludes that *Shari'ah* perception is playing a vital role in enhancing the customer satisfaction in Islamic microfinance. It has important implications for policy-makers and Islamic microfinance

providers to design *Shari'ah*awareness programs to enhance the *Shari'ah* perception of low income population.

Web URL: ***http://www.tandfonline.com/doi/full/10.1080/23322039.2017.1315206***

21. Iftikhar, S., & Mahmood, H. Z.(2017). Human capital development and food security nexus: An empirical appraisal from districts of Punjab province. ***Journal of Food and Drug Research.5(1). 18-24***

ABSTRACT:

It is proven fact that human capital development plays a pivotal role in enhancing industrial and agricultural productivity and economic growth. Comprehensive research has been rendered by scientists to observe the relationships of human capital development (HCD) with multiple dimensions but none of the scientists explored, yet, connections between HCD and food security. This study is an endeavor to explore ranking of districts of Punjab province of Pakistan with respect to different indicators of HCD including overall literacy rate, farmers' literacy rates and population per school. Moreover, relationships between food security and target variables are also quantified. Data are collected from Punjab Development Statistics (Government of Punjab 2009) and Food Insecurity report 2009 (SDPI, SDC and WFP 2009). Moreover, values of the target variables are arranged in descending order to explore the ranks of the districts in the province while bidirectional Pearson correlation analysis is rendered to know the direction of relationships between food insecure population (%) and overall and farmers' literacy rates and population per school. Negative relationships are found between food insecure populations and rest of other indicators. Therefore, it is strongly recommended that policy maker must make necessary arrangements to augment literacy rates to secure food for the masses in the province.

Web URL:

https://pdfs.semanticscholar.org/bf01/5c3ba9063a933cd9833741ea438d34bacea8.pdf

22. Damalas, C. A., & Khan, M. (2017). Pesticide use in vegetable crops in Pakistan: Insights through an ordered probit model. ***Crop Protection*****,** ***99*****, 59-64.**

ABSTRACT:

Pesticide application issues are a major concern in farmers' production practices, but little is known about the knowledge levels and the behaviour of farmers when handling pesticides. Farmers' knowledge of pesticide use practices and factors affecting application of the current practices were explored in the Lodhran and Vehari districts of Pakistan. The ordered probit model was used to analyze data from selected small-scale farmers dealing with vegetable production. All farmers were using chemical pesticides for pest control, but more than one-third of the pesticides belonged to the category highly hazardous (34.2%) or moderately hazardous (35%) pesticides. Moreover, the majority of the farmers were using mixtures for better control of different pests or diseases. Most farmers (58.1%) showed moderate levels of knowledge of common application issues. In addition, only 16.1% of the farmers had received basic training on pesticide use and only 12.9% had access to information. The ordered probit model showed that basic training on pesticide use, access to advice, education, reading pesticide labels, and years of applying pesticides contributed positively to farmers' knowledge of pesticide handling. By contrast, applying pesticide mixtures had a negative impact on farmers' knowledge. Overall, the data shed light on patterns of pesticide handling practices by small-scale farmers in vegetable crops in the Lodhran and Vehari districts of Pakistan, for which research data are lacking from the literature. Overreliance of farmers on pesticides, poor access to training on pesticides, and poor knowledge of proper handling practices imply high risk of pesticide exposure and pesticide residues on crops. Effective extension programs and smooth access to advice are necessary for improving farmers' knowledge on proper use of pesticides and thus reducing the adverse effects on their health and the environment

Web URL: **http://www.sciencedirect.com/science/article/pii/S0261219417301205**

23. Khan, S. A., Yosuf, N. Sheikh, U & Najam, I. (2017). Impact of HR Practices on University Teachers' job motivation: A case study of the Universities of Lahore, Pakistan. ***EUROPEAN ACADEMIC RESEARCH.*** **4(11).**

ABSTRACT:

The purpose of this study is to investigate the impact of HR practices on university teachers' job motivation in Lahore, Pakistan. The study consists of three variables: Administrative Policies (AP), Rewards/Incentives (RI) and Teachers Motivation (TM) where administrative policies and incentives/rewards are considered independent variables whereas motivation level is used as a dependent variable. Five point Likert scale questionnaire was adopted to collect the data. The data was processed through SPSS 20 and correlation & linear regression analysis was used to analyze the data. The results of the study carry significance and elucidate that rewards/incentives and administrative policies affect the motivation level of university teachers in Lahore, Pakistan.

Web URL: **http://euacademic.org/UploadArticle/3050.pdf**

24. Abdullah, M. I., Ashraf, S., & Sarfraz, M. (2017). The Organizational Identification Perspective of CSR on Creative Performance: The Moderating Role of Creative Self-Efficacy. *Sustainability*, *9*(11), 2125.

ABSTRACT:

Corporate social responsibility (CSR) is an emerging and fast-growing concept for both academic research and organizations. In recent years, the far-reaching influence of CSR practices on stakeholders has made both researchers and practitioners pay heed to this dimension. Employees are one of the most important stakeholders influenced by CSR practices. CSR brings in many ideas, concepts, and techniques. In the past, different antecedents and consequences of corporate social responsibility have been studied, but there is still a deficit in regard to whether employee creative performance is an outcome of corporate social responsibility, and the interlinked variables that might enhance this relationship. The main objective of this study is to examine how CSR practices enhance employee performances within the organization, and which other variables may enhance this relationship. The literature suggests that employees who value CSR campaigns and other practices identify with their company to a greater degree, work with more devotion and loyalty, and show more creativity in their work performance. In this study, organizational identification has been taken as the mediator, and creative self-efficacy has been taken as

the moderator. The hypotheses were tested within the sample of companies engaging in CSR practices in Pakistan. A questionnaire survey was conducted using simple random sampling. Simple linear regression, hierarchical regression, and Barron and Kenny tests were applied through SPSS (Statistical Package for the Social Science) for data analysis, and results were found according to the proposed model of the study.

Web URL: **http://www.mdpi.com/2071-1050/9/11/2125/htm**

25. Mahmood, A. Ayub, T. Abdullah, I. & Sarfraz, M. (2017). Linking Fashion Clothing Involvement with Attitude towards Luxury Brands. *Pacific Business Review International*. 9(10).

ABSTRACT:

The purpose of this study is to examine the relationship between fashion clothing involvement (FCI) and the attitude towards luxury brands (ATLB), mediating role of social comparison (S_COM) and status consumption (S_CON). The study aims to expand the scope of fashion marketing research within the context of luxury clothing brand market. The paper opted for a descriptive study involving 251 respondents. Data were collected through online and offline survey methods. Structural equation modelling was employed to test the research hypotheses. The study found that status consumption performs a partial mediating role on the relationship between FCI and ATLB. Non-probability sampling technique was used to collect the data. Due to lack of representation, the findings of this study cannot be projected or generalized beyond the sample unit used. The paper includes implications for market practitioners to effectively targetfashionconscious consumers by developing marketing strategies that involves the element of attracting status consuming buyers. This paper extends the empirical model of FCI by incorporating fashion Clothing involvement as an antecedent of ATLB along with two mediators S_Com and S_Con.

Web URL: **http://pbr.co.in/April%202017/10.pdf**

26. Ellahi, N., Maroof, Z., Mehmood, H. Z., & Kiani, A. (2017). EDUCATION AND SOCIOECONOMIC DEVELOPMENT: FINDING THE WAY FORWARD. *Science International*, *29*(2), 361-361.

ABSTRACT:

Economic theories within the endogenous growth framework introduced the concept of human capital, which postulates that education is a critical factor to economic growth and socioeconomic development. Another view of human development paradigm states that education level contributes to economic growth through the channels of productivity and social change. Present paper discusses the role of basic education to reduce food insecurity. It is a fact documented in literature that basic education that can help people in enhancing their capacity in developing countries to live a decent life and escape from hunger and poverty. It is achieved through higher awareness on diversification of assets and activities with which they are better able to get information on health and sanitation, further there is a psychological contribution and a role through social relations as well. These entire factors contribute to ensure food security in the long run. There are various channels Specific Objectives of the paper include analyzing whether basic education and higher education help to fight against food security in Pakistan. The proposed study is a combination of theoretical and empirical analysis and it included both the indicators of basic and higher education along with available data on food security variables. Moreover, it intends to apply econometric techniques to find short run and long run elasticities along with short run diagnostic tests. In addition to this, this paper theoretically compares the state of Pakistan with the other countries in South Asian region. In sum, present study is planned to test the validity of the hypothesis that reduction in food insecurity is an important end of development for developing countries. In addition this study presents policy recommendations on the basis of theoretical facts and empirical findings which further helps to find the way forward.

Web URL: **http://www.sci-int.com/pdf/636300161324048875.pdf**

DEPARTMENT OF CHEMICAL ENGINEERING

Journal Papers

1. Akhtar, M. A., Riaz, S., Hayat, A., Nasir, M., Muhammad, N., Rahim, A., & Nawaz, M. H. (2017). Poly (ethylene oxide) tethered trans-porphyrin: Synthesis, self-assembly with fullerene (C 60) and DNA binding studies. *Journal of Molecular Liquids*, *225*, 235-239.

ABSTRACT:

Trans-Porphyrin containing phenyl group at both ends was synthesized via corresponding dipyrromethanes (DPM) in the presence of TFA and DDQ. The polyethyleneglycole (PEG) chains were attached at the trans positions of ABA type porphyrinic moiety. The prepared PEGylated porphyrin (with PEG arms at the periphery) P-$(PEO)_2$ was self-assembled into spheres of uniform diameter while their DMF solution was dialyzed into water. Furthermore, the addition of fullerene (C_{60}) to P-$(PEO)_2$ caused complexation between porphyrin and fullerene which lead to interesting and trenchant morphology having worm like lateral aggregates. The assembly process and the as-prepared edifices were characterized using UV–vis absorption spectroscopy and the morphology of these assemblies was investigated using transmission electron microscope (TEM). Furthermore, the DNA binding with porphyrin aggregates has been demonstrated via electrochemical (cyclic voltammetric) response of screen printed electrodes modified. The obvious increase in redox current disclosed the intermolecular interactions of the adducts with the DNA. These studies of unprecedented adducts can further be explored for potential applications in biosensors.

Web URL: http://www.sciencedirect.com/science/article/pii/S016773221633149X

2. Abu-Jrai, A. M., Jamil, F., Ala'a, H., Baawain, M., Al-Haj, L., Al-Hinai, M., ... & Rafiq, S. (2017). Valorization of waste Date pits biomass for biodiesel production in presence of green carbon catalyst. *Energy Conversion and Management*, *135*, 236-243.

ABSTRACT:

In this study, an efficient utilization of waste Date pits biomass for synthesizing green carbon catalyst as well as production of biodiesel were investigated. The green carbon catalyst was

modified by KOH and characterized by XRD, SEM, EDX, TEM and BET. Taguchi method in Response Surface Methodology (RSM) was applied to study the effect of several process parameters such as reaction temperature, time, catalysts type and methanol to oil ratio, on the yield of the produced biodiesel. The optimized yield obtained was 91.6% when the process temperature was 65 °C, with catalyst type C3 (6 wt% KOH on carbon) within 1 h and with 9:1 methanol to oil ratio. The produced biodiesel was completely characterized in order to verify its quality, compared with the international standards. Fuel properties of the produced biodiesel were found to be a cetane number 60.31, density 881 kg/m^3, viscosity 4.24 mm^2/s, cloud point 3.9 °C, cold filter plugging point −0.62 °C, pour point −1.4 °C and flash point 141 °C, which lies within the limits specified by the international standards of ASTM and EN. Waste Date pits biomass can be a promising platform for the production of green carbon catalysts as well as biodiesel production.

Web URL: ***http://www.sciencedirect.com/science/article/pii/S0196890416311785***

3. Saeed, M., Rafiq, S., Bergersen, L. H., & Deng, L. (2017). Tailoring of water swollen PVA membrane for hosting carriers in CO 2 facilitated transport membranes. ***Separation and Purification Technology*****,** ***179*****, 550-560.**

ABSTRACT:

Facilitated transported composite membranes were synthesized for efficient CO_2/N_2separation by incorporation surface modified multi-walled carbon nanotubes (CNTs) in polyvinyl alcohol (PVA) and adjusting the pH of the membrane casting solution from acidic to basic. The membranes were developed for post-combustion CO_2 capture operating under humidified condition and low CO_2 partial pressure. The membrane was tailored by adding different concentrations of surface modified CNTs (0–2%) with respect to PVA and adjusting pH from 5 to 12. An optimal CNT loading along with membrane pH was determined based on experimental results from gas permeation tests.

By optimizing the CNT loading and pH of the membrane, the CO_2 permeance was increased from 0.18 ± 0.02 m^3 (STP)/m^2 bar h to 0.44 ± 0.02 m^3 (STP)/m^2 bar h at a constant CO_2/N_2 selectivity of 60 ± 1. The membrane swelling degree was also increased from 154 ± 20

to 254 ± 30. The thickness of the selective layer was reduced from ~0.85 μm to 0.45 μm which resulted in further increase in permeance to 0.48 m^3 (STP)/m^2 bar h. The developed membrane showed a stable operation over a period of 1 month.

Web URL: ***http://www.sciencedirect.com/science/article/pii/S1383586616326387***

4. Cho, H. J., Ahmed, F., Kim, T. Y., Kim, B. S., & Yeo, Y. K. (2017). A comparative study of teaching-learning-self-study algorithms on benchmark function optimization. *Korean Journal of Chemical Engineering*, *34*(3), 628-641.

ABSTRACT:

In typical optimization problems, the number of design variables may be large and their influence on the specific objective function can be complicated; the objective function may have some local optima while most chemical engineers are interested only in the global optimum. For any new optimization algorithms, it is essential to validate their performance, compare with other existing algorithms and check whether they provide the global optimum solutions, which can be done effectively by solving benchmark problems. In this work, seven typical optimization algorithms including the newly proposed TLBO (Teaching-learning-based optimization) based algorithms such as the TLSO (Teaching-learning-self-study optimization) algorithm have been reviewed and tested by using a set of 20 benchmark functions for unconstrained optimization problems to validate the performance and to assess these optimization algorithms. It was found that the TLSO algorithm shows the fastest convergence speed to the optimum and outperforms other algorithms for most test functions.

Web URL: ***https://link.springer.com/content/pdf/10.1007/s11814-016-0317-x.pdf***

5. Xin, L., Yang, W., Zhao, Q., Dong, R., Liang, X., Xiu, Z., ... & Wu, G. (2017). Effect of extrusion treatment on the microstructure and mechanical behavior of SiC nanowires reinforced Al matrix composites. *Materials Science and Engineering: A*, *682*, 38-44.

ABSTRACT:

In the present work, microstructure and mechanical performance of extruded SiCnw/Al composites have been investigated. The extrusion treatment leads to the alignment of SiC nanowires and the densification of the composites. The average length of SiC nanowires has been shortened after extrusion. High density dislocation tangles have been observed in Al matrix after extrusion. As the "non-deformable" phases, SiC nanowires inhabited the movement and deformation of surrounding Al matrix, leading to the formation of the grain boundaries. Therefore, SiC nanowires were mainly found at the boundary of Al grains in the extruded composites. Regardless of content of SiC nanowires, the yield strength, tensile strength and elongation of SiCnw/6061Al composites have been improved after extrusion treatment. Based on generalized mixture rule considering the effect of porosity, the increase of elastic modulus of SiCnw/6061Al composites is mainly due to the densification effect. The strengthening factor and efficiency of SiC nanowires are highest among all SiC reinforcements, and the strengthening behavior of SiC reinforced Al matrix composites could be well explain by the modified shear-lag model. The ratio of strengthening efficiency of SiCnw/Al composites before and after extrusion was about 0.6, indicating that orientation optimization of SiC nanowires is an effective method to improve the mechanical properties of SiCnw/Al composites.

Web URL: ***http://www.sciencedirect.com/science/article/pii/S0921509316313958***

6. Xin, L., Yang, W., Zhao, Q., Dong, R., Wu, P., Xiu, Z., ... & Wu, G. (2017). Strengthening behavior in SiC nanowires reinforced pure Al composite. ***Journal of Alloys and Compounds*****, *695*, 2406-2412.**

ABSTRACT:

Recently, it has been found that SiC nanowires have significant strengthening effect on Al matrix. The shear-lag model was used to explain the strengthening behavior after considering the aspect ratio of reinforcement in the previous work. However, the effect of alloying elements has not been considered yet. Moreover, the significant strengthening effect of SiC nano-particles over micron-scale particles could not been explained by the modified shear-lag model due to their same aspect ratio. Therefore, pure Al matrix composites reinforced with SiC

nanowires, which could minimize the strengthening effect of the alloying elements, were selected to explore in this work. SiCnw/pure Al composites with different fractions (15, 20 and 25 vol%) have been prepared by pressure infiltration method. The yield strength was improved with the increased content of SiC nanowires. Based on the previous work, the modified shear-lag model has been further developed after considering the surface-to-volume ratio of the reinforcement. It has been taken into account that initially the effective atoms participated into the interfacial load transferring, and eventually the strengthening behavior of Al composites reinforced with SiC-type reinforcements was explored. Based on the developed model, the key research fields have also been discussed in order to exploit the strengthening effect of SiC nanowires.

Web URL: ***http://www.sciencedirect.com/science/article/pii/S0925838816336027***

7. Amin, M. R., Al-Harthi, M. A., Imran, S. M., & Hussain, M. (2018). Effect of Nanoparticles on Mechanical and Flame-retardant Properties of Polyether-Block-Polyamide Polymer Nanocomposites. ***Polymer-Plastics Technology and Engineering*****,** ***57*****(1), 38-45.**

ABSTRACT:

In this study, polyester elastomer-based thermoplastic (TPEE) nanocomposites were fabricated for flame-retardant applications. Small amounts of graphene and nanoclay were added to the nanocomposites to investigate their effects on the mechanical and thermal properties of the nanocomposites. The addition of a phosphorous flame-retardant additive resulted in a significant improvement of the Young's modulus and thus yield stress in the synthesized nanocomposites as compared to those made with the virgin TPEE. There was no synergistic improvement in mechanical properties with the addition of graphene and nanoclay to the nanocomposites. However, thermal properties, mainly the heat deflection temperature and fire performance (UL-94 V0), were improved significantly by the addition of graphene and nanoclay and a synergistic effect was observed. Heat distortion temperature and thermogravimetric analysis were used to analyze the thermal properties of the nanocomposites. The UL-94 testing method was used to investigate the fire performance of the nanocomposites. Scanning electron microscopy was used to observe the polymer fracture surface morphology. The dispersion of

the graphene and nanoclay particles was confirmed by transmission electron microscopy analysis.

Web URL: ***http://www.tandfonline.com/doi/abs/10.1080/03602559.2017.1300814***

8. Jang, N., Yasin, M., Park, S., Lovitt, R. W., & Chang, I. S. (2017). Determination of volumetric gas–liquid mass transfer coefficient of carbon monoxide in a batch cultivation system using kinetic simulations. *Bioresource Technology*, *239*, 387-393.

ABSTRACT:

A mathematical model of microbial kinetics was introduced to predict the overall volumetric gas–liquid mass transfer coefficient (k_La) of carbon monoxide (CO) in a batch cultivation system. The cell concentration (X), acetate concentration (C_{ace}), headspace gas (N_{co} and Nco2), dissolved CO concentration in the fermentation medium (C_{co}), and mass transfer rate (R) were simulated using a variety of $k_La$values. The simulated results showed excellent agreement with the experimental data for a k_La of 13/hr. The C_{co} values decreased with increase in cultivation times, whereas the maximum mass transfer rate was achieved at the mid-log phase due to vigorous microbial CO consumption rate higher than R. The model suggested in this study may be applied to a variety of microbial systems involving gaseous substrates.

Web URL: ***http://www.sciencedirect.com/science/article/pii/S0960852417306624***

9. Jamshaid, A., Hamid, A., Muhammad, N., Naseer, A., Ghauri, M., Iqbal, J., ... & Shah, N. S. (2017). Cellulose-based Materials for the Removal of Heavy Metals from Wastewater–An Overview. *ChemBioEng Reviews*.

ABSTRACT:

Water pollution due to increase in population and high rates of wastewater generation have become serious concerns since the last few decades. Heavy metals are amongst the main wastewater pollutants due to their ability to persist in the environment. Materials and techniques are being investigated for the treatment of heavy metals in wastewater. Cellulose is one of the materials gaining attention due to its excellent physical, chemical, and mechanical properties. Cellulose-based materials are being widely studied for the adsorption of heavy

metals. This overview highlights research efforts to enhance the role of cellulose in wastewater treatment through cellulose-based materials. It also discusses the effects of cellulose modifications such as cellulose gels, cellulose composites, cellulose derivatives, functionalized cellulose, and nanocrystalline cellulose on the capacity of heavy metals adsorption.

Web URL: **http://onlinelibrary.wiley.com/doi/10.1002/cben.201700002/full**

10. Yang, W. S., Chen, G. Q., Wu, P., Hussain, M., Song, J. B., Dong, R. H., & Wu, G. H. (2017). Electrical Discharge Machining of Al2024-65 vol% SiC Composites. ***Acta Metallurgica Sinica (English Letters)*****,** ***30*****(5), 447-455.**

ABSTRACT:

In the present work, the wire electrical discharge machining (WEDM) process of the 65 vol% SiCp/2024Al composite prepared by pressure infiltration methods has been investigated. The microstructure of the machined composite was characterized by scanning electron microscope, the average surface roughness (Ra), X-ray diffraction, X-ray photoelectron spectroscopy and transmission electron microscopy (TEM) techniques. Three zones from the surface to the interior (melting zone, heat affected zone and un-affected zone) were found in the machined composites, while the face of SiC particles on the surface toward the outside was “cut” to be flat. Increase in Al and Si but decrease in C and O were observed in the core areas of the removed particles. Si phase, which was generated due to the decomposition of SiC, was detected after the WEDM process. The irregular and spherical particles were further observed by TEM. Based on the microstructure observation, it is suggested that the machining mechanism of 65 vol% SiCp/2024Al composite was the combination of the melting of Al matrix and the decomposition of SiC particles.

Web URL: ***https://link.springer.com/article/10.1007/s40195-016-0515-x***

11. Munnawar, I., Iqbal, S. S., Anwar, M. N., Batool, M., Tariq, S., Faitma, N., ... & Ahmad, N. M. (2017). Synergistic effect of Chitosan-Zinc Oxide Hybrid Nanoparticles on antibiofouling and water disinfection of mixed matrix polyethersulfone nanocomposite membranes. ***Carbohydrate polymers*****,** ***175*****, 661-670.**

ABSTRACT:

Antifouling polyethersulfone (PES) membranes for water disinfection were fabricated by incorporating varying concentrations of carbohydrate polymer chitosan and Zinc oxide hybrid nanoparticles (CS-ZnO HNPS). The CS-ZnO HNPS were prepared using chemical precipitation method and were characterized using SEM, XRD and FTIR. The membranes were then fabricated by incorporating nanoparticles of CS-ZnO HNPS with three different concentrations of 5%, 10% and 15% w/w in the casting solution of PES through phase inversion method. The influence of nano-sized CS-ZnO HNPS on the properties of PES was characterized to study morphology, contact angle, water retention, surface roughness and permeability flux. The membranes with the maximum concentrations of 15% HNPS resulted in larger mean pore sizes and lowest contact angle value as compare to the pristine PES membrane. The prepared membranes exhibited significant water permeability, hydrophilicity and prevention against microbial fouling. The prepared membranes were observed to have significant antibacterial as well as antifungal properties due to the synergistic effect of chitosan and ZnO against both bacteria of the type of S. Aureus, B. *Cereus*, E. coli, and fungi such as S. typhi, A. fumigatus and *F. solani.*

Web URL: https://www.sciencedirect.com/science/article/pii/S0144861717309128

12. Yang, W., Chen, G., Qiao, J., Liu, S., Xiao, R., Dong, R., ... & Wu, G. (2017). Graphene nanoflakes reinforced Al-20Si matrix composites prepared by pressure infiltration method. *Materials Science and Engineering: A*.

ABSTRACT:

It has not been reported in the existed literatures that whether it is possible to prepare GNFs/Al composites by pressure infiltration method due to the poor wettability and severe reaction behavior between carbon and molten Al. In the present study, microstructure and mechanical behavior of graphene nanoflakes (GNFs) reinforced Al-20Si (GNFs/Al-20Si) composites prepared by the pressure infiltration method have been thoroughly investigated. The Al-20Si matrix was chosen to inhibit the formation of Al_4C_3. It has found that the GNFs and Al alloy matrix has been well bonded without formation of Al_4C_3, which authenticated the effectiveness of the alloying treatment. Moreover, the hardness and the elastic modulus of the composites were increased

linearly with the increase in the GNFs content. After addition of 1.5 wt% GNFs, the ultimate tensile strength and bending strength attained the peak values, which increased 130% and 230% to that of Al matrix, respectively. To the best of our knowledge, it is the highest strengthening ratio in Al matrix composites reinforced with graphene reinforcements. Furthermore, based on the modified shear-lag model and combined with the literatures' data, the strengthening behavior of GNFs/Al composites has been extensively discussed. It is concluded that the pressure infiltration method is the most feasible and successful way to prepare GNFs/Al composites without formation of Al_4C_3 and with high strengthening ratio.

Web URL: ***http://www.sciencedirect.com/science/article/pii/S0921509317307906***

13. Hussain, M., Akhter, P., Iqbal, J., Ali, Z., Yang, W., Shehzad, N., ... & Russo, N. (2017). VOCs photocatalytic abatement using nanostructured titania-silica catalysts. ***Journal of Environmental Chemical Engineering*****.**

ABSTRACT:

In this work, different quantities of TiO_2 incorporated into TiO_2-KIT6 nanostructured catalysts were considered to improve the photocatalytic abatement of volatile organic compounds (VOCs; ethylene, propylene) at ambient temperature. The best optimized activity and stability of the catalysts toward(s) ethylene and propylene degradation has been shown for 30 wt% TiO_2, while the worst conversion has been observed for a 90 wt% TiO_2 loading. This was likely due to the dispersion and stabilization of the anatase TiO_2 with 30 wt% on KIT-6, which in turn allowed more VOCs adsorption and better light penetration than 90% TiO_2/KIT-6 in which it showed a bulk phase and large agglomerates with light penetration limitations. VOC abatement has been found to be not only influenced directly by the dispersed TiO_2 contents but also by the calcination temperatures, and 500 °C has been found to be the best calcination condition to achieve the highest propylene conversion. The optimized nanostructured photocatalyst developed for ethylene and propylene, could also be promising candidate for other VOCs and different applications.

Web URL: ***http://www.sciencedirect.com/science/article/pii/S2213343717302646***

14. Majeed, K., Hassan, A., & Abu Bakar, A. (2015). Barrier, Biodegradation, and mechanical properties of (Rice husk)/(Montmorillonite) hybrid filler-filled low-density polyethylene nanocomposite films. *Journal of Vinyl and Additive Technology*.

ABSTRACT:

Rice husk (RH)/montmorillonite (MMT) hybrid filler-filled low-density polyethylene nanocomposite films were prepared by extrusion blown film. RH was used as a biodegradable filler in various concentrations (2, 5, and 7 parts per hundred composite), while the amount of MMT was held constant at 2 wt%. Delamination of MMT platelets and distribution of RH were investigated by X-ray diffraction and scanning electron microscopy. Diffractograms revealed the formation of intercalated structures, regardless of the RH content. Barrier properties revealed that MMT platelets have the potential to retard the diffusion of permeating molecules while, on the other hand, barrier efficiency of MMT is balanced by the subsequent incorporation of RH in RH/MMT hybrid filler-filled composite films. Despite an increase in permeability, the selectivity ratio (CO_2/O_2 permeability) increased with increasing RH contents in the hybrid filler-filled composite films showing the potential of these films in the development of modified atmosphere for fresh fruits and vegetables. The colonization of fungus and formation of holes as observed in micrographs of the test samples subjected to soil burial revealed that the biodegradation rate increased with the incorporation of RH in the hybrid composites. The composite films with higher contents of RH in hybrid filler are also more biodegradable than those having lower contents. Addition of RH contents in the hybrid filler increased the tensile modulus, while decreasing the tensile and tear strength. Addition of RH in the hybrid filler increased the melting and crystallization temperatures of the resulting nanocomposite films as well

Web URL: ***http://onlinelibrary.wiley.com/doi/10.1002/vnl.21499/full***

15. Jamshaid, A., Hamid, A., Muhammad, N., Naseer, A., Ghauri, M., Iqbal, J., ... & Shah, N. S. (2017). Cellulose-based Materials for the Removal of Heavy Metals from Wastewater–An Overview. *ChemBioEng Reviews*.

ABSTRACT:

Water pollution due to increase in population and high rates of wastewater generation have become serious concerns since the last few decades. Heavy metals are amongst the main wastewater pollutants due to their ability to persist in the environment. Materials and techniques are being investigated for the treatment of heavy metals in wastewater. Cellulose is one of the materials gaining attention due to its excellent physical, chemical, and mechanical properties. Cellulose-based materials are being widely studied for the adsorption of heavy metals. This overview highlights research efforts to enhance the role of cellulose in wastewater treatment through cellulose-based materials. It also discusses the effects of cellulose modifications such as cellulose gels, cellulose composites, cellulose derivatives, functionalized cellulose, and nanocrystalline cellulose on the capacity of heavy metals adsorption.

Web URL: ***http://onlinelibrary.wiley.com/doi/10.1002/cben.201700002/full***

16. Ur Rehman, R., Rafiq, S., Muhammad, N., Khan, A. L., Ur Rehman, A., TingTing, L., ... & Gu, X. (2017). Development of ethanolamine-based ionic liquid membranes for efficient CO2/CH4 separation. ***Journal of Applied Polymer Science*****,** ***134*****(44).**

ABSTRACT:

This study is focused on the development of ionic liquids (ILs) based polymeric membranes for the separation of carbon dioxide (CO2) from methane (CH4). The advantage of ILs in selective CO2 absorption is that it enhances the CO2 selective separation for the ionic liquid membranes (ILMs). ILMs are developed and characterized with two different ILs using the solution-casting method. Three different blend compositions of ILs and polysulfone (PSF) are selected for each ILMs 10, 20, and 30 wt %. Effect of the different types of ILs such as triethanolamine formate (TEAF) and triethanolamine acetate (TEAA) are investigated on PSF-based ILMs. Field emission scanning electron microscopy analysis of the membranes showed reasonable homogeneity between the ILs and PSF. Thermogravimetric analysis showed that by increasing the ILs loading thermal stability of the membranes improved. Mechanical analysis on developed membranes showed that ILs phase reduced the amount of plastic flow of the PSF phase and therefore, fracture takes place at gradually lower strains with increasing ILs content. Gas permeation evaluation was carried out on the developed membranes for CO2/CH4 separation between 2

bar to 10 bar feed pressure. Results showed that CO2 permeance increases with the addition of ILs 10–30 wt % in ILMs. With 20–30 wt % TEAF-ILMs and TEAA-ILMs, the highest selectivity of a CO2/CH4 53.96 6 0.3, 37.64 6 0.2 and CO2 permeance 69.5 6 0.6, 55.21 6 0.3 is observed for treated membrane at 2–10 bar. The selectivity using mixed gas test at various CO2/CH4 compositions shows consistent results with the ideal gas selectivity.

Web URL:

https://www.researchgate.net/profile/Rashid_Rehman4/publication/317343847_Development_of_ethanol_amine_based_ionic_liquid_membranes_for_efficient_CO2CH4_separation/links/5983560daca272a947c72828/Development-of-ethanol-amine-based-ionic-liquid-membranes-for-efficient-CO2-CH4-separation.pdf

17. Ghauri, M., Shahzad, K., Khurram, M. S., Jaffery, M. H., Ali, N., Khan, W. A., & Cliffe, K. R. (2017). Development of a Temperature Programmed Identification Technique to Characterize the Organic Sulphur Functional Groups in Coal. *Energies*, *10*(6), 782.

ABSTRACT:

The Temperature Programmed Reduction (TPR) technique is employed for the characterisation of various organic sulphur functional groups in coal. The TPR technique is modified into the Temperature Programmed Identification technique to investigate whether this method can detect various functional groups corresponding to their reduction temperatures. Ollerton, Harworth, Silverdale, Prince of Wales coal and Mequinenza lignite were chosen for this study. High pressure oxydesulphurisation of the coal samples was also done. The characterization of various organic sulphur functional groups present in untreated and treated coal by the TPR method and later by the TPI method confirmed that these methods can identify the organic sulphur groups in coal and that the results based on total sulphur are comparable with those provided by standard analytical techniques. The analysis of the untreated and treated coal samples showed that the structural changes in the organic sulphur matrix due to a reaction can be determined.

Web URL: **http://www.mdpi.com/1996-1073/10/6/782/htm**

18. Usman, M., Akhtar, J., & Iqbal, J. (2017). Adsorption of Gold onto γ-aminopropyltriethoxysilane Grafted Coconut Pith. ***Journal of the Chemical Society of Pakistan*****,** ***39*****(6).**

ABSTRACT:

This study was carried out to investigate adsorption kinetic and adsorption thermodynamics of Au(III) ions onto γ-aminopropyltriethoxysilane grafted coconut pith. The results from equilibrium adsorption were fitted in various adsorption isotherm models such as Langmuir, Freundlich, Temkin and Dubinin-Radushkevich and the best fit for the experimental data was Langmuir isotherm. The maximum adsorption capacity for virgin coconut pith (VCP) and the grafted coconut pith (GCP) were 256.41 and 285.59 mg/g, respectively. The kinetic data was verified using pseudo-first-order, pseudo-second-order, elovich equation and intraparticle diffusion model. The correlation results suggested that the pseudo-second-order model fits the experimental data well. A thermodynamic study revealed the endothermic nature of reaction due to positive enthalpy (ΔH°) values and negative values of Gibbs free energy (ΔG°) describes the spontaneity of adsorption process. The regenerability of VCP and GCP adsorbents were investigated with NaOH (1.0 M).

Web URL:

http://web.a.ebscohost.com/abstract?direct=true&profile=ehost&scope=site&authtype=crawler&jrnl=02535106&AN=127027261&h=Ehsb65mD17hTMnHscaOLbpNJ%2f6JzQvvFHFA55hmnf9t7%2btsTNMXlMK1trA6vdZ0imrYoMqkBWdtOYUy2a7nanA%3d%3d&crl=c&resultNs=AdminWebAuth&resultLocal=ErrCrlNotAuth&crlhashurl=login.aspx%3fdirect%3dtrue%26profile%3dehost%26scope%3dsite%26authtype%3dcrawler%26jrnl%3d02535106%26AN%3d127027261

19. Liu, Y., Rehman, F., & Zimmerman, W. B. (2017). Reaction engineering of carbon monoxide generation by treatment with atmospheric pressure, low power CO2 DBD plasma. ***Fuel*****,** ***209*****, 117-126.**

ABSTRACT:

One of the greatest challenges faced by humanity is the changing global environmental trends. Evidence points out to the increased greenhouse gas emission by humans as the main cause.

One of the possible solutions to reduce CO2 emissions is to produce value added products or the precursors which can be used as the feedstock for the former. In the current study CO2 is converted to CO by dielectric barrier discharge (DBD)-corona hybrid plasma treatment while maintaining low power consumption. The kinetics of CO formation by CO2 plasmolysis is studied and analysed in detail. A well mixed system kinetics model has been proposed to estimate the reaction time for the experimental studies. Optical emission spectroscopy has been used to study CO2 plasma and mixtures of CO2/N2, CO2/water vapour and CO2/Ar plasma. A parametric study varying length of electrode, voltage, frequency, CO2 flow rate and pressure in plasma chamber is conducted. CO formation was found to be favoured at 600 mL/min flow rate, 1 atm pressure, 4.8 kV voltage at 40 kHz of frequency with 9 cm electrode.

Web URL: **https://www.sciencedirect.com/science/article/pii/S0016236117309596**

20. Yang, W., Chen, G., Wang, P., Qiao, J., Hu, F., Liu, S., ... & Wu, G. (2017). Enhanced thermal conductivity in Diamond/Aluminum composites with tungsten coatings on diamond particles prepared by magnetron sputtering method. ***Journal of Alloys and Compounds*****,** ***726*****, 623-631.**

ABSTRACT:

In the present work, tungsten (W) coatings with thickness range of 35e130 nm on the diamond particles were prepared by magnetron sputtering method, and then the Diamond/Al composites were prepared by the vacuum infiltration method. The prepared W coatings were smooth and dense on all the facets of the diamond particles. Moreover, the presence of W-coatings inhibited the interfacial debonding phenomenon and improved the interfacial bonding between diamond particles and Al matrix. The Diamond/Al composite with the 45 nm W-coating achieved the maximum thermal conductivity (622 W/(m$K)). To the best of our knowledge, it is the highest thermal conductivity obtained in the Al matrix composites reinforced with 100 mm diamond particles with coatings. Based on the Hasselman and Johnson (H-J) model, the thermal conductivity behavior of the Diamond/Al composites has been discussed. It indicates that the magnetron sputtering is a feasible and successful method to prepare thin and reliable tungsten coatings for the Diamond/Al composites.

Web URL: **https://www.sciencedirect.com/science/article/pii/S0925838817327834**

21. Ashfaq, M., Noor, N., Saif-Ur-Rehman, M., Sun, Q., Mustafa, G., Faizan Nazar, M., & Yu, C. P. (2017). Determination of Commonly used pharmaceuticals in Hospital waste of Pakistan and evaluation of their ecological risk assessment. *CLEAN–Soil, Air, Water*, *45*(6).

ABSTRACT:

In this study, six human pharmaceuticals in wastewater, sediments, and solid waste samples of five hospitals in Gujrat, Pakistan, were detected by a validated high performance liquid chromatography-ultraviolet method and then their ecological risk assessment was conducted. The pharmaceuticals include paracetamol, naproxen, diclofenac, ibuprofen, amlodipine, and rosuvastatin and were chromatographed on a C-18 column at 254 nm using liquid–liquid extraction. The highest concentration obtained was of paracetamol and it was also detected in all the five hospitals and all the sample matrices (max. 696 ng/mL) whereas, the concentration of other pharmaceuticals were also very high although they were not detected in all the sample matrices. Maximum concentrations of other pharmaceuticals detected were naproxen (220 ng/mL), diclofenac (186 ng/mL), ibuprofen (596 ng/mL), amlodipine (303 ng/mL), and rosuvastatin (104 ng/mL). Risk assessment in terms of risk quotient (RQ) was also calculated based on maximum measured concentration and the RQ values were very high for all pharmaceuticals. The maximum RQ values obtained from different pharmaceuticals were paracetamol (696 against daphnia), naproxen (84 against fish), diclofenac (9300 against O*ncorhynchus mykiss*), ibuprofen (16 000 against *Oryzias latipes*), and amlodipine (471 against green algae). The results from this study demand for comprehensive monitoring of pharmaceuticals from different points sources and treatment of all type of wastes including hospital waste.

Web URL: **http://onlinelibrary.wiley.com/doi/10.1002/clen.201500392/full**

22. Waqas, H., Shan, A., Khan, Y. G., Nawaz, R., Rizwan, M., Saif-Ur-Rehman, M., ... & Jabeen, M. (2017). Human health risk assessment of arsenic in groundwater aquifers of Lahore, Pakistan. *Human and Ecological Risk Assessment: An International Journal*, 1-15.

ABSTRACT:

The present study was conducted to estimate As concentration in groundwater and resulting human health risk in terms of chronic daily intake, hazard quotient (HQ), hazard index (HI), and carcinogenic risk (CR) both for oral and dermal exposure to As. Groundwater samples (*n* = 100) were collected from ten different towns of Lahore District (Pakistan). Arsenic concentration ranged from 2 to 111 µg L^{-1} in groundwater samples of the study area, which was significantly greater than the safe limit of As (10 µg L^{-1}) in drinking water set by the World Health Organization. Health risk assessment of As showed that HQ (0.1–11) for oral exposure and HI (0.1–11) values also exceeded the typical toxic risk index value of 1. 9.75 × E-05–4.59 × E-03 and 5.89 × E-07–2.77 × E-05 for oral and dermal As exposure, respectively. Both CR and cancer index (CIs) values were higher than United States Environmental Protection Agency limit (10^{-6}), suggesting that people are at high risk of As-induced carcinogenicity from oral and dermal exposure to As in drinking water. It was concluded that As contamination of groundwater causes carcinogenic and noncarcinogenic health effects to the people; therefore, urgent management and remedial actions are required to protect people from As poisoning.

Web URL: **http://www.tandfonline.com/doi/abs/10.1080/10807039.2017.1288561**

23. Ahmed, M. A., Rehman, M. S. U., Terán-Hilares, R., Khalid, S., & Han, J. I. (2017). Optimization of twin gear-based pretreatment of rice straw for bioethanol production. *Energy Conversion and Management*, *141*, 120-125.

ABSTRACT:

A laboratory twin-gear reactor (TGR) was investigated as a new means for the pretreatment of high solid lignocelluloses. Response surface methodology based on Box Behnken Design was used to optimize the enzymatic digestibility with respect to the pretreatment process variables: temperature of 50–90 C, NaOH concentration of 2–6% and no. of cycles of 30–60. The results revealed that the TGR-based pretreatment led to the significant structural alterations through increases in pore size, pore volume, cellulose crystallinity and surface area. SEM images also confirmed the surface modifications in the pretreated rice straw. A response surface quadratic model predicted 90% of the enzymatic digestibility, and it was confirmed experimentally and

through the analysis of variance (ANOVA) as well. The TGR extrusion proved to be an effective means for exceedingly high solids lignocellulose.

Web URL: **http://www.sciencedirect.com/science/article/pii/S0196890416305015**

24. Ashfaq, M., Khan, K. N., Rehman, M. S. U., Mustafa, G., Nazar, M. F., Sun, Q., ... & Yu, C. P. (2017). Ecological risk assessment of pharmaceuticals in the receiving environment of pharmaceutical wastewater in Pakistan. *Ecotoxicology and environmental safety*, *136*, 31-39.

ABSTRACT:

The pharmaceutical industry of Pakistan is growing with an annual growth rate of 10%. Besides this growth, this industry is not complying with environmental standards, and discharging its effluent into domestic wastewater network. Only limited information is available about the occurrence of pharmaceutical compounds (PCs) in the environmental matrices of Pakistan that has motivated us to aim at the occurrence and ecological risk assessment of 11 PCs of different therapeutic classes in the wastewater of pharmaceutical industry and in its receiving environmental matrices such as sludge, solid waste and soil samples near the pharmaceutical formulation units along Shiekhupura road, Lahore, Pakistan. Target PCs (paracetamol, naproxen, diclofenac, ibuprofen, amlodipine, rosuvastatin, ofloxacin, ciprofloxacin, moxifloxacin, sparfloxacin and gemifloxacin) were quantified using in-house developed HPLC-UV. Ibuprofen (1673 μg/L, 6046 μg/kg, 1229 μg/kg and 610 μg/kg), diclofenac (836 μg/L, 4968 μg/kg, 6632 μg/kg and 257 μg/kg) and naproxen (464 μg/L, 7273 μg/kg, 4819 μg/ kg and 199 μg/kg) showed the highest concentrations among 11 target PCs in wastewater, sludge, solid waste and soil samples, respectively. Ecological risk assessment, in terms of risk quotient (RQ), was also carried out based on the maximum measured concentration of PCs in wastewater. The maximum RQ values obtained were with paracetamol (64 against daphnia), naproxen (177 against fish), diclofenac (12,600 against Oncorhynchus mykiss), ibuprofen (167,300 against Oryzias latipes), ofloxacin (81,000 against Pseudomonas putida) and ciprofloxacin (440 against Microcystis aeruginosa). These results show a high level of ecological risk due to the discharge of untreated wastewater from pharmaceutical units. This risk may further lead to food web contamination and drug resistance in pathogens. Thus, further studies are needed to detect the

PCs in crops as well as the government should strictly enforce environmental legislation on these pharmaceutical units.

Web URL: **http://www.sciencedirect.com/science/article/pii/S014765131630433X**

25. Park, S., Yasin, M., Jeong, J., Cha, M., Kang, H., Jang, N., ... & Chang, I. S. (2017). Acetate-assisted increase of butyrate production by Eubacterium limosum KIST612 during carbon monoxide fermentation. *Bioresource technology*, *245*, 560-566.

ABSTRACT:

The acetate-assisted cultivation of Eubacterium limosum KIST612 was found to provide a way for enhancing cell mass, the carbon monoxide (CO) consumption rate, and butyrate production using CO as an electron and energy source. Cell growth (146%), μmax (121%), and CO consumption rates (151%) increased significantly upon the addition of 30 mM acetate to microbial cultures. The main product of CO fermentation by E. limosum KIST612 shifted from acetate to butyrate in the presence of acetate, and 5.72 mM butyrate was produced at the end of the reaction. The resting cell experimental conditions indicated acetate uptake and an increase in the butyrate concentration. Three routes to acetate assimilation and energy conservation were suggested based on given experimental results and previously genome sequencing data. Acetate assimilation via propionate CoAtransferase (PCT) was expected to produce 1.5 mol ATP/mol butyrate, and was thus anticipated to be the most preferred route.

Web URL: **https://www.sciencedirect.com/science/article/pii/S0960852417314463**

26. Ilyas, A., Muhammad, N., Gilani, M. A., Ayub, K., Vankelecom, I. F., & Khan, A. L. (2017). Supported protic ionic liquid membrane based on 3-(trimethoxysilyl) propan-1-aminium acetate for the highly selective separation of CO2. *Journal of Membrane Science*, *543*, 301-309.

ABSTRACT:

The ability to tailor ionic liquids can result in very high separation efficiency for CO2/CH4 and CO2/N2. In this study, a new protic ionic liquid was synthesized with high CO2 absorption capacity employing (3-aminopropyl) trimethoxysilane and acetic acid, both of these have been

reported to exhibit high affinity for CO2. The synthesized ionic liquid was characterized by FTIR and the supported ionic liquid membrane was tested to determine the separation of CO2 from CH4. Experiments were conducted at different temperatures and feed conditions, and pure and mixed gas permeability/selectivity data were reported. This combination of silyl ether functionalized cation and acetate ion dramatically improved the membrane separation performance as the SILM displayed CO2 permeance of 23 GPU combined with CO2/CH4 selectivity of 41. The synthesized SILM was stable upto 10 bar as no leaching of ionic liquid was observed and the permeance increased from 23 to 31 GPU as the temperature was raised from 25 °C to 65 °C, while the selectivity slightly 2 decreased from 41 to 35 over the same temperature range. The exceptionally high selectivity of CO2/CH4 makes [APTMS][Ac] a promising room temperature ionic liquid for CO2 separation without facilitated transport. A synergistic effect of methoxy groups from [APTMS] part of the ionic liquid caused the enhanced permeability of CO2 as supported by theoretical calculations.

Web URL: **https://www.sciencedirect.com/science/article/pii/S0376738817314023**

27. Shahid, M. Z., Usman, M. R., Akram, M. S., Khawaja, S. Y., & Afzal, W. (2017). Initial Interfacial Tension for Various Organic–Water Systems and Study of the Effect of Solute Concentration and Temperature. ***Journal of Chemical & Engineering Data*****,** ***62*****(4), 1198-1203.**

ABSTRACT:

Interfacial tension is an important thermophysical property for operations involving multifluid phases such as liquid–liquid extraction. This work aims at presenting a rapid experimental method and initial interfacial tension data of nine organic compounds and water binary systems. The organic compounds include *n*-butyl acetate, cyclohexanol, cyclohexanone, diethyl ether, ethyl acetate, methyl ethyl ketone, methylcyclohexane, 1-octanol, and toluene. The effect of temperature on the initial interfacial tension was also studied. These systems are chosen to cover a wide range of interfacial tension (1–51 mN/m). Comparisons between the data sets from this work and those from the literature, whenever available, show generally very good agreement. This work also presents new data of initial interfacial tension for several ternary systems with four organic compounds and water with varying quantities of propionic

acid or propanoic (0–0.25 mass fraction) at ambient conditions; the organic compounds include *n*-butyl acetate, cyclohexanone, 1-octanol, and toluene. The results show that the impact of propionic acid concentration as solute in water is large, especially at the higher solute concentrations. The initial and final (mutually saturated phases) interfacial tensions are found in agreement for different immiscible binary systems studied in this work. The method presented may be used as a rapid way of finding interfacial tensions.

Web URL: **http://pubs.acs.org/doi/abs/10.1021/acs.jced.6b00703**

28. Khawaja, S. Y., Usman, M. R., Nasif, M., Akram, M. S., Afzal, W., & Akhtar, N. A. (2017). Mass transfer efficiency of a tall and low plate free area liquid pulsed sieve-plate extraction column. *International Journal of Industrial Chemistry*, *8*(4), 397-410.

ABSTRACT:

Mass transfer performance is studied in a tall, thin, and low plate free area liquid pulsed sieve-plate extraction column. The 5.0 cm internal diameter column consists of eighty sieve plates with percent free area of only 13.5. The effects of pulsation intensity (product of amplitude and frequency) and dispersed phase velocity are studied on the extraction efficiency of the column for the acetic acid–kerosene–water system. A mass transfer correlation for the measurement of overall mass transfer coefficient is developed that best-fits the experimental data obtained in the present study. Mathematical analysis of the column is carried out that shows the insignificance of axial diffusivities in the column.

Web URL: **https://link.springer.com/article/10.1007/s40090-017-0129-9**

29. Inayat, A., Ahmad, M. M., Mutalib, M. A., Yusup, S., & Khan, Z. (2017). Economic analysis and optimization for bio-hydrogen production from oil palm waste via steam gasification. *Energy Sources, Part B: Economics, Planning, and Policy*, *12*(2), 158-165.

ABSTRACT:

Biomass steam gasification with in situ carbon dioxide capture using CaO exhibits good prospects for the production of hydrogen-rich gas. In Malaysia, due to abundance of palm waste, it is a good candidate to be used as a feedstock for hydrogen production. The present

work focuses on the mathematical modeling of detailed economic analysis and cost minimization of the flow sheet design for hydrogen production from palm waste using MATLAB. The influence of the operating parameters on the economics is studied. It is predicted that hydrogen cost decreases by increasing both temperature and steam/biomass ratio. Meanwhile, the hydrogen cost increases when increasing sorbent/biomass ratio. Cost minimization solves to give optimum cost of 1.9105 USD/kg with hydrogen purity, hydrogen yield, hydrogen efficiency, and thermodynamic efficiency are 79.9 mol%, 17.97 g/h, 81.47%, and 79.85%, respectively. The results indicate that this system has the potential to offer low production cost for hydrogen production from palm waste.

Web URL: **http://www.tandfonline.com/doi/abs/10.1080/15567249.2014.937881**

30. Khan, Z., Yusup, S., & Watson, I. (2017). Assessment of Energy Flows in Integrated Catalytic Adsorption (ICA) Steam Gasification for Hydrogen Production.

ABSTRACT:

Biomass has a potential to produce sustainable and renewable hydrogen due to its low sulphur and nitrogen content (low NOx and SOx emissions) and contributes towards net CO2 cycle. Biomass steam gasification is found to be most promising among thermal conservation processes for renewable hydrogen production. The energy required for gasification using steam is high compared to other gasification agents e.g. air or pure oxygen. The integrated catalytic adsorption (ICA) utilizes catalyst and CO2 adsorbent together in the single fluidized bed gasifier. The present study investigates the energy flows to optimize the gasification energy requirement with respect to hydrogen concentration and yield in the ICA process at 600, 650 and 750 °C. The overall gasification energy required increased with increasing gasification temperature from 675 to 750 °C. However, a slight reduction in required energy was observed from 600 °C to 675 °C which might be due to strong CO2 adsorption, an exothermic reaction, and contributes to the energy requirements of the process. This was further verified with zero CO2 and highest hydrogen compositions (82 vol%) at 675 °C. However, ICA steam gasification is found to be a high energy consuming process and heat integration has to be considered for an economical hydrogen generation process.

Web URL:

https://www.sciencedirect.com/science/article/pii/S1876610217363671/pdf?md5=b0178c90ed5386d27e8ed09d0981ec91&pid=1-s2.0-S1876610217363671-main.pdf&_valck=1

31. Capper, S., Khan, Z., Kamble, P., Sharp, J., & Watson, I. (2017). Progression towards Online Tar Detection Systems. *Energy Procedia*, *142*, 892-897.

ABSTRACT:

The most prohibitive aspect with the commercialisation of biomass gasification technology is tar fouling of the product gas. The presence of tar impacts the efficiency of gasification systems and compromises gas quality, rendering it less useful for some downstream applications sensitive to gas quality. Various tar detection methods are reported in the literature which can be differentiated into offline and online techniques. However, offline techniques are found to be time consuming, expansive and require sufficient instrumentation and knowledge to achieve reliable results. Recent advances in online tar detection based on spectral information of individual tar component have attracted much research attention. Among these, fluorescence spectroscopy is a highly promising technique for the provision of distinctive, non-invasive and real time data collection for tar levels which can be easily installed on gasification product gas streams. This paper presents the initial work on developing a low cost tar detection system based on LED induced fluorescence. The detection system mainly consists of a photomultiplier tube (PMT), LED (emission wavelength of 280 nm) and 300 nm longpass colour glass filter. Initial experiments have been carried out with different concentrations (0 to 100 wt%) of phenol (used as a model tar compound) and bio-oil samples from an in-house, downdraft (throated) fixed bed gasification system. The results show a linear increase of fluorescence with phenol and the gasifier bio-oil at different concentrations.

Web URL: https://www.sciencedirect.com/science/article/pii/S187661021735871X

32. Kamble, P., Khan, Z., Capper, S., Sharp, J., & Watson, I. (2017). Improving Downdraft Gasifier Stability by Robust Instrumentation and Control Systems.

ABSTRACT:

Not Found

Web URL:

33. Farooq, A., Khurram, M. S., Rafiq, S., Memon, S. A., Ghauri, M., Shahzad, K., ... & Muhammad, N. (2017). Biomass gasification for energy generation: parametric investigation on continuous updraft Gasifier. *Journal of Engineering Technology*. 6

ABSTRACT:

Biomass has gained inevitable importance as a distributed source of energy after coal, oil and natural gas. The gasification is one of the cleaner technology to convert biomass into environmental friendly gaseous fuel. An updraft gasifier was designed and experiments were carried out using mustard seed(s) as feed. It was observed that the temperature distribution improved using circulation. The temperature achieved lied in the range of 600oC-800oC with and without circulation. Increasing the temperature from 400oC- 800oC and equivalence ratio (ER) from 0.15-0.3, increases the amount of H2/CO from 0.29-2.67; whereas in the case of circulation it decreases from 0.65-0.41. The CO2 produced is 70% with circulation and 50% without circulation. Increasing temperature reduces the fluctuating amount of NOx from 1976 ppm to573 ppm under normal conditions. While SO2 is 229 ppm without circulation and is almost zero for circulation. At the optimum ER value of 0.23, maximum value of lower heating value (LHV) and higher heating value (HHV) without circulation were observed to be 7743 Btu/lb and 8995 Btu/lb respectively while 3801 Btu/lb and 4397 Btu/lb with circulation.

Web URL:

https://www.researchgate.net/profile/Abid_Farooq/publication/321096407_Biomass_gasification_for_energy_generation_parametric_investigation_on_continuous_updraft_Gasifier/links/5a0d103fa6fdcc39e9bfbec0/Biomass-gasification-for-energy-generation-parametric-investigation-on-continuous-updraft-Gasifier.pdf

34. Sultan, T., Ahmad, Z., Anwar, Z., & Khurram, M. S. (2017). Impact of asymmetric lamp positioning on the performance of a closed-conduit UV reactor. *Ain Shams Engineering Journal*.

ABSTRACT:

Computational fluid dynamics (CFD) analyses for the performance improvement of a closed-conduit ultraviolet (UV) reactor were performed by changing the lamp positions from symmetric to asymmetric. The asymmetric lamp positioning can be useful for UV reactor design and optimization. This goal was achieved by incorporating the two performance factors, namely reduction equivalent dose (RED) and system dose performance. Four cases were carried out for asymmetric lamp positioning within the UV reactor chamber and each case consisted of four UV lamps that were simulated once symmetrically and four times asymmetrically. The results of the four asymmetric cases were compared with the symmetric one. Moreover, these results were evaluated by using CFD simulations of a closed-conduit UV reactor. The fluence rate model, UVCalc3D was employed to validate the simulations results. The simulation results provide detailed information about the dose distribution, pathogen track modeling and RED. The RED value was increased by approximately 15% by using UVCalc3D fluence rate model. Additionally, the asymmetric lamp positioning of the UV lamps had more than 50% of the pathogens received a better and a higher UV dose than in the symmetric case. Consequently, the system dose performance was improved by asymmetric lamp positioning. It was concluded that the performance parameters (higher RED and system dose performance) were improved by using asymmetric lamp positioning.

Web URL: **http://www.sciencedirect.com/science/article/pii/S2090447917300230**

DEPARTMENT OF MATHEMATICS

Journal Papers

1. Nazar, K., Murid, A. H., & Sangawi, A. W. (2017, January). The computation of zeros of Ahlfors map for multiply connected regions. In *AIP Conference Proceedings* (Vol. 1795, No. 1, p. 020003). AIP Publishing.

ABSTRACT:

The relation between the Ahlfors map and Szegö kernel $S(z, a)$ is classical. The Szegö kernel is a solution of a Fredholm integral equation of the second kind with the Kerzman-Stein kernel. The exact zeros of the Ahlfors map are known for a particular family of doubly connected regions and a particular triply connected region. This paper presents a numerical method for computing the zeros of the Ahlfors map of any bounded multiply connected regions with smooth boundaries. The method depends on the values of $S(z(t), a)$, $S'(z(t), a)$ and $\vartheta'(t)$, where $\vartheta(t)$ is the boundary correspondence function of Ahlfors map. A formula is derived for computing $S'(z(t), a)$. An integral equation for $\vartheta'(t)$ is used for finding the zeros of Ahlfors map. The numerical examples presented here demonstrate the method.

Web URL: **http://aip.scitation.org/doi/pdf/10.1063/1.4972147**

2. Islam, W., Younis, M., & Rizvi, S. T. R. (2017). Optical solitons with time fractional nonlinear Schrödinger equation and competing weakly nonlocal nonlinearity. *Optik-International Journal for Light and Electron Optics*, *130*, 562-567.

ABSTRACT:

The optical solitons have been extracted from the model that describes the dynamics of solitons in nonlinear optics with competing weakly nonlocal nonlinearity. The diffraction coefficient and parabolic law nonlinearity are also consider in this time fractional model. The constraint conditions, for the existence of the dark and singular soliton solutions, are also listed. Additionally, a couple of other solutions known as singular periodic solutions, fall out as a by-product of this scheme.

Web URL: ***http://www.sciencedirect.com/science/article/pii/S0030402616312797***

3. Rizvi, S. T. R., Bashir, S., Ali, K., & Ahmad, S. (2017). Jacobian elliptic periodic traveling wave solutions for Biswas–Milovic equation. *Optik-International Journal for Light and Electron Optics*, *131*, 582-587.

ABSTRACT:

The Biswas–Milovic equation can also be treated as the generalized version of usual nonlinear Schrodinger's equation. With the help of *F*-expansion method, the explicit Jacobian elliptic periodic traveling wave solutions for Biswas–Milovic equations are constructed. Here we will discuss the two nonlinear media; those are Kerr law and the power law.

Web URL: ***http://www.sciencedirect.com/science/article/pii/S0030402616314668***

4. Sohail, A., Maqbool, K., Akbar, N. S., & Younas, M. (2017). Advanced Study of Unsteady Heat and Chemical Reaction with Ramped Wall and Slip Effect on a Viscous Fluid. *Communications in Theoretical Physics*, *67*(3), 301.

ABSTRACT:

This paper investigate the effect of slip boundary condition, thermal radiation, heat source, Dufour number, chemical reaction and viscous dissipation on heat and mass transfer of unsteady free convective MHD flow of a viscous fluid past through a vertical plate embedded in a porous media. Numerical results are obtained for solving the nonlinear governing momentum, energy and concentration equations with slip boundary condition, ramped wall temperature and ramped wall concentration on the surface of the vertical plate. The influence of emerging parameters on velocity, temperature and concentration fields are shown graphically.

Web URL:

http://159.226.161.111/EN/article/downloadArticleFile.do?attachType=PDF&id=16999

5. Rizvi, S. T. R., & Ali, K. (2017). Jacobian elliptic periodic traveling wave solutions in the negative-index materials. *Nonlinear Dynamics*, *87*(3), 1967-1972.

ABSTRACT:

The aim of this work is to present an analytical study on optical solitons in nonlinear negative-index materials. Three types of nonlinearities that are Kerr law, power law and parabolic law are taken into account. With the help of *F*-expansion method, the explicit Jacobian elliptic periodic traveling wave solutions are constructed.

Web URL: ***https://link.springer.com/article/10.1007/s11071-016-3166-6***

6. Mehmood, N., Agarwal, R. P., Butt, S. I., & Pečarić, J. (2017). New generalizations of Popoviciu-type inequalities via new Green's functions and Montgomery identity. ***Journal of Inequalities and Applications*****,** ***2017*****(1), 108.**

ABSTRACT:

The inequality of Popoviciu, which was improved by Vasić and Stanković (Math. Balk. 6:281-288, 1976), is generalized by using new identities involving new Green's functions. New generalizations of an improved Popoviciu inequality are obtained by using generalized Montgomery identity along with new Green's functions. As an application, we formulate the monotonicity of linear functionals constructed from the generalized identities, utilizing the recent theory of inequalities for n-convex functions at a point. New upper bounds of Grüss and Ostrowski type are also computed.

Web URL: ***https://link.springer.com/article/10.1186/s13660-017-1379-y***

7. Rizvi, S. T. R., Ali, K., Sardar, A., Younis, M., & Bekir, A. (2017). Symbolic computation and abundant travelling wave solutions to KdV–mKdV equation. ***Pramana*****,** ***88*****(1), 16.**

ABSTRACT:

In this article, the novel (G'/G)-expansion method is successfully applied to construct the abundant travelling wave solutions to the KdV–mKdV equation with the aid of symbolic computation. This equation is one of the most popular equation in soliton physics and appear in many practical scenarios like thermal pulse, wave propagation of bound particle, etc. The method is reliable and useful, and gives more general exact travelling wave solutions than the existing methods. The solutions obtained are in the form of hyperbolic, trigonometric and rational functions including solitary, singular and periodic solutions which have many potential applications in physical science and engineering. Many of these solutions are new and some have already been constructed. Additionally, the constraint conditions, for the existence of the solutions are also listed.

Web URL: ***https://link.springer.com/article/10.1007/s12043-016-1315-6***

8. Younis, M., ur Rehman, H., Rizvi, S. T. R., & Mahmood, S. A. (2017). Dark and singular optical solitons perturbation with fractional temporal evolution. *Superlattices and Microstructures*, *104*, 525-531.

ABSTRACT:

The article studies the dynamics of dark, singular, combined optical solitons and many other periodic solutions to fractional temporal perturbed nonlinear Schrödinger equation in nonlinear optics. The fractional extended Fan sub-equation method is first time used for any fractional temporal nonlinear Schrödinger equation. The solutions are of qualitatively different nature, depending on the five parameters. The constraint conditions, for the existence of the solitons, are also listed. Moreover a couple of other solutions known as combined soliton and combined periodic solution, fall out as a by product in limiting cases.

Web URL: ***http://www.sciencedirect.com/science/article/pii/S0749603616318924***

9. Ali, K., Rizvi, S. T. R., Ahmad, S., Bashir, S., & Younis, M. (2017). Bell and kink type soliton solutions in birefringent nano-fibers. *Optik-International Journal for Light and Electron Optics*.

ABSTRACT:

In this paper we have obtained the explicit Jacobian elliptic periodic traveling wave solutions in birefringent fibers with spatio-temporal dispersion with the help of *F*-expansion method. Two nonlinear media are used that are Kerr and parabolic law. There are constraint conditions that evolve with the solution structure.

Web URL: **http://www.sciencedirect.com/science/article/pii/S0030402617306812**

10. Imran, M., Baig, A. Q., Siddiqui, H. M. A., & Sarawar, R. (2017). On molecular topological properties of diamond like networks. *Canadian Journal of Chemistry*, (ja).

ABSTRACT:

The Randi´c (product) connectivity index and its derivative called the sum-connectivity index are well known topological indices and these both descriptors correlate well among themselves and with the π-electronic energies of benzenoid hydrocarbons. The general n-connectivity of a molecular graph G is defined as nχ(G)= X vi1 vi2 vi3 ...vin+1 1 p di1 di2 ...din+1 and the n-sum

connectivity of a molecular graph G is defined as nX(G) = X vi1 vi2 vi3 ...vin+1 1 p di1 + di2 + ... + din+1 , where the paths of length n in G are denoted by vi1 , vi2 ...vin+1 and the degree of each vertex vi is denoted by di. In this paper, we discuss third connectivity and third sum-connectivity indices of diamond like networks and compute analytical closed results of these indices for diamond like networks.

Web URL: ***https://tspace.library.utoronto.ca/bitstream/1807/77568/1/cjc-2017-0206.pdf***

11. Abbas, G., Khan, M. S., Ahmad, Z., & Zubair, M. (2017). Higher-dimensional inhomogeneous perfect fluid collapse in f (R) gravity. ***The European Physical Journal C*****, *77*(7), 443.**

ABSTRACT:

This paper is about the *[Math Processing Error]n+2*-dimensional gravitational contraction of an inhomogeneous fluid without heat flux in the framework of a *f*(*R*) metric theory of gravity. Matching conditions for two regions of a star are derived by using the Darmois junction conditions. For the analytic solution of the equations of motion in modified *f*(*R*) theory of gravity, we have taken the scalar curvature constant. Hence the final result of gravitational collapse in this framework is the existence of black hole and cosmological horizons, and both of these form earlier than the singularity. It is shown that a constant curvature term *[Math Processing Error]f(R0)* (*[Math Processing Error]R0* is the constant scalar curvature) slows down the collapsing process.

Web URL: **https://link.springer.com/article/10.1140/epjc/s10052-017-5003-6**

12. Siddiqui, A. M., Sohail, A., & Maqbool, K. (2017). Analysis of a channel and tube flow induced by cilia. ***Applied Mathematics and Computation*****, *309*, 133-141.**

ABSTRACT:

Power law metachronal wave motion, responsible for the cilia transport is investigated in this paper using numerical tools. The dynamical analysis is made in channel and in tube to demonstrate the quantitative effect of the geometry. Similarity transformations are employed to convert the governing partial differential equations into a set of coupled ordinary differential equations. A swift and accurate collocation algorithm is applied to the boundary value problem

(BVP) of coupled ordinary differential equations. A nondimensional graphical analysis of the waving amplitude is reported by varying the flow consistency and flow behavior indices.

Web URL: ***http://www.sciencedirect.com/science/article/pii/S0096300317302436***

13. Rizvi, S. T. R., Ali, K., Bashir, S., Younis, M., Ashraf, R., & Ahmad, M. O. (2017). Exact soliton of (2+ 1)-dimensional fractional Schrödinger equation. *Superlattices and Microstructures*, *107*, 234-239.

ABSTRACT:

The nonlinear fractional Schrödinger equation is the basic equation of fractional quantum mechanics introduced by Nick Laskin in 2002. We apply three tools to solve this mathematical-physical model. First, we find the solitary wave solutions including the trigonometric traveling wave solutions, bell and kink shape solitons using the *F*-expansion and Improve *F*-expansion method. We also obtain the soliton solution, singular soliton solutions, rational function solution and elliptic integral function solutions, with the help of the extended trial equation method.

Web URL: ***http://www.sciencedirect.com/science/article/pii/S074960361730770X***

14. Hassan, M., Zeeshan, A., Majeed, A., & Ellahi, R. (2017). Particle shape effects on ferrofuids flow and heat transfer under influence of low oscillating magnetic field. *Journal of Magnetism and Magnetic Materials*, *443*, 36-44.

ABSTRACT:

The purpose of this study is to theoretically examine nanoparticle shapes behavior on mass and heat flow of ferrofluid over a rotating disk with the presence of low oscillating magnetic field. Ferrofluid is prepared by water and iron nanoparticles of three different shapes like sphere, oblate ellipsoid and prolate ellipsoid. The problem has been formulated by employing the controllable force into the fundamental hydrodynamic equations and its effect along with particle shape factor on physical properties of fluid is discussed. These equations are converted into a system of ordinary differential equations by employing appropriate similarity approach and then solved by HAM based Bvph2 package. Effects of particle shape, particle volume

fraction and magnetization parameter on axial, radial and tangential velocities along with temperature profile are demonstrated through graphically. The results for local Nusselt number are calculated and analyzed and the path for enhancement in heat transfer is also proposed.

Web URL: ***https://www.sciencedirect.com/science/article/pii/S0304885317313367***

15. Rafiullah, M., & Jabeen, D. (2017). New Eighth and Sixteenth Order Iterative Methods to Solve Nonlinear Equations. ***International Journal of Applied and Computational Mathematics*****, *3*(3), 2467-2476.**

ABSTRACT:

In this work we proposed two new higher order iterative methods to solve nonlinear equations. These methods based on the method Rafiullah (Numer Anal Appl 4(3):239–243, 2011) which is fifth-order. The Lagrange interpolation is used to improve the convergence order and efficiency index of the method. Convergence order of new methods are proved analytically. Some test problems are given to show the efficiency of the proposed methods.

Web URL: ***https://link.springer.com/article/10.1007/s40819-016-0245-9***

16. Rizvi, S. T. R., Salim, S., Ali, K., & Younis, M. (2017). New Thirring optical solitons with vector-coupled Schrödinger equations in birefringent fibers. ***Waves in Random and Complex Media*****, *27*(2), 359-366.**

ABSTRACT:

The article studies the dynamics of Thirring optical solitons in birefrigent fibers with vector-coupled nonlinear Schrödinger equations. The G'/G-expansion scheme has been used to extract the dark and singular soliton solutions along with constraint conditions. It may also be noted that a couple of other solutions known as singular periodic solutions, fall out as a by-product of this scheme.

Web URL: ***http://www.tandfonline.com/doi/full/10.1080/17455030.2016.1246781***

17. Ashraf, R., Ahmad, M. O., Younis, M., Ali, K., & Rizvi, S. T. R. (2017). Dipole and Gausson soliton for ultrashort laser pulse with high order dispersion. *Superlattices and Microstructures*.

ABSTRACT:

In this paper, we find the dipole soliton (dark-in-the bright) for higher order nonlinear Schrödinger equation (HNLSE) with kerr law. This equation represents the propagation of a nonlinear ultrashort laser pulse in the optical fiber. We use the ansatz method of Choudhuri and Porsezian to find the solitary wave solution, which is combination of product of dark and bright solitary waves. We also find single Gausson soliton solution for (HNLSE) with log law nonlinearity described in optical nano fibers.

Web URL: ***http://www.sciencedirect.com/science/article/pii/S0749603617310868***

18. Rizvi, S. T. R., Ali, K., & Hussain, M. (2017). Cycle-supermagic labelings of the disjoint union of graphs. *Utilitas Mathematica*, *104*, 215-226.

ABSTRACT:

In this paper we formulate cycle-supermagic labelings for the disjoint union of isomorphic copies of different families of graphs. We also prove that disjoint union of non isomorphic copies of fans and ladders are cycle-supermagic.

Web URL: ***https://arxiv.org/abs/1506.06087***

19. Khalid, M., Rizvi, S. T. R., & Ali, K. (2017). Note on cycle-(super) magic labelings of disconnected graphs. *UTILITAS MATHEMATICA*, *104*, 315-320.

ABSTRACT: Not Found

Web URL:

20. Ahmad, U., Ahmad, S., & Yousaf, R. (2017). Computation of Zagreb and atom–bond connectivity indices of certain families of dendrimers by using automorphism group action. *J. Serb. Chem. Soc.*, *82*(2), 151-162.

ABSTRACT:

In QSAR/QSPR studies, topological indices are utilized to predict the bioactivity of chemical compounds. In this paper, the closed forms of different Zagreb indices and atom–bond connectivity indices of regular dendrimers $G[n]$ and $H[n]$ in terms of a given parameter n are determined by using the automorphism group action. It was reported that these connectivity indices are correlated with some physicochemical properties and are used to measure the level of branching of the molecular carbon-atom skeleton.

Web URL: **http://shd-pub.org.rs/index.php/JSCS/article/download/3398/416**

21. Jawad, A., Ilyas, A., & Ahmad, S. (2017). Shaft potential inspired warm inflation. ***International Journal of Geometric Methods in Modern Physics*****,** ***14*****(06), 1750088.**

ABSTRACT:

We discuss the warm inflation in the presence of shaft potential (V(φ)=M4pφ2n−2(φn+gn)2−2n)V(φ)=Mp4φ2n−2(φn+gn)2−2n, tachyon scalar field and the generalized form of dissipative coefficient Γ=a0Tqφq−1Γ=a0Tqφq−1. In this respect, we investigate the inflationary parameters (slow-roll parameters, number of e-folds, scalar-tensor power spectra, spectral indices, tensor-to-scalar ratio and running of scalar spectral index) in both strong and weak dissipative regimes. It is interesting to mention that our inflationary parametric results (tensor-scalar ratio, spectral index and running of spectral) are consistent with the recent observational data such as BICEP22, WMAP99 and latest Planck data.

Web URL:

http://www.worldscientific.com/doi/abs/10.1142/S0219887817500888?journalCode=ijgmmp

22. Younis, M., ur Rehman, H., Rizvi, S. T. R., & Mahmood, S. A. (2017). Dark and singular optical solitons perturbation with fractional temporal evolution. ***Superlattices and Microstructures*****,** ***104*****, 525-531.**

ABSTRACT:

The article studies the dynamics of dark, singular, combined optical solitons and many other periodic solutions to fractional temporal perturbed nonlinear Schr¨odinger equation in

nonlinear optics. The fractional extended Fan sub-equation method is first time used for any fractional temporal nonlinear Schr¨odinger equation. The solutions are of qualitatively different nature, depending on the five parameters. The constraint conditions, for the existence of the solitons, are also listed. Moreover a couple of other solutions known as combined soliton and combined periodic solution, fall out as a by product in limiting cases.

Web URL: **http://www.sciencedirect.com/science/article/pii/S0749603616318924**

23. Ashraf, S., Kerre, E. E., & Qayyum, M. (2017). THE INTUITIONISTIC FUZZY MULTI-CRITERIA DECISION MAKING BASED ON INCLUSION DEGREE. *COMPTES RENDUS DE L ACADEMIE BULGARE DES SCIENCES*, *70*(7), 925-934.

ABSTRACT:

Not Found

Web URL:

24. Rizvi, S. T. R., Ali, K., Salman, M., Nawaz, B., & Younis, M. (2017). Solitary wave solutions for quintic complex Ginzburg–Landau model. *Optik-International Journal for Light and Electron Optics*, *149*, 59-62.

ABSTRACT:

The article studies dark in the bright (dipole) soliton solutions and the solitary wave (Combo) solutions for Quintic complex Ginzburg-Landau model (CGLQ). The model is generated from cubic complex GinzburgLandau equation (CGLC), derived from nonlinear Schr¨odinger equation (NLSE). We use ansatz method of Li [21] to get combo soliton solutions for (CGLQ) model. To get the dipole soliton solution, we use the ansatz method of Choudhuri [20].

Web URL: **https://www.sciencedirect.com/science/article/pii/S0030402617310872**

25. Afzal, S. S., Younis, M., & Rizvi, S. T. R. (2017). Optical dark and dark-singular solitons with anti-cubic nonlinearity. *Optik-International Journal for Light and Electron Optics*, *147*, 27-31.

ABSTRACT:

This paper studies the dynamics of optical dark and dark-singular solitons for nonlinear Schr¨odinger equation under anti-cubic nonlinearity with extended direct algebraic method.

The constraint conditions for the existence of optical dark and dark-singular solitons are also listed. Additionally, a couple of other solutions known as singular periodic, fall out as a by-product of this scheme.

Web URL: **https://www.sciencedirect.com/science/article/pii/S0030402617309592**

26. Nawaz, B., Ali, K., Rizvi, S. T. R., & Younis, M. (2017). Soliton solutions for quintic complex Ginzburg-Landau model. ***Superlattices and Microstructures*****,** ***110*****, 49-56.**

ABSTRACT:

In this paper, we find the rational function solution, confluent hypergeometric functions solutions and solitary wave solutions for quintic complex Ginzburg-Landau (CGLQ) model by using extended trial equation method. We also find some new solitary wave soliton solutions for CGLQ equation by using modified extended tanh-function method.

Web URL: **https://www.sciencedirect.com/science/article/pii/S0749603617319559**

27. Imran, S., Hussain, M., Siddiqui, M. K., & Numan, M. (2017). Super face d-antimagic labeling for disjoint union of toroidal fullerenes. ***Journal of Mathematical Chemistry*****,** ***55*****(3), 849-863.**

ABSTRACT:

The discovery of the fullerene molecules and related forms of carbon such as nanotubes has generated an explosion of activity in chemistry, physics, and materials science. Classical fullerene is an all-carbon molecule in which the atoms are arranged on a pseudospherical framework made up entirely of pentagons and hexagons. A toroidal fullerene (toroidal polyhex) is a cubic bipartite graph embedded on the torus such that each face is a hexagon. In this paper we examine the existence of entire labeling, where face-weights of all 6-sided faces of disjoint union of toroidal fullerenes form an arithmetic progression with common difference d∈{1,2,3}d∈{1,2,3}.

Web URL: **https://link.springer.com/article/10.1007/s10910-016-0713-9**

28. Alolaiyan, H, Cheema, I. Z & Hussain, M. (2017). Magic labeling on line graph of different graphs. ***Journal of Computational and Theoretical Nanosciences. 14(12).***

ABSTRACT:

The aim of this paper is to investigate fan, friendship, ladder and wheel line graphs and to study the super magic and anti-supermagic vertex-edge-face labeling of such graphs and their isomorphic copies. An anti-supermagic labeling of the extension of cycle graphs is also formulated.

Web URL:

http://www.ingentaconnect.com/content/asp/jctn/2017/00000014/00000012/art00009

29. Mehmood, T., Mahmood, H., & Hussain, M. (2017). Edge Irregularity Strength of Multi Middle and Extended Prism Graphs. *Journal of Computational and Theoretical Nanoscience*, *14*(11), 5248-5252.

ABSTRACT:

Vertex labeling for simple graph G is a mapping $f: V(G) \rightarrow \{1, 2, 3, 4, \ldots, m\}$ called m-labeling. The weight of edge uv in graph G denoted by $W_t(uv)$ is sum of labels of end vertices u and v i.e., $W_t(uv) = f(u) + f(v)$. A vertex m-labeling is defined as an edge irregular m-labeling of graph G if for every two different edges a and b their weights are different i.e., $W_t(a) \neq W_t(b)$. The minimum m for which graph G has an edge irregular m-labeling is named as the edge irregularity strength of graph G denoted by $es(G)$. In this paper we estimate the bounds of the edge irregularity strength and calculate the accurate value for some families of graphs.

Web URL: http://www.ingentaconnect.com/content/asp/jctn/2017/00000014/00000011/art00014

30. SOHAIL, A., LI, Z. W., IFTIKHAR, M., MOHAMED, M., & BÉG, O. A. (2017). STOCHASTIC ANALYSIS OF A DETERMINISTIC AND SEASONALLY-FORCED SEI MODEL FOR IMPROVED DISEASE SPREAD SIMULATION. *Journal of Mechanics in Medicine and Biology*, 1750067.

ABSTRACT:

The geographic distribution of different viruses has developed widely, giving rise to an escalating number of cases during the past two decades. The deterministic Susceptible, Exposed, Infectious (SEI) models can demonstrate the spatio-temporal dynamics of the diseases

and have been used extensively in modern mathematical and mechano-biological simulations. This article presents a functional technique to model the stochastic effects and seasonal forcing in a reliable manner by satisfying the Lipschitz criteria. We have emphasized that the graphical portrayal can prove to be a powerful tool to demonstrate the stability analysis of the deterministic as well as the stochastic modeling. Emphasis is made on the dynamical effects of the force of infection. Such analysis based on the parametric sweep can prove to be helpful in predicting the disease spread in urban as well as rural areas and should be of interest to mathematical biosciences researchers.

Web URL:

http://www.worldscientific.com/doi/abs/10.1142/S0219519417500671?journalCode=jmmb

31. Javed, S., Hussain, M., Riasat, A., Kanwal, S., Imtiaz, M., & Ahmad, M. O. Deficiency of forests. *Open Mathematics*, *15*(1), 1431-1439.

ABSTRACT:

An edge-magic total labeling of an (n,m)-graph $G = (V,E)$ is a one to one map λ from $V(G) \cup E(G)$ onto the integers $\{1,2,\ldots,n+m\}$ with the property that there exists an integer constant c such that $\lambda(x) + \lambda(y) + \lambda(xy) = c$ for any $xy \in E(G)$. It is called super edge-magic total labeling if $\lambda(V(G)) = \{1,2,\ldots,n\}$. Furthermore, if G has no super edge-magic total labeling, then the minimum number of vertices added to G to have a super edge-magic total labeling, called super edge-magic deficiency of a graph G, is denoted by $\mu_s(G)$ [4]. If such vertices do not exist, then deficiency of G will be $+\infty$. In this paper we study the super edge-magic total labeling and deficiency of forests comprising of combs, 2-sided generalized combs and bistar. The evidence provided by these facts supports the conjecture proposed by Figueroa-Centeno, Ichishima and Muntaner-Bartle [2].

Web URL: **https://www.degruyter.com/view/j/math.2017.15.issue-1/math-2017-0122/math-2017-0122.xml**

32. Javed, S., Sohail, A., Maqbool, K., Butt, S. I., & Chaudhry, Q. A. (2017). The Lattice Boltzmann method and computational analysis of bone dynamics-I. *Complex Adaptive Systems Modeling*, *5*(1), 12.

ABSTRACT:

Bone is comprised of an enormously hierarchical construction that promotes transportation of necessary fluids and solids, guaranteeing accurate function and growth. Bone remodeling is a combined process of bone creation and destruction. A number of mathematical models have been developed for the balanced and imbalanced bone remodeling. A brief overview regarding mathematical modeling of bone remodeling is provided. The Lattice Boltzmann method (LBM) has widely been implemented in CFD simulations, and it is becoming more suitable in the application of image processing amongst several others. Mainly, the LBM simulates the communication between synthetic particles dispersed in a lattice. Canaliculi and tortuous channels that have more or less roughly circular structure link among oval bodies identified as lacunae, and are vital to the function of bone. As there is a lack of equipment to inspect flow in channels on the order of measure of canaliculi, so the use of computational methods are more advantageous to give perceptivities into the nature of the flows. In this article, the computational fluid dynamics analysis is descried, using the Lattice Boltzmann method, to examine the result of the microscopic surface roughness of the canalicular wall, which is formed by collagen fibrils, on the flow profiles in the pericellular space.

Web URL: **https://link.springer.com/article/10.1186/s40294-017-0051-1**

33. Khan, N. A., Sohail, A., & Sultan, F. (2017). Effect of anisotropic slip and magnetic field on the flow and heat transfer of Eyring-Powell fluid over an infinite rotating disk. ***International Journal of Fluid Mechanics Research*****,** ***44*****(3).**

ABSTRACT:

This study aims to investigate the effects of magnetic field and anisotropic slip on the flow of Eyring-Powell fluid and heat transfer over an infinite rotating disk. Flows driven by the rotation of a disk have many practical applications in various areas of physics and engineering. The investigation of Eyring-Powell fluid flow due to the rotational motion of an infinite disk is extended for a case where anisotropic slip appears on the surface of the disk. The slip-length boundary condition has been made direction dependent by stipulating the independent slip-length values in the streamwise and spanwise direction. The flow is governed by the second-

order approximation of Eyring-Powell fluid, and the numerical solution has been obtained by using bvp4c. The effects of several physical parameters such as Eyring-Powell parameter, magnetic field, and the Prandtl number have been investigated on the velocity and temperature profiles and physical quantities. The existence of a slip-length boundary condition greatly affects both the velocity and temperature profiles. The results are presented through graphs and tables, and to check their validity, a comparison has been made.

Web URL:

http://www.dl.begellhouse.com/journals/71cb29ca5b40f8f8,17826c7b54f59419,1c3b109a558c39a6.html

34. Abbas, G., Shah, S. M., & Zubair, M. (2017). Collapse and expansion of plane symmetric charged anisotropic source. *Canadian Journal of Physics*, *95*(2), 114-118.

ABSTRACT:

In this paper, we have investigated the final evolutionary stages of charged non-static plane symmetric anisotropic source. To this end, we have solved the Einstein-Maxwell field equations with the charged plane symmetric source. We have found that vanishing of radial heat flux in the gravitating source provides the parametric form of the metric functions. The new form of the metric functions can generate a class of physically acceptable solutions depending on the choice parameter. These solutions may be classified as expanding or collapsing solutions with the particular values of generating parameter. The gravitational collapse in this case end with the formation of single apparent horizon while there exists two such horizon in case of charged spherical anisotropic source.

Web URL: **https://tspace.library.utoronto.ca/bitstream/1807/75319/1/cjp-2016-0741.pdf**

35. Zubair, M., Bahamonde, S., & Jamil, M. (2017). Generalized second law of thermodynamic in modified teleparallel theory. *The European Physical Journal C*, *77*(7), 472.

ABSTRACT:

This study is conducted to examine the validity of the generalized second law of thermodynamics (GSLT) in flat FRW for modified teleparallel gravity involving coupling

between a scalar field with the torsion scalar *T* and the boundary term B=2\nabla _{\mu }T^{\mu }. This theory is very useful, since it can reproduce other important well-known scalar field theories in suitable limits. The validity of the first and second law of thermodynamics at the apparent horizon is discussed for any coupling. As examples, we have also explored the validity of those thermodynamics laws in some new cosmological solutions under the theory. Additionally, we have also considered the logarithmic entropy corrected relation and discuss the GSLT at the apparent horizon.

Web URL: **https://link.springer.com/article/10.1140/epjc/s10052-017-5043-y**

36. Noureen, I., & Zubair, M. (2017). Axially symmetric shear-free fluids in f (R, T) gravity. *International Journal of Modern Physics D*, *26*(11), 1750128.

ABSTRACT:

In this work, we have discussed the implications of shear-free condition on axially symmetric anisotropic gravitating objects in f(R,T)f(R,T) theory. Restricted axial symmetry ignoring rotation and reflection entries containing three independent metric functions is taken into account for establishment of instability range. Implementation of linear perturbation on constitutive modified dynamical equations yield evolution equation. This equation associates adiabatic index ΓΓ with material and dark source components of physical parameters defining stable and unstable regions in Newtonian (N) and post-Newtonian (pN) approximations. It is remarked that the axial system evolving under shear-free condition implicates high levels of stability in anisotropic environment.

Web URL:

http://www.worldscientific.com/doi/abs/10.1142/S0218271817501280?journalCode=ijmpd

37. Zubair, M., Azmat, H., & Noureen, I. (2017). Dynamical analysis of cylindrically symmetric anisotropic sources in f (R, T) gravity. *The European Physical Journal C*, *77*(3), 169.

ABSTRACT:

In this paper, we have analyzed the stability of cylindrically symmetric collapsing object filled with locally anisotropic fluid in $f(R, T)$ theory, where R is the scalar curvature and T is the trace of stress-energy tensor of matter. Modified field equations and dynamical equations are

constructed in $f(R, T)$ gravity. The evolution or collapse equation is derived from dynamical equations by performing a linear perturbation on them. The instability range is explored in both the Newtonian and the post-Newtonian regimes with the help of an adiabetic index, which defines the impact of the physical parameters on the instability range. Some conditions are imposed on the physical quantities to secure the stability of the gravitating sources.

Web URL: https://link.springer.com/article/10.1140/epjc/s10052-017-4723-y

38. Azmat, H., Zubair, M., & Noureen, I. (2018). Dynamics of shearing viscous fluids in f (R, T) gravity. *International Journal of Modern Physics D*, *27*(01), 1750181.

ABSTRACT:

In this paper, we have analyzed the dynamical stability of shearing viscous anisotropic fluid with cylindrical symmetry in f(R,T)f(R,T) theory. We have chosen two viable f(R,T)f(R,T) models for dynamical analysis, and explored their nature and role for stable stellar configuration. Modified field equations and corresponding dynamical equations have been constructed, perturbation approach is adopted to deal with complexity of these equations. With the help of perturbed dynamical equations, the evolution equation has been established to analyze the role of shear viscosity and pressure anisotropy on dynamics of cylindrical system. The adiabatic index ΓΓ is used to investigate the instabilities appearing in Newtonian (N) and post-Newtonian (pN) approximations. Some conditions are found for material variables that are required to meet the stability criterion. We compare the outcomes of our analysis with the results of various models available in literature to reach at more comprehensive conclusion.

Web URL: http://www.worldscientific.com/doi/abs/10.1142/S0218271817501814

39. Zubair, M., & Kousar, F. (2017). Inflationary cosmology for f (R, φ) models with different potentials. *Canadian Journal of Physics*, *95*(11), 1074-1085.

ABSTRACT:

We examine inflation in f(R, φ)-theory, where scalar field is coupled to gravity. We have constructed the Rf(φ) models using exponential and power law potentials and study inflation for these models which can support the early-time acceleration with a useful cosmological constant at high curvature. We have calculated the slow-roll parameters, scalar-to-tensor ratio

and spectral index for these models and analyzed them graphically to check the viability according to recent observational data. We have also presented the evolution of effective equation of state and energy density.

Web URL: **http://inspirehep.net/record/1603368/files/fulltext.pdf**

40. Zubair, M., Mustafa, G., Waheed, S., & Abbas, G. (2017). Existence of stable wormholes on a non-commutative-geometric background in modified gravity. *The European Physical Journal C*, *77*(10), 680.

ABSTRACT:

In this paper, we discuss spherically symmetric wormhole solutions in $f(R, T)$ modified theory of gravity by introducing well-known non-commutative geometry in terms of Gaussian and Lorentzian distributions of string theory. For analytic discussion, we consider an interesting model of $f(R, T)$ gravity defined by $f(R,T)=f1(R)+\lambda T$. By taking two different choices for the function $f1(R)$, that is, $f1(R)=R$ and $f1(R)=R+\alpha R2+\gamma Rn$, we discuss the possible existence of wormhole solutions. In the presence of non-commutative Gaussian and Lorentzian distributions, we get exact and numerical solutions for both these models. By taking appropriate values of the free parameters, we discuss different properties of these wormhole models analytically and graphically. Further, using an equilibrium condition, it is found that these solutions are stable. Also, we discuss the phenomenon of gravitational lensing for the exact wormhole model and it is found that the deflection angle diverges at the wormhole throat.

Web URL: **https://link.springer.com/article/10.1140/epjc/s10052-017-5251-5**

41. Nadeem, M. F., Zafar, S., & Zahid, Z. (2017). Some Topological Indices of L (S (CNCk [n])). *Punjab University Journal of Mathematics*, *49*(1), 13-17.

ABSTRACT:

A topological index is a function which associates real number to the graphs. Graph theory is significant in the subject of structural chemistry. In this paper we calculated $R\alpha$, $M\alpha$, $\chi\alpha$, ABC, GA, ABC4 and GA5 indices of L(S(CNCk[n])).

Web URL: http://pu.edu.pk/images/journal/maths/PDF/Paper-2_49_1_17.pdf

42. Mufti, Z. S. , Zafar,S., Zahid, Z. & Nadeem, F. (2017). Study of the Paraline Graphs of Certain Benzenoid Structures Using Topological Indices. MAGNT Research Report 4(3) 110-116.

ABSTRACT:

Topological indices are valuable in the study of QSAR/QSPR. There are numerous applications of graph theory in the field of structural chemistry. In this paper, we computed generalized Randic, general Zagreb, general sum-connectivity, ABC ,GA , ABC4 , and GA5 indices of the paraline graphs of triangular and linear parallelogram Benzenoid structures.

Web URL: http://brisjast.com/wp-content/uploads/2017/07/MRR-July-14-17.pdf

43. Gao, Y., Nadeem, M. F., Zafar, S., Zahid, Z., Husin, M. N., & Farahani, M. R. (2017). About the certain topological indices of the line graph of V-Pantacenic nanotube. ***International Journal of Pharmaceutical Sciences and Research*****.**

ABSTRACT:

A topological index is a numeric quantity associated with a graph which characterizes the topology of the graph and is invariant under graph automorphism. Topological indices such Randić, atom-bond connectivity (ABC) and geometric (GA) indices are used to predict the bioactivity of different chemical compounds. Recently, the edge version of atom-bond connectivity and geometric arithmetic indices of graph G are introduced based on the degree of an edge of line graph of G. In this paper, the closed formulas of edge version of atom-bond connectivity and geometric-arithmetic indices for V- Pantacenic nanotube are computed.

Web URL:

https://www.researchgate.net/profile/Mohammad_Farahani3/publication/318085341_About_the_certain_topological_indices_of_the_line_graph_of_V-Pantacenic_nanotube_344/links/5a2706e44585155dd4241273/About-the-certain-topological-indices-of-the-line-graph-of-V-Pantacenic-nanotube-344.pdf

44. GAO, W., NADEEM, M., ZAFAR, S., ZAHID, Z., & FARAHANI, M. ON THE PARA-LINE GRAPHS OF CERTAIN NANOSTRUCTURES BASED ON TOPOLOGICAL INDICES.

ABSTRACT:

Topological indices are valuable in the study of QSAR/QSPR. There are numerous applications of graph theory in the field of structural chemistry. In this paper, we computed generalized Randić, general Zagreb, general sum-connectivity, ABC, GA, ABC4 and GA5 indices of the Para-line graph of V-Pantacenic nanotube, H-Pantacenic nanotube and V-Pantacenic nanotorus.

Web URL: **https://www.scientificbulletin.upb.ro/rev_docs_arhiva/rez4dd_769395.pdf**

45. Zhang, X., Zahid, Z., Zafar, S., Farahani, M. R., & Nadeem, M. F. (2017). Study of the Para-Line Graphs of Certain Polyphenyl Chains using Topological Indices. ***INTERNATIONAL JOURNAL OF ADVANCED BIOTECHNOLOGY AND RESEARCH*****, *8*(3), 2435-2442.**

ABSTRACT:

The applications of topological indices appear in mathematical chemistry especially in the study of QSAR/QSPR. In this paper, we computed generalized Randić, general Zagreb, general sum-connectivity, ABC, GA; ABC4 and GA5 indices of the para-line graphs of ortho-polyphenyl chain, meta-polyphenyl chain and para-polyphenyl chain..

Web URL:

https://www.researchgate.net/profile/Mohammad_Farahani3/publication/318085259_STUDY_OF_THE_PARA-LINE_GRAPHS_OF_CERTAIN_POLYPHENYL_CHAINS_USING_TOPOLOGICAL_INDICES_315/links/5a09e575aca272d40f411d07/STUDY-OF-THE-PARA-LINE-GRAPHS-OF-CERTAIN-POLYPHENYL-CHAINS-USING-TOPOLOGICAL-INDICES-315.pdf

46. Ahmed, A. (2017). On Super Edge-Magic Deficiency of Unicyclic Graphs. Hacettepe Journal of Mathematics and Statistics.

ABSTRACT:

A graph G is called edge-magic if there exists a bijective function phi : V (G) boolean OR E(G) -> {1,2,...,vertical bar V(G)vertical bar + vertical bar E(G)vertical bar} such that phi(x) + phi(xy) +

phi(y) = c(phi) is a constant for every edge xy is an element of E(G), called the valence of ck. Moreover, G is said to be super edge-magic if phi(V(G)) = {1, 2,..., vertical bar V(C)vertical bar}. The super edge-magic deficiency of a graph G, denoted by mu(s)(G), is the minimum…

Web URL: **https://www.researchgate.net/publication/317282400_On_super_edge-magic_deficiency_of_certain_Toeplitz_graphs**

47. Abid, M., Wajid, H. A., Iqbal, M. Z., Najam, S., Arshad, A., & Ahmad, A. (2017). DESIGN AND ANALYSIS OF AN AERODYNAMIC DOWNFORCE PACKAGE FOR A FORMULA STUDENT RACE CAR. *IIUM Engineering Journal*, *18*(2), 212-224.

ABSTRACT:

This paper presents design of aerodynamic downforce generating devices (front wing, rear wing and diffuser) to enhance the performance of the Formula Student Race Car using numerical and experimental studies. Numerical results using computational fluid dynamics (CFD) studies were primarily validated with the experimental results performed in the wind tunnel. It was concluded that the use of a downforce package can enhance the performance of the vehicle in the competition.

Web URL:

http://journals.iium.edu.my/ejournal/index.php/iiumej/article/download/679/486

48. Abid, M., Hussain, M., Khan, A., & Wajid, H. A. (2017). Application of monotonic adaptive kernel for optimization: A case study. *Proceedings of the Institution of Mechanical Engineers, Part E: Journal of Process Mechanical Engineering*, 0954408916688501.

ABSTRACT:

Optimization is considered to be the integral part of designing a wide range of engineering solutions. Manual optimization is a hectic job to obtain desired optimized results using hit and trial method. Monotonic adaptive kernel algorithm optimizes the solution to the target stress by using linear interpolation function and checking current values on every iterative step and computing differential load. Using monotonic adaptive kernel algorithm, numerical simulations are conducted on gasketed bolted flange pipe joints to achieve required preload in the bolts as

per industrial guidelines for their optimized performance. It is observed that the monotonic adaptive kernel algorithm produces more accurate and fast results conforming to the desired target values as compared to the manual and semiautomatic optimization techniques implemented for the gasketed bolted flange pipe joint.

Web URL: **http://journals.sagepub.com/doi/abs/10.1177/0954408916688501**

49. Ellahi, R., Tariq, M. H., Hassan, M., & Vafai, K. (2017). On boundary layer nano-ferroliquid flow under the influence of low oscillating stretchable rotating disk. ***Journal of Molecular Liquids*****,** ***229*****, 339-345.**

ABSTRACT:

A new model is here proposed to investigate the effects of nano-Ferroliquid under the influence of low oscillating over stretchable rotating disk. The basic governing equations are formulated under the effects of magnetic field. The resulting system of partial differential equations is first reduced in non-dimensional form by using proper transformations and then reduced coupled system of differential equations is solved analytically by means of homotopy analysis method (HAM). The physical interpretation of velocity and temperature towards different emerging parameters such as particle concentration and effective magnetization parameter are discussed graphically. The physical parameters such as shear stress at wall, heat transfer rate through wall, boundary layer thickness and volume flow rate in axial direction are also presented in tabular form. Finally a comparison with the existing literature is made as a limiting case of the reported problem and found in good agreement.

Web URL: **http://www.sciencedirect.com/science/article/pii/S0167732216339113**

50. Zeeshan, A., Hassan, M., Ellahi, R., & Nawaz, M. (2017). Shape effect of nanosize particles in unsteady mixed convection flow of nanofluid over disk with entropy generation. ***Proceedings of the Institution of Mechanical Engineers, Part E: Journal of Process Mechanical Engineering*****,** ***231*****(4), 871-879.**

ABSTRACT:

The aim of this paper is to study the different shapes of nanoparticles on mixed convective steady flow over a rotating disk. For nanofluid, the copper nanoparticles of disk, cylindrical, and spherical shapes of different sizes and water as base fluid are considered. The physical problem is first modeled and then the governing equations are transformed into nonlinear ordinary differential equations. These equations are dimensionless using geometrical and physical flowfield-dependent parameters and solved analytically. A very good agreement is observed between the obtained results of the current study and previously published study in limiting cases. The shape effects on velocity profiles in radial, tangential, axial directions, and temperature distribution are displayed graphically with the reflection of specific range of nanolayer thickness and its conductivity. In addition, irreversibility due to heat and fluid friction is investigated that supports the heat transfer enhancement in renewable energy systems and industrial thermal management. For the analysis of the averaged entropy generation number, the results are shown in pie charts and tablet form. It is evident from the study that proper choice of nanoparticles will be helpful in controlling velocity and heat transfer. It is also observed that irreversibility process can be reduced by using nanoparticles, especially the spherical particles.

Web URL: **http://journals.sagepub.com/doi/abs/10.1177/0954408916646139**

51. Ellahi, R., Hassan, M., & Zeeshan, A. (2017). Shape effects of spherical and nonspherical nanoparticles in mixed convection flow over a vertical stretching permeable sheet. *Mechanics of Advanced Materials and Structures*, 1-8.

ABSTRACT:

In this article, two-dimensional heat transfer mixed convection flow of a nanofluid over a vertical stretching permeable sheet is investigated. Simultaneous effects of spherical and nonspherical shapes of nanoparticles with different sizes in nanolayer are taken into account. The human engineered fluids with Nimonic 80a metal nanoparticles are used as base fluids. Analytic solutions of velocity and temperature under the influence of the Buoyancy force (assists or opposes) are first obtained and then the role of pertinent parameters, such as volume friction, mixed convection, porosity, stretching, power law index, and temperature

index, is illustrated through graphs and tables. In addition, correlation of Nusselt number and skin friction corresponding to active parameters are also analyzed.

Web URL: **http://www.tandfonline.com/doi/full/10.1080/15376494.2016.1232454**

52. Amin, N., Afzal, R. M., Yousaf, M., & Javid, M. A. (2017). Comparison amongst pulse sequences for enhanced contrast to noise ratio in magnetic resonance imaging. *JPMA. The Journal of the Pakistan Medical Association*, *67*(2), 225.

ABSTRACT:

Objective: To provide optimised pulse sequence and imaging protocols for contrast-to-noise ratio and for tissues that have different signal intensities in magnetic resonance imaging. Methods: A tissue equivalent material, ferrous benzoic xylenol orange gel, was prepared using gelatine, ferrous ammonium sulfate,sulfuric acid, xylenol orange tetrasodium salt and benzoic acid. The gel wasirradiated using 6MV photonsfrom a Varian Clinac 600C linear accelerator, with a dose of 5, 10, 15, 20 and 25 gray. Experimental variations in imaging parameters were performed in echo time and repetition time. The quantitative analysis consisted of contrast-to-noise ratio. Results: Conventional spin echo and fast spin echo were equivalent for the tissues of comparable signal intensities and for entities moderate difference between signal intensities. Conventional spin echo provided remarkable contrast for tissues where signal intensity difference was extremely high in T1, T2-weighted study. An appropriate inversion time of fast fluid attenuated inversion recovery made it significant to measure contrast between tissues where signal intensity difference was the smallest and ordinary.

Web URL: **http://www.jpma.org.pk/PdfDownload/8082.pdf**

53. Raza, Z., & Ahmad, M. (2017). Structure of the unitary subgroup of the group algebra $\mathbb{F}$ 2 n (QD) 1 6. *Journal of Algebra and Its Applications*, 1850060.

ABSTRACT:

In this paper, we established the structure of unitary unit subgroup V∗(F2n(QD)16)V∗(𝔽2n(QD)16) of the group algebra F2n(QD16)𝔽2n(QD16), where QD16QD16 is the Quasi-dihedral [D. S. Dummit and R. Foote, *Abstract Algebra*, 3rd edn.

(Wiley, 2004), pp. 71–72] (Semi-Dihedral [B. Huppert, *Endliche Gruppen* (Springer, 1967), pp. 90–93]) group of order 16 and F2nℙ2n is any finite field of characteristic 2 with 2n2n elements.

Web URL:

http://www.worldscientific.com/doi/abs/10.1142/S0219498818500603?journalCode=jaa

54. Arshad, S., Huang, J., Khaliq, A. Q., & Tang, Y. (2017). Trapezoidal scheme for time–space fractional diffusion equation with Riesz derivative. ***Journal of Computational Physics*****, *350*, 1-15.**

ABSTRACT:

In this paper, a finite difference scheme is proposed to solve time-space fractional diffusion equation which has second-order accuracy in both time and space direction. The time and space fractional derivatives are considered in the senses of Caputo and Riesz, respectively. First, the centered difference approach is used to approximate the Riesz fractional derivative in space. Then, the obtained fractional ordinary differential equations are transformed into equivalent Volterra integral equations. And then, the trapezoidal rule is utilized to approximate the Volterra integral equations. The stability and convergence of our scheme are proved via mathematical induction method. Finally, numerical experiments are performed to confirm the high accuracy and efficiency of our scheme.

Web URL: https://www.sciencedirect.com/science/article/pii/S0021999117306150

55. Arshad, S., Bu, W., Huang, J., Tang, Y., & Zhao, Y. (2017). Finite difference method for time–space linear and nonlinear fractional diffusion equations. ***International Journal of Computer Mathematics*****, 1-16.**

ABSTRACT:

In this paper a finite difference method is presented to solve time–space linear and nonlinear fractional diffusion equations. Specifically, the centred difference scheme is used to approximate the Riesz fractional derivative in space. A trapezoidal formula is used to solve a system of Volterra integral equations transformed from spatial discretization. Stability and convergence of the proposed scheme is discussed which shows second-order accuracy both in

temporal and spatial directions. Finally, examples are presented to show the accuracy and effectiveness of the schemes.

Web URL: **http://www.tandfonline.com/doi/abs/10.1080/00207160.2017.1344231**

56. Arshad, S., Baleanu, D., Bu, W., & Tang, Y. (2017). Effects of HIV infection on CD4+ T-cell population based on a fractional-order model. ***Advances in Difference Equations*****, *2017*(1), 92.**

ABSTRACT:

In this paper, we study the HIV infection model based on fractional derivative with particular focus on the degree of T-cell depletion that can be caused by viral cytopathicity. The arbitrary order of the fractional derivatives gives an additional degree of freedom to fit more realistic levels of $CD4^+$ cell depletion seen in many AIDS patients. We propose an implicit numerical scheme for the fractional-order HIV model using a finite difference approximation of the Caputo derivative. The fractional system has two equilibrium points, namely the uninfected equilibrium point and the infected equilibrium point. We investigate the stability of both equilibrium points. Further we examine the dynamical behavior of the system by finding a bifurcation point based on the viral death rate and the number of new virions produced by infected $CD4^+$ T-cells to investigate the influence of the fractional derivative on the HIV dynamics. Finally numerical simulations are carried out to illustrate the analytical results.

Web URL: **https://link.springer.com/article/10.1186/s13662-017-1143-0**

57. Imran, M., Baby, S., Siddiqui, H. M. A., & Shafiq, M. K. (2017). On the bounds of degree-based topological indices of the Cartesian product of F-sum of connected graphs. ***Journal of inequalities and applications*****, *2017*(1), 305.**

ABSTRACT:

Topological indices are the mathematical tools that correlate the chemical structure with various physical properties, chemical reactivity or biological activity numerically. A topological index is a function having a set of graphs as its domain and a set of real numbers as its range. In QSAR/QSPR study, a prediction about the bioactivity of chemical compounds is made on the basis of physico-chemical properties and topological indices such as Zagreb, Randić and

multiple Zagreb indices. In this paper, we determine the lower and upper bounds of Zagreb indices, the atom-bond connectivity (ABC) index, multiple Zagreb indices, the geometric-arithmetic (GA) index, the forgotten topological index and the Narumi-Katayama index for the Cartesian product of *F*-sum of connected graphs by using combinatorial inequalities.

Web URL: https://link.springer.com/article/10.1186/s13660-017-1579-5

58. Binyamin, M. A., Siddiqui, H. M. A., & Shehzad, A.(2017). A Combinatorial Approach to the Classification of Resolution Graphs of Weighted Homogeneous plane Curve Singularities.

ABSTRACT:

In this article we describe the classification of the resolution graphs of weighted homogeneous plane curve singularities in terms of their weights by using the concepts of graph theory and combinatorics. The classification shows that the resolution graph of a weighted homogeneous plane curve singularity is always a caterpillar.

Web URL:

https://www.researchgate.net/profile/Muhammad_Banyamin/publication/313770171_A_Combinatorial_Approach_to_the_Classification_of_Resolution_Graphs_of_Weighted_Homogeneous_plane_Curve_Singularities/links/58a57914aca27206d986e807/A-Combinatorial-Approach-to-the-Classification-of-Resolution-Graphs-of-Weighted-Homogeneous-plane-Curve-Singularities.pdf

59. Sohail, A., Maqbool, K., & Ellahi, R. (2018). Stability analysis for fractional-order partial differential equations by means of space spectral time Adams-Bashforth Moulton method. *Numerical Methods for Partial Differential Equations*, *34*(1), 19-29.

ABSTRACT:

In this article, a new numerical scheme space Spectral time Fractional Adam Bashforth Moulton method for the solution of fractional partial differential equations is offered. The proposed method is obtained by modifying, in a suitable way; the spectral technique and the method of lines. The attention is focused on the stability properties and hence an elegant stability analysis for the current approach is also provided. Finally, two examples are presented to illustrate the

effectiveness of the reported method. Obtained results confirm the convergence and spectral accuracy of the proposed method in both space and time. In addition, a comparison with the existing studies is also made as a limiting case of the considered problem at the end and found in good agreement.

Web URL: **http://onlinelibrary.wiley.com/doi/10.1002/num.22171/full**

60. Gao, y., Imran, M,. Farahani, M. R. & Siddiqui, H. M. A. (2017). Some connectivity indices and Zagreb Index of honeycomb graphs. ***International Journal of Pharmaceutical Sciences and Research.***

ABSTRACT:

Abstract: In this paper, we investigate several topological indices in honeycomb graphs: Randić connectivity index, sum-connectivity index, atom-bond connectivity index, geometric-arithmetic index, First and Second Zagreb indices and Zagreb polynomials. Formulas for computing the above topological descriptors in honeycomb graphs are given.

Web URL:

https://www.researchgate.net/publication/320384033_Some_connectivity_indices_and_Zagreb_Index_of_honeycomb_graphs_327

61. Jawad, A., Rani, S., & Ilyas, A. (2017). Quartic potential inspired warm standard and tachyon scalar fields brane-world inflation. ***International Journal of Modern Physics D*****,** ***26*****(13), 1750144.**

ABSTRACT:

A warm inflationary universe in the brane-world scenario is being studied by assuming the standard scalar and tachyon field models. For this purpose, the quartic potential (σφ44σφ44) is being utilized which is ruled out by current data in cold inflation but in our models it is analyzed that it is in agreement with recent observational data. Moreover, the generalized form of dissipative coefficient (Γ=a0Tm˜φm˜−1)(Γ=a0Tm˜φm˜−1) is being considered. Within this setup, the inflationary parameters in the weak dissipative regime are being analyzed. It is observed that the ranges of our results of tensor-to-scalar ratio, scalar spectral index and running of

spectral favor observational data like BICEP2, WMAP9 and Planck.

Web URL:

http://www.worldscientific.com/doi/abs/10.1142/S0218271817501449?journalCode=ijmpd

62. Jawad, A., & Shahzad, M. U. (2017). Accreting fluids onto regular black holes via Hamiltonian approach. *The European Physical Journal C*, *77*(8), 515.

ABSTRACT:

We investigate the accretion of test fluids onto regular black holes such as Kehagias–Sfetsos black holes and regular black holes with Dagum distribution function. We analyze the accretion process when different test fluids are falling onto these regular black holes. The accreting fluid is being classified through the equation of state according to the features of regular black holes. The behavior of fluid flow and the existence of sonic points is being checked for these regular black holes. It is noted that the three-velocity depends on critical points and the equation of state parameter on phase space.

Web URL: https://link.springer.com/article/10.1140%2Fepjc%2Fs10052-017-5075-3

63. Jawad, A., Gulshan, F., & Rani, S. (2017). Warm Standard Scalar Field Modified Chaplygin Gas Inflation Inspired by Generalized Dissipative Coefficient on the Brane. *Communications in Theoretical Physics*, *68*(2), 272.

ABSTRACT:

We discuss the warm inflation in the presence of standard scalar field model and modified Chaplygin gas in brane-world scenario. We consider weak and strong dissipative regimes with generalized dissipative coefficient. We extract various inflationary parameters. For example, we analyze the behavior of different ratios (ratio of dissipative co-efficient and Hubble parameter Γ/3H, ratio of temperature and Hubble parameter T/H, scalar-to-tensor ratio r) with respect to spectral index n_s for the weak and strong dissipative regimes through parametric plotting. It is found that T/H and Γ/3H satisfied the required conditions in both dissipative

regimes. It is also noted that the spectral index (n_s) attain the range $n_s = 0.96^{+0.10}_{-0.10}$. It is remarked here that our results are consistence with observational data WMAP7, WMAP9, and recent Planck data.

Web URL: **http://iopscience.iop.org/article/10.1088/0253-6102/68/2/272/meta**

64. Jawad, A., Rani, S., & Saleem, M. (2017). Cosmological study of reconstructed f (T) models. ***Astrophysics and Space Science*****,** ***362*****(4), 63.**

ABSTRACT:

In this paper, we construct f(T)f(T) models by using some dark energy models taking FRW space-time under reconstruction scenario. These dark energy models consist of pilgrim dark energy model with event horizon and Granda-Oliveros as infrared cutoff and higher order time derivatives of Hubble parameter. Using these models we drive the cosmological parameters such as equation of state, square speed of sound and ωT−ω′TωT−ωT′ plane taking power-law form of scale factor. We discuss these parameters graphically for different values of scale factor parameter. The first and second models represent quintessence and phantom era with stable behavior and freezing region for smaller values of scale factor parameter. The third model shows unstable behavior while phantom era of the universe.

Web URL: **https://link.springer.com/article/10.1007/s10509-017-3040-0**

65. Jawad, A., & Shahzad, M. U. (2017). Effects of thermal fluctuations on non-minimal regular magnetic black hole. ***The European Physical Journal C*****,** ***77*****(5), 349.**

ABSTRACT:

We analyze the effects of thermal fluctuations on a regular black hole (RBH) of the non-minimal Einstein–Yang–Mill theory with gauge field of magnetic Wu–Yang type and a cosmological constant. We consider the logarithmic corrected entropy in order to analyze the thermal fluctuations corresponding to non-minimal RBH thermodynamics. In this scenario, we develop various important thermodynamical quantities, such as entropy, pressure, specific heats, Gibb's free energy and Helmholtz free energy. We investigate the first law of thermodynamics in the presence of logarithmic corrected entropy and non-minimal RBH. We

also discuss the stability of this RBH using various frameworks such as the γγ factor (the ratio of heat capacities), phase transition, grand canonical ensemble and canonical ensemble. It is observed that the non-minimal RBH becomes globally and locally more stable if we increase the value of the cosmological constant.

Web URL: **https://link.springer.com/article/10.1140/epjc/s10052-017-4914-6**

66. Jawad, A., Videla, N., & Gulshan, F. (2017). Dynamics of warm power-law plateau inflation with a generalized inflaton decay rate: predictions and constraints after Planck 2015. *The European Physical Journal C*, *77*(5), 271.

ABSTRACT:

In the present work, we study the consequences of considering a new family of single-field inflation models, called power-law plateau inflation, in the warm inflation framework. We consider the inflationary expansion is driven by a standard scalar field with a decay ratio Γhaving a generic power-law dependence with the scalar field φ and the temperature of the thermal bath *T* given by Γ(φ,T)=CφTaφa−1. Assuming that our model evolves according to the strong dissipative regime, we study the background and perturbative dynamics, obtaining the most relevant inflationary observable as the scalar power spectrum, the scalar spectral index and its running and the tensor-to-scalar ratio. The free parameters characterizing our model are constrained by considering the essential condition for warm inflation, the conditions for the model evolves according to the strong dissipative regime and the 2015 Planck results through the ns–*r* plane. For completeness, we study the predictions in the ns–dns/dlnk plane. The model is consistent with a strong dissipative dynamics and predicts values for the tensor-to-scalar ratio and for the running of the scalar spectral index consistent with current bounds imposed by Planck and we conclude that the model is viable.

Web URL: **https://link.springer.com/article/10.1140/epjc/s10052-017-4846-1**

67. Jawad, A., Ilyas, A., & Rani, S. (2017). Warm modified Chaplygin gas shaft inflation. *The European Physical Journal C*, *77*(2), 131.

ABSTRACT:

In this paper, we examine the possible realization of a new inflation family called “shaft inflation” by assuming the modified Chaplygin gas model and a tachyon scalar field. We also consider the special form of the dissipative coefficient Γ=a0T3φ2Γ=a0T3φ2 and calculate the various inflationary parameters in the scenario of strong and weak dissipative regimes. In order to examine the behavior of inflationary parameters, the nsns–φ,nsφ,ns–*r*, and nsns–αsαs planes (where ns,αs,rns,αs,r, and φφ represent the spectral index, its running, tensor-to-scalar ratio, and scalar field, respectively) are being developed, which lead to the constraints r<0.11r<0.11, ns=0.96±0.025ns=0.96±0.025,
and αs=−0.019±0.025αs=−0.019±0.025. It is quite interesting that these results of the inflationary parameters are compatible with BICEP2, WMAP (7+9)(7+9) and recent Planck data.

Web URL: **https://link.springer.com/article/10.1140/epjc/s10052-017-4691-2**

68. Jawad, A., & Umair Shahzad, M. (2017). Particle dynamics around time conformal regular black holes via Noether symmetries. ***International Journal of Modern Physics D*****, *26*(07), 1750059.**

ABSTRACT:

The time conformal regular black hole (RBH) solutions which are admitting the time conformal factor eϵg(t)eϵg(t), where g(t)g(t) is an arbitrary function of time and ϵϵ is the perturbation parameter are being considered. The approximate Noether symmetries technique is being used for finding the function g(t)g(t) which leads to τατα. The dynamics of particles around RBHs are also being discussed through symmetry generators which provide approximate energy as well as angular momentum of the particles. In addition, we analyze the motion of neutral and charged particles around two well known RBHs such as charged RBH using Fermi–Dirac distribution and Kehagias–Sftesos asymptotically flat RBH. We obtain the innermost stable circular orbit and corresponding approximate energy and angular momentum. The behavior of effective potential, effective force and escape velocity of the particles in the presence/absence of magnetic field for different values of angular momentum near horizons are also being

analyzed. The stable and unstable regions of particle near horizons due to the effect of angular momentum and magnetic field are also explained.

Web URL:

http://www.worldscientific.com/doi/abs/10.1142/S0218271817500596?journalCode=ijmpd

69. Jawad, A., Rani, S., Salako, I. G., & Gulshan, F. (2017). Pilgrim dark energy models in fractal universe. *International Journal of Modern Physics D*, *26*(06), 1750049.

ABSTRACT:

We discuss the cosmological implications of interacting pilgrim dark energy (PDE) models (with Hubble, Granda–Oliveros and generalized ghost cutoffs) with cold dark matter (ΛΛCDM) in fractal cosmology by assuming the flat universe. We observe that the Hubble parameter lies within observational suggested ranges while deceleration parameter represents the accelerated expansion behavior of the universe. The equation of state (EoS) parameter (ωDωD) corresponds to the quintessence region and phantom region for different cases of uu. Further, we can see that ωDωD–ω′DωD′ (where prime indicates the derivative with respect to natural logarithmic of scale factor) plane describes the freezing and thawing regions and also corresponds to ΛCDMΛCDM limit for some cases of uu (PDE parameter). It is also noted that the rr–ss (state-finder parameters) plane corresponds to ΛCDMΛCDM limit and also shows the Chaplygin as well as phantom/quintessence behavior. It is observed that pilgrim dark energy models in fractal cosmology expressed the consistent behavior with recent observational schemes.

Web URL:

http://www.worldscientific.com/doi/abs/10.1142/S0218271817500493?journalCode=ijmpd

70. Jawad, A., Azhar, N., & Rani, S. (2017). Entropy corrected holographic dark energy models in modified gravity. *International Journal of Modern Physics D*, *26*(04), 1750040.

ABSTRACT:

We consider the power law and the entropy corrected holographic dark energy (HDE) models with Hubble horizon in the dynamical Chern–Simons modified gravity. We explore various

cosmological parameters and planes in this framework. The Hubble parameter lies within the consistent range at the present and later epoch for both entropy corrected models. The deceleration parameter explains the accelerated expansion of the universe. The equation of state (EoS) parameter corresponds to quintessence and cold dark matter (ΛΛCDM) limit. The ωΛ−ω′ΛωΛ−ωΛ′ approaches to ΛΛCDM limit and freezing region in both entropy corrected models. The statefinder parameters are consistent with ΛΛCDM limit and dark energy (DE) models. The generalized second law of thermodynamics remain valid in all cases of interacting parameter. It is interesting to mention here that our results of Hubble, EoS parameter and ωΛ−ω′ΛωΛ−ωΛ′ plane show consistency with the present observations like Planck, WP, BAO, H0H0, SNLS and nine-year WMAP.

Web URL:

http://www.worldscientific.com/doi/abs/10.1142/S0218271817500407?journalCode=ijmpd

71. Jawad, A., Ilyas, A., & Rani, S. (2017). Dynamics of modified Chaplygin gas inflation on the Brane with bulk viscous pressure. *International Journal of Modern Physics D*, *26*(04), 1750031.

ABSTRACT:

We investigate the role of bulk viscous pressure on the warm inflationary modified Chaplygin gas (MCG) in braneworld framework in the presence of standard scalar field. We assume the intermediate inflationary scenario in strong dissipative regime and constructed the inflaton, potential, entropy density, slow-roll parameters, scalar and tensor power spectra, scalar spectral index and tensor-to-scalar ratio. We develop various trajectories such as ns−Nns−N, ns−rns−r and ns−αsns−αs (where nsns is the spectral index, αsαs is the running of spectral index, NN is the number of e-folds and rr is tensor-to-scalar ratio) for variable as well as constant dissipation and bulk viscous coefficients at high dissipative regime. It is interesting to remark here that our results of these parameters are compatible with recent observational data such as WMAP 7+97+9, BICEP22 and Planck data.

Web URL:

http://www.worldscientific.com/doi/abs/10.1142/S0218271817500316?journalCode=ijmpd

72. Jawad, A., Rani, S., Salako, I. G., & Gulshan, F. (2017). Cosmological study in loop quantum cosmology through dark energy model. *International Journal of Modern Physics D*, *26*(02), 1750007.

ABSTRACT:

The interacting generalized ghost version of pilgrim dark energy (GGPDE) is discussed in the framework of loop quantum cosmology (LQC). We analyze the behavior of cosmological parameters (Hubble, equation of state (EoS), deceleration) and cosmological planes (ωD−ω′DωD−ωD′ and rr-ss) in the present scenario (ωDωD represents the EoS parameter and ω′DωD′ indicates the evolution of the EoS parameter, rr,ss are statefinder parameters). It is observed that the deceleration parameter corresponds to the accelerated expansion of the universe. The EoS parameter lies in vacuum and phantom regions for all cases of uu (pilgrim dark energy (PDE) parameter). The ωD−ω′DωD−ωD′ plane lies in thawing region for all cases of uu. The r−sr−s plane corresponds to ΛΛ cold dark matter (CDM) and Chaplygin gas model. We have also mentioned the constraints on calculated cosmological parameters and found that all the trajectories of cosmological parameters and planes show the consistence behavior with the observational schemes.

Web URL:

http://www.worldscientific.com/doi/abs/10.1142/S0218271817500079?journalCode=ijmpd

73. Shahzad, M. U., & Jawad, A. (2017). Tidal forces in Kiselev black hole. *The European Physical Journal C*, *77*(6), 372.

ABSTRACT:

The aim of this paper is to examine the tidal forces occurring in a Kiselev black hole surrounded by radiation and dust fluids. It is noted that the radial and angular components of the tidal force change the sign between event and Cauchy horizons. We solve the geodesic

deviation equation for radially free-falling bodies toward Kiselev black holes. We explain the geodesic deviation vector graphically and point out the location of the event and Cauchy horizons for specific values of the radiation and dust parameters.

Web URL: **https://link.springer.com/article/10.1140/epjc/s10052-017-4935-1**

74. Jawad, A., Hussain, S., Rani, S., & Videla, N. (2017). Impact of generalized dissipative coefficient on warm inflationary dynamics in the light of latest Planck data. *The European Physical Journal C*, *77*(10), 700.

ABSTRACT:

The warm inflation scenario in view of the modified Chaplygin gas is studied. We consider the inflationary expansion to be driven by a standard scalar field whose decay ratio \Gamma has a generic power-law dependence with the scalar field \phi and the temperature of the thermal bath *T*. By assuming an exponential power-law dependence in the cosmic time for the scale factor *a*(*t*), corresponding to the intermediate inflation model, we solve the background and perturbative dynamics considering our model to evolve according to (1) weak dissipative regime and (2) strong dissipative regime. Specifically, we find explicit expressions for the dissipative coefficient, scalar potential, and the relevant inflationary observables like the scalar power spectrum, scalar spectral index, and tensor-to-scalar ratio. The free parameters characterizing our model are constrained by considering the essential condition for warm inflation, the conditions for the model evolves according to weak or strong dissipative regime, and the 2015 Planck results through the n_s–*r* plane.

Web URL: **https://link.springer.com/article/10.1140/epjc/s10052-017-5264-0**

75. Jawad, A., Chaudhary, S., & Videla, N. (2017). Dynamics of polynomial Chaplygin gas warm inflation. *The European Physical Journal C*, *77*(11), 808.

ABSTRACT:

In the present work, we study the consequences of a recently proposed polynomial inflationary potential in the context of the generalized, modified, and generalized cosmic Chaplygin gas models. In addition, we consider dissipative effects by coupling the inflation

field to radiation, i.e., the inflationary dynamics is studied in the warm inflation scenario. We take into account a general parametrization of the dissipative coefficient \Gamma for describing the decay of the inflaton field into radiation. By studying the background and perturbative dynamics in the weak and strong dissipative regimes of warm inflation separately for the positive and negative quadratic and quartic potentials, we obtain expressions for the most relevant inflationary observables as the scalar power spectrum, the scalar spectral, and the tensor-to-scalar ratio. We construct the trajectories in the n_\mathrm{s}–*r* plane for several expressions of the dissipative coefficient and compare with the two-dimensional marginalized contours for (n_\mathrm{s},r) from the latest Planck data. We find that our results are in agreement with WMAP9 and Planck 2015 data.

Web URL: **https://link.springer.com/article/10.1140/epjc/s10052-017-5377-5**

76. Sohail, A., Ahmad, Z., Bég, O. A., Arshad, S., & Sherin, L. (2017). A review on hyperthermia via nanoparticle-mediated therapy. *Bulletin du Cancer*.

ABSTRACT:

Hyperthermia treatment, generated by magnetic nanoparticles (MNPs) is promising since it is tumour-focused, minimally invasive and uniform. The most unique feature of magnetic nanoparticles is their reaction to and manipulation by a magnetic force which is responsible for enabling their potential as heating mediators for cancer therapy. With magnetic nanoparticle hyperthermia, a tumour is preferentially loaded with systemically administered nanoparticles with high-absorption cross section for transduction of an extrinsic energy source to heat. To maximize the energy deposited in the tumour while limiting the exposure in healthy tissues, the heating is achieved by exposing the region of tissue containing magnetic nanoparticles to an alternating magnetic field. The magnetic nanoparticles dissipate heat from relaxation losses thereby heating localized tissue above normal physiological ranges. Besides thermal efficiency, the biocompatibility of magnetite nanoparticles assists in their deployment as efficient drug carriers for targeted therapeutic regimes. In the present article we provide a state-of-the-art review focused on progress in nanoparticle induced hyperthermia treatments which have several potential advantages over both global and local hyperthermia treatments achieved

without nanoparticles. Green bio-nanotechnology has attracted substantial attention and has demonstrable abilities to improve cancer therapy. Furthermore we have listed the challenges associated with this treatment along with future opportunities in this field which it is envisaged will be of interest to biomedical engineers, bio-materials scientists, medical researchers and pharmacological research groups.

Web URL:

http://usir.salford.ac.uk/41346/1/E__USIR%20repository_2017_BULLETIN%20DU%20CANCER%20Hyper-thermia%20magnetic%20nanosystems%20ACCEPTED%20Feb%206th%202017.pdf

77. **Beg, O. A., Uddin, M. J., Sohail, A., & Ismail, A. I. M. (2017). Numerical solution of MHD slip flow of a nanofluid past a radiating plate with Newtonian heating: a lie group approach. *Alexandria Engineering Journal*.**

ABSTRACT:

In this paper, we have examined the magnetohydrodynamic flow of a nanofluid past a radiating sheet. The Navier velocity slip, Newtonian heating and passively controlled wall boundary conditions are considered. The governing equations are reduced into similarity equations with the help of Lie group. A collocation method is used for simulation. The influence of emerging parameters on velocity, temperature, nanoparticle volumetric fraction profiles, as well as on local skin friction factor and local Nusselt number are illustrated in detail. It is found that the friction (heat transfer rate) is lower (higher) for passively controlled boundary conditions as compared to the case of an actively controlled boundary condition. The magnetic field decreases both the skin friction and the rate of heat transfer. The findings are validated with existing results and found an excellent agreement. The model explores new applications in solar collectors with direct solar radiative input using magnetic nanofluids.

Web URL:

http://usir.salford.ac.uk/41564/1/ALEXANDRIA%20ENG%20JOURNAL%20magnetoconvective%20nanofluid%20dynamic%20slip%20modelling%20ACCEPTED%20March%204th%202017.pdf

78. Siddiqui, A. M., Sohail, A., Naqvi, S., & Haroon, T. (2017). Analysis of Stokes flow through periodic permeable tubules. *Alexandria Engineering Journal*, *56*(1), 105-113.

ABSTRACT:

This article reports the detailed analysis of the Stokes flow through permeable tubes. The objective of this investigation was to search for exact solutions to the Stokes flow and thereby observe the effects on radial flow component, provided the permeability on the tubular surface is an elementary trigonometric function. Mathematical expressions for the pressure distribution, velocity components, volume flux, average wall shear stress and leakage flux are presented explicitly. Graphical analysis of the fluid flow is presented for a set of parametric values. Important conclusions are drawn for Stokes flow through tubes with low as well as high permeability. The classical Poiseuille flow is presented as a limiting case of this immense study of Stokes flow.

Web URL: **http://www.sciencedirect.com/science/article/pii/S1110016816302770**

79. Arshad, S., Siddiqui, A. M., Sohail, A., Maqbool, K., & Li, Z. (2017). Comparison of optimal homotopy analysis method and fractional homotopy analysis transform method for the dynamical analysis of fractional order optical solitons. *Advances in Mechanical Engineering*, *9*(3).

ABSTRACT:

In this article, dynamical analysis of fractional order Schrödinger equation governing the optical wave propagation is reported in detail. The validity criteria for the application of the semi-analytic asymptotic methods are exploited. Comparison between the solutions obtained by the two asymptotic techniques, that is, the fractional homotopy analysis transform method and the optimal homotopy analysis method is performed to select the most accurate technique for the stated problem.

Web URL: **http://journals.sagepub.com/doi/full/10.1177/1687814017692946**

DEPARTMENT OF ELECTRICAL ENGINEERING

Journal Papers

1. Asif, M. R., Chun, Q., Hussain, S., Fareed, M. S., & Khan, S. (2017). Multinational vehicle license plate detection in complex backgrounds. ***Journal of Visual Communication and Image Representation*****, *46*, 176-186.**

ABSTRACT:

Many methods for multinational License Plate Detection (LPD) have been proposed in recent times but most of them are not sophisticated enough to handle complex backgrounds. Moreover, their ability to handle various environmental and illumination conditions has been

limited and still needs improvement. In this paper, we propose a novel technique to detect license plates of vehicles regardless of their color, size, and content. As the rear vehicle lights are an essential part of any vehicle, we reduce the image processing area to eliminate the complex background by detecting the rear-lights as the license plates are in a certain range of these lights. Heuristic Energy Map (HEM) of the vertical edge information in the Region of Interest (ROI) is calculated and area with the dense edges is selected using a unique histogram approach which is considered to be the license plate. The proposed algorithm is tested on 855 images from various countries including China, Pakistan, Serbia, Italy and various states of America. Experimental results show that the proposed method is able to detect license plates 90.4% of times despite of complex backgrounds in 0.25 s on average that can achieve real time performance.

Web URL: **http://www.sciencedirect.com/science/article/pii/S1047320317300883**

2. Khan, S., Jaffery, M. H., Hanif, A., & Asif, M. R. (2017). Teaching Tool for a Control Systems Laboratory Using a Quadrotor as a Plant in MATLAB. *IEEE Transactions on Education*.

ABSTRACT:

This paper presents a MATLAB-based application to teach the guidance, navigation, and control concepts of a quadrotor to undergraduate students, using a graphical user interface (GUI) and 3-D animations. The Simulink quadrotor model is controlled by a proportional integral derivative controller and a linear quadratic regulator controller. The GUI layout's many components can be easily programmed to perform various experiments by considering the simulation of the quadrotor as a plant; it incorporates control systems (CS) fundamentals such as time domain response, transfer function and state-space form, pole-zero location, root locus, frequency domain response, steady-state error, position and disturbance response, controller design and tuning, unity, and the use of a Kalman filter as a feedback sensor. 3-D animations are used to display the quadrotor flying in any given condition selected by the user. For each simulation, users can view the output response in the form of 3-D animations, and can run time plots. The quadrotor educational tool (QET) helps students in the CS laboratory understand

basic CS concepts. The QET was evaluated based on student feedback, grades, satisfaction, and interest in CS.

Web URL: ***http://ieeexplore.ieee.org/abstract/document/7836322/***

3. Masood, B., & Baig, S. (2016). Standardization and deployment scenario of next generation NB-PLC technologies. *Renewable and Sustainable Energy Reviews*, *65*, 1033-1047.

ABSTRACT:

Several efforts have been made in the recent decades with a goal to implement the Advanced Metering Infrastructure (AMI) in the power grid. These efforts laid foundation for the implementation of next generation Narrowband Power Line Communications (NB-PLC) technologies. In the recent past, standardization process has been completed by IEEE and ITU-T for the deployment of transceivers, based on Orthogonal Frequency Division Multiplexing (OFDM) NB-PLC. In this paper significance of NB-PLC with a focus on CENELEC band in the context of standardization and deployment is discussed. A comprehensive comparative analysis of Power Related Intelligent Metering Evolution (PRIME), G3-PLC and IEEE 1901.2 along with their routing techniques is presented. Moreover, deployment aspects and worldwide PLC research projects by academia are discussed.

Web URL: ***http://www.sciencedirect.com/science/article/pii/S1364032116303884***

4. Masood, B., Haider, A., & Baig, S. (2017). Modeling and Characterization of Low Voltage Access Network for Narrowband Powerline Communications. *Journal of Electrical Engineering & Technology*, *12*(1), 443-450.

ABSTRACT:

Nowadays, Power Line Communication (PLC) is gaining high attention from industry and electric supply companies for the services like demand response, demand side management and Advanced Metering Infrastructure (AMI). The reliable services to consumers using PLC can be provided by utilizing an efficient PLC channel for which sophisticated channel modeling is very important. This paper presents characterization of a Low Voltage (LV) access network for Narrowband Power Line Communications (NB-PLC) using transmission line (TL) theory and a

Simulink model. The TL theory analysis not only includes the constant parameters but frequency selectivity is also introduced in these parameters such as resistance, conductance and impedances. However, the proposed Simulink channel model offers an analysis and characterization of capacitive coupler, network impedance and channel transfer function for NB-PLC. Analysis of analytical and simulated results shows a close agreement of the channel transfer function. In the absence of a standardized NBPLC channel model, this research work can prove significant in improving the efficiency and accuracy of NB-PLC communication transceivers for Smart Grid communications.

Web URL:

http://www.jeet.or.kr/LTKPSWeb/uploadfiles/be/201605/130520161459574535000.pdf

5. Javed, A., Larijani, H., Ahmadinia, A., & Emmanuel, R. (2017). RANDOM NEURAL NETWORK LEARNING HEURISTICS. *Probability in the Engineering and Informational Sciences*, 1-21.

ABSTRACT:

The random neural network (RNN) is a probabilitsic queueing theory-based model for artificial neural networks, and it requires the use of optimization algorithms for training. Commonly used gradient descent learning algorithms may reside in local minima, evolutionary algorithms can be also used to avoid local minima. Other techniques such as artificial bee colony (ABC), particle swarm optimization (PSO), and differential evolution algorithms also perform well in finding the global minimum but they converge slowly. The sequential quadratic programming (SQP) optimization algorithm can find the optimum neural network weights, but can also get stuck in local minima. We propose to overcome the shortcomings of these various approaches by using hybridized ABC/PSO and SQP. The resulting algorithm is shown to compare favorably with other known techniques for training the RNN. The results show that hybrid ABC learning with SQP outperforms other training algorithms in terms of mean-squared error and normalized root-mean-squared error.

Web URL: ***https://www.cambridge.org/core/journals/probability-in-the-engineering-and-informational-sciences/article/random-neural-network-learning-heuristics/2FD3C90B26A129A9551679C47316AD0A***

6. Javed, A., Larijani, H., Ahmadinia, A., Emmanuel, R., Mannion, M., & Gibson, D. (2017). Design and Implementation of a Cloud Enabled Random Neural Network-Based Decentralized Smart Controller With Intelligent Sensor Nodes for HVAC. *IEEE Internet of Things Journal*, *4*(2), 393-403.

ABSTRACT:

Building Energy Management Systems (BEMS) monitor and control the Heating Ventilation and Air Conditioning (HVAC) of buildings in addition to many other building systems and utilities. Wireless Sensor Networks (WSN) have become the integral part of BEMS at the initial implementation phase or latter when retro fitting is required to upgrade older buildings. WSN enabled BEMS however have several challenges which are managing data, controllers, actuators, intelligence, and power usage of wireless components (which might be battery powered). The wireless sensor nodes have limited processing power and memory for embedding intelligence in the sensor nodes. In this work, we present a random neural network (RNN) based smart controller on a Internet of Things (IoT) platform integrated with cloud processing for training the RNN which has been implemented and tested in an environment chamber. The IoT platform is modular and not limited to but has several sensors for measuring temperature, humidity, inlet air coming from the HVAC duct and PIR. The smart RNN controller has three main components:base station, sensor nodes, and the cloud with embedded intelligence on each component for different tasks. This IoT platform is integrated with cloud processing for training the RNN. The RNN based occupancy estimator is embedded in sensor node which estimates the number of occupants inside the room and sends this information to the base station. The base station is embedded with RNN models to control the HVAC on the basis of setpoints for heating and cooling. The HVAC of the environment chamber consumes 27.12% less energy with smart controller as compared to simple rule based controllers. The occupancy estimation time is reduced by our proposed hybrid algorithm for occupancy estimation that combines RNN based occupancy estimator with door sensor node (equipped with PIR and magnetic reed switch). The results show that accuracy of hybrid RNN occupancy estimator is 88%.

Web URL:

http://researchonline.gcu.ac.uk/portal/files/24481811/H.Larijani_FINAL_VERSION.pdf

7. Javed, A., Larijani, H., Ahmadinia, A., & Gibson, D. (2017). Smart random neural network controller for HVAC using cloud computing technology. ***IEEE Transactions on Industrial Informatics*****,** ***13*****(1), 351-360.**

ABSTRACT:

Smart homes reduce human intervention in controlling the Heating Ventilation and Air Conditioning (HVAC) systems for maintaining a comfortable indoor environment. The embedded intelligence in the sensor nodes is limited due to the limited processing power and memory in the sensor node. Cloud computing has become increasingly popular due to its capability of providing computer utilities as internet services. In this work, a model for intelligent controller by integrating Internet of Things (IoT) with cloud computing and web services is proposed. The wireless sensor nodes for monitoring the indoor environment and HVAC inlet air, and wireless base station for controlling the actuators of HVAC have been developed. The sensor nodes and base station communicate through RF transceivers at 915 MHz. Random neural network (RNN) models are used for estimating the number of occupants, and for estimating the Predicted mean vote (PMV) based setpoints for controlling the heating, ventilation and cooling of the building. Three test cases are studied (Case 1- data storage and implementation of RNN models on the cloud, Case 2- RNN models implementation on base station, Case 3- distributed implementation of RNN models on sensor nodes and base stations) for determining the best architecture in terms of power consumption. The results have shown that by embedding the intelligence in the base station and sensor nodes (i.e. Case 3), the power consumption of the intelligent controller was 4.4% less than Case 1 and 19.23 % less than Case 2

Web URL: ***http://ieeexplore.ieee.org/abstract/document/7529229/***

8. Hamayun, M. T., Ijaz, S., & Bajodah, A. H. (2017). Output integral sliding mode fault tolerant control scheme for LPV plants by incorporating control allocation. ***IET Control Theory & Applications*****.**

ABSTRACT:

An integrated integral sliding mode fault tolerant control scheme is proposed for the linear parameter varying (LPV) plants in the output feedback framework. To estimate the unavailable plant states, an unknown input LPV observer is employed. The feedback and observer gains are designed using linear matrix inequalities approach to ensure closed-loop stability nominally and in the situation of actuator faults/failures. An integral sliding modes approach in the LPV framework together with control allocation maintains the nominal performance in the presence of permissible set of actuator faults/failures. A rigorous closed-loop stability analysis is carried out and to show the feasibility of the proposed approach it is tested in simulations on the non-linear plant of a passenger aircraft.

Web URL: **http://digital-library.theiet.org/content/journals/10.1049/iet-cta.2016.1247**

9. Majed, A., Salam, Z., & Amjad, A. M. (2017). Harmonics elimination PWM based direct control for 23-level multilevel distribution STATCOM using differential evolution algorithm. *Electric Power Systems Research*, *152*, 48-60.

ABSTRACT:

This work describes the application of a soft computing technique—known as the differential evolution (DE) to implement the harmonics elimination pulse-width modulation (HEPWM) for the direct control of distribution static synchronous compensator (D-STATCOM). The main contribution of the work is the application of DE to solve eleven HEPWM switching angles to synthesize a 23-level cascaded multilevel voltage source inverter (MVSI). The key feature of this algorithm is the wide modulation index (M_I) range that can be produced (i.e. 5.40–8.15 p.u) with very small step size (0.01), while maintaining the total harmonic distortion (THD) of the MVSI output voltage below 5%. Furthermore, the utilization of high levels MVSI allows for the output voltage of the D-STATCOM to be sufficiently high, thus avoiding the use of step-up transformer. The correctness of the computed HEPWM angles is validated using single phase 23-level cascaded MVSI experimental rig. Then, the proposed method is compared to the phase-shifted PWM (PS-PWM) using a ±6.5 MVAr/11 kV D-STATCOM modelled in MATLAB-Simulink. For the same switching frequency, the HEPWM switching results in a superior

harmonics spectra and lower switching losses. Furthermore, if the switching frequency is fixed to a particular value, the size of the series coupling inductor can be reduced to at least half. Dynamically, the steady state value of the reactive current (i_{Cq}) is reached in less than one mains cycle when a transition from the full inductive to full capacitive modes is imposed.

Web URL: ***https://www.sciencedirect.com/science/article/pii/S0378779617302717***

10. Khalid, A., & Asif, H. M. (2017). OCDMA and OSTBC based VLC transceiver design using NI cDAQ. *Photonic Network Communications*, 1-12.

ABSTRACT:

Visible light communication (VLC) is a novel technology especially for short-range data communication. IEEE has standardized VLC for 5*G* systems as a means to short-range wireless communication. In this paper, a complete state-of-the-art VLC software-defined radio is designed using NI cDAQ components tools developed in LabVIEW/MATLAB. The main objectives in designing a VLC transceiver are the suitable envelope for driving LEDs (transmitters) and a high data rate. The current work makes use of optical code division multiple access mainly to achieve the said objectives. It is shown through comparison with existing system that the proposed system is computationally less expensive and provides improved data rate. Finally, simulation programs are also developed and the proposed system is compared with the existing system in terms of bit error rate.

Web URL: **https://link.springer.com/article/10.1007/s11107-017-0722-z**

11. Ghous, I., Xiang, Z., & Karimi, H. R. (2017). H∞ control of 2-D continuous Markovian jump delayed systems with partially unknown transition probabilities. *Information Sciences*, *382*, 274-291.

ABSTRACT:

This study focuses on stochastic stability and H_∞ control of two-dimensional (2-D) continuous delayed Markovian jump systems (MJSs) with partial information on transition probability. At first, a sufficient condition for the stochastic stability of 2-D MJSs is proposed by choosing an appropriate Lyapunov–Krasovskii functional. Then, the results are developed by designing a state feedback controller that guarantees the stochastic stability of the resultant closed-loop

system with a prescribed H_∞performance level γ. Finally, the proposed results are validated with the help of examples.

Web URL: ***http://www.sciencedirect.com/science/article/pii/S0020025516320369***

12. Khan, A. A., & Brown, A. K. (2017). Optimisation of Scanning Difference Pattern and Monopulse Feed. ***International Journal of Antennas and Propagation*****, *2017*.**

ABSTRACT:

Certain radar applications may require maintaining the difference pattern slope and twin beam shape, while main null is scanning in the presence of mutual coupling. It is also desirable in monopulse radar applications to be able to generate acceptable sum and difference patterns using single simplified feed structure. This paper focuses on these problems and provides a solution based on Intelligent -Plane Boundary Condition-Particle Swarm Optimiser (IzBC-PSO) to compensate for the difference pattern degradation while scanning a small coupled array (). In second case, a simplified feed is proposed that only requires phase flip for 50% of elements to produce sum and difference patterns for the monopulse array, consisting of isotropic elements.

Web URL: ***http://downloads.hindawi.com/journals/ijap/2017/3869085.pdf***

13. Khan, A., Arif, A., Nawaz, T., & Baig, S. (2017). Walsh Hadamard transform based transceiver design for SC-FDMA with discrete wavelet transform. ***China Communications*****, *14*(5), 193-206.**

ABSTRACT:

This article proposes a new transceiver design for Single carrier frequency division multiple access (SCFDMA) system based on discrete wavelet transform (DWT). SCFDMA offers almost same structure as Orthogonal frequency division multiple access (OFDMA) with extra advantage of low Peak to Average Power Ratio (PAPR). Moreover, this article also suggests the application of Walsh Hadamard transform (WHT) for linear precoding (LP) to improve the PAPR performance of the system. Supremacy of the proposed transceiver over conventional Fast Fourier transform (FFT) based SCFDMA is shown through simulated results in terms of PAPR, spectral efficiency (SE) and bit error rate (BER).

Web URL: ***http://ieeexplore.ieee.org/abstract/document/7942326/***

14. Hanif, A., Bhatti, A. I., & Ahmed, Q. (2017). Managing Thermally Derated Torque of an Electrified Powertrain through LPV Control. ***IEEE/ASME Transactions on Mechatronics*****.**

ABSTRACT:

Vehicle with electrified powertrains exhibit degraded performance when operated in hot environments. When the operating and surrounding temperatures rise, an electric drive suffers from torque derating as its parameters change. This paper proposes a Linear Parameter Varying (LPV) based observer controller pair to address this problem. The feedback Field Oriented Control (FOC) is the most commonly adopted instantaneous torque control method for an electrified powertrain drive system. The flux and torque performance of a conventional feedback FOC deteriorates under the vast uncertainties in rotor and stator resistance due to temperature variations during Electric Vehicle (EV) operation. To cater for these uncertain scenarios, a robust closed-loop observer is designed to estimate the thermally derated torque and flux. The stability of the whole LPV scheme is established. The efficacy of the proposed algorithm is demonstrated for an EV operating in Federal Urban Driving Schedule (FUDS) with a dynamic temperature profile. The nonlinear simulation results confirm the LPV observer capability to successfully estimate the flux and derated torque in an EV drive system. The proposed technique, after validating in simulation environment, is verified experimentally on an Induction Machine (IM) drive controlled by NI myRIO-1900.

Web URL: **http://ieeexplore.ieee.org/abstract/document/8214268/**

15. Baig, S., Ahmad, M., Asif, H. M., Shahzad, M. N., & Jaffery, M. H. (2017). Dual PHY Layer for Non-Orthogonal Multiple Access Transceiver in 5G Networks. ***IEEE Access*****.**

ABSTRACT:

Non-orthogonal multiple access (NOMA) is a promising multiple access technique, proposed in literature for the fifth generation (5G) mobile networks. The NOMA system model consists of the conventional orthogonal frequency division multiplexing (OFDM), as a pulse shaping technique in conjunction with a variable power domain for various users, allocated in

proportion to each user's channel gain. OFDM technique based on wavelet filter banks, namely Wavelet OFDM (WOFDM) has been utilized in digital communication to improve the system robustness to noise and adjacent channel interference, and is therefore anticipated to be adopted for the NOMA technique. WOFDM in NOMA (WNOMA) outperforms OFDM based conventional NOMA (CNOMA) with reference to interference mitigation, bandwidth efficiency, spectral confinement and multi-user capacity. Most of the fourth generation (4G) networks are based on OFDM and its variants. Therefore, in this research work, keeping in view the interoperability with the fourth generation networks and the latency requirements in 5G, a dual physical layer based on conventional OFDM and WOFDM as pulse shaping methods, is proposed for the NOMA transceiver. Performance of WNOMA and CNOMA is analyzed for bit error rate in the presence of channel impairments including additive noise and IQ imbalance and multiuser capacity is also computed. Comparison of various parametersindicates the advantage of adopting WNOMA over its conventional counterpart for relatively poor channel conditions.

Web URL: **http://ieeexplore.ieee.org/stamp/stamp.jsp?arnumber=8239813**

DEPARTMENT OF COMPUTER SCIENCE

Journal Papers

1. Mushtaq, Z., Rasool, G., & Shahzad, B. (2017). Detection of J2EE Patterns based on Customizable. International Journal of Advanced Computer Science and Applications, 8(1). 361-376

ABSTRACT:

Design patterns support extraction of design information for better program understanding, reusability and reengineering. With the advent of contemporary applications, the extraction of design information has become quite complex and challenging. These applications are multilingual in nature i.e. their design information is spread across various language components that are interlinked with each other. At present, no approach is available that is

capable to extract design information of multilingual applications by using design patterns. This paper lays foundation for the analysis of multilingual source code for the detection of J2EE Patterns. J2EE Patterns provide design solutions for effective enterprise applications. A novel approach is presented for the detection of J2EE Patterns from multilingual source code of J2EE applications. For this purpose, customizable and reusable feature types are presented as definitions of J2EE Patterns catalogue. A prototype implementation is evaluated on a corpus that contains the repository of multilingual source code of J2EE Patterns. Additionally, the tool is tested on open source applications. The accuracy of the tool is validated by successfully recognizing J2EE Patterns from the multilingual source code. The results demonstrate the significance of customizable definitions of J2EE Pattern's catalogue and capability of prototype.

Web URL:

https://pdfs.semanticscholar.org/0470/2b72848054f43803a1b08e1085af0343f591.pdf

2. Sargano, A. B., Angelov, P., & Habib, Z. (2017). A comprehensive review on handcrafted and learning-based action representation approaches for human activity recognition. *Applied Sciences*, *7*(1), 110.

ABSTRACT:

Human activity recognition (HAR) is an important research area in the fields of human perception and computer vision due to its wide range of applications. These applications include: intelligent video surveillance, ambient assisted living, human computer interaction, human-robot interaction, entertainment, and intelligent driving. Recently, with the emergence and successful deployment of deep learning techniques for image classification, researchers have migrated from traditional handcrafting to deep learning techniques for HAR. However, handcrafted representation-based approaches are still widely used due to some bottlenecks such as computational complexity of deep learning techniques for activity recognition. However, approaches based on handcrafted representation are not able to handle complex scenarios due to their limitations and incapability; therefore, resorting to deep learning-based techniques is a natural option. This review paper presents a comprehensive survey of both handcrafted and learning-based action representations,

offering comparison, analysis, and discussions on these approaches. In addition to this, the well-known public datasets available for experimentations and important applications of HAR are also presented to provide further insight into the field. This is the first review paper of its kind which presents all these aspects of HAR in a single review article with comprehensive coverage of each part. Finally, the paper is concluded with important discussions and research directions in the domain of HAR.

Web URL: ***http://www.mdpi.com/2076-3417/7/1/110/htm***

3. Khan, A., Noreen, I., Ryu, H., Doh, N. L., & Habib, Z. (2017). Online complete coverage path planning using two-way proximity search. ***Intelligent Service Robotics*****,** ***10*****(3), 229-240.**

ABSTRACT:

This paper presents an efficient online approach for complete coverage path planning of mobile robots in an unknown workspace based on online boustrophedon motion and an optimized backtracking mechanism. The presented approach first performs a single continuous boustrophedon motion until a critical point is reached. In order to completely cover the environment, next starting point is decided by using the accumulated knowledge of the environment map. An efficient backtracking technique based on proposed Two-way Proximity Search algorithm is used to plan a path from the critical point to the new starting point. Simulation results show the efficiency of proposed backtracking approach with improved total coverage time, coverage path length and memory requirements.

Web URL: ***https://link.springer.com/article/10.1007/s11370-017-0223-z***

4. Athar, A., Ahmed, K., Abbas, S., & Saeed, Y. (2017). Modeling Cooperative and Competitive Emotions Using Parallel SOM for Artificially Intelligent Agents. ***International Journal of Computer Science and Network Security (IJCSNS)*****,** ***17*****(2), 270.**

ABSTRACT:

As an interactive structure in human mind the emotions contribute to the adaptive learning, rational decision making and communication proficiency. According to the psychological scheme of human mind, emotions have temporal dynamics and activate concurrently due to

the variance of environmental stimuli. The affective exposition of mind can express and communicate the shared or diverse effects of simultaneous emotions to the environment. The role of emotions in the nature of agency has been identified and partially addressed. However, in multi-agent scenarios (MAS) it is required to facilitate agents with the mechanism of interactive emotional dynamics to resolve conflicts and respond quickly. Inspired from neuropsychology, and by considering the function of emotions in the establishment of agency this paper attempts to analyze and design the synergy of emotional dynamics that addresses the cooperation and competition in emotions due to the change in their determining parameters to achieve autonomy.

Web URL: ***http://paper.ijcsns.org/07_book/201702/20170235.pdf***

5. Asghar, K., Habib, Z., & Hussain, M. (2017). Copy-move and splicing image forgery detection and localization techniques: a review. ***Australian Journal of Forensic Sciences*****,** ***49*****(3), 281-307.**

ABSTRACT:

Digital image acquisition is now a simple task and information in the form of digital images is drastically increasing on social media, which has both positive and negative impacts on a society in many different ways. Advanced user-friendly tools have made it easy to manipulate image content in order to gain illegal advantage or to make false propaganda, and digital images and videos are not acceptable in courts of law as evidence without reliable forensic analysis. A lot of research has been done in order to address this problem and many techniques exist that detect and localize copy-move and splicing forgeries. However, it is very important to know whether these methods are robust, properly modelling the structural changes that have occurred in images due to copy-move and/or splicing forgeries, and can reliably classify a digital image as a genuine or modified image. In this paper, we present an extensive literature review of the state-of-the-art techniques on copy-move and splicing forgeries, highlighting their limitations, and we provide future research directions.

Web URL: ***http://www.tandfonline.com/doi/abs/10.1080/00450618.2016.1153711***

6. Mehdi, M. M., Raza, I., & Hussain, S. A. (2017). A game theory based trust model for Vehicular Ad hoc Networks (VANETs). ***Computer Networks*****,** ***121*****, 152-172.**

ABSTRACT:

Vehicular Ad hoc Networks (VANETs) facilitate road safety, transportation security, reliability and management. This paper presents a game theory based trust model for VANETs. The proposed model is based on an attacker and defender security game to identify and counter the attacker/malicious nodes. The parameters considered for attackers and defender's strategy are majority opinion, betweenness centrality, and node density. The outcome of the specific game is determined by the game matrix which contains the cost (payoff) values for possible action-reaction combination. Nash equilibrium when applied to calculate the best strategy for attacker and defender vehicles. The model is simulated in Network Simulator (ns2), and results show that the proposed model performs better than the schemes with random malicious nodes and existing game theory based approach in terms of throughput, retransmission attempts and data drop rate for different attacker and defender scenarios.

Web URL: ***http://www.sciencedirect.com/science/article/pii/S1389128617301573***

7. Munawar, S., Hamid, M., Khan, M. S., Ahmed, A., & Hameed, N. (2017). Health Monitoring Considering Air Quality Index Prediction Using Neuro Fuzzy Inference Model: A Case Study of Lahore, Pakistan. ***Journal of Basic and Applied Sciences*****,** ***13*****, 123-132.**

ABSTRACT:

For many years, improving air quality has been great attention of the whole world. It has been recognized that air pollution as a hypothetically hazardous type of environmental pollution and polluted air directly affects the human health. In Asian countries, it has converged less attention of ever growing most alarming and hazardous issue of air pollution. This paper presents a case study of Lahore city of Pakistan for the prediction of Air Quality Index (AQI) using hybrid approach of Neuro Fuzzy (NF) inference system. The ambient air data of Lahore was taken from the Environmental Protection Department (EPD) working under government of the Punjab. For results evaluation, data was recorded at different station in the period from April 2007 to May 2015. The fuzzy rules have been generated according to the Pakistan

Environmental Protection Agency (PAK-EPA) standard of AQI. The NF Inference Model took the air pollutants such as Particulate Matter (PM2.5), Ozone (O3), Carbon Monoxide (CO), Sulphur Dioxide (SO2) and Nitrogen Dioxide (NO2) as inputs and predicted the air quality index as good, moderate, or unhealthy air. The results showed that NF based AQI prediction model classifies the AQI proficiently, robustly, and accurately as compared to conventional method.

Web URL: ***http://lifescienceglobal.com/pms/index.php/jbas/article/viewFile/4559/2588***

8. Qayum, M. A., & Naseer, M. (2017). A fast approach for finding design repeat in textile rotary printing for fault detection. *The Journal of The Textile Institute*, *108*(1), 62-65.

ABSTRACT:

Speed is the most critical factor for real-time defect detection in fabric rotary printing systems. Most of the methods proposed in the literature work by acquiring an error-free image and registering this image with subsequent images captured during the production. In these methods, major time-consuming problem is to find the design repeat in the sample image before further processing. We proposed a fast method for finding the design repeat. The method is tuned up according to the textile printing domain. During the printing process, the fabric moves in a horizontal direction, so the image registration can be restricted to the same direction. To further speed up the process, the image registration method is applied using few initial pixel columns of the reference image with the sample image. This bunch of selected columns of the reference image is matched with the same number of columns selected from the sample image by moving this bunch on the sample image column by column. The maximum matching position is marked as a start of the design repeat. Since the repeat size is always fixed, we can extract the complete design pattern from an acquired image for further processing of fault detection. Experimental results on different fabric designs using the above-mentioned method are very promising.

Web URL: ***http://www.tandfonline.com/doi/abs/10.1080/00405000.2015.1135579***

9. Rasool, G., & Arshad, Z. (2017). A Lightweight Approach for Detection of Code Smells. *Arabian Journal for Science and Engineering*, *42*(2), 483-506.

ABSTRACT:

The accurate removal of code smells from source code supports activities such as refactoring, maintenance, examining code quality etc. A large number of techniques and tools are presented for the specification and detection of code smells from source code in the last decade, but they still lack accuracy and flexibility due to different interpretations of code smell definitions. Most techniques target just detection of few code smells and render different results on the same examined systems due to different informal definitions and threshold values of metrics used for detecting code smells. We present a flexible and lightweight approach based on multiple searching techniques for the detection and visualization of all 22 code smells from source code of multiple languages. Our approach is lightweight and flexible due to application of SQL queries on intermediate repository and use of regular expressions on selected source code constructs. The concept of approach is validated by performing experiments on eight publicly available open source software projects developed using Java and C# programming languages, and results are compared with existing approaches. The accuracy of presented approach varies from 86–97 % on the eight selected software projects.

Web URL: ***https://link.springer.com/content/pdf/10.1007/s13369-016-2238-8.pdf***

10. Sharjeel, M., Nawab, R. M. A., & Rayson, P. (2017). COUNTER: corpus of Urdu news text reuse. ***Language Resources and Evaluation*****,** ***51*****(3), 777-803.**

ABSTRACT:

Text reuse is the act of borrowing text from existing documents to create new texts. Freely available and easily accessible large online repositories are not only making reuse of text more common in society but also harder to detect. A major hindrance in the development and evaluation of existing/new mono-lingual text reuse detection methods, especially for South Asian languages, is the unavailability of standardized benchmark corpora. Amongst other things, a gold standard corpus enables researchers to directly compare existing state-of-the-art methods. In our study, we address this gap by developing a benchmark corpus for one of the widely spoken but under resourced languages i.e. Urdu. The COrpus of Urdu News TExt Reuse (COUNTER) corpus contains 1200 documents with real examples of text reuse from the field of journalism. It has been manually annotated at document level with three

levels of reuse: wholly derived, partially derived and non derived. We also apply a number of similarity estimation methods on our corpus to show how it can be used for the development; evaluation and comparison of text reuse detection systems for the Urdu language. The corpus is a vital resource for the development and evaluation of text reuse detection systems in general and specifically for Urdu language.

Web URL: **https://link.springer.com/article/10.1007/s10579-016-9367-2**

11. Khan, A., Noreen, I., & Habib, Z. (2017). On Complete Coverage Path Planning Algorithms for Non-holonomic Mobile Robots: Survey and Challenges. ***Journal of Information Science & Engineering*****, *33*(1).**

ABSTRACT:

The problem of determining a collision free path within a region is an important area of research in robotics. One significant aspect of this problem is coverage path planning, which is a process to find a path that passes through each reachable position in the desired area. This task is fundamental to many robotic applications such as cleaning, painting, underwater operations, mine sweeping, lawn mowing, agriculture, monitoring, searching, and rescue operations. The total coverage time is significantly influenced by total number of turns, optimization of backtracking sequence, and smoothness in the complete coverage path. There is no comprehensive literature review on backtracking optimization and path smoothing techniques used in complete coverage path planning. Although the problem of coverage path planning has been addressed by many researchers. However, existing state of the art needs to be significantly improved, particularly in terms of accuracy, efficiency, robustness, and optimization. This paper aims to present the latest developments, challenges regarding backtracking sequence optimization, smoothness techniques, limitations of existing approaches, and future research directions.

Web URL:

https://pdfs.semanticscholar.org/ee6b/dd20dd58de3c4fe646103e76b46237821d38.pdf

12. Hussain, S. A., Khan, N. A., Sadiq, A., & Ahmad, F. (2010). Simulation, modeling and analysis of master node election algorithm based on signal strength for VANETs through Colored Petri nets. *Neural Computing and Applications*, 1-17.

ABSTRACT:

The broadcast storm problem causes redundancy, contention and collision of messages in a network, particularly in vehicular ad hoc networks (VANETs) where number of participants can grow arbitrarily. This paper presents a solution to this problem in which a node is designated as a master through an election process. Moreover, an algorithm is proposed for asynchronous *VANETs* to select a master node, where the participants (i.e., vehicles) can communicate with each other directly (single-hop). The proposed algorithm is extrema-finding in a way that a node having maximum signal strength is elected as a master node and each vehicle continues communication with the master until the master node keeps its signal strength at the highest level and remains operational too. This paper further presents the Petri net-based modeling of the proposed algorithm for evaluation which is going to be presented for the first time in leader election algorithm in *VANETs*. Verification of the proposed algorithm is carried out through state space analysis technique.

Web URL: ***https://link.springer.com/article/10.1007/s00521-016-2622-z***

13. Shah, N., Abid, S. A., Qian, D., & Mehmood, W. (2017). A survey of P2P content sharing in MANETs. *Computers & Electrical Engineering*, *57*, 55-68.

ABSTRACT:

Recently, several approaches have been proposed for Peer-to-peer (P2P) content/file sharing in mobile ad hoc networks (MANETs). In this article, we apprise a comprehensive survey of researches related to P2P overlay networks for sharing the content at the application layer in MANETs. We compare and contemplate the features, vitality, and vulnerability of these approaches and highlight indispensable research challenges that are imperative to address and will have substantial vantages. The fallout of the analysis would serve as a substantial guide for anyone willing to delve into research on the topic of P2P overlay over MANETs.

Web URL: ***http://www.sciencedirect.com/science/article/pii/S004579061631062X***

14. Hussain, S. A., Iqbal, M., Saeed, A., Raza, I., Raza, H., Ali, A., ... & Baig, A. (2017). An Efficient Channel Access Scheme for Vehicular Ad Hoc Networks. ***Mobile Information Systems*****, *2017*.**

ABSTRACT:

Vehicular Ad Hoc Networks (VANETs) are getting more popularity due to the potential Intelligent Transport Systems (ITS) technology. It provides many efficient network services such as safety warnings (collision warning), entertainment (video and voice), maps based guidance, and emergency information. VANETs most commonly use Road Side Units (RSUs) and Vehicle-to-Vehicle (V2V) referred to as Vehicle-to-Infrastructure (V2I) mode for data accessing. IEEE 802.11p standard which was originally designed for Wireless Local Area Networks (WLANs) is modified to address such type of communication. However, IEEE 802.11p uses Distributed Coordination Function (DCF) for communication between wireless nodes. Therefore, it does not perform well for high mobility networks such as VANETs. Moreover, in RSU mode timely provision of data/services under high density of vehicles is challenging. In this paper, we propose a RSU-based efficient channel access scheme for VANETs under high traffic and mobility. In the proposed scheme, the contention window is dynamically varied according to the times (deadlines) the vehicles are going to leave the RSU range. The vehicles with shorter time deadlines are served first and vice versa. Simulation is performed by using the Network Simulator (NS-3) v. 3.6. The simulation results show that the proposed scheme performs better in terms of throughput, backoff rate, RSU response time, and fairness.

Web URL: ***http://downloads.hindawi.com/journals/misy/2017/8246050.pdf***

15. Iqbal, J., Asif, M., Hanif, M. K., Hunain, M. Q., & Chaudary, M. H. (2017). Ad Tracking: Advertisement Tracking using Graphics Processing Unit. ***Journal of Engineering Technology (ISSN: 0747-9964)*****, *6*(2), 232-252.**

ABSTRACT:

Introduction: In this era of electronics communication, companies typically rely on the electronic media for marketing and advertisement campaigns to reach a broad audience. However, they have to bear a very high cost. The challenge through electronic media

advertisement is transparent pricing. Advertisers require a mechanism to avoid extra payment. There exists different advertisement tracking software's which is expensive and requires substantial processing power.

Methodology: In this research, an effective ad tracking software architecture is proposed using graphics processing unit to achieve better performance. This system will guaranty the accurate pricing of advertisement by calculating the exact amount of time slot for which the advertisement was on-air. **Result & Conclusion:** The proposed system provides an efficient and cost-effective solution for advertisement tracking. In a nutshell, it is concluded that advertisement through electronic media is a primary concern in these days and the proposed system will help companies transparent and accurate pricing.

Web URL: ***http://www.joetsite.com/wp-content/uploads/2017/07/Vol.-62-20-2017.pdf***

16. Tahir, A., Abid, S. A., & Shah, N. (2017). Logical Clusters in DHT-Paradigm for Scalable Routing in MANETs. ***Computer Networks*****.**

ABSTRACT:

Connectivity of nodes in the logical network is the minimal requirement for the functionality of a distributed hash table (DHT)-based routing protocol. In case of high mobility, frequent changes to the network topology introduce higher maintenance overhead for updating the mapping information that worsens not only the performance of these protocols, but also restricts their pertinence only to the networks with low mobility. In addition, the route to the destination node in such protocols is not immediately available which result in high lookup latency for the requesting node.

In this paper, we proposes a novel 3-dimensional logical cluster-based DHT routing protocol for mobile ad hoc network (MANETs) that use logical clustering and an effective replication strategy to reduce the routing overhead and lookup latency introduced by the above problems. Simulation results substantiate the effectiveness of the proposed protocol in terms of reducing the delay by slightly increasing the control overhead.

Web URL: ***http://www.sciencedirect.com/science/article/pii/S1389128617302499***

17. Fatima, M., Hasan, K., Anwar, S., & Nawab, R. M. A. (2017). Multilingual author profiling on Facebook. *Information Processing & Management*, *53*(4), 886-904.

ABSTRACT:

Author profiling is the identification of demographic features of an author by examining his written text. Recently, it has attracted the attention of research community due to it's potential applications in forensic, security, marketing, fake profiles identification on online social networking sites, capturing sender of harassing messages etc. We need benchmark corpora to develop and evaluate techniques for author profiling. Majority of the existing corpora are for English and other European languages but not for under–resourced South Asian languages, like Roman Urdu (written using English alphabets). Roman Urdu is used in daily communication by a large number of native speakers of Urdu around the world particularly in Facebook posts/comments, Twitter tweets, blogs, chat blogs and SMS messaging. The construction of sentences of Urdu while using alphabets of English transforms the language properties of the text. We aim to investigate the behavior of existing author profiling techniques for multilingual text consisting of English and Roman Urdu, concretely for gender and age identification. We here focus on author profiling on Facebook by (i) developing a multilingual (Roman Urdu and English) corpus, (ii) manually building of a bilingual dictionary for translating Roman Urdu words into English, (iii) modeling existing state-of-the-art author profiling techniques by using content based features (word and character N–grams) and 64 different stylistic based features (11 lexical word based features, 47 lexical character based features and 6 vocabulary richness measures) for age and gender identification on multilingual and translated corpora, (iv) evaluating and comparing the behavior of above mentioned techniques on multilingual and translated corpora. Our extensive empirical evaluation shows that (i) existing author profiling techniques can be used for multilingual text (Roman Urdu + English) as well as monolingual text (corpus obtained after translating multilingual corpus using bilingual dictionary), (ii) content based methods outperform stylistic based methods for both gender and age identification task and (iii) translation of multilingual corpus to monolingual text does not improve results.

Web URL: **https://www.sciencedirect.com/science/article/pii/S0306457316302424**

18. Rathore, S., Habes, M., Iftikhar, M. A., Shacklett, A., & Davatzikos, C. (2017). A review on neuroimaging-based classification studies and associated feature extraction methods for Alzheimer's disease and its prodromal stages. *NeuroImage*.

ABSTRACT:

Neuroimaging has made it possible to measure pathological brain changes associated with Alzheimer's disease (AD) in vivo. Over the past decade, these measures have been increasingly integrated into imaging signatures of AD by means of classification frameworks, offering promising tools for individualized diagnosis and prognosis. We reviewed neuroimaging-based studies for AD and mild cognitive impairmentclassification, selected after online database searches in Google Scholar and PubMed (January, 1985–June, 2016). We categorized these studies based on the following neuroimaging modalities (and sub-categorized based on features extracted as a post-processing step from these modalities): i) structural magnetic resonance imaging[MRI] (tissue density, cortical surface, and hippocampal measurements), ii) functional MRI (functional coherence of different brain regions, and the strength of the functional connectivity), iii) diffusion tensor imaging (patterns along the white matter fibers), iv) fluorodeoxyglucose positron emission tomography (FDG-PET) (metabolic rate of cerebral glucose), and v) amyloid-PET (amyloid burden). The studies reviewed indicate that the classification frameworks formulated on the basis of these features show promise for individualized diagnosis and prediction of clinical progression. Finally, we provided a detailed account of AD classification challenges and addressed some future research directions.

Web URL: **https://www.sciencedirect.com/science/article/pii/S1053811917302823**

19. Gilanie, G., Ullah, H., Mehmood, M., Bajwa, U. I., & Habib, Z. (2017). Colored Representation of Brain Gray Scale MRI Images to Potentially Underscore the Variability and Sensitivity of Images. *Current Medical Imaging Reviews*, *13*, 000-000.

ABSTRACT:

Objective: The drive of this research activity is to report a colorization method to enhance the visualization, cell characterization and interpretation of brain Magnetic Resonance (MR) images, indicative of the underlying physical density of bio tissues.

Background: In daily health care environments, medical scanners are being used to generate gray scale images of anatomical structures.

Method: Severity of diseases is determined from this luminance component only. Irrefutably, if this high dimensional gray scale, medical data is visualized in colored versions, the definitive and more accurate the pathological assessment process will be. A number of methods have been reported to represent brain Magnetic Resonance Images (MRI) data in color with the cost of computational complexity. In this research work, an efficient method of colorization using frequencies from visible range of color spectrum, has been proposed to embody the variations and sensitivity of the brain MRI images

Web URL:

https://www.researchgate.net/profile/Ghulam_Gilanie/publication/316738329_Colored_Representation_of_Brain_Gray_Scale_MRI_Images_to_potentially_underscore_the_variability_and_sensitivity_of_images/links/59c52416aca272c71bb8d856/Colored-Representation-of-Brain-Gray-Scale-MRI-Images-to-potentially-underscore-the-variability-and-sensitivity-of-images.pdf

20. Mushtaq, Z., Rasool, G., & Shehzad, B. (2017). Multilingual source code analysis: A systematic literature review. *IEEE Access*.

ABSTRACT:

Contemporary software applications are developed using cross-language artifacts which are interdependent with each other. The source code analysis of these applications requires the extraction and examination of artifacts which are build using multiple programming languages along with their dependencies. A large number of studies presented on multilingual source code analysis and its applications in the last one and half decade. The objective of this systematic review (SLR) is to summarize state of the art and prominent areas for future research. This systematic literature review is based on different techniques, tools and methodologies to analyze multilingual source code applications. We finalized 56 multi-discipline

published papers relevant to multilingual source code analysis and its applications out of 3820 papers, filtered through multi-stage search criterion. Based on our findings, we highlight research gaps and challenges in the field of multilingual applications. The research findings are presented in the form of research problems, research contributions, challenges and future prospects. We identified 46 research issues and requirements for analyzing multilingual applications and grouped them in 13 different software engineering domains. We examined the research contributions and mapped them with individual research problems. We presented the research contributions in the form of tools techniques and approaches that are presented in the form of research models, platforms, frameworks, prototype models and case studies. Every research has its limitations or prospects for future research. We highlighted the limitations and future perspectives and grouped them in various software engineering domains. Most of the research trends and potential research areas are identified in static source code analysis, program comprehension, refactoring, reverse engineering, detection, and traceability of crosslanguage links, code coverage, security analysis, crosslanguage parsing and abstraction of source code models.

Web URL: **http://ieeexplore.ieee.org/stamp/stamp.jsp?arnumber=7953501**

21. Rasool, G., & Arshad, Z. (2017). A Lightweight Approach for Detection of Code Smells. *Arabian Journal for Science and Engineering*, *42*(2), 483-506.

ABSTRACT:

The accurate removal of code smells from source code supports activities such as refactoring, maintenance, examining code quality etc. A large number of techniques and tools are presented for the specification and detection of code smells from source code in the last decade, but they still lack accuracy and flexibility due to different interpretations of code smell definitions. Most techniques target just detection of few code smells and render different results on the same examined systems due to different informal definitions and threshold values of metrics used for detecting code smells. We present a flexible and lightweight approach based on multiple searching techniques for the detection and visualization of all 22 code smells from source code of multiple languages. Our approach is lightweight and flexible

due to application of SQL queries on intermediate repository and use of regular expressions on selected source code constructs. The concept of approach is validated by performing experiments on eight publicly available open source software projects developed using Java and C# programming languages, and results are compared with existing approaches. The accuracy of presented approach varies from 86–97 % on the eight selected software projects.

Web URL: **https://link.springer.com/content/pdf/10.1007/s13369-016-2238-8.pdf**

22. Noreen, I., Khan, A., Ryu, H., Doh, N. L., & Habib, Z. (2017). Optimal path planning in cluttered environment using RRT*-AB. *Intelligent Service Robotics*, 1-12.

ABSTRACT:

Rapidly exploring Random Tree Star (RRT*) has gained popularity due to its support for complex and high-dimensional problems. Its numerous applications in path planning have made it an active area of research. Although it ensures probabilistic completeness and asymptotic optimality, its slow convergence rate and large dense sampling space are proven problems. In this paper, an off-line planning algorithm based on RRT* named RRT*-adjustable bounds (RRT*-AB) is proposed to resolve these issues. The proposed approach rapidly targets the goal region with improved computational efficiency. Desired objectives are achieved through three novel strategies, i.e., connectivity region, goal-biased bounded sampling, and path optimization. Goal-biased bounded sampling is performed within boundary of connectivity region to find the initial path. Connectivity region is flexible enough to grow for complex environment. Once path is found, it is optimized gradually using node rejection and concentrated bounded sampling. Final path is further improved using global pruning to erode extra nodes. Robustness and efficiency of proposed algorithm is tested through experiments in different structured and unstructured environments cluttered with obstacles including narrow and complex maze cases. The proposed approach converges to shorter path with reduced time and memory requirements than conventional RRT* methods.

Web URL: **https://link.springer.com/article/10.1007/s11370-017-0236-7**

23. Idris, A., Iftikhar, A., & ur Rehman, Z. (2017). Intelligent churn prediction for telecom using GP-AdaBoost learning and PSO undersampling. *Cluster Computing*, 1-15.

ABSTRACT:

Nowadays, telecom industry faces fierce competition in satisfying its customers. This competition thus requires an efficient churn prediction system to identify customers who are ready to quit. Such churn customers are then retained through addressing relevant reasons identified by the churn prediction system. Therefore, now the role of churn prediction system is not only restricted to accurately predict churners but also to interpret customer churn behavior. In this paper, searching capabilities of genetic programming (GP) and classification capabilities of AdaBoost are integrated in order to evolve a high-performance churn prediction system having better churn identification abilities. For this, frequently selected features in various GP expressions evaluated through AdaBoost based learning, are marked and analyzed. Moreover, the issue of imbalance present in telecom datasets is also addressed through particle swarm optimization (PSO) based undersampling method, which provides unbiased distribution of training set to GP-AdaBoost based prediction system. Particle swarm optimization based undersampling method in combination with GP-AdaBoost results a churn prediction system (ChP-GPAB), which offers better learning of churners and also identifies underlying factors responsible for churn behavior of customers. Two standard telecom data sets are used for evaluation and comparison of the proposed ChP-GPAB system. The results show that the proposed ChP-GPAB system yields 0.91 AUC and 0.86 AUC on Cell2Cell and Orange datasets, in addition to identifying the reasons of churning.

Web URL: **https://link.springer.com/article/10.1007/s10586-017-1154-3**

24. Ahmad, S., Asif, M., Talib, R., Adeel, M., Yasir, M., & Chaudary, M. H. (2017). Surveillance of intensity level and geographical spreading of dengue outbreak among males and females in Punjab, Pakistan: A case study of 2011. *Journal of infection and public health*.

ABSTRACT:

Background

Dengue fever is viral disease which spreads due to the bite of the *Aedes aegypti*mosquito. In recent years, it has affected around 40% population of the world. Its endemic flow has led to a large disease burden, in terms of human and financial resources.

Methods

Geographical Information Systems (GIS) are normally used to develop epidemiological thematic maps. This study explores the patterns and hotspots, associated with the catastrophic outbreak of dengue, in Punjab, in 2011. The ArcView software was used to analyze the data reported by the district hospitals of Punjab. Twenty-one-thousand cases were reported from March to December 2011, with 300 causalities.

Results and conclusion

This research reveals that from among the total 37 epidemiological weeks, the maximum impact was observed between weeks 22 and 27. The geographical flow and hotspots associated with dengue have been shown through thematic maps. A positive correlation between the risk for dengue and age was observed. The findings of this research can help health officials and decision-makers alert the public about future outbreaks and take preventive measures to considerably reduce the mortality and morbidity associated with the disease.

Web URL: **https://www.sciencedirect.com/science/article/pii/S1876034117302770**

25. Ahmad, S., Asif, M., Majid, M., Ashraf, M. W., Chaudary, M. H., & Iqbal, M. An Effective Study of Geographical Pattern and Intensity of Dengue Epidemic among Females in Punjab, Pakistan.

ABSTRACT:

Introduction: An emerging issue all over the world, especially in the tropical countries, is dengue fever now a day. It is a viral communicating disease which flows from one person to other through female mosquito is known as Aedes aegypti. In the short time, its outburst ruins the human and financial resources. Most of the countries with limited technical infrastructure are unable to fight with this disease in a proficient way.

Methodology: Geographical Information System (GIS) is a smart way to express Epidemiological information in the form of thematic maps which represent geographical pattern and intensity of outbreak.

Result & Conclusion: In this research study, we used ArcView tool to express female patient's data of Dengue outbreak in 2011.Almost seven thousand females were affected due to Dengue fever in Punjab Province in thirty-seven epidemiological weeks from March 2011 to December 2011.Our research revealed Geographical Pattern and Intensity of Dengue fever among females of all ages in Punjab province. It can assist administrative authorities and health departments for future awareness and preventive measures to take in time action to save human and financial resources.

Web URL: **http://www.joetsite.com/wp-content/uploads/2017/11/Vol.-63-5-17.pdf**

26. Ahmad, A., Whitworth, B., Zeshan, F., Bertino, E., & Friedman, R. (2017). Extending social networks with delegation. *Computers & Security*, *70*, 546-564.

ABSTRACT:

Despite their enormous growth, current social networks lack a systematic approach to delegate rights – when an entity authorizes another to access the resources on its behalf. This paper proposes a delegation model based on socio-technical design and theory of cooperation and collaboration that best suits the requirements of social networks. The model is formulated through formal methods, designed using ontologies and implemented through Facebook APIs. The model's expressiveness is examined for overlapping policies of multiple users, its consistency is analyzed for conflicting and redundant policies and user acceptance testing is performed for acceptability. For social validity, the model is also compared with 27 previous delegation models with respect to socio-technical validity parameters derived from social principles already accepted in the human society.

Web URL: **https://www.sciencedirect.com/science/article/pii/S0167404817301517**

27. Zeshan, F., Mohamad, R., Ahmad, M. N., Hussain, S. A., Ahmad, A., Raza, I., ... & Babar, I. (2017). Ontology-based service discovery framework for dynamic environments. *IET Software*, *11*(2), 64-74.

ABSTRACT:

With all the recent advancements in the electronic world, hardware is becoming smaller, cheaper and more powerful; while the software industry is moving towards service-oriented integration technologies. Hence, service oriented architecture is becoming a popular platform for the development of applications for distributed embedded real-time system (DERTS). With rapidly increasing diversity of services on the internet, new demands have been raised concerning the efficient discovery of heterogeneous device services in the dynamic environment of DERTS. Context-awareness principles have been widely studied for DERTS; hence, it can be used as an additional set of service selection criteria. However, in order to use context information effectively, it should be presented in an unambiguous way and the dynamic nature of the embedded and real-time systems should be considered. To address these challenges, the authors present a service discovery framework for DERTS which uses context-aware ontology of embedded and real-time systems and a semantic matching algorithm to facilitate the discovery of device services in embedded and real-time system environments. The proposed service discovery framework also considers the associated priorities with the requirements posed by the requester during the service discovery process

Web URL: **http://ieeexplore.ieee.org/document/7907373/**

28. Jamal, M. H., Prakash, A., & Kulkarni, M. (2017). Exploiting semantics of temporal multi-scale methods to optimize multi-level mesh partitioning. ***International Journal for Numerical Methods in Engineering*****.**

ABSTRACT:

Multi-scale problems are often solved by decomposing the problem domain into multiple subdomains, solving them independently using different levels of spatial and temporal refinement, and coupling the subdomain solutions back to obtain the global solution. Most commonly, finite elements are used for spatial discretization, and finite difference time stepping is used for time integration. Given a finite element mesh for the global problem domain, the number of possible decompositions into subdomains and the possible choices for associated time steps is exponentially large, and the computational costs associated with different decompositions can vary by orders of magnitude. The problem of finding an optimal

decomposition and the associated time discretization that minimizes computational costs while maintaining accuracy is nontrivial. Existing mesh partitioning tools, such as METIS, overlook the constraints posed by multi-scale methods and lead to suboptimal partitions with a high performance penalty. We present a multi-level mesh partitioning approach that exploits domain-specific knowledge of multi-scale methods to produce nearly optimal mesh partitions and associated time steps automatically. Results show that for multi-scale problems, our approach produces decompositions that outperform those produced by state-of-the-art partitioners like METIS and even those that are manually constructed by domain experts.

Web URL: **http://onlinelibrary.wiley.com/doi/10.1002/nme.5506/full**

29. Hussain, S. A., Fatima, M., Saeed, A., Raza, I., & Shahzad, R. K. (2017). Multilevel classification of security concerns in cloud computing. ***Applied Computing and Informatics*****,** ***13*****(1), 57-65.**

ABSTRACT:

Threats jeopardize some basic security requirements in a cloud. These threats generally constitute privacy breach, data leakage and unauthorized data access at different cloud layers. This paper presents a novel multilevel classification model of different security attacks across different cloud services at each layer. It also identifies attack types and risk levels associated with different cloud services at these layers. The risks are ranked as low, medium and high. The intensity of these risk levels depends upon the position of cloud layers. The attacks get more severe for lower layers where infrastructure and platform are involved. The intensity of these risk levels is also associated with security requirements of data encryption, multi-tenancy, data privacy, authentication and authorization for different cloud services. The multilevel classification model leads to the provision of dynamic security contract for each cloud layer that dynamically decides about security requirements for cloud consumer and provider.

Web URL: **https://www.sciencedirect.com/science/article/pii/S2210832716300011**

30. Adnan, M., Latif, M. A., & Nazir, M. (2017). Estimating Evapotranspiration using Machine Learning Techniques. ***INTERNATIONAL JOURNAL OF ADVANCED COMPUTER SCIENCE AND APPLICATIONS*****,** ***8*****(9), 108-113.**

ABSTRACT:

The measurement of evapotranspiration is the most important factor in irrigation scheduling. Evapotranspiration means loss of water from the surface of plant and soil. Evaporation parameters are being used in studying water balances, water resource management, and irrigation system design and for estimating plant growth and height as well. Evapotranspiration is measured by different methods by using various parameters. Evapotranspiration varies with the climate change and as the climate has a lot of variation geographically, the pre-developed systems have not used all available meteorological data hence not robust models. In this research work, a model is developed to estimate evapotranspiration with more authentic and accurate reduced meteorological parameters using different machine learning techniques. The study reveals to learn and generalize the relationship among different parameters. The dataset with reduced dimension is modeled through time series neural network giving the regression value R=83%.

Web URL:

https://pdfs.semanticscholar.org/239d/064c337903805feb8e5339cb37583d62ebcf.pdf

31. Jadoon, N. K., Anwar, W., Bajwa, U. I., & Ahmad, F. (2017). Statistical machine translation of Indian languages: a survey. *Neural Computing and Applications*, 1-13.

ABSTRACT:

In this study, performance analysis of a state-of-art phrase-based statistical machine translation (SMT) system is presented on eight Indian languages. State of the art in SMT on different Indian languages to English language has also been discussed briefly. The motivation of this study was to promote the development of SMT and linguistic resources for these Indian language pairs, as the current systems are in infancy stage due to sparse data resources. EMILLE and crowdsourcing parallel corpora have been used in this study for experimental purposes. The study is concluded by presenting the performance of baseline SMT system for Indian languages (Bengali, Gujarati, Hindi, Malayalam, Punjabi, Tamil, Telugu and Urdu) into English with average 10–20 % accurate results for all the language pairs. As a result of this study, both of these annotated parallel corpora resources and SMT system will

serve as benchmarks for future approaches to SMT in Hindi → English, Urdu → English, Punjabi → English, Telugu → English, Tamil → English, Gujarati → English, Bengali → English and Malayalam → English.

Web URL: **https://link.springer.com/article/10.1007/s00521-017-3206-2**

32. Rahman, U. U., Sargano, A. B., & Bajwa, U. I. (2017). Android-Based Verification System for Banknotes. *Journal of Imaging*, *3*(4), 54.

ABSTRACT:

With the advancement in imaging technologies for scanning and printing, production of counterfeit banknotes has become cheaper, easier, and more common. The proliferation of counterfeit banknotes causes loss to banks, traders, and individuals involved in financial transactions. Hence, it is inevitably needed that efficient and reliable techniques for detection of counterfeit banknotes should be developed. With the availability of powerful smartphones, it has become possible to perform complex computations and image processing related tasks on these phones. In addition to this, smartphone users have increased greatly and numbers continue to increase. This is a great motivating factor for researchers and developers to propose innovative mobile-based solutions. In this study, a novel technique for verification of Pakistani banknotes is developed, targeting smartphones with android platform. The proposed technique is based on statistical features, and surface roughness of a banknote, representing different properties of the banknote, such as paper material, printing ink, paper quality, and surface roughness. The selection of these features is motivated by the X-ray Diffraction (XRD) and Scanning Electron Microscopy (SEM) analysis of genuine and counterfeit banknotes. In this regard, two important areas of the banknote, i.e., serial number and flag portions were considered since these portions showed the maximum difference between genuine and counterfeit banknote. The analysis confirmed that genuine and counterfeit banknotes are very different in terms of the printing process, the ingredients used in preparation of banknotes, and the quality of the paper. After extracting the discriminative set of features, support vector machine is used for classification. The experimental results confirm the high accuracy of the proposed technique.

Web URL: **http://www.mdpi.com/2313-433X/3/4/54/htm**

33. Obaid, I., Kazmi, S. A. R., & Qasim, A. (2017). Modeling and Verification of Payment System in E-Banking. ***INTERNATIONAL JOURNAL OF ADVANCED COMPUTER SCIENCE AND APPLICATIONS*****, *8*(8), 195-201.**

ABSTRACT:

Formal modeling and verification techniques have been used to ensure the reliability and accuracy of multiple systems to be verified. In contrast to ordinary testing techniques which exhibit the presence of flaws and errors in a system, formal methods prove their absence. Electronic banking (ebanking) services have become very popular with the escalating development in the information and communication technology. Due to the presence of complexity, an e-banking system requires an efficient security model. One important approach to ensure the reliability and security of the e-banking system is through the use of formal methodologies. This study explores the opportunity of modeling interbank payment system through a case study of 1- link Automated Teller Machine (ATM). A generic verification system SPIN (Simple Promela Interpreter) is, therefore, employed to model and then to verify the integrity and security of payment system in e-banking. Linear temporal logic formulas are further summarized to assure the security of the e-banking system. The principal conclusion of the work includes a complete procedure of verification and modeling of the payment system in 1-link ATMs.

Web URL:

https://pdfs.semanticscholar.org/2071/c1ad9e4a6e7f5b20d54a9711d25de2405c77.pdf

34. Sameen, S., Sharjeel, M., Nawab, R. M. A., Rayson, P., & Muneer, I. (2017). Measuring Short Text Reuse For The Urdu Language. ***IEEE Access*****.**

ABSTRACT:

Text reuse occurs when one borrows the text (either verbatim or paraphrased) from an earlier written text. A large and increasing amount of digital text is easily and readily available, making it simpler to reuse but difficult to detect. As a result, automatic detection of text reuse has

attracted the attention of the research community due to the wide variety of applications associated with it. To develop and evaluate automatic methods for text reuse detection, standard evaluation resources are required. In this work, we propose one such resource for a significantly under-resourced language - Urdu, which is widely used in day to day communication and has a large digital footprint particularly in the Indian subcontinent. Our proposed Urdu Short Text Reuse Corpus contains 2,684 short Urdu text pairs, manually labelled as verbatim (496), paraphrased (1,329), and independently written (859). In addition, we describe an evaluation of the corpus using various state-of-the-art text reuse detection methods with binary and multi-classification settings and a set of four classifiers. Output results show that Character n-gram Overlap using J48 classifier outperform other methods for the Urdu short text reuse detection task.

Web URL: **http://ieeexplore.ieee.org/stamp/stamp.jsp?arnumber=8118088**

35. Asghar, K., Gilanie, G., Saddique, M., & Habib, Z. (2017). Automatic Enhancement Of Digital Images Using Cubic Bézier Curve And Fourier Transformation. ***Malaysian Journal of Computer Science*****,** ***30*****(4), 300-310.**

ABSTRACT:

Image enhancement is one of the most important and visually appealing areas of digital image processing and computer vision. It is considered as a very important part of pre-processing for the development of industrial, security, forensic, medical, and many other applications. Although significant efforts were devoted in the past, a completely automatic image enhancement for all types of input and applications is still a big challenge in the domain of image processing. In this paper, we have proposed a multi-disciplinary approach to enhance the image automatically by intensity transformation in the spatial domain through cubic Bézier curve on images filtered with low and high pass Butterworth in the frequency domain. Results are promising when compared with the existing state-of-the-arts techniques for both visually and quantitatively, which proved that the proposed method can ensure better contrast enhancement.

Web URL: **http://mjes.um.edu.my/index.php/MJCS/article/view/9894**

36. Gilanie, G., Bajwa, U. I., Waraich, M. M., Habib, Z., Ullah, H., & Nasir, M. (2017). Classification of normal and abnormal brain MRI slices using Gabor texture and support vector machines. *Signal, Image and Video Processing*, 1-9.

ABSTRACT:

In computational and clinical environments, autoclassification of brain magnetic resonance image (MRI) slices as normal and abnormal is challenging. The purpose of this study is to investigate the computer vision and machine learning methods for classification of brain magnetic resonance (MR) slices. In routine health-care units, MR scanners are being used to generate a massive number of brain slices, underlying the anatomical details. Pathological assessment from this medical data is being carried out manually by the radiologists or neuro-oncologists. It is almost impossible to analyze each slice manually due to the large amount of data produced by MRI devices at each moment. Irrefutably, if an automated protocol performing this task is executed, not only the radiologist will be assisted, but a better pathological assessment process can also be expected. Numerous schemes have been reported to address the issue of autoclassification of brain MRI slices as normal and abnormal, but accuracy, robustness and optimization are still an open issue. The proposed method, using Gabor filter and support vector machines, classifies brain MRI slices as normal or abnormal. Accuracy, sensitivity, specificity and ROC-curve have been used as standard quantitative measures to evaluate the proposed algorithm. To the best of our knowledge, this is the first study in which experiments have been performed on Whole Brain Atlas-Harvard Medical School (HMS) dataset, achieving an accuracy of 97.5%, sensitivity of 99%, specificity of 92% and ROC-curve as 0.99. To test the robustness against medical traits based on ethnicity and to achieve optimization, a locally developed dataset has also been used for experiments and remarkable results with accuracy (96.5%), sensitivity (98%), specificity (92%) and ROC-curve (0.97) were achieved. Comparison with state-of-the-art methods proved the overall efficacy of the proposed method.

Web URL: **https://link.springer.com/article/10.1007/s11760-017-1182-8**

37. Bajwa, U. I., Shah, A. A., Waqas, M. Gilanie, G. & Bajwa, S. E. (2017). Computer-Aided Detection (CADe) System for Detection of Malignant Lung Nodules in CT Slices – A Key for Early Lung Cancer Detection. ***Current Medical Imaging Reviews. 13.***

ABSTRACT:

Lung cancer is the most common cancer in terms of both incidence and mortality. Where medical science is playing its role to overcome this deadly disease, new advancement's and research is also going on in computer science especially in the domain of image processing to support doctors and radiologists to tackle it. Developments are going on in image processing and CAD evaluation for applications that include cancer screening, diagnosis, and image-guided intervention, and treatment. The most efficient way to stop the cancer is to detect and diagnose it at early stage. Most of the existing CAD systems monitor the growth of lung nodules over a period of time, which is not possible at the early stage of lung cancer. In case of lung cancer treatment in Pakistan, even if the cancer is at later stages there are no such archives in which the history of patient is maintained. So in that case it becomes extremely important to develop such system which detects lung cancer at its early stage without depending on the requirement of patient history. Secondly majority of the CAD systems requires training prior to use and after the training they still can't produce satisfactory results. And the last point is most of the scanners comes with built-in software and most of the scanners doesn't support third party software's. In this study, a CAD system is proposed for the detection of malignant nodules through traditional image processing techniques fused with the techniques used by radiologists. The system goes through three main phases pre-processing, segmentation and 3D reconstruction. In first phase, pre-processing techniques were used to remove unwanted information and enhance the image for further processing. During second phase, the nodule was detected and localized and in the last phase, 3D reconstruction of the nodule performed for better visualization that supports the radiologist and the surgeon/doctor. By the end of the study we discussed the performance of our CAD system on LIDC dataset. This dataset consists of 1018 cases from which we randomly selected 340 cases and compared the results of our methodology using four different scenarios against studies which have used Artificial Neural

Networks (ANN) and Support Vector Machine (SVM). The methodology used in this study, clearly outperforms in two out of the four scenarios when compared to ANN and SVM

Web URL: **http://www.eurekaselect.com/node/153171/article/computer-aided-detection-cade-system-for-detection-of-malignant-lung-nodules-in-ct-slices-a-key-for-early-lung-cancer-detection**

38. Khan, M. S., & Younas, M. (2017). Analyzing readers behavior in downloading articles from IEEE digital library: a study of two selected journals in the field of education. *Scientometrics*, *110*(3), 1523-1537.

ABSTRACT:

In this study, we investigate the downloads behavior of readers for two well-known IEEE journals in the field of education, i.e., IEEE Transactions on Learning Technologies (TLT) and IEEE Transactions on Education (ToE). In our analysis, we found that articles in both journals are not downloaded rapidly in earlier months. The majority of articles reach to 50 and 80% of their first 12 months downloads' total in later months. Using linear regression analysis, we discovered that the cumulative first 12 months downloads of articles cannot be predicted by earlier months downloads. However, it can be predicted more accurately by using cumulative downloads count of later months. Moreover, we found that average downloads of articles in both journals increases rapidly as soon as they are assigned to an issue. In case of TLT which follows a delayed open access policy, we observed that average downloads after open access increases marginally for 2 months, and then it declines and continues to progress more or less in a consistent manner for 2 years. While in ToE which does not follow such policy, the average downloads decreases persistently.

Web URL: **https://link.springer.com/article/10.1007/s11192-016-2232-7**

39. Hannan, A., Bajwa, A. E., Riaz, S., Arshad, U., Saleem, S., & Bajwa, U. I. (2018). In vitro Salmonella typhi biofilm formation on gallstones and its disruption by Manuka honey. *Pakistan Journal of Pharmaceutical Sciences*, *31*(1).

ABSTRACT:

Biofilm is a complex community of single or different types of microorganisms (bacteria, viruses, fungi, protozoa) attached to a surface and stick to each other through production of extracellular matrix. Salmonella typhi forms biofilm on cholesterol gallstones resulting in carrier state. Once formed, biofilm is difficult to treat. To date cholecystectomy is the only cure for this condition. Manuka honey is known to have tremendous antibiofilm activity against various organisms. S. typhi biofilm was grown in vitro on clinical samples of human cholesterol gallstones by Gallstone tube assay method for 12 days. Biofilm mass was quantified on day 1, 5, 7, 9 and 12 by crystal violet assay and was also examined by scanning electron microscope. Three concentrations w/v of Manuka honey (40%, 60% and 80%) were used, each one at 24, 48 and 72 hours. The most effective concentration (80% w/v) was repeated on two sets of gallstones. Biofilm mass was re quantified by crystal violet assay and was examined by scanning electron microscope. S. typhi formed uniform biofilm on cholesterol gallstone surface. The optical density measurements exhibited a rising pattern with time thereby indicating an increase in biofilm mass. It was 0.2 on day 1 and 0.9 on day 12. With 80% w/v Manuka honey, biofilm mass decreased most effectively with 0.5 OD after 72 hours. Biofilm formation by S, typhi on gallstones is surface specific and bile dependant. Either increasing the duration (beyond 72 hours) of the effective concentration (80% w/v) of honey or increasing the concentration (above 80%) of honey for a specific duration (72 hour) may cause complete disruption of the S. typhi biofilm on gallstone. S. typhi forms biofilm on cholesterol gallstones surface in vitro and it can be visualized by scanning electron microscopy. Biofilm mass can be quantified using crystal violet assay. Among various concentrations 80% Manuka honey for 72 hours is most effective in disrupting S. typhi biofilm on gallstones in vitro as evident from crystal violet assay.

Web URL:

http://web.a.ebscohost.com/abstract?direct=true&profile=ehost&scope=site&authtype=crawler&jrnl=1011601X&AN=126675067&h=yoOM1yKYLxbghFA8ZNRSLNL%2f3EgDYU3KJx%2fF8yp%2bgv%2fmERvLmpc4aK7nCAjBhEc2a0xzVcjK4Of1FUcOmvMwng%3d%3d&crl=c&resultNs=AdminWebAuth&resultLocal=ErrCrlNotAuth&crlhashurl=login.aspx%3fdirect%3dtrue%26prof

ile%3dehost%26scope%3dsite%26authtype%3dcrawler%26jrnl%3d1011601X%26AN%3d126675067

40. Abbas, S., & Athar, A. (2017). Advance Modeling of Agriculture Farming Techniques Using Internet of Things. *IJCSNS*, *17*(12), 114.

ABSTRACT:

Now a days large number of problem occur in farming, Lack of water availability, poor soil condition, bad weather condition and no proper timings for cultivating crops. These problems arise due to static nature of values that are used for calculating all these problems. The problem can only be resolved by making a system dynamic. This paper presents the emerging IOT techniques that help in resolving such problems by using dynamic methodology. Smart framework will be developed that is having centralized control for water sprinkle, for soil condition a separate module will be developed that will check the soil composition and accordingly allows water intake. For weather condition and crop timings problem advance modeling will be done.

Web URL: http://paper.ijcsns.org/07_book/201712/20171216.pdf

41. Ahmad, F., Chen, Y., Hu, L., Wang, S., Wang, J., Chen, Z., ... & Shen, J. (2017). BrainStorm: a psychosocial game suite design for non-invasive cross-generational cognitive capabilities data collection. *Journal of Experimental & Theoretical Artificial Intelligence*, *29*(6), 1311-1323.

ABSTRACT:

Currently available traditional as well as videogame-based cognitive assessment techniques are inappropriate due to several reasons. This paper presents a novel psychosocial game suite, BrainStorm, for noninvasive cross-generational cognitive capabilities data collection, which additionally provides cross-generational social support. A motivation behind the development of presented game suite is to provide an entertaining and exciting platform for its target users in order to collect gameplaybased cognitive capabilities data in a non-invasive manner. An extensive evaluation of the presented game suite demonstrated high acceptability and

attraction for its target users. Besides, the data collection process is successfully reported as transparent and non-invasive.

Web URL:

https://pdfs.semanticscholar.org/ff3c/c5b4408fcdd8538e3198e95fe27df6384ff4.pdf

42. Mahmoodl, M. K., & Ahmad, F. (2017). An Informal Enumeration of Squares of 2 (k) Using Rooted Trees Arising From Congruences. *UTILITAS MATHEMATICA*, *105*, 41-51.

ABSTRACT:* *Not Found

Web URL:

43. Mian, N. A., & Ahmad, F. (2017). Modeling and Analysis of MAPE-K loop in Self Adaptive Systems using Petri Nets. *IJCSNS*, *17*(12), 158.

ABSTRACT:

Feedback loop plays a pivotal role in modeling of systems that have capability to adapt to new requirements during execution. These systems are categorized as self-adaptive systems (SAS) which can alter their working according to the inputs received from the environment. At present, we are surrounded by software systems that are either adaptive or self-adaptive. In both cases feedback loop has a major role in the adaptation process. Hence, reliable and efficient working of this loop is critical towards successful development of software systems that have ability to work with requirements that were not known at the time of development. Formal methods are mathematics of software and hardware systems, these methods include modeling languages and tools to model and analyze systems with use of concrete mathematical principles. Petri-Nets is a formal specification language that is used for analysis, modeling and testing of complex systems. In this paper we have presented an initial model of feedback loop using Petri-Nets. It has been observed that modeling and analysis of feedback loop using Petri-nets has been useful in verification of system at an abstract level and the generated model is free from deadlock and has capability to expand in future. This is an abstract model with limited inputs, invariants and constraints, this model will be enhanced for a complete SAS in future research.

Web URL: http://paper.ijcsns.org/07_book/201712/20171223.pdf

DEPARTMENT OF IRCBM

Journal Papers

1. Rahim, M. I., Weizbauer, A., Evertz, F., Hoffmann, A., Rohde, M., Glasmacher, B., ... & Mueller, P. P. (2017). Differential magnesium implant corrosion coat formation and contribution to bone bonding. ***Journal of Biomedical Materials Research Part A*****,** ***105*****(3), 697-709.**

ABSTRACT:

Magnesium alloys are presently under investigation as promising biodegradable implant materials with osteoconductive properties. To study the molecular mechanisms involved, the potential contribution of soluble magnesium corrosion products to the stimulation of osteoblastic cell differentiation was examined. However, no evidence for the stimulation of osteoblast differentiation could be obtained when cultured mesenchymal precursor cells were differentiated in the presence of metallic magnesium or in cell culture medium containing elevated magnesium ion levels. Similarly, in soft tissue no bone induction by metallic magnesium or by the corrosion product magnesium hydroxide could be observed in a mouse model. Motivated by the comparatively rapid accumulation solid corrosion products physicochemical processes were examined as an alternative mechanism to explain the stimulation of bone growth by magnesium-based implants. During exposure to physiological solutions a structured corrosion coat formed on magnesium whereby the elements calcium and phosphate were enriched in the outermost layer which could play a role in the established biocompatible behavior of magnesium implants. When magnesium pins were inserted into avital bones, corrosion lead to increases in the pull out force, suggesting that the expanding corrosion layer was interlocking with the surrounding bone. Since mechanical stress is a well-established inducer of bone growth, volume increases caused by the rapid accumulation of corrosion products and the resulting force development could be a key mechanism and provide an explanation for the observed stimulatory effects of magnesium-based implants in hard tissue.

Web URL: **http://onlinelibrary.wiley.com/doi/10.1002/jbm.a.35943/full**

2. Khan, U. S., Rahim, A., Khan, N., Muhammad, N., Rehman, F., Ahmad, K., & Iqbal, J. (2017). Aging study of the powdered magnetite nanoparticles. *Materials Chemistry and Physics*, *189*, 86-89.

ABSTRACT:

Magnetite nanoparticles were produced via co-precipitation method and then stored at room temperature for 6 years in aerobic atmosphere. Variations in the inherent solid phase and solid

interfacial properties of the prepared magnetite nanoparticles were investigated. For this purpose the fresh and aged samples were characterized using transmission electron microscopy, vibrating sample magnetometer, X-ray diffractometer and energy dispersive X-ray spectrometer. The solid phase transformations of magnetite nanoparticles to maghemite nanoparticles as well as formation of other iron oxides were happened. After aging of 6 years, no change was occurred in the magnetic features; however increase in particle size from 9.6 to 18.5 measured by transmission electron microscopy was confirmed. The crystallite size and vibrating sample magnetometer values were measured before and after aging and found to increase from 8.98 nm and 47.23 emu/g to 16.18 nm and 58.36 emu/g respectively. The formation of other iron oxides, recrystallization and agglomeration during aging process, caused a significant decrease in the specific surface area from 124.43 to 45.00 m^2/g of the stored sample.

Web URL: ***http://www.sciencedirect.com/science/article/pii/S0254058416309609***

3. Yar, M., Shahzadi, L., Farooq, A., Imran, S. J., Cerón-Carrasco, J. P., den-Haan, H., ... & Dvorak, Z. (2017). In vitro modulatory effects of functionalized pyrimidines and piperidine derivatives on Aryl hydrocarbon receptor (AhR) and glucocorticoid receptor (GR) activities. ***Bioorganic Chemistry*****,** ***71*****, 285-293.**

ABSTRACT:

The development of biologically active molecules based on molecular recognition is an attractive and challenging task in medicinal chemistry and the molecules that can activate/deactivate certain receptors are of great medical interest. In this contribution, selected pyrimidine/piperidine derivatives were synthesized and tested for the ability to activate/deactivate Aryl hydrocarbon receptor (AhR) and Glucocorticoid receptor (GR). Tested compounds are shown to activate the receptors but to much lesser extent than positive controls, dioxin and dexamethasone for Ahr and GR, respectively. However, some of them antagonized the positive controls action. Although further *in vivo* studies are needed to fully characterize the bioactivities of these compounds, the reported *in vitro* evidences demonstrate that they might be used as the modulators of AhR and GR activities

Web URL: ***http://www.sciencedirect.com/science/article/pii/S0045206816302115***

4. Rehman, F., Ahmed, K., Airoldi, C., Gaisford, S., Buanz, A., Rahim, A., ... & Volpe, P. L. (2017). Amine bridges grafted mesoporous silica, as a prolonged/controlled drug release system for the enhanced therapeutic effect of short life drugs. ***Materials Science and Engineering: C*****, *72*, 34-41.**

ABSTRACT:

Hybrid mesoporous silica SBA-15, with surface incorporated cross-linked long hydrophobic organic bridges was synthesized using stepwise synthesis. The synthesized materials were characterized by elemental analysis, infrared spectroscopy, nuclear magnetic resonance spectroscopy, nitrogen adsorption, X-rays diffraction, thermogravimetry and scanning and transmission electron microscopy. The functionalized material showed highly ordered mesoporous network with a surface area of 629.0 $m^2 g^{-1}$. The incorporation of long hydrophobic amine chains on silica surface resulted in high drug loading capacity (21% Mass/Mass) and prolonged release of ibuprofen up till 75.5 h. The preliminary investigations suggests that the synthesized materials could be proposed as controlled release devices to prolong the therapeutic effect of short life drugs such as ibuprofen to increase its efficacy and to reduce frequent dosage.

Web URL: ***http://www.sciencedirect.com/science/article/pii/S0928493116308074***

5. Nasir, M., Nawaz, M. H., Latif, U., Yaqub, M., Hayat, A., & Rahim, A. (2017). An overview on enzyme-mimicking nanomaterials for use in electrochemical and optical assays. ***Microchimica Acta*****, 1-20.**

ABSTRACT:

Various kinds of nanomaterials have been described in recent years that represent stable and low-cost alternatives to biomolecules (such as enzymes) for use in (bio)analytical methods. The materials typically include, metal/metal oxides, metal complexes, nanocomposites, porphyrins, phthalocyanines, smart polymers, and carbonaceous nanomaterials. Due to their biomimetic and other properties, such nano-materials may replace natural enzymes in

chemical sensors, biosensors, and in various kinds of bioassays. This overview (with 252 references) highlights the analytical potential of such nanomaterials. It is divided into sections on (a) the types of nanomaterials according to their intrinsic nature, (b) non-enzymatic sensor designs (including electrochemical, colorimetric, fluorescent and chemiluminescent methods), and (c), applications of non-enzymatic sensors in the biomedical, environmental and food analysis fields. We finally address current challenges and future directions.

Web URL: ***https://link.springer.com/article/10.1007/s00604-016-2036-8***

6. Afzal, A., Mujahid, A., Schirhagl, R., Bajwa, S. Z., Latif, U., & Feroz, S. (2017). Gravimetric Viral Diagnostics: QCM Based Biosensors for Early Detection of Viruses. *Chemosensors*, *5*(1), 7.

ABSTRACT:

Viruses are pathogenic microorganisms that can inhabit and replicate in human bodies causing a number of widespread infectious diseases such as influenza, gastroenteritis, hepatitis, meningitis, pneumonia, acquired immune deficiency syndrome (AIDS) etc. A majority of these viral diseases are contagious and can spread from infected to healthy human beings. The most important step in the treatment of these contagious diseases and to prevent their unwanted spread is to timely detect the disease-causing viruses. Gravimetric viral diagnostics based on quartz crystal microbalance (QCM) transducers and natural or synthetic receptors are miniaturized sensing platforms that can selectively recognize and quantify harmful virus species. Herein, a review of the label-free QCM virus sensors for clinical diagnostics and point of care (POC) applications is presented with major emphasis on the nature and performance of different receptors ranging from the natural or synthetic antibodies to selective macromolecular materials such as DNA and aptamers. A performance comparison of different receptors is provided and their limitations are discussed.

Web URL: ***http://www.mdpi.com/2227-9040/5/1/7/htm***

7. Xu, P., Zuo, H., Chen, B., Wang, R., Ahmed, A., Hu, Y., & Ouyang, J. (2017). Doxorubicin-loaded platelets as a smart drug delivery system: An improved therapy for lymphoma. *Scientific Reports*, *7*.

ABSTRACT:

Chemotherapy is majorly used for the treatment of many cancers, including lymphoma. However, cytotoxic drugs, utilized in chemotherapy, can induce various side effects on normal tissues because of their non-specific distribution in the body. Natural platelets are used as drug carriers because of their biocompatibility and specific targeting to vascular disorders, such as cancer, inflammation, and thrombosis. In this work, doxorubicin (DOX) was loaded in natural platelets for treatment of lymphoma. Results showed that DOX was loaded into platelets with high drug loading and encapsulation efficiency. DOX did not significantly induce morphological and functional changes in platelets. DOX-platelet facilitated intracellular drug accumulation through "tumor cell-induced platelet aggregation" and released DOX into the medium in a pH-controlled manner. This phenomenon reduced the adverse effects and enhanced the therapeutic efficacy. The growth inhibition of lymphoma Raji cells was enhanced, and the cardiotoxicity of DOX was reduced when DOX was loaded in platelets. DOX-platelet improved the anti-tumor activity of DOX by regulating the expression of apoptosis-related genes. Thus, platelets can serve as potential drug carriers to deliver DOX for clinical treatment of lymphoma

Web URL: ***https://www.ncbi.nlm.nih.gov/pmc/articles/PMC5309782/***

8. Khan, A. S., Man, Z., Arvina, A., Bustam, M. A., Nasrullah, A., Ullah, Z., ... & Muhammad, N. (2017). Dicationic imidazolium based ionic liquids: Synthesis and properties. *Journal of Molecular Liquids*, *227*, 98-105.

ABSTRACT:

In the present work, four dicationic ionic liquids (DILs) having 1,1-Bis(3-methylimidazolium-1-yl) butylene ($[C_4(Mim)_2]$) cation with counter anions namely hydrogensulfate, methanesulfonate, trifluoromethanesulfonate, and paratoluene sulfonate were synthesized and characterized. The structures of ILs were confirmed by ^{1}H NMR, ^{13}C and elemental analysis (CHNS). The effect of temperature and anion type on thermophysical properties such as refractive index, density and

viscosity were studied. Density and viscosity values were measured within the temperature range of 293.15–273.15 K. Moreover, thermal expansion coefficient, molecular volume, molar volume, free volume, standard entropy, and lattice energy were derived from the density and viscosity values. Viscosity values were used for calculation of activation energy using the Arrhenius equation. Refractive index values were measured in the temperature range of 293.15–323.15 K and the values of refractive index were used further to estimate the electronic polarizability using Lorenz-Lorentz equation. Thermal properties of the synthesized DILs were determined using thermogravimetric analyzer (TGA) and differential scanning calorimetry (DSC).

Web URL: ***http://www.sciencedirect.com/science/article/pii/S0167732216323364***

9. Akhtar, M. A., Riaz, S., Hayat, A., Nasir, M., Muhammad, N., Rahim, A., & Nawaz, M. H. (2017). Poly (ethylene oxide) tethered trans-porphyrin: Synthesis, self-assembly with fullerene (C 60) and DNA binding studies. ***Journal of Molecular Liquids*****, *225*, 235-239.**

ABSTRACT:

Trans-Porphyrin containing phenyl group at both ends was synthesized via corresponding dipyrromethanes (DPM) in the presence of TFA and DDQ. The polyethyleneglycole (PEG) chains were attached at the trans positions of ABA type porphyrinic moiety. The prepared PEGylated porphyrin (with PEG arms at the periphery) P-$(PEO)_2$ was self-assembled into spheres of uniform diameter while their DMF solution was dialyzed into water. Furthermore, the addition of fullerene (C_{60}) to P-$(PEO)_2$ caused complexation between porphyrin and fullerene which lead to interesting and trenchant morphology having worm like lateral aggregates. The assembly process and the as-prepared edifices were characterized using UV–vis absorption spectroscopy and the morphology of these assemblies was investigated using transmission electron microscope (TEM). Furthermore, the DNA binding with porphyrin aggregates has been demonstrated via electrochemical (cyclic voltammetric) response of screen printed electrodes modified. The obvious increase in redox current disclosed the intermolecular interactions of the adducts with the DNA. These studies of unprecedented adducts can further be explored for potential applications in biosensors.

Web URL: **http://www.sciencedirect.com/science/article/pii/S016773221633149X**

10. Bazin, I., Tria, S. A., Hayat, A., & Marty, J. L. (2017). New biorecognition molecules in biosensors for the detection of toxins. *Biosensors and Bioelectronics*, *87*, 285-298.

ABSTRACT:

Biological and synthetic recognition elements are at the heart of the majority of modern bioreceptor assays. Traditionally, enzymes and antibodies have been integrated in the biosensor designs as a popular choice for the detection of toxin molecules. But since 1970s, alternative biological and synthetic binders have been emerged as a promising alternative to conventional biorecognition elements in detection systems for laboratory and field-based applications. Recent research has witnessed immense interest in the use of recombinant enzymatic methodologies and nanozymes to circumvent the drawbacks associated with natural enzymes. In the area of antibody production, technologies based on the modification of in vivo synthesized materials and in vitro approaches with development of "display "systems have been introduced in the recent years. Subsequently, molecularly-imprinted polymers and Peptide nucleic acid (PNAs) were developed as an attractive receptor with applications in the area of sample preparation and detection systems. In this article, we discuss all alternatives to conventional biomolecules employed in the detection of various toxin molecules We review recent developments in modified enzymes, anozymes, nanobodies, aptamers, peptides, protein scaffolds and DNazymes. With the advent of nanostructures and new interface materials, these recognition elements will be major players in future biosensor development.

Web URL: ***http://www.sciencedirect.com/science/article/pii/S0956566316306236***

11. Sharma, A., Goud, K. Y., Hayat, A., Bhand, S., & Marty, J. L. (2016). Recent Advances in Electrochemical-Based Sensing Platforms for Aflatoxins Detection. *Chemosensors*, *5*(1), 1.

ABSTRACT:

Mycotoxin are small (MW ~700 Da), toxic secondary metabolites produced by fungal species that readily colonize crops and contaminate them at both pre- and post-harvesting. Among all, aflatoxins (AFs) are mycotoxins of major significance due to their presence in common

food commodities and the potential threat to human health worldwide. Based on the severity of illness and increased incidences of AFs poisoning, a broad range of conventional and analytical detection techniques that could be useful and practical have already been reported. However, due to the variety of structural analogous of these toxins, it is impossible to use one common technique for their analysis. Numerous recent research efforts have been directed to explore alternative detection technologies. Recently, immunosensors and aptasensors have gained promising potential in the area of sample preparation and detection systems. These sensors offer the advantages of disposability, portability, miniaturization, and on-site analysis. In a typical design of an aptasensor, an aptamer (ssDNA or RNA) is used as a bio-recognition element either integrated within or in intimate association with the transducer surface. This review paper is focused on the recent advances in electrochemical immuno- and aptasensing platforms for detection of AFs in real samples.

Web URL: **http://www.mdpi.com/2227-9040/5/1/1/htm**

12. Nasir, M., Rauf, S., Muhammad, N., Nawaz, M. H., Chaudhry, A. A., Malik, M. H., ... & Hayat, A. (2017). Biomimetic nitrogen doped titania nanoparticles as a colorimetric platform for hydrogen peroxide detection. ***Journal of colloid and interface science*****, *505*, 1147-1157.**

ABSTRACT:

Nanoparticles proved a viable alternative to the already used sensing and diagnostics methods due to their low cost, good stability, easy availability and easy synthesis. In the present approach, nitrogen doped titania nanoparticles are prepared through freeze drying method, and subsequently stabilized through ionic liquid. These nanoparticles were characterized through various techniques such as X-ray diffraction (XRD), Fourier transformation infrared spectroscopy (FTIR), Scanning electron microscopy (SEM), BET pore size and surface area analyzer, X-ray photoelectron spectroscopy (XPS) and UV–Visible diffuse reflectance spectroscopy (UV–Vis. DRS). The synthesized nitrogen doped titania nanoparticles were proved to be a novel peroxidase mimetic with great potential to catalyze oxidation of 3,3’,5,5’-tetramethylbenzidine (TMB) in the presence of hydrogen peroxide (H_2O_2) to form a blue color product. As a proof of concept, this new enzyme mimic was used as a robust nanoprobe for the

detection of hydrogen peroxide with improved analytical characteristics. A linear response for hydrogen peroxide detection was obtained in the range of 10–300 µmol/L, with a detection limit of 2.5 µmol/L. Taking into account the valuable intrinsic peroxidase activity, the present work may find widespread applications in the field of sensors and biosensors for diverse applications.

Web URL: ***https://www.sciencedirect.com/science/article/pii/S0021979717307828***

13. Ur Rehman, R., Rafiq, S., Muhammad, N., Khan, A. L., Ur Rehman, A., TingTing, L., ... & Gu, X. (2017). Development of ethanolamine-based ionic liquid membranes for efficient CO2/CH4 separation. ***Journal of Applied Polymer Science*****,** ***134*****(44).**

ABSTRACT:

This study is focused on the development of ionic liquids (ILs) based polymeric membranes for the separation of carbon dioxide (CO2) from methane (CH4). The advantage of ILs in selective CO2 absorption is that it enhances the CO2 selective separation for the ionic liquid membranes (ILMs). ILMs are developed and characterized with two different ILs using the solution-casting method. Three different blend compositions of ILs and polysulfone (PSF) are selected for each ILMs 10, 20, and 30 wt %. Effect of the different types of ILs such as triethanolamine formate (TEAF) and triethanolamine acetate (TEAA) are investigated on PSF-based ILMs. Field emission scanning electron microscopy analysis of the membranes showed reasonable homogeneity between the ILs and PSF. Thermogravimetric analysis showed that by increasing the ILs loading thermal stability of the membranes improved. Mechanical analysis on developed membranes showed that ILs phase reduced the amount of plastic flow of the PSF phase and therefore, fracture takes place at gradually lower strains with increasing ILs content. Gas permeation evaluation was carried out on the developed membranes for CO2/CH4 separation between 2 bar to 10 bar feed pressure. Results showed that CO2 permeance increases with the addition of ILs 10–30 wt % in ILMs. With 20–30 wt % TEAF-ILMs and TEAA-ILMs, the highest selectivity of a CO2/CH4 53.96 6 0.3, 37.64 6 0.2 and CO2 permeance 69.5 6 0.6, 55.21 6 0.3 is observed for treated membrane at 2–10 bar. The selectivity using mixed gas test at various CO2/CH4 compositions shows consistent results with the ideal gas selectivity.

Web URL:

https://www.researchgate.net/profile/Rashid_Rehman4/publication/317343847_Development_of_ethanol_amine_based_ionic_liquid_membranes_for_efficient_CO2CH4_separation/links/5983560daca272a947c72828/Development-of-ethanol-amine-based-ionic-liquid-membranes-for-efficient-CO2-CH4-separation.pdf

14. Jamshaid, A., Hamid, A., Muhammad, N., Naseer, A., Ghauri, M., Iqbal, J., ... & Shah, N. S. (2017). Cellulose-based Materials for the Removal of Heavy Metals from Wastewater–An Overview. *ChemBioEng Reviews*.

ABSTRACT:

Water pollution due to increase in population and high rates of wastewater generation have become serious concerns since the last few decades. Heavy metals are amongst the main wastewater pollutants due to their ability to persist in the environment. Materials and techniques are being investigated for the treatment of heavy metals in wastewater. Cellulose is one of the materials gaining attention due to its excellent physical, chemical, and mechanical properties. Cellulose-based materials are being widely studied for the adsorption of heavy metals. This overview highlights research efforts to enhance the role of cellulose in wastewater treatment through cellulose-based materials. It also discusses the effects of cellulose modifications such as cellulose gels, cellulose composites, cellulose derivatives, functionalized cellulose, and nanocrystalline cellulose on the capacity of heavy metals adsorption.

Web URL: ***http://onlinelibrary.wiley.com/doi/10.1002/cben.201700002/full***

15. Sarwono, A., Man, Z., Bustam, M. A., Subbarao, D., Idris, A., Muhammad, N., ... & Ullah, Z. (2017). Swelling Mechanism of Urea Crosslinked Starch-Lignin Films in Water. *Environmental Technology*, (just-accepted), 1-31.

ABSTRACT:

Coating fertilizer particles with thin films is a possibility to control fertilizer release rates. It is observed that novel urea cross-linked starch–lignin composite thin films, prepared by solution casting, swell on coming into contact with water due to the increase in volume by water uptake

by diffusion. The effect of lignin content, varied from 0% to 20% in steps of 5% at three different temperatures (25°C, 35°C and 45°C), on swelling of the film was investigated. By gravimetric analysis, the equilibrium water uptake and diffusion coefficient decrease with lignin content, indicating that the addition of lignin increases the hydrophobicity of the films. When temperature increases, the diffusion coefficient and the amount of water absorbed tend to increase. Assuming that swelling of the thin film is by water uptake by diffusion, the diffusion coefficient is estimated. The estimated diffusion coefficient decreases from 4.3 to 2.1×10^{-7} cm^2/s at 25°C, from 5.3 to 2.9×10^{-7} cm^2/s at 35°C and from 6.2 to 3.8×10^{-7} cm^2/s at 45°C depending on the lignin content. Activation energy for the increase in diffusion coefficient with temperature is observed to be 16.55 kJ/mol. An empirical model of water uptake as a function of percentage of lignin and temperature was also developed based on Fick's law.

Web URL: ***http://www.tandfonline.com/doi/abs/10.1080/09593330.2017.1332108***

16. Khan, Z. U. H., Khan, A., Wan, P., Khan, A. U., Tahir, K., Muhammad, N., ... & Khan, Z. U. (2017). New natural product-an efficient antimicrobial applications of new newly synthesized pyrimidine derivatives by the electrochemical oxidation of hydroxyl phenol in the presence of 2-mercapto-6-(trifluoromethyl) pyrimidine-4-ol as nucleophile. ***Natural Product Research*****.**

ABSTRACT:

Some new pyrimidine derivatives have been synthesised by electrochemical oxidation of catechol (**1a**) in the existence of 2-mercapto-6-(trifluoromethyl) pyrimidine-4-ol (**3**) as a nucleophile in aqueous solution using Cyclic Voltammetric and Controlled Potential Coulometry. The catechol has been oxidised to *o*-quinone through electrochemical method and participative in Michael addition reaction, leading to the development of some new pyrimidine derivatives. The products were achieved in good yield with high pureness. The mechanism of the reaction has been conformed from the Cyclic Voltammetric data and Controlled Potential Coulometry. After purification, the compounds were characterised using modern techniques. The synthesised materials were screened for antimicrobial actions using Gram positive and Gram negative strain of bacteria. These new synthesised pyrimidine derivatives showed very good antimicrobial activity.

Web URL: ***http://www.tandfonline.com/doi/abs/10.1080/14786419.2017.1326043***

17. Chen, J., Lei, S., Zeng, K., Wang, M., Asif, A., & Ge, X. (2017). Catalase-imprinted Fe3O4/Fe@ fibrous SiO2/polydopamine nanoparticles: An integrated nanoplatform of magnetic targeting, magnetic resonance imaging, and dual-mode cancer therapy. ***Nano Research*****, *10*(7), 2351-2363.**

ABSTRACT:

Recent advances in the research on the molecular mechanism of cell death and methods for preparation of nanomaterials make the integration of various therapeutic approaches, targeting, and imaging modes into a single nanoscale complex a new trend for the development of future nanotherapeutics. Hence, a novel ellipsoidal composite nanoplatform composed of a magnetic Fe3O4/Fe nanorod core (~120 nm) enwrapped by a catalase (CAT)-imprinted fibrous SiO2/ polydopamine (F-SiO2/PDA) shell with thickness 70 nm was prepared in this work. In vitro experiments showed that the Fe3O4/Fe@F-SiO2/PDA nanoparticles can selectively inhibit the bioactivity of CAT in tumor cells by the molecular imprinting technique. As a result, the H2O2 level in tumor cells was elevated dramatically. At the same time, the Fe3O4/Fe core released Fe ions to catalyze the conversion of H2O2 to ·OH in tumor cells. Eventually, the concentration of ·OH in tumor cells rapidly rose to a lethal level thus triggering apoptosis. Combined with the remarkable near-infrared light (NIR) photothermal effect of the CATimprinted PDA layer, the Fe3O4/Fe@F-SiO2/PDA nanoparticles can effectively kill MCF-7, HeLa, and 293T tumor cells but are not toxic to nontumor cells. Furthermore, these nanoparticles show good capacity for magnetic targeting and suitability for magnetic resonance imaging (MRI). Therefore, the integrated multifunctional nanoplatform opens up new possibilities for high-efficiency visual targeted nonchemo therapy for cancer.

Web URL: ***https://link.springer.com/content/pdf/10.1007/s12274-017-1431-8.pdf***

18. Khan, A. S., Hussain, A. N., Sidra, L., Sarfraz, Z., Khalid, H., Khan, M., ... & Rehman, I. U. (2017). Fabrication and in vivo evaluation of hydroxyapatite/carbon nanotube electrospun fibers for biomedical/dental application. ***Materials Science and Engineering: C***.

ABSTRACT:

The aim was to synthesize bioactive electrospun fibers for biomedical and dental application with improved biocompatibility. In situ precipitation of nano-hydroxyapatite (nHA) was performed with various concentrations (0.5%, 1%, 2%, 3%, and 5% wt/wt) of functionalized multi-walled-carbon nanotubes (MWCNTs) by using microwave irradiation technique. The obtained composites were characterized by Fourier Transform Infrared (FTIR), X-ray Diffraction (XRD), Thermogravimetric Analysis/Differential Scanning Calorimetry (TGA/DSC), and the cylindrical discs were made for mechanical testing. The failure behavior was analyzed by Scanning Electron Microscope (SEM). CNT and HA/CNT were silanized with γ-methacryloxypropyl-trimethoxysilane (MPTS) and mixed with polyvinyl alcohol (10% wt./vol.) and electrospun to fabricate fibers. The biocompatibility of both fibers was accessed by their effects on angiogenesis in a chick chorioallantoic membrane (CAM) assay. The electrospun fibers were analyzed by SEM. FTIR confirmed the structural behavior of pre and post-silanized HA/CNT. XRD showed the phase purity and crystallinity before and after heat treatment. Mechanical properties showed that 3% loaded HA/CNT has higher compressive strength (100.5 ± 5.9 MPa) compared to others and the failure behavior exhibited dispersion of CNT in HA matrix. The HA/CNT electrospun fibers showed significantly more blood vessels formation compared to CNT fibers. These HA/CNT electrospun fibers showed promising results in terms of biocompatibility and with improved mechanical properties of CNT reinforced composites, they can be used in load bearing clinical applications.

Web URL: ***http://www.sciencedirect.com/science/article/pii/S0928493116321956***

19. Ahtzaz, S., Nasir, M., Shahzadi, L., Amir, W., Anjum, A., Arshad, R., ... & ur Rehman, I. (2017). A study on the effect of zinc oxide and zinc peroxide nanoparticles to enhance angiogenesis-pro-angiogenic grafts for tissue regeneration applications. ***Materials & Design*****, *132*, 409-418.**

ABSTRACT:

Angiogenesis is a process of formation of new small blood vessels from existing vessels and is very critical for proper and rapid tissue healing. As reactive oxygen species (ROS) are known for

their ability to promote angiogenesis, in this study zinc oxide (ZnO) and zinc peroxide (ZnO_2) nano-particles (NP's) encapsulated chitosan (CS) and cellulose based hydrogels were synthesized. ZnO_2 is comparatively stronger oxidizing agent as compared to ZnO, therefore, in this study it was hypothesized that ZnO_2 would deliver better angiogenic potential than ZnO. Three types of hydrogels were prepared; control hydrogel (without nano-particles), hydrogel having ZnO NP's and hydrogel having ZnO_2 NP's. The hydrogels were characterized by scanning electron microscopy (SEM) for structural morphology, Fourier transform infrared spectroscopy (FTIR) for chemical functional groups analyses and X-ray Diffraction (XRD) to investigate the crystalline or amorphous structure of NP's. The solution absorption capacity was tested in PBS and degradation was investigated in PBS, PBS/H_2O_2 and PBS/lysozyme solutions. The angiogenic behavior of these materials was studied in chorioallantoic membrane (CAM) assay and ZnO_2 based material showed significant higher angiogenesis.

Web URL: **https://www.sciencedirect.com/science/article/pii/S0264127517306846**

20. Mahmood, H., Moniruzzaman, M., Yusup, S., Muhammad, N., Iqbal, T., & Akil, H. M. (2017). Ionic liquids pretreatment for fabrication of agro-residue/thermoplastic starch based composites: A comparative study with other pretreatment technologies. ***Journal of Cleaner Production*****.**

ABSTRACT:

Ionic liquids (ILs) pretreatment has emerged as a promising technology toward environmentally benign conversion of lignocellulosic residues into high value cellulosic fiber as sustainable raw material for biocomposite fabrication. This study presents a comparison of ILs-assisted pretreatment of oil palm fronds (OPF) fiber with dilute acid, alkaline, and hot compressed water pretreatments on the mechanical and thermal properties of their fabricated thermo-molded biocomposites with thermoplastic starch as a biopolymer binder. A comparison of energy consumption for ILs pretreatment with other pretreatment methods was also performed and the comparative impact of ILs pretreatment on OPF fiber was investigated by lignocellulosic composition, crystallinity and thermal stability analysis for untreated and all pretreated fibers. Results indicate that ILs pretreatment is superior in terms of delignification of OPF and

produces cellulose rich fiber (CRF) with 48–50% reduced crystallinity as compared to those of acidic, alkaline, and hot water pretreated fibers. However, the flexural strength of the IL [emim][dep] treated composite (13.8 MPa) was significantly improved over that of untreated composite with value of 5.3 MPa, but was slightly higher than acidic and hot water pretreatments which were 13.5 MPa and 10.8 MPa, respectively. ILs pretreatment consumed about 0.5–2.0 folds more energy per kg of OPF residue as compared to other methods. In the premises of the present findings, we believe that ILs-based pretreatment could be a new, clean and promising alternative processing approach for conversion of a wide variety of agro-based lignocellulosic waste materials into cellulose-rich fibers for manufacturing of engineered biocomposite panels.

Web URL: ***http://www.sciencedirect.com/science/article/pii/S0959652617310508***

21. Steenbergen, P. J., Bardine, N., & Sharif, F. (2017). Kinetics of glucocorticoid exposure in developing zebrafish: A tracer study. *Chemosphere*, *183*, 147-155.

ABSTRACT:

In the current study the dynamics of glucocorticoid uptake by zebrafish chorionated embryos from the surrounding medium were studied, using 2.5 μM cortisol or dexamethasone solutions complemented with their tritiated variant. We measured the uptake of radioactive cortisol by embryos during a 1 h submersion. Interestingly, the signal in chorionated embryos was 85% (exposure: 1–2 hpf) or 78% (exposure: 48–49 hpf) of the signal present in an equal volume medium. By comparing embryos measured without chorion, we found that 18–20% of the radioactivity present in chorionated embryos is actually bound to the chorion or located in the perivitelline space. Consequently, embryonic tissue contains radioactivity levels of 60% of a similar volume of medium after 1 h incubation. During early developmental stages (1–48 hpf) exposure of more than 24 h in cortisol was needed to achieve radioactivity levels similar to an equal volume of medium within the embryonic tissue and more than 48 h for dexamethasone. In glucocorticoid-free medium, radioactivity dropped rapidly below 10% for both glucocorticoids, suggesting that the major portion of the embryonic radioactivity was a result of simple diffusion. During later developmental stages (48–96 hpf) initial uptake dynamics were similar, but showed a decrease of tissue radioactivity to 20% of an equal volume of medium

after hatching, probably due to development and activation of the hypothalamic pituitary interrenal axis. Uptake is dependent on the developmental stage of the embryo. Furthermore, the presence of the chorion during exposure should be taken into account even when small lipophilic molecules are being tested.

Web URL: **http://www.sciencedirect.com/science/article/pii/S0045653517307634**

22. Khan, M. I., Khan, H. U., Azizli, K., Sufian, S., Man, Z., Siyal, A. A., ... & ur Rehman, M. F. (2017). The pyrolysis kinetics of the conversion of Malaysian kaolin to metakaolin. *Applied Clay Science*, *146*, 152-161.

ABSTRACT:

The aim of this work was to study the pyrolysis kinetics of the thermal transformation of kaolin to metakaolin with the aid of models and model free isoconversional methods. Thermal treatment in the range of 600–850 °C is used to convert kaolin into an amorphous and highly reactive metakaolin (MK). In this study, the thermal transformation of kaolin to metakaolin was investigated using thermokinetics and instrumental analysis. Kaolin was subjected to thermogravimetric analysis (TGA) at heating rates of 10, 20 and 40 °C/min, in the temperature range of 50–800 °C. Approximately, 14.2% of mass loss was recorded during the TG analysis. 95% of the degree of dehydroxylation was attained at 635 °C, representing the minimum temperature for this process. The TGA and its related data were analyzed using model free (based on DTG, DTA and TG) and model based kinetics methods. Both DTG and DTA peak temperatures were employed for the thermokinetics of kaolin using Ozawa, Kissinger and Starink methods; giving an E_a in the range of 246.6–252.5 kJ·mol^{-1}. A slight higher average E_a (266–267 kJ·mol^{-1} vs 246.6–252.5 kJ·mol^{-1}) was observed when TGA based integral methods (KAS, FWO and Starink) were used. The mechanism of the thermokinetics was investigated using the Redfern model and the best fitting was given by 3rd order chemical reaction (F_3) function. Both model-free and model based thermokinetics methods could be used to validate the thermal transformation of kaolinite to metakaolinite.

Web URL: ***http://www.sciencedirect.com/science/article/pii/S0169131717302132***

23. Mishra, R. K., Nawaz, M. H., Hayat, A., Nawaz, M. A. H., Sharma, V., & Marty, J. L. (2017). Electrospinning of graphene-oxide onto screen printed electrodes for heavy metal biosensor. *Sensors and Actuators B: Chemical*, *247*, 366-373.

ABSTRACT:

We present an electrospinning of graphene-oxide (GO) onto screen printed carbon electrodes (SPCE) for heavy metals (HMs) bio-sensing. The GO was dispersed in poly (vinyl alcohol) (PVA) diluted aqueous solution, and the mixture was electrospun into GO/PVA composite nanofibers. The morphology of GO and SPCE modified with electrospun nanofiber was studied using SEM micrographs and confirmed the uniform distribution of GO sheets in nanofibers. The Alkaline Phosphatase (ALP) was immobilized onto nanofibers grown on the SPCE and activity was checked using 1-napthyl phosphate (1-NP) by applying differential pulse voltammetry (DPV). The ALP activity was inhibited in the presence of HMs and a difference in activity was recorded after inhibition. The inhibition was calculated based on the data of pre and post inhibition current values. The inhibition of ALP was observed with mercury (Hg^{2+}), lead (Pb^{2+}) and cadmium (Cd^{2+}) with a detection limit of 0.0075, 0.015 and 0.0312 ppb respectively. The developed biosensor was also tested to evaluate the matrix suitability through recovery studies. Excellent HM recoveries were obtained in the range 94.6–99.75 with%RSD value of 3.77.

Web URL: ***http://www.sciencedirect.com/science/article/pii/S0925400517304768***

24. Khan, Z. U. H., Khan, A., Chen, Y. M., Shah, N. S., Muhammad, N., Khan, A. U., ... & Qaisrani, S. A. (2017). Biomedical applications of green synthesized Nobel metal nanoparticles. *Journal of Photochemistry and Photobiology B: Biology*.

ABSTRACT:

Synthesis of Nobel metal nanoparticles, play a key role in the field of medicine. Plants contain a substantial number of organic constituents, like phenolic compounds and various types of glycosides that help in synthesis of metal nanoparticles. Synthesis of metal nanoparticles by green method is one of the best and environment friendly methods. The major significance of the green synthesis is lack of toxic by-products produced during metal nanoparticle synthesis. The nanoparticles, synthesized by green method show various significant biological activities.

Most of the research articles report the synthesized nanoparticles to be active against gram positive and gram negative bacteria. Some of these bacteria include *Escherichia coli*, *Bacillus*subtilis, *Klebsiella pneumonia* and *Pseudomonas* fluorescens. The synthesized nanoparticles also show significant antifungal activity against *Trichophyton* simii, *Trichophyton mentagrophytes* and *Trichophyton rubrum* as well as different types of cancer cells such as breast cancer cell line. They also exhibit significant antioxidantactivity. The activities of these Nobel metal nano-particles mainly depend on the size and shape. The particles of small size with large surface area show good activity in the field of medicine. The synthesized nanoparticles are also active against leishmanial diseases. This research article explores in detail the green synthesis of the nanoparticles and their uses thereof.

Web URL: ***http://www.sciencedirect.com/science/article/pii/S1011134417304980***

25. Abbas, S. K., Aslam, M. A., Amir, M., Atiq, S., Ahmed, Z., Siddiqi, S. A., & Naseem, S. (2017). Electrical impedance functionality and spin orientation transformation of nanostructured Sr-substituted BaMnO 3 hexagonal perovskites. ***Journal of Alloys and Compounds*****, *712*, 720-731.**

ABSTRACT:

Eliminating the undesirable pyrochlore phase is quite essential in order to determine the viable dielectric and magnetic characteristics of perovskite-based materials. In this work, we report the synthesis of stoichiometric Sr-substituted barium manganite namely, $Ba_{1-x}Sr_xMnO_3$ (x = 0.0, 0.2, 0.4, 0.6 and 0.8) to reveal the improved structural, dielectric and magnetic properties with increase in Sr contents. X-ray diffraction and subsequent Rietveld refinement reveals that with successful substitution of Sr at Ba-site, the pyrochlore phase diminishes and pure perovskite phase is achieved. Scanning electron microscopy demonstrates gradually improved grain shapes and uniformity in sizes in the series. Electrical impedance spectroscopy was performed using an impedance analyzer, to obtain frequency response of dielectric constant, giving tenable information about a sustainable change in electrical permittivity due to Sr-substitution which could be used for multilayered chip inductors. Dense dielectric materials with low losses are credible for multilayered components which make these oxides more feasible than ferrites

to be used as sheets inside the multilayered chip inductors. Contribution of grains and grain boundaries effect on electrical resistivity, losses and quality factors are also distinguished. The coupling between the magnetic and dielectric order is also confirmed through magneto-dielectric measurement. Low temperature magnetic studies reveals the multiferroic characteristic of the material as the ferromagnetic transition temperature of 55 K, found experimentally has never been reported before.

Web URL: ***http://www.sciencedirect.com/science/article/pii/S0925838817313609***

26. Nawaz, S., Shah, N. S., Khan, J. A., Sayed, M., Ala'a, H., Andersen, H. R., ... & Khan, H. M. (2017). Removal efficiency and economic cost comparison of hydrated electron-mediated reductive pathways for treatment of bromate. ***Chemical Engineering Journal*****,** ***320*****, 523-531.**

ABSTRACT:

Bromate, a potential carcinogen, is a well known highly persistent and environmentally recalcitrant contaminant. UV-254/sulfite-based advanced reductive pathways (ARPs) were proposed to eliminate bromate successfully from water. Experiments with N_2, N_2O, 2-chlorophenol, inorganic ions, and different pH (highly acidic to highly basic) proved that UV-254/sulfite successfully provides aqueous electron that effectively participate in bromate removal from water. Significant removal, 86%, of initially 39.0 μM bromate was achieved by UV-254/sulfite under conditions that dominate aqueous electron based pathways. The high second-order rate constant of 5.3×10^9 M^{-1} s^{-1} determined proved high reactivity of aqueous electron with bromate. The kinetic and removal efficiency of bromate showed linear relationship with the rate of aqueous electron formation. An increase in kinetic and removal efficiency of bromate was observed with increasing initial sulfite concentration and decreasing bromate concentration. The impacts of different initial concentrations of the typical ions commonly found in water were studied in detail to extend the UV-254/sulfite-based process for potential practical applications. The lower molar absorptivity of bromate at 254 nm determined proved insignificant removal of bromate under direct photolysis. The impacts of initial sulfite concentration on removal of bromate in UV-254/sulfite-based process also minimized role of

direct photolysis. The cost evaluation and rapid decomposition of bromate into bromide proved UV-254/sulfite-based ARPs to be economical and highly rewarding in efficient decomposition of bromate and other inorganic oxyhalides.

Web URL: ***http://www.sciencedirect.com/science/article/pii/S1385894717303480***

27. Gonfa, G., Bustam, M. A., Muhammad, N., & Ullah, S. (2017). Effect of task specific thiocyanate based ionic liquids on relative volatility of cyclohexane and benzene azeotropic mixture. ***Journal of Molecular Liquids*****,** ***238*****, 208-214.**

ABSTRACT:

The relative volatilities of cyclohexane (Cy) to benzene (Bz) in the presence of eight task-specific imidazolium thiocyanate ionic liquids (ILs) were measured using headspace gas chromatography. The ILs contain nitrile, ally, benzyl and hydroxyl functional group in their imidazolium cations and thiocyanate as anion. The effects of incorporation of nitrile, allyl, benzyl and hydroxyl functional groups in imidazolium alkyl chain on the relative volatility of Cy to Bz were investigated using experiment and quantum calculations. COSMO-RS model was used to study the polarity (charge distribution) of the ILs and the solutes. Density functional theory (DFT) was employed to investigate the cation-anion interaction energies and IL-Bz/Cy binding energies. The structural variations of the imidazolium cation influence the performance of the ILs. Moreover, the performances of the ILs were compared with two typical conventional entrainers, dimethyl sulfoxide (DMSO) and N,N-dimethylformamide (DMF). Except two hydroxyl containing ILs, the remaining six ILs show higher Cy to Bz relative volatility values compared to the bench marked conventional solvents.

Web URL: ***http://www.sciencedirect.com/science/article/pii/S0167732217313491***

28. Feroze, A., Idrees, M., Kim, D. K., Nadeem, M., Siddiqi, S. A., Shaukat, S. F., ... & Siddique, M. (2017). Low Temperature Synthesis and Properties of BiFeO3. ***Journal of Electronic Materials*****, 1-8.**

ABSTRACT:

Extensive efforts have been made to synthesize single phase and stoichiometric BiFeO3. Some modified techniques have been tried in synthesizing BiFeO3 as compared with the conventionally used co-precipitation method. Thermogravimetric Analysis/Differential Scanning Calorimetry and x-ray diffraction experiments were used exclusively to explore the effects of heat treatment temperature and time on crystallographic behavior of the prepared BiFeO3 powder. Field emission scanning electron microscopy was used to explore the microstructure of the synthesized BiFeO3. The appearance of different magnetic phases in 57Fe Mo¨ssbauer spectra and field dependent magnetization was confirmed on the basis of particle size distribution. In this research, an easy, low cost and high-yield method for the low temperature single phase and stoichiometric synthesis of BiFeO3 has been suggested.

Web URL: ***https://link.springer.com/content/pdf/10.1007/s11664-017-5463-3.pdf***

29. Mansha, S., Imran, M., Shah, A. M. U. H., Jamal, M., Ahmed, F., Atif, M., & Bilal Waqar, A. (2017). Hepatitis B and C Virus Infections Among Human Immunodeficiency Virus-Infected People Who Inject Drugs in Lahore, Pakistan. *Viral Immunology*.

ABSTRACT:

Hepatitis B virus (HBV) and hepatitis C virus (HCV) are the major cause of the global burden of hepatitis. One of the main routes of transmission for both viruses is through exposure to infected blood, which includes sharing blood-contaminated syringes and needles. Human immunodeficiency virus (HIV) attacks the immune system and results in acquired immune deficiency syndrome and opportunistic infections. The objective of this study was to assess the epidemiology of HBV and HCV infections among HIV-infected people who inject drugs (PWID). The study enrolled 100 PWID from different addiction centers of the city of Lahore in Pakistan. All subjects were HIV-infected males and were above 16 years of age. Screening of HBV and HCV infections was performed through immunochromatography tests and enzyme-linked immunosorbent assays. The prevalence of HCV and HBV infections among the 100 HIV-infected PWID was 55% and 6%, respectively. HIV monoinfection was found in 37% of the subjects, while triple infection was detected in 2% of the subjects. Majority of the HIV-infected PWID were using heroin and Avil injections (65%). Half of the subjects had used injection drugs for 1–5

years, while 32% had used injection drugs for 6–10 years. HCV infection was more common than HBV infection among the enrolled subjects. Most of the PWID were practicing heroin and Avil injections.

Web URL:

https://www.researchgate.net/profile/Muhsin_Jamal2/publication/317077161_Hepatitis_B_and_C_Virus_Infections_Among_Human_Immunodeficiency_Virus-Infected_People_Who_Inject_Drugs_in_Lahore_Pakistan/links/5924559a0f7e9b997954b083/Hepatitis-B-and-C-Virus-Infections-Among-Human-Immunodeficiency-Virus-Infected-People-Who-Inject-Drugs-in-Lahore-Pakistan.pdf

30. Farooq, U., Danish, M., Lu, S., Naqvi, M., Gu, X., Fu, X., ... & Nasir, M. (2017). Synthesis of nZVI@ reduced graphene oxide: an efficient catalyst for degradation of 1, 1, 1-trichloroethane (TCA) in percarbonate system. *Research on Chemical Intermediates*, *43*(5), 3219-3236.

ABSTRACT:

Graphene-oxide-supported nano zero-valent iron (nZVI) composite (nZVI–rGO) was synthesized and tested as an efficient percarbonate activator for degradation of 1,1,1-trichloroethane (TCA). Significant dispersion of nZVI on the surface of reduced graphene oxide (rGO) was observed, with good limitation of nanoparticle agglomeration and aggregation. Good TCA degradation efficiency of 90% was achieved in 2.5 h in presence of 0.8 g/l nZVI–rGO catalyst and 30 mM sodium percarbonate (SPC) oxidant; however, excessive catalyst or oxidant concentration reduced the degradation efficiency. Investigation of reactive oxygen species using radical probe compounds as well as radical scavengers confirmed presence of hydroxyl ($OH^{\cdot}$) and superoxide ($O^{\cdot-}2O2^{\cdot-}$) radicals that are responsible for the TCA degradation. The morphology and surface characteristics of the heterogeneous catalyst were analyzed by transmission electron microscopy and scanning electron microscopy. Brunauer–Emmett–Teller analysis revealed that the synthesized catalyst had large surface area and small particle size of 299.12 m^2/g and 20.10 nm, respectively, compared with 5.33 m^2/g and 1.12 µm for bare graphene oxide. X-ray diffraction analysis revealed good dispersion of nZVI

on the surface of rGO. Fourier-transform infrared characteristic peaks confirmed strong attachment of Fe onto the rGO surface. Energy-dispersive spectroscopy analysis validated the stoichiometric composition of the prepared Fe/rGO material. In conclusion, use of nZVI–rGO-activated SPC could represent an alternative technique for remediation of TCA-contaminated groundwater.

Web URL: ***https://link.springer.com/article/10.1007/s11164-016-2821-3***

31. Yar, M., Shahzad, S., Shahzadi, L., Shahzad, S. A., Mahmood, N., Chaudhry, A. A., ... & MacNeil, S. (2017). Heparin binding chitosan derivatives for production of pro-angiogenic hydrogels for promoting tissue healing. ***Materials Science and Engineering: C*****, *74*, 347-356.**

ABSTRACT:

Our aim was to develop a biocompatible hydrogel that could be soaked in heparin and placed on wound beds to improve the vasculature of poorly vascularized wound beds. In the current study, a methodology was developed for the synthesis of a new chitosan derivative (CSD-1). Hydrogels were synthesized by blending CSD-1 for either 4 or 24 h with polyvinyl alcohol (PVA). The physical/chemical interactions and the presence of specific functional groups were confirmed by Fourier transform infrared (FT-IR) spectroscopy and proton nuclear magnetic resonance (^{1}H NMR). The porous nature of the hydrogels was confirmed by scanning electron microscopy (SEM). Thermal gravimetric analysis (TGA) showed that these hydrogels have good thermal stability which was slightly increased as the blending time was increased. Hydrogels produced with 24 h of blending supported cell attachment more and could be loaded with heparin to induce new blood vessel formation in a chick chorionic allantoic membrane assay.

Web URL: **http://www.sciencedirect.com/science/article/pii/S0928493116325279**

32. Muhammad, N., Gonfa, G., Rahim, A., Ahmad, P., Iqbal, F., Sharif, F., ... & Rehman, I. U. (2017). Investigation of ionic liquids as a pretreatment solvent for extraction of collagen biopolymer from waste fish scales using COSMO-RS and experiment. ***Journal of Molecular Liquids*****, *232*, 258-264.**

ABSTRACT:

Collagen being an abundant natural biopolymer and also has many applications for bio-medical and non-biomedical uses, were extracted from waste fish scales using green route of ionic liquid pretreatment. To get insight on dissolution and extraction of collagen from fish scale using ionic liquids, COSMO-RS computational approach was used to identify the best ionic liquid. The 1-ethyl-3-methylimidazolium acetate ($[C_2C_1im][Ac]$) ionic liquid based on low activity coefficient (inverse of solubility) and best fit sigma profile was selected for pretreatment. The ground fish scales were pretreated with $[C_2C_1im][Ac]$ ionic liquid and further subjected to separation for obtaining the collagen. The collagen was obtained in the form of thin film with yield of 3.1 ± 0.5% at 100 °C for 12 h treatment time. The obtained collagen was characterized using Fourier Transform Infrared Spectroscopy (FTIR), UV–Vis spectrometer, Powder X-rays Diffraction (PXRD), Thermal Gravimetric Analysis (TGA), Field Emission Scanning Microscopy (FE-SEM), Energy Dispersive X-rays spectroscopy (EDX). The FTIR, UV–Vis and XRD analysis shows the characteristic peaks assigned to the collagen. The SEM analysis confirms the dissolution of collagen fibers in ionic liquid. The TGA analysis shows lower thermal stability of extracted collagen as compared to fish scales.

Web URL: ***http://www.sciencedirect.com/science/article/pii/S0167732216339745***

33. Yousaf, M., Rafique, H. M., Amin, M., Ramay, S. M., Atiq, S., Alzayed, N. S., & Siddiqi, S. A. (2017). VISIBLE-LIGHT-INDUCED Fe-DOPED ZnO MAGNETIC PHOTOCATALYST NANOPARTICLES FOR DEGRADATION OF METHYLENE BLUE. ***Digest Journal of Nanomaterials & Biostructures (DJNB)*****,** ***12*****(1).**

ABSTRACT:

Visible-light-induced Fe-doped zinc oxide photocatalysts with nominal compositions Zn1-xFexO (x=0.0, 0.05) via sol-gel combustion method have been investigated. The structural, thermal, morphological, elemental, magnetic and optical properties have been investigated systematically using X-ray diffractometer, thermogravimetric analysis, field emission scanning electron microscope equipped with energy dispersive X-ray spectroscopy, physical properties measurement system and UV/vis-spectrophotometer, respectively. Wurtzite-type hexagonal crystal structure was evident from the diffraction analysis. The doping of Fe3+ at Zn-site in ZnO

helped to reduce its bandgap energy, attributed to the creation of an extra level near band edges. The synthesized materials exhibited an enhanced photocatalytic activity visualized using degradation of methylene blue under the irradiation of visible-light. Pseudo-first-order rate law was also applied to study the reaction kinetics of methylene blue catalyzed by visible-light irradiation.

Web URL: ***http://www.chalcogen.ro/91_YousefM.pdf***

34. Liu, C., Shi, H., Yang, H., Yan, S., Luan, S., Li, Y., ... & Yin, J. (2017). Fabrication of antibacterial electrospun nanofibers with vancomycin-carbon nanotube via ultrasonication assistance. *Materials & Design*, *120*, 128-134.

ABSTRACT:

The aggregation of multi-walled carbon nanotubes (MWCNT) into the polymer matrix and weak bactericidal property of MWCNT usually limit the application of MWCNT in the infection resistance. To solve the above problem, vancomycin hydrochloride modified multi-walled carbon nanotube (Van-MWCNT) via the chemical reaction of the MWCNT's inherent carboxyl group and the Van's amide group was well designed and synthesized. Then, Van-MWCNT was *in-situ* anchored onto thermoplastic polyurethane (TPU) electrospun nanofibers (TPU/Van-MWCNT) by ultrasonication assistance to achieve the bactericidal property. The above preparation process was facile, non-toxic with the green solvent-water as medium. At the same time, it also effectively reduced the aggregation of Van-MWCNT into the electrospun nanofibers. The minimal inhibitory concentration (MIC) of Van-MWCNT against *S. aureus* was obviously lower than that of MWCNT. And the TPU/Van-MWCNT exhibited excellent antibacterial properties evaluated through the spread plate test and field emission scanning electron microscope (FESEM). The as-prepared antibacterial TPU electrospun nanofibers have potential application in wound dressing.

Web URL: ***http://www.sciencedirect.com/science/article/pii/S0264127517301363***

35. Zeng, K., Lin, F. X., Xie, J., Wang, M. Z., Rong, J. L., Zhao, Y., ... & Ge, X. W. (2017). Chitosan modified by γ-ray-induced grafting of poly (tributyl-(4-vinylbenzyl) phosphonium) as a biosafe and high-efficiency gene carrier. *New Journal of Chemistry*, *41*(10), 4182-4189.

ABSTRACT:

The development of gene carriers with high delivery efficiency and enough biosafety to replace the current viral vectors and cationic liposomes has long been a key project to achieve the practical application of gene therapy. As an abundant natural polymer, chitosan (CS) possesses incomparably high biocompatibility. However, when it is used as a gene carrier, the gene transfection efficiency is rather disappointing. Herein, we prepared a novel chitosan derivative, poly(tributyl-(4-vinylbenzyl)phosphonium)-grafted CS (CS-P), *via* γ-ray radiation-induced grafting copolymerization of tributyl-(4-vinylbenzyl)phosphonium in an acidic solution of CS. The CS-P could combine with *p*EGFP through a complex coacervation method to form *p*EGFP-loaded CS-P complex particles with a size of about 150 nm and a high positive zeta potential of 41.7 ± 6.1 mV. Agarose gel electrophoresis and an MTT assay show that the *p*EGFP-loaded CS-P particles have excellent biosafety, superior to *p*EGFP-loaded unmodified CS particles. *In vitro* and *in vivo* gene transfection experiments based on HeLa cells confirmed that *p*EGFP loaded into CS-P particles exhibits much higher gene transfection efficiency than that loaded into unmodified CS. This work provides not only a new way to modify CS with quaternary phosphonium, but also a useful and feasible way to obtain new CS-based gene vectors with high gene transfection efficiency and biosafety for potentially practical clinic applications.

Web URL: ***http://pubs.rsc.org/-/content/articlelanding/2017/nj/c7nj00008a/unauth#!divAbstract***

36. Mishra, R. K., Hayat, A., Mishra, G. K., Catanante, G., Sharma, V., & Marty, J. L. (2017). A novel colorimetric competitive aptamer assay for lysozyme detection based on superparamagnetic nanobeads. *Talanta*, *165*, 436-441.

ABSTRACT:

Lysozyme (Lys) commonly presents in wines and are known to cause toxicological impact on human health. The need of highly sensitive and reliable detection methods are evident in such matrix. In this work, we developed a competitive aptamer based assay for detection of Lys by employing carboxylated magnetic beads as a support to immobilize the target molecule Lys. The used aptamer sequence was biotinylated which further binds with Streptavidin-Alkaline

phosphatase (Stp-ALP) in the micro wells. Colorimetric tests were performed in order to optimize different experimental parameters. The Lys assay showed a good linearity in the range of 5–140 nM with a limit of detection (LOD) 10 nM. The mid-point value (IC_{50}) 110 nM and the analysis time (60 min) validated the developed aptasensor as a promising tool for routine use. The assay displayed good recoveries of Lys in the range 99.00–99.27% and was demonstrated for the detection of Lys in wine samples.

Web URL: ***http://www.sciencedirect.com/science/article/pii/S0039914016310359***

37. Majdinasab, M., Yaqub, M., Rahim, A., Catanante, G., Hayat, A., & Marty, J. L. (2017). An Overview on Recent Progress in Electrochemical Biosensors for Antimicrobial Drug Residues in Animal-Derived Food. ***Sensors*****,** ***17*****(9), 1947.**

ABSTRACT:

Anti-microbial drugs are widely employed for the treatment and cure of diseases in animals, promotion of animal growth, and feed efficiency. However, the scientific literature has indicated the possible presence of antimicrobial drug residues in animal-derived food, making it one of the key public concerns for food safety. Therefore, it is highly desirable to design fast and accurate methodologies to monitor antimicrobial drug residues in animal-derived food. Legislation is in place in many countries to ensure antimicrobial drug residue quantities are less than the maximum residue limits (MRL) defined on the basis of food safety. In this context, the recent years have witnessed a special interest in the field of electrochemical biosensors for food safety, based on their unique analytical features. This review article is focused on the recent progress in the domain of electrochemical biosensors to monitor antimicrobial drug residues in animal-derived food.

Web URL: ***http://www.mdpi.com/1424-8220/17/9/1947/htm***

38. Shahzadi, L., Zeeshan, R., Yar, M., Qasim, S. B., Chaudhry, A. A., Khan, A. F., & Muhammad, N. (2017). Biocompatibility Through Cell Attachment and Cell Proliferation Studies of Nylon 6/Chitosan/Ha Electrospun Mats. ***Journal of Polymers and the Environment*****, 1-9.**

ABSTRACT:

Novel cefixime loaded chitosan/HA/Nylon 6 electropsun mats were prepared with excellent swelling properties and were tested for cell attachment and cell proliferation. FTIR spectra shows that hydrogen bonding is developed between composite fibers, as pronounced shape change could be seen in amide I and II peaks. SEM analysis displayed completely different morphology (fiber diameters, general appearance, pore-size and shape) of composite fibers as compared to N6 fibers. Composite fibers showed high thermal stability in thermal gravimetric analysis. The ultimate tensile strength of fiber films was around 4.45 MPa. Both composite and Nylon 6 fibers demonstrated sustained drug release up to 24 h. Although the composite and control (Nylon 6) fibers, both, provided compatible favorable environment for the osteoblast cells, the composite fibers provided a better suited environment for the osteoblast cells differentiation and in parallel supporting cellular population also composite fibers exhibited superior swelling properties than the control which in turn complement the healing properties of wound dressings.

Web URL: ***https://link.springer.com/article/10.1007/s10924-017-1100-8***

39. Gonfa, G., Muhammad, N., & Bustam, M. A. (2017). Probing the interactions between DNA nucleotides and biocompatible liquids: COSMO-RS and molecular simulation study. *Separation and Purification Technology*.

ABSTRACT:

Ionic liquid (ILs) have been attracting significant attention as an alternative solvent for DNA extraction/purification and stabilization/storage. In this work, we investigated the interaction between DNA nucleotides and bio-base ILs to get insight into the effect of structural variations of the ILs on the ILs-DNA complex formations. COSMO-RS based quantum calculations and molecular simulation were used to investigate the interaction between the bio-base ILs and DNA nucleotides. Deoxyadenosine 5’ monophosphate (A), Deoxythymidyine 5’ monophosphate (T), Deoxycytidine 5’ monophosphate (C), Deoxyguanosine 5’ monophosphate (G) and their dimers were used to model DNA. 260 ILs (13 cations and 20 amino acid based anions) were evaluated. Activity coefficients at infinite dilution of the DNA nucleotides and excess enthalpy

of mixing of the systems were predicted using COSMO-RS model. Solvation free energies of the DNA nucleotides were estimated employing molecular dynamics simulations. The activity coefficients of DNA nucleotides decrease with increasing nucleotides chain length. This implies solubility of the nucleotides is higher for longer DNA nucleotide chain. Piperidinium and pyrrolidinium based ILs show lower activity coefficient than choline and morpholinium based ILs. ILs with anions containing nonpolar side chain amino acids show lower activity coefficient compared to those with polar side chains. This implies strong interaction between the nucleotides and ILs with anions containing nonpolar side chain amino acids compared to anions with polar side chains. Moreover, ILs based on anions with nonpolar side chain show higher negative excess enthalpy of mixing compared to those with polar side chain. Further, solvation free energies of DNA nucleotides in the ILs are negative. Solvation free energy is more negative for dimers compared to monomer nucleotides. ILs based on anions with nonpolar side chain show more negative solvation free energies compared to those with polar side chains.

Web URL: **https://www.sciencedirect.com/science/article/pii/S1383586617312662**

40. Jamal, A., Shahzadi, L., Ahtzaz, S., Zahid, S., Chaudhry, A. A., ur Rehman, I., & Yar, M. (2018). Identification of anti-cancer potential of doxazocin: Loading into chitosan based biodegradable hydrogels for on-site delivery to treat cervical cancer. ***Materials Science and Engineering: C*****,** ***82*****, 102-109.**

ABSTRACT:

In this study, an effective, biocompatible and biodegradable *co*-polymer comprising of chitosan (CS) and polyvinyl alcohol (PVA) hydrogels, chemically crosslinked and impregnated with doxazocin, is reported. The chemical structural properties of the hydrogels were evaluated by Fourier Transform Infrared spectroscopy (FTIR) and physical properties were analysed by scanning electron microscopy (SEM). The swelling behaviour is an important parameter for drug release mechanism and was investigated to find out the solution absorption capacity of the synthesized hydrogels. MTT assay revealed that doxazocin loaded hydrogels significantly hindered the cell viability. Flow cytometry analysis was performed to analyse the effect of 8CLH and 4CLH on regulation of cell cycle. Moreover, in vivo anti-cancer potential of synthesized

hydrogels was assessed by CAM Assay. Results displayed that 8CLH with 1 mg/ml of doxazocin had prominently decreased the angiogenesis and significantly increased the number of cells in G1 phase of cell cycle. These results declared that 8CLH will be a good addition among hydrogels used for treatment of cancer by onsite delivery of drug.

Web URL: ***https://www.sciencedirect.com/science/article/pii/S0928493117320246***

41. Khan, A. S., Man, Z., Bustam, M. A., Kait, C. F., Nasrullah, A., Ullah, Z., ... & Muhammad, N. (2018). Dicationic ionic liquids as sustainable approach for direct conversion of cellulose to levulinic acid. *Journal of Cleaner Production*, *170*, 591-600.

ABSTRACT:

The conversion of cellulose to platform chemicals and renewable energies is the most promising and sustainable route to solve the crisis of fossil fuel resources. With this aim, the one-pot conversion of cellulose to industrial important levulinic acid (LA) using dicationic ionic liquids as a catalyst has been investigated. In the present research work, dicationic ionic liquids, containing 1,1-bis(3-methylimidazolium-1-yl) butylene ($[C_4(Mim)_2]$) cation with counter anions hydrogensulfate, dihydrogensulfate, methanesulfonate, and trifluoromethanesulfonate has been synthesized and applied for one-pot conversion of cellulose to LA. The structures, thermal stability, and acidity of ILs were determined by ^1H NMR, CHNS values, thermogravimetric analyzer (TGA) and Hammet acidity function, respectively. Among the synthesized ionic liquids, $[C_4(Mim)_2][(2HSO_4)(H_2SO_4)_2]$ showed higher catalytic activity for conversion of cellulose to LA (55%) without using any additional catalyst or solvent at 100 °C for 3 h, which is the best result compared to previous reports. A mechanism to explain the reaction route toward LA formation is proposed. Moreover, the recycling of IL was easily achieved without structural changes or any impurities. This one-pot production of levulinic acid from untreated cellulose will open new opportunity for the conversion of sustainable biomass resources into valuable chemicals.

Web URL: **https://www.sciencedirect.com/science/article/pii/S0959652617320930**

42. Ilyas, A., Muhammad, N., Gilani, M. A., Ayub, K., Vankelecom, I. F., & Khan, A. L. (2017). Supported protic ionic liquid membrane based on 3-(trimethoxysilyl) propan-1-aminium

acetate for the highly selective separation of CO2. *Journal of Membrane Science*, *543*, 301-309.

ABSTRACT:

The ability to tailor ionic liquids can result in very high separation efficiency for CO_2/CH_4 and CO_2/N_2. In this study, a new protic ionic liquid was synthesized with high CO_2 absorption capacity employing (3-aminopropyl) trimethoxysilane and acetic acid, both of these have been reported to exhibit high affinity for CO_2. The synthesized ionic liquid was characterized by FTIR and the supported ionic liquid membrane was tested to determine the separation of CO_2 from CH_4. Experiments were conducted at different temperatures and feed conditions, and pure and mixed gas permeability/selectivity data were reported. This combination of silyl ether functionalized cation and acetate ion dramatically improved the membrane separation performance as the SILM displayed CO_2 permeance of 23 GPU combined with CO_2/CH_4 selectivity of 41. The synthesized SILM was stable upto 10 bar as no leaching of ionic liquid was observed and the permeance increased from 23 to 31 GPU as the temperature was raised from 25 °C to 65 °C, while the selectivity slightly decreased from 41 to 35 over the same temperature range. The exceptionally high selectivity of CO_2/CH_4 makes [APTMS][Ac] a promising room temperature ionic liquid for CO_2 separation without facilitated transport. A synergistic effect of methoxy groups from [APTMS] part of the ionic liquid caused the enhanced permeability of CO_2 as supported by theoretical calculations.

Web URL: ***https://www.sciencedirect.com/science/article/pii/S0376738817314023***

43. Ullah, Z., Bustam, M. A., Man, Z., Khan, A. S., Muhammad, N., & Sarwono, A. (2017). Preparation and kinetics study of biodiesel production from waste cooking oil using new functionalized ionic liquids as catalysts. *Renewable Energy*, *114*, 755-765.

ABSTRACT:

In this work, 1,4-sultone and benzimidazolium-based ionic liquids (ILs) with four different anions were synthesized, and their structures were confirmed by nuclear magnetic resonance (NMR) and elemental analysis (CHNS). The acidity of the synthesized ILs was studied using Hammett acidity function and COSMO-RS. The waste cooking oil was used as a raw material for

biodiesel production and their different fatty acids were determined by gas chromatography coupled with flame ionization detector (GC-FID). These four ILs, as catalysts, were screened and comparatively IL 3-methyl-1-(4-sulfo-butyl)-benzimidazolium trifluoromethanesulfonate [BSMBIM][CF_3SO_3] was selected for further detailed optimization study. This IL experimental efficiency results supported the Hammett acidity function and COSMO-RS study. The catalyst performance was studied and optimised the different parameters. The catalyst efficiency was studied in one and two-step reactions. [BSMBIM][CF_3SO_3] as a catalyst showed the esterification of waste cooking oil up to 78.13% in a single step reaction. Potassium hydroxide was used in the second step to *trans*-esterify the waste cooking oil up to 94.52%. The catalyst was reused for seven times with high-yield production. The obtained biodiesel was characterized by GC, NMR, FTIR, thermogravimetric (TGA) and their physicochemical properties were compared with the already established standards. The kinetic study of this transesterification reaction was evaluated and followed the first-order reaction mechanism.

Web URL: ***https://www.sciencedirect.com/science/article/pii/S0960148117307127***

44. Khan, A. S., Hussain, A. N., Sidra, L., Sarfraz, Z., Khalid, H., Khan, M., ... & Rehman, I. U. (2017). Fabrication and in vivo evaluation of hydroxyapatite/carbon nanotube electrospun fibers for biomedical/dental application. *Materials Science and Engineering: C*.

ABSTRACT:

The aim was to synthesize bioactive electrospun fibers for biomedical and dental application with improved biocompatibility. In situ precipitation of nano-hydroxyapatite (nHA) was performed with various concentrations (0.5%, 1%, 2%, 3%, and 5% wt/wt) of functionalized multi-walled-carbon nanotubes (MWCNTs) by using microwave irradiation technique. The obtained composites were characterized by Fourier Transform Infrared (FTIR), X-ray Diffraction (XRD), Thermogravimetric Analysis/Differential Scanning Calorimetry (TGA/DSC), and the cylindrical discs were made for mechanical testing. The failure behavior was analyzed by Scanning Electron Microscope (SEM). CNT and HA/CNT were silanized with γ-methacryloxypropyl-trimethoxysilane (MPTS) and mixed with polyvinyl alcohol (10% wt./vol.) and electrospun to fabricate fibers. The biocompatibility of both fibers was accessed by their

effects on angiogenesis in a chick chorioallantoic membrane (CAM) assay. The electrospun fibers were analyzed by SEM. FTIR confirmed the structural behavior of pre and post-silanized HA/CNT. XRD showed the phase purity and crystallinity before and after heat treatment. Mechanical properties showed that 3% loaded HA/CNT has higher compressive strength (100.5 ± 5.9 MPa) compared to others and the failure behavior exhibited dispersion of CNT in HA matrix. The HA/CNT electrospun fibers showed significantly more blood vessels formation compared to CNT fibers. These HA/CNT electrospun fibers showed promising results in terms of biocompatibility and with improved mechanical properties of CNT reinforced composites, they can be used in load bearing clinical applications.

Web URL: ***http://www.sciencedirect.com/science/article/pii/S0928493116321956***

45. Khan, Z. U. H., Khan, A., Chen, Y., ullah Khan, A., Shah, N. S., Muhammad, N., ... & Wan, P. (2017). Photo catalytic applications of gold nanoparticles synthesized by green route and electrochemical degradation of phenolic Azo dyes using AuNPs/GC as modified paste electrode. ***Journal of Alloys and Compounds*****,** ***725*****, 869-876.**

ABSTRACT:

A highly efficient, quick and environmentally benign protocol has been adopted to synthesize AuNPs using the plant extract of *Sueda fruciotosa*. UV–vis spectroscopy, XRD, HRTEM, SEM and FTIR were used to characterize the prepared AuNPs. Different concentrations of plant extract were used to optimize the size, morphology and distribution of AuNPs. AuNPs were of small size and spheroid in shape at lower concentration. AuNPs showed a surface plasmon resonance at 443 nm. According to HRTEM the average size of AuNPs was 6–8 nm. The AuNPs were appraised for their photo degradation activity on methylene blue (MB) as an experimental substrate. Photo-catalytic activity of AuNPs was found to be dependent on the concentration of catalyst, irradiation time, size and aggregation of AuNPs. Furthermore, AuNPs exhibited an excellent electro-catalytic activity. The sensitivity of modified AuNPs was also studied for phenolic Azo dyes (PAD) which showed its good degradation activity. These gold nanoparticles found to be significantly applicable in the field of electrochemistry, sensors, catalysis, nano-devices, treatment of waste water and conversion of toxic agents into less toxic compound.

Web URL: ***https://www.sciencedirect.com/science/article/pii/S0925838817325987***

46. Aleem, A. R., Shahzadi, L., Alvi, F., Khan, A. F., Chaudhry, A. A., ur Rehman, I., & Yar, M. (2017). Thyroxin releasing chitosan/collagen based smart hydrogels to stimulate neovascularization. ***Materials & Design*****,** ***133*****, 416-425.**

ABSTRACT:

The development of new biomaterials with tailored properties is highly desired in tissue engineering field. The neovascularization is essential part of tissue regeneration which provides food and nutrients to cells. There is a real need for proangiogenic biomaterials to assist wound healing. The ideal dressing should be inexpensive and achieve rapid healing with minimal inconvenience to the patient. In this paper, new porous thyroxin containing pro-angiogenic hydrogels were generated via freeze gelation protocol. The chemical structural analysis of the synthesized hydrogels was investigated by Fourier Transform Infrared (FTIR) spectroscopy. The morphology and pore dimensions were studied by scanning electron microscopy (SEM). In swelling studies, 10 μg thyroxine loaded hydrogel (TLH-10) showed greater degree of swelling as compared to 1 μg loaded thyroxine material (TLH-1) and control. The degradation studies were tested in three different media, i.e. phosphate buffer saline (PBS), lysozyme and hydrogen peroxide and relatively higher degradation was seen in hydrogen peroxide. The synthesized materials were implanted on the chick chorioallantoic membrane to investigate their angiogenic potential. The TLH-1 hydrogel stimulated angiogenesis greater than the TLH-10; in this case blood vessels were attached and very much grown into the scaffold.

Web URL: ***https://www.sciencedirect.com/science/article/pii/S0264127517307219***

47. Rauf, S., Nawaz, M. A. H., Muhammad, N., Raza, R., Shahid, S. A., Marty, J. L., & Hayat, A. (2017). Protic ionic liquids as a versatile modulator and stabilizer in regulating artificial peroxidase activity of carbon materials for glucose colorimetric sensing. ***Journal of Molecular Liquids*****,** ***243*****, 333-340.**

ABSTRACT:

Nanoparticles proved a viable alternative to the already used sensing and diagnostics methods due to their low cost, good stability, easy availability and easy synthesis. In the present approach, nitrogen doped titania nanoparticles are prepared through freeze drying method, and subsequently stabilized through ionic liquid. These nanoparticles were characterized through various techniques such as X-ray diffraction (XRD), Fourier transformation infrared spectroscopy (FTIR), Scanning electron microscopy (SEM), BET pore size and surface area analyzer, X-ray photoelectron spectroscopy (XPS) and UV–Visible diffuse reflectance spectroscopy (UV–Vis. DRS). The synthesized nitrogen doped titania nanoparticles were proved to be a novel peroxidase mimetic with great potential to catalyze oxidation of 3,3′,5,5′-tetramethylbenzidine (TMB) in the presence of hydrogen peroxide (H_2O_2) to form a blue color product. As a proof of concept, this new enzyme mimic was used as a robust nanoprobe for the detection of hydrogen peroxide with improved analytical characteristics. A linear response for hydrogen peroxide detection was obtained in the range of 10–300 μmol/L, with a detection limit of 2.5 μmol/L. Taking into account the valuable intrinsic peroxidase activity, the present work may find widespread applications in the field of sensors and biosensors for diverse applications.

Web URL: ***https://www.sciencedirect.com/science/article/pii/S0021979717307828***

48. Iqbal, B., Muhammad, N., Jamal, A., Ahmad, P., Khan, Z. U. H., Rahim, A., ... & Rehman, I. U. (2017). An application of ionic liquid for preparation of homogeneous collagen and alginate hydrogels for skin dressing. ***Journal of Molecular Liquids*****,** ***243*****, 720-725.**

ABSTRACT:

Ionic liquid due to its green nature as well as having the ability to dissolve biopolymer, was used in the preparation of collagen and alginate hydrogels. The collagen and alginate hydrogels were prepared in different ratios of collagen and alginate, labeled CA5040, CA6030 and CA7020. The prepared hydrogels were characterized with Fourier-transform infrared spectroscopy (FTIR), Scanning electron microscope (SEM), Thermogravimetric analysis (TGA) analysis. The samples were evaluated for water uptake behavior and mechanical properties using electrodynamic fatigue testing system. The biocompatibility was assessed through hemolysis and MTT assay on rat mesenchymal stem cells (rMSC) which showed satisfactory results. The drug loading and

subsequent antibacterial properties were also performed. The prepared collagen and alginate hydrogels are suggested to be used for skin dressing.

Web URL: **https://www.sciencedirect.com/science/article/pii/S0167732217327435**

49. Rafiq, M. Y., Iqbal, F., Aslam, F., Bilal, M., Munir, N., Sultana, I., ... & Razaq, A. (2017). Fabrication and characterization of ZnO/MnO2 and ZnO/TiO2 flexible nanocomposites for energy storage applications. ***Journal of Alloys and Compounds*****,** ***729*****, 1072-1078.**

ABSTRACT:

ZnO based nanostructure composites are attractive for high-tech applications of energy conversion and energy storage due to wide range in operating potential window. This study presents about fabrication of ZnO/MnO_2 and ZnO/TiO_2composites via hydrothermal method in two consecutive steps. Furthermore lignocelluloses fiber directly collected form self-growing plant Monochoria Vagina, were incorporated in fabricated ZnO/MnO_2 and ZnO/TiO_2 composites for development of flexible and bulk paper composite electrode. The structural and morphological analysis were carried out using X-ray Diffraction (XRD), Scanning Electron Microscopy (SEM), respectively. XRD analysis confirm the crystalline structures for ZnO/MnO_2 and ZnO/TiO_2 samples with crystallite size ~62 nm and ~63 nm, respectively. SEM images shows the sheet-like and nanorods morphology for ZnO and MnO_2 nanostructures, respectively. Fourier Transform Infrared (FTIR) Spectroscopy absorbance spectrum reveal the composite formation of ZnO/MnO_2/LC and ZnO/TiO_2/LC as bulk paper electrodes whereas cyclic Voltammetry measurement showed the capacitive behavior of composite paper electrodes for the suitable applications in supercapacitors and batteries.

Web URL: ***https://www.sciencedirect.com/science/article/pii/S0925838817333030***

50. Ahmad, P., Khandaker, M. U., Shah, S. T., Rehman, F., Khan, G., Muhammad, N., ... & Numan, A. (2017). Controlled synthesis of anisotropic hexagonal boron nitride nano-web. ***Materials Science in Semiconductor Processing*****,** ***66*****, 44-49.**

ABSTRACT:

The assembly of one-dimensional (1D), two-dimensional (2D), and three-dimensional (3D) nanomaterial show entirely different properties than their individual counterparts. Since the shape of nanomaterials plays a crucial role in designing devices with desired applications, relentless efforts are on-going to obtain the parameters for controlling the shape of the final product. Present study concerns the synthesis and growth of a combined 2D and 3D structure of Hexagonal Boron Nitride Nanofibers Web (BNNFs-Web) from 1D structure of BNNFs. Magnesium catalytic layer deposited on Silicon substrate produces Web-like nucleation sites when etches with NH_3 flow at 300 °C. The precursor's mixture of B, γ-Fe_2O_3 and MgO annealed at 500 °C uses these nucleation sites as a pattern, and grow BNNFs-Web in a unique 2D and 3D configuration at 1000 °C. XRD, Raman and FTIR spectroscopies confirmed the h-BN phase of the as-synthesized BNNFs-Web. This unique 2D and 3D material can offer distinguish features with improved properties as compared to other nanostructures of h-BN. Such a material can be a much better choice for its potential applications in different fields of bio-medical, microelectronic mechanical system and solid state neutron detectors.

Web URL: ***http://www.sciencedirect.com/science/article/pii/S1369800116307417***

51. Goud, K. Y., Hayat, A., Catanante, G., Satyanarayana, M., Gobi, K. V., & Marty, J. L. (2017). An electrochemical aptasensor based on functionalized graphene oxide assisted electrocatalytic signal amplification of methylene blue for aflatoxin B1 detection. *Electrochimica Acta*, *244*, 96-103.

ABSTRACT:

In this work, we developed an electrochemical aptasensor by using methylene blue (MB) redox probe labeled aptamer as a signaling fragment and functional graphene oxide (FGO) as the signal-enlarging platform. The role of functionalized graphene oxide was not mere to serve as a covalent immobilization support for aptamer sequences, but its catalytic signal amplification behavior towards methylene blue was demonstrated for the first time in the present work. The functionalized graphene oxide was cast on screen-printed carbon electrodes (SPCE), and then the MB-tagged aptamer was covalently immobilized on SPCE by using hexamethylenediamine (HMDA) as a spacer via carbodiimide amide-bonding chemistry. Aflatoxin B1 (AFB1) analyte

molecule detection was accomplished by the aptamer conjugated redox probe, which undergoes/involves a conformational change in the complex structure of aptamer consequent to AFB1 binding. The proposed assay permitted to detect AFB1 in the linear range of 0.05-6.0 ng mL(-1) with a very low limit of detection (LOD) (0.05 ng mL(-1)). The present principle aptasensor was tested to screen the alcoholic beverage samples for AFB1 detection and good recovery values were obtained.

Web URL: ***https://www.cheric.org/research/tech/periodicals/view.php?seq=1550571***

52. Sarwono, A., Man, Z., Muhammad, N., Khan, A. S., Hamzah, W. S. W., Rahim, A. H. A., ... & Wilfred, C. D. (2017). A new approach of probe sonication assisted ionic liquid conversion of glucose, cellulose and biomass into 5-hydroxymethylfurfural. ***Ultrasonics Sonochemistry*****, *37*, 310-319.**

ABSTRACT:

5-Hydroxymethylfurfural (HMF) has been identified as a promising biomass-derived platform chemical. In this study, one pot production of HMF was studied in ionic liquid (IL) under probe sonication technique. Compared with the conventional heating technique, the use of probe ultrasonic irradiation reduced the reaction time from hours to minutes. Glucose, cellulose and local bamboo, treated with ultrasonic, produced HMF in the yields of 43%, 31% and 13% respectively, within less than 10 min. The influence of various parameters such as acoustic power, reaction time, catalysts and glucose loading were studied. About 40% HMF yield at glucose conversion above 90% could be obtained with 2% of catalyst in 3 min. Negligible amount of soluble by-product was detected, and humin formation could be controlled by adjusting the different process parameters. Upon extraction of HMF, the mixture of ionic liquid and catalyst could be reused and exhibited no significant reduction of HMF yield over five successive runs. The purity of regenerated $[C_4C_1im]Cl$ and HMF was confirmed by NMR spectroscopy, indicating neither changes in the chemical structure nor presence of any major contaminants during the conversion under ultrasonic treatment. ^{13}C NMR suggests that $[C_4C_1im]Cl/CrCl_3$ catalyses mutarotation of α-glucopyranose to β-glucopyranose leading to

isomerization and finally conversion to HMF. The experimental results demonstrate that the use of probe sonication technique for conversion to HMF provides a positive process benefit.

Web URL: ***http://www.sciencedirect.com/science/article/pii/S1350417717300378***

53. Obasi, H. C., Chaudhry, A. A., Ijaz, K., Akhtar, H., & Malik, M. H.(2017). Development of biocomposites from coir fibre and poly (caprolactone) by solvent casting technique. ***Polymer Bulletin*****, 1-13.**

ABSTRACT:

In this study, blends of poly (caprolactone) (PCL) with different content of coir fibre (CF) (2, 2.5 and 5 wt%) were fabricated by solvent casting technique to obtain a biodegradable composite. The PCL/CF composites obtained have been characterised using the X-ray diffraction (XRD), Fourier transform infrared spectroscopy (FTIR), scanning electron microscopy (SEM) and Electrodynamic fatigue testing machines. According to XRD patterns, the intensity of the peak in the pure PCL spectrum was found to decrease by the addition of coir fibre which then disappears when the CF content is 5 wt% is indicating that coir fibre inhibited the diffusion and deposition of PCL molecules. The FTIR absorption spectra for the PCL/CF blends showed that there was no new peak to represent the chemical interaction between the functional groups of coir fibre and poly (caprolactone). The SEM micrographs of the composites indicate inadequate wetting of coir fibre as filler content increases due to poor dispersion and interfacial adhesion. The tensile strength of the composites samples was found to increase with an increase in the fibre content up to 2.5 wt% on addition of coir fibre but with a reduction from 16.79 N/mm^2 for the neat polymer to 5.08 N/mm^2 for the blend with 5 wt% coir fibre (a 69.74% decrease). The addition of coir fibre reduces the elongation at break of the composites, whereas the Young modulus value of composites goes on increasing up to 182 N/mm^2 for coir fibres volume fraction of 2.5 wt%. The behaviour of samples with high fibre content could be explained by insufficient fibre wetting and poor interfacial adhesion with no coupling agent in addition to the low aspect ratio of the coir particles.

Web URL: ***https://link.springer.com/article/10.1007/s00289-017-2122-z***

54. Yar, M., Shahzadi, L., Mehmood, A., Raheem, M. I., Román, S., Chaudhry, A. A., ... & MacNeil, S. (2017). Deoxy-sugar releasing biodegradable hydrogels promote angiogenesis and stimulate wound healing. *Materials Today Communications*, *13*, 295-305.

ABSTRACT:

Vascular endothelial growth factor (VEGF) stimulates endothelial cells to migrate, proliferate and form new blood vessels. However direct delivery of VEGF has not become clinically adopted as a means of stimulating blood vessel formation and wound healing because of its relatively poor stability and its production of immature blood vessels. A simpler way of stimulating production of VEGF *in situ* is explored in this study following reports of deoxy sugars involved in inducing VEGF production. The pro-angiogenic effect of L and D isomers of deoxy sugars (ribose, fucose and rhamnose) loaded into biodegradable chitosan/collagen hydrogels was examined using a chick chorionic allantoic membrane assay. The L-sugars were all pro-angiogenic but only the 2-deoxy-D-ribose had strong effects on angiogenesis. Furthermore, these sugars could not be metabolised by four strains of *Staphylococcus aureus*, as a metabolic substrate for growth, although some of these could be metabolised by another typical pathogen, *Pseudomonas aeruginosa*. The effects of 2-deoxy-D-ribose in a chitosan/collagen hydrogel on wound healing were also assessed. This biomaterial doubled the rate of cutaneous wound healing in rats associated with an increase in vascularisation detected by staining for CD34 positive cells.

Web URL: https://www.sciencedirect.com/science/article/pii/S2352492817302581

55. Babar, A., Yar, M., Tarazi, H., Duarte, V., Alshammari, M. B., Gilani, M. A., ... & Khan, A. F. (2017). Molecular docking and glucosidase inhibition studies of novel N-arylthiazole-2-amines and Ethyl 2-[aryl (thiazol-2-yl) amino] acetates. *Medicinal Chemistry Research*, *26*(12), 3247-3261.

ABSTRACT:

This study describes an efficient synthesis of a series of novel ethyl 2-[aryl(thiazol-2-yl)amino]acetates (**4a–l**) from *N*-arylthiazole-2-amines (**3a–l**). The reaction conditions were optimized and the best results were obtained when ethyl chloroacetate was used as alkylating agent and NaH as base in THF. α-glucosidase and β-glucosidase inhibition activities

of *N*-arylthiazole-2-amines (**3a–l**) and ethyl 2-[aryl(thiazol-2-yl)amino]acetates (**4a–l**) were determined, which revealed that most of the compounds showed high percentage inhibition towards the enzymes. Among the synthesized compounds, **4e** appeared to have the highest inhibition towards α-glucosidase having IC_{50} value of 150.4 ± 1.9 µM which was almost two folds as compared to acarbose (336.9 ± 9.0 µM) taken as standard. Molecular docking of the compounds **3g**, **3f**, **4a**, and **4e** was also performed which showed their bonding modes to the enzyme's active sites via amino and acetate groups, respectively.

Web URL: **https://link.springer.com/article/10.1007/s00044-017-2018-3**

56. Iqbal, H., Ali, M., Zeeshan, R., Mutahir, Z., Iqbal, F., Nawaz, M. A. H., ... & Khan, A. F. (2017). Chitosan/hydroxyapatite (HA)/hydroxypropylmethyl cellulose (HPMC) spongy scaffolds-synthesis and evaluation as potential alveolar bone substitutes. ***Colloids and Surfaces B: Biointerfaces*****,** ***160*****, 553-563.**

ABSTRACT:

Alveolar bone loss is associated with infections and its augmentation is a pre-requisite for the success of dental implants. In present study, we aim to develop and evaluate novel freeze dried doxycycline loaded chitosan (CS)/hydroxyapatite (HA) spongy scaffolds where hydroxypropylmethyl cellulose (HPMC) was added as a crosslinker. Scaffolds displayed compressive strength of 14 MPa/cm^3 and 0.34 as elastic response. The interconnected pore diameter was 41–273 µm, favorably provided the template supporting cells and transport. An overall 10% degradation was seen after 14 day's studies at pH 7.4 in PBS. Doxycycline hyclate, a frequently used drug to counter oral infections, demonstrated an initial burst release (6–8 h), followed by a sustain release profile for the remaining 64 h. CS/HA/HPMC scaffolds were nontoxic and promoted pre-osteoblast cell viability as seen with live/dead calcein staining after 24 h where scaffolds with 10% and 25% HPMC by weight of scaffold had more viable cells. Scaffolds with 10%, 20% and 25% HPMC by weight of scaffold showed efficient cellular adhesion as seen in scanning electron microscopy images (day 8) indicating that pre-osteoblast cells were able to adhere well on the surface and into the porous structure via cytoplasmic extensions. Hoechst 33258 nuclear staining at day 2 and 8 indicated cell proliferation which was

further supported byMTT assay at day 2, 4 and 8. Although all scaffolds supported pre-osteoblast cell viability, alkaline phosphatase (ALP) staining demonstrated that upon induction, differentiation was pronounced in case of scaffolds with 10% HMPC scaffolds. Conclusively, these materials having all the required mechanical and biological properties are potential candidates for alveolar bone regeneration.

Web URL: **https://www.sciencedirect.com/science/article/pii/S0927776517306379**

57. Rahim, A., Rehman, Z. U., Mir, S., Muhammad, N., Rehman, F., Nawaz, M. H., ... & Chaudhry, A. A. (2017). A non-enzymatic glucose sensor based on CuO-nanostructure modified carbon ceramic electrode. *Journal of Molecular Liquids*, *248*, 425-431.

ABSTRACT:

Mesoporous silica-graphite composite (SiO_2/C-graphite) was synthesized by the sol-gel technique. The surface area (S_{BET} = 98.93 m^2/g), pore volume (0.30 cm^3/g) and pore size (12.16 nm) were characterized by BET. The novelty of this work lays in the fabrication of material in which ceramic material (SiO_2/C-graphite) was decorated with copper oxide (CuO) nanostructure. SEM images revealed material compactness without phase segregation and EDX mapping showed a homogenous structure. Pressed disk electrode fabricated with SiO_2/C/CuO nanocomposite material was evaluated as an amperometric non-enzymatic glucose sensor in 0.1 M NaOH solution. The linear response range, sensitivity, detection limit, and quantification limit were 0.02–20.0 mmol L^{-1}, 0.06 µmol L^{-1}, 472 µA $mmol^{-1}$ L^{-1} cm^{-2}, and 0.76 mmol L^{-1}, respectively. The electrode response time is < 1 s with the addition of 0.02 mmol L^{-1}glucose. The electrode is chemically stable, exhibits rapid and excellent sensitivity and does not show any interference from coexisting species present in the blood samples. The proposed sensor repeatability was assessed as 1.9% RSD for ten measurements of 13.0 mmol L^{-1} glucose solution. The sensor tested to ascertain glucose in blood serum showed to be a promising tool for the future evolution of non-enzymatic glucose sensors.

Web URL: **https://www.sciencedirect.com/science/article/pii/S0167732217342800**

58. Jiang, R., Xin, Z., Xu, S., Shi, H., Yang, H., Song, L., ... & Li, Y. (2017). Enzyme-mimicking polymer brush-functionalized surface for combating biomaterial-associated infections. *Applied Surface Science*, *423*, 869-880.

ABSTRACT:

Biomaterial-associated infections critically compromise the functionality and performance of the medical devices, and pose a serious threat to human healthcare. Recently, natural DNase enzyme has been recognized as a potent material to prevent bacterial adhesion and biofilm formation. However, the vulnerability of DNase dramatically limits its long-term performance in antibacterial applications. In this work, DNase-mimicking polymer brushes were constructed to mimic the DNA-cleavage activity as well as the macromolecular scaffold of the natural DNase. The bacteria repellent efficacy of DNase-mimicking polymer brush-functionalized surface was comparable to that of the DNase-functionalized surface. More importantly, due to their inherent stability, DNase-mimicking polymer brushes presented the much better performance in inhibiting bacterial biofilm development for prolonged periods of time, as compared to the natural DNase. The as-developed DNase-mimicking polymer brush-functionalized surface presents a promising approach to combat biomaterial-associated infections.

Web URL: https://www.sciencedirect.com/science/article/pii/S0169433217318871

59. Ferrucci, D., Biancardi, M. F., Nishan, U., Rosa-Ribeiro, R., & Carvalho, H. F. (2017). Desquamation takes center stage at the origin of proliferative inflammatory atrophy, epithelial–mesenchymal transition, and stromal growth in benign prostate hyperplasia. *Cell biology international*, *41*(11), 1265-1270.

ABSTRACT:

In this commentary, we propose a relationship between desquamation, initially described as the collective detachment and deletion of epithelial cell in the prostate gland after castration, and proliferative inflammatory atrophy (PIA) and stromal growth in benign prostate hyperplasia (BPH). First, in response to diverse stimuli, including inflammatory mediators, epithelial cells desquamate and leave a large surface of the luminal side of the basement membrane (BM) exposed. Basal cells are activated into intermediate-type cells, which change morphology to

cover and remodel the exposed BM (simple atrophy) to a new physiological demand (such as in the hypoandrogen environment, simulated by surgical and/or chemical castration) and/or to support re-epithelialization (under normal androgen levels). In the presence of inflammation (that might be the cause of desquamation), the intermediate-type cells proliferate and characterize PIA. Second, in other circumstances, desquamation is an early step of epithelial-to-mesenchymal transition (EMT), which contributes to stromal growth, as suggested by some experimental models of BPH. The proposed associations correlate unexplored cell behaviors and reveal the remarkable plasticity of the prostate epithelium that might be at the origin of prostate diseases.

Web URL: **http://onlinelibrary.wiley.com/doi/10.1002/cbin.10867/full**

60. Goud, K. Y., Hayat, A., Satyanarayana, M., Kumar, V. S., Catanante, G., Gobi, K. V., & Marty, J. L. (2017). Aptamer-based zearalenone assay based on the use of a fluorescein label and a functional graphene oxide as a quencher. ***Microchimica Acta*****,** ***184*****(11), 4401-4408.**

ABSTRACT:

A versatile and cost-effective aptamer-based fluorescence quenching assay is described for the detection of the mycotoxin zearalenone (ZEN). Exfoliated functional graphene oxide (FGO) of high water-dispersibility is adopted as an effective fluorescence quencher of the fluorescence of FAM. Quenching properties of graphite, graphene oxide (GO) and FGO were investigated, and FGO is found to be the most efficient quencher. FGO therefore was used in an aptamer-based detection format that allows ZEN to be determined in the concentration range of 0.5 to 64 $ng \cdot mL^{-1}$ with a limit of detection of 0.5 $ng \cdot mL^{-1}$. The aptamer assay has good repeatability and reproducibility ($n \geq 4$). Selectivity of the aptamer assay against a set of possible interferents is substantiated. This aptasensing assay was successfully applied to the determination of ZEN in (spiked) alcoholic beverage samples, beer and wine, and recovery values in the range of 87 to 96% were obtained for the determination of ZEN at levels as low as 1–16 ng mL^{-1}.

Web URL: **https://link.springer.com/article/10.1007/s00604-017-2487-6**

61. Wang, X., Yan, S., Song, L., Shi, H., Yang, H., Luan, S., ... & Zhao, J. (2017). Temperature-Responsive Hierarchical Polymer Brushes Switching from Bactericidal to Cell Repellency. *ACS applied materials & interfaces*, *9*(46), 40930-40939.

ABSTRACT:

Unlike conventional poly(*N*-isopropylacrylamide) (PNIPAM)-based surfaces switching from bactericidal activity to bacterial repellency upon decreasing temperature, we developed a hierarchical polymer architecture, which could maintain bactericidal activities at room temperature while presenting bacterial repellency at physiological temperature. In this architecture, a thermoresponsive bactericidal upper layer consisting of PNIPAM-based copolymer and vancomycin (Van) moieties was built on an antifouling poly(sulfobetaine methacrylate) (PSBMA) bottom layer via sequential surface-initiated photoiniferter-mediated polymerization. At room temperature below the lower critical solution temperature (LCST), the PNIPAM-based upper layer was stretchable, facilitating contact killing of bacteria by Van. At physiological temperature (above the LCST), the PNIPAM-based layer collapsed, thus leading to the burial of Van and exposure of bottom PSBMA brushes, finally displaying notable performances in bacterial inhibition, dead bacteria detachment, and biocompatibility, simultaneously. Our strategy provides a novel pathway in the rational design of temperature-sensitive switchable surfaces, which shows great advantages in the real-world infection-resistant applications.

Web URL: **http://pubs.acs.org/doi/abs/10.1021/acsami.7b09968**

62. Rhouati, A., Bulbul, G., Latif, U., Hayat, A., Li, Z. H., & Marty, J. L. (2017). Nano-Aptasensing in Mycotoxin Analysis: Recent Updates and Progress. *Toxins*, *9*(11), 349.

ABSTRACT:

Recent years have witnessed an overwhelming integration of nanomaterials in the fabrication of biosensors. Nanomaterials have been incorporated with the objective to achieve better analytical figures of merit in terms of limit of detection, linear range, assays stability, low production cost, etc. Nanomaterials can act as immobilization support, signal amplifier, mediator and artificial enzyme label in the construction of aptasensors. We aim in

this work to review the recent progress in mycotoxin analysis. This review emphasizes on the function of the different nanomaterials in aptasensors architecture. We subsequently relate their features to the analytical performance of the given aptasensor towards mycotoxins monitoring. In the same context, a critically analysis and level of success for each nano-aptasensing design will be discussed. Finally, current challenges in nano-aptasensing design for mycotoxin analysis will be highlighted.

Web URL: **http://www.mdpi.com/2072-6651/9/11/349/htm**

63. Farooq, A., Khurram, M. S., Rafiq, S., Memon, S. A., Ghauri, M., Shahzad, K., ... & Muhammad, N. Biomass gasification for energy generation: parametric investigation on continuous updraft Gasifier.

ABSTRACT:

Biomass has gained inevitable importance as a distributed source of energy after coal, oil and natural gas. The gasification is one of the cleaner technology to convert biomass into environmental friendly gaseous fuel. An updraft gasifier was designed and experiments were carried out using mustard seed(s) as feed. It was observed that the temperature distribution improved using circulation. The temperature achieved lied in the range of 600oC-800oC with and without circulation. Increasing the temperature from 400oC- 800oC and equivalence ratio (ER) from 0.15-0.3, increases the amount of H2/CO from 0.29-2.67; whereas in the case of circulation it decreases from 0.65-0.41. The CO2 produced is 70% with circulation and 50% without circulation. Increasing temperature reduces the fluctuating amount of NOx from 1976 ppm to573 ppm under normal conditions. While SO2 is 229 ppm without circulation and is almost zero for circulation. At the optimum ER value of 0.23, maximum value of lower heating value (LHV) and higher heating value (HHV) without circulation were observed to be 7743 Btu/lb and 8995 Btu/lb respectively while 3801 Btu/lb and 4397 Btu/lb with circulation.

Web URL:

https://www.researchgate.net/profile/Abid_Farooq/publication/321096407_Biomass_gasification_for_energy_generation_parametric_investigation_on_continuous_updraft_Gasifier/lin

ks/5a0d103fa6fdcc39e9bfbec0/Biomass-gasification-for-energy-generation-parametric-investigation-on-continuous-updraft-Gasifier.pdf

64. Imran, M., Waheed, Y., Ghazal, A., Ullah, S., Safi, S. Z., Jamal, M., ... & Ullah, F. (2017). Modern biotechnology-based therapeutic approaches against HIV infection. ***Biomedical reports*****, *7*(6), 504-507.**

ABSTRACT:

The causative agent of acquired immune deficiency syndrome (AIDS) is human immunodeficiency virus (HIV). Since its discovery before 30 years, a number of drugs known as highly active antiretroviral therapy have been developed to suppress the life cycle of the virus at different stages. With the current therapeutic approaches, ending AIDS means providing treatment to 35 million individuals living with HIV for the rest of their lives or until a cure is developed. Additionally, therapy is associated with various other challenges such as potential of drug resistance, toxicity and presence of latent viral reservoir. Therefore, it is imperative to search for treatments and to identify new therapeutic approaches against HIV infection to avoid daily intake of drugs. The aim of the current review was to summarize different therapeutic strategies against HIV infection, including stem cell therapy, RNA interference, CRISPR/Cas9 pathways, antibodies, intrabodies and nanotechnology. Silencing RNA against chemokine receptor 5 and other HIV RNAs have been tested and found to elicit homology-based, post-transcriptional silencing. The CRISPR/Cas9 is a gene editing technology that produces a double-stranded nick in the virus DNA, which is repaired by the host machinery either by non-homology end joining mechanism or via homology recombination leading to insertion, deletion mutation which further leads to frame shift mutation and non-functional products. Intrabodies are intracellular-expressed antibodies that are directed towards the targets inside the cell unlike the naturally expressed antibodies which target outside the cell. Different nanotechnology-based therapeutic approaches are also in progress against HIV. HIV eradication is not feasible without deploying a cure or vaccine alongside the treatment.

Web URL: https://www.spandidos-publications.com/br/7/6/504/download

65. Mushtaq, S., Khan, J. A., Rabbani, F., Latif, U., Arfan, M., & Yameen, M. A. (2017). Biocompatible biodegradable polymeric antibacterial nanoparticles for enhancing the effects of a third-generation cephalosporin against resistant bacteria. *Journal of medical microbiology*, *66*(3), 318-327.

ABSTRACT:

Purpose. In the present study, enhancement of the the antibacterial activity of ceftriaxone against Gram-positive (meticillin-resistant *Staphylococcus aureus*; MRSA) and Gram-negative (*Escherichia coli*) bacteria with a biodegradable polymer was attempted.

Methodology. MRSA and *E. coli* were collected and identified by biochemical and molecular tests. Blank and ceftriaxone-loaded chitosan nanoparticles (CNPs) were prepared by the ionic gelation method. *In vitro* antibiotic-susceptibility studies were performed by disc diffusion, agar well plate method, Etest and time-kill assay. *In vivo* activity was assessed using the neutropenic mouse thigh model and cytotoxicity was estimated by MTT (methylthiazolyldiphenyl tetrazolium bromide) assay with the MCF-7 cancer cell line.

Results. MRSA showed 97 % and *E. coli* 83 % resistance against ceftriaxone in the disc diffusion test. The isolates showing a ≥1024 mg l^{-1} MIC value for ceftriaxone were selected for further evaluation. In the agar well plate method, the mean zones of inhibition for blank and ceftriaxone-loaded CNPs were 17 and 23 mm, respectively, for MRSA isolates and 15 and 25 mm, respectively, for *E. coli* isolates. In the time-kill assay, ~1 $\log_{10}$ to ~2.5 $\log_{10}$ reduction in viability was seen with both isolates when treated with ceftriaxone-loaded CNPs over 24 h. The *in vivo* studies also showed the enhanced antibacterial activity of ceftriaxone-loaded CNPs, with a 41 % reduction in MRSA and a 27 % reduction in *E. coli* burden. A low cytotoxicity of blank and ceftriaxone-loaded CNPs was seen, with a slight reduction in the percentage viability of cells from 87 to 83 % and from 88 to 81 %, respectively.

Conclusion. The synergistic effect of ceftriaxone-loaded CNPs is a useful finding for the treatment of MRSA and *E. coli* infections.

Web URL:

http://jmm.microbiologyresearch.org/content/journal/jmm/10.1099/jmm.0.000445

66. Khan, A. S., Man, Z., Bustam, M. A., Gonfa, G., Chong, F. K., Ullah, Z., ... & Muhammad, N. (2017). Effect of Structural Variations on the Thermophysical Properties of Protic Ionic Liquids: Insights from Experimental and Computational Studies. *Journal of Chemical & Engineering Data*, *62*(10), 2993-3003.

ABSTRACT:

In this work, new protic ionic liquids (PILs) based on 1-methylimidazolium/1-propanenitrileimidazolium cations with hydrogen sulfate, methanesulfonate, trifluoromethanesulfonate, *para*-toluenesulfonate, trifluoroacetate, and acetate anions were synthesized. The structures and purity of the products were confirmed by using ^{1}H and ^{13}C NMR and CHNS elemental analysis. The effect of structural variations on the thermophysical properties, namely, refractive index, density, and viscosity, was evaluated in a wide temperature range. The viscosity and density values were measured within the temperature range of 293.15–373.15 K. The density values were used further to calculate more properties like thermal expansion coefficient, molecular volume, standard entropy, and the lattice energy. Moreover, the experimental values of viscosity were used for the calculation of activation energy. Refractive indices were measured within the temperature range of 293.15–323.15 K, and these values were also used in the calculation of electronic polarizability. Acid numbers of the prepared PILs were measured and correlated with their structure moiety. In addition, the density functional theory (DFT) calculations were performed to get a deeper insight into the effect of structural variations of the ion pairs on their physical properties.

Web URL: http://pubs.acs.org/doi/abs/10.1021/acs.jced.6b00450

67. Khan, A. S., Khalid, H., Sarfraz, Z., Khan, M., Iqbal, J., Muhammad, N., ... & Rehman, I. U. (2017). Vibrational spectroscopy of selective dental restorative materials. *Applied Spectroscopy Reviews*, *52*(6), 507-540.

ABSTRACT:

Recently, significant advancement has occurred in vibrational (Fourier transform infrared [FTIR] and Raman) spectroscopy associated with dental materials. FTIR and Raman spectroscopies have emerged as significant breakthrough techniques and offer exciting new possibilities in the area of dental materials. These techniques have been used to obtain chemical images of formulations and allow researchers to find out the *in situ*structure of materials. This review summarizes the information obtained from these two techniques and their application in dental material sciences. The presented database of vibrational spectroscopy facilitated the appropriate identification of frequently used dental materials ranging from filling, obturating, adhesive, lining/luting materials, and prosthodontics materials. Spectral peaks that are related to these materials are discussed in detail, which provided crucial data in understanding the chemical structural properties. The application of vibrational spectroscopy allowed for a quick differential identification of typical dental materials composed of organic and inorganic compounds. From our study as well as the literature reviewed, it appeared that investigators uniformly confirmed the benefits of vibrational spectroscopy concerning identification of chemical functional groups of different chemical compositions. The diagnostic and prognostic tools based on these technologies have the potential to revolutionize our concepts leading to improve materials sciences and clinical application.

Web URL: **http://www.tandfonline.com/doi/abs/10.1080/05704928.2016.1244069**

68. Iqbal, J., Du, Y., Howari, F., Bataineh, M., Muhammad, N., & Rahim, A. (2017). Simultaneous Enrichment and On-line Detection of Low-Concentration Copper, Cobalt, and Nickel Ions in Water by Near-Infrared Diffuse Reflectance Spectroscopy Combined with Chemometrics. *Journal of AOAC International*, *100*(2), 560-565.

ABSTRACT:

Sensitive detection of heavy metal ions in water is of great importance considering the effects that heavy metals have on public health. A developed fluidized bed enrichment technique was used to concentrate and detect low concentrations of Cu^{2+}, Co^{2+}, and Ni^{2+} in water samples by near-IR diffuse reflectance (NIDR) spectroscopy (NIDRS) directly without using any chemicals or reagents. The NIDR spectra of adsorbent were measured on-line, and quantitative detection

was achieved by applying a built partial least-squares chemometric model. Sensitivity and accuracy was improved significantly because large-volume mixture solutions were used in the enrichment process. Root mean square error of cross-validation values for Cu^{2+}, Co^{2+}, and Ni^{2+} were 0.29, 0.41, and 0.35 µg/mL, respectively, with mean relative error values in the acceptable range of 6.56–10.27%. This study confirms the potential application of fluidized bed enrichment combined with NIDRS and chemometrics for the simultaneous detection of trace heavy metal ions in water, with low relative error.

Web URL:

http://www.ingentaconnect.com/contentone/aoac/jaoac/2017/00000100/00000002/art00033

69. Ullah, Z., Bustam, M. A., Man, Z., Khan, A. S., Muhammad, N., Sarwono, A., ... & Mengal, A. N. (2017). A Detail Description on Catalytic Conversion of Waste Palm Cooking Oil into Biodiesel and Its Derivatives: New Functionalized Ionic Liquid Process. *ChemistrySelect*, *2*(27), 8583-8595.

ABSTRACT:

This work is focusing on the synthesis and application of new potential ionic liquids (ILs) for biodiesel production from waste palm cooking oil. For this propose total eleven ionic liquids were synthesized containing various types of cations and anions and characterized with nuclear magnetic resonance (NMR), fourier-transform infrared (FTIR) and elemental analyser (CHNS). The Hammett acidity of the ionic liquids were determined using Ultraviolet (**UV**) visible spectrometer and correlated with their catalytic properties. The process of biodiesel preparation has been optimized with respect of different factors (catalysts concentrations, methanol to oil ratio, temperature, agitation speed and time) affecting the transesterification reaction. The highest yield of 96.25% for 3-methyl-1-(4-sulfo-butyl)-3H-imidazol-1-ium trifluoromethanesulfonate [BSMIM][CF_3SO_3] was obtained under optimal conditions. The obtained product was characterized using gas chromatography (GC), NMR, FTIR, Thermogravimetric analysis (TGA) techniques. The physicochemical properties like kinematic viscosity, flash point, density etc were determined and compared with the standard of

American Society of Testing Materials (ASTM) and European Standard (EN) methods. The by-product of reaction i.e. glycerol was further esterified to minimize the waste of glycerol. The kinetic study shows that the transesterification reaction catalysed by prepared ILs follow the pseudo-first order reaction. The kinetic energy (*Ea*) of the reaction was calculated around 19.89 kJ/mol.

Web URL: **http://onlinelibrary.wiley.com/doi/10.1002/slct.201701099/full**

70. Nasrullah, A., Bhat, A. H., Isa, M. H., Danish, M., Naeem, A., Muhammad, N., & Khan, T. (2017). Efficient removal of methylene blue dye using mangosteen peel waste: kinetics, isotherms and artificial neural network (ANN) modeling. ***DESALINATION AND WATER TREATMENT*****,** ***86*****, 191-202.**

ABSTRACT:

In this work, mangosteen peel (MP) waste was used as a new biosorbent for removal of methylene blue (MB) dye from aqueous solution. Surface area, surface functional groups, surface charge and surface morphology were analyzed through Brunauer Emmett Teller, Fourier transform infrared, pHzpc and field emission scanning electron microscopy/energy dispersive X-ray spectroscopy techniques, respectively. The major functional groups were –CO, –COO and –OH. Batch adsorption experiments were conducted with varying MP dose (0.01–0.08 g), pH (2–12), contact time (10–60 min), temperature (25°C–45°C) and concentration of MB solution (50–150 mg/L). The study examined the implementation of artificial neural network for the prediction of MB adsorption from aqueous solution by MP, based on 30 experimental sets of batch adsorption study. Optimum number of neurons determined was 4 for Levenberg– Marquardt training algorithm; at which the highest value of R2 and lowest mean square error were found to be 0.997 and 2.972, respectively. Among the various kinetic models applied, the pseudo-second-order kinetic model was identified to be the most suitable to represent the adsorption of MB on the surface of MP. Langmuir, Freundlich, Temkin and Harkins–Jura isotherm models were employed to study the adsorption equilibrium. Langmuir isotherm model was identified as the most suitable. The calculated values of thermodynamic

factors, ΔS°, ΔG°, S*, Ea and ΔH°, showed that the adsorption phenomenon is spontaneous, feasible and endothermic in nature.

Web URL: **http://www.deswater.com/DWT_abstracts/vol_86/86_2017_191.pdf**

71. Safi, S. Z., Qvist, R., Ong, G., Karimian, H., Imran, M., & Shah, I. (2017). Stimulation of β-adrenergic receptors plays a protective role via increased expression of RAF-1 and PDX-1 in hyperglycemic rat pancreatic islet (RIN-m5F) cells. ***Archives of medical science: AMS*****,** ***13*****(2), 470.**

ABSTRACT:

Introduction

It is a widely held view that a progressive reduction of beta-cell mass occurs in the progression of diabetes. RAF-1 kinase and pancreas duodenal homeobox 1 (PDX-1) are major factors that promote survival of cells and maintain normal insulin functions. In this study we investigated the effect of a β-adrenergic receptor agonist and antagonist on RAF-1 and PDX-1, and their respective effects on apoptosis and insulin release in RIN-m5F cells.

Material and methods

RIN-m5F cells were cultured in normal (5 mM) and high (25 mM) glucose to mimic diabetic conditions, followed by treatment with 5 µM, 10 µM and 20 µM of isoproterenol and isoproterenol + propranolol for 6, 12 and 24 h. Western blotting and reverse transcription analysis were performed to examine the expression of RAF-1 and PDX-1. Annexin-V-FITC and terminal deoxynucleotidyl transferase dUTP nick-end labeling (TUNEL) assays were used to investigate apoptosis. ELISA was used to measure insulin levels. Reverse transcription polymerase chain reaction was conducted to investigate the expression of genes.

Results

Stimulation of β-adrenergic receptors with isoproterenol significantly induced RAF-1 and PDX-1 genes in a concentration-dependent and time-independent manner. Changes were significant

both at protein and mRNA levels. Up-regulation of RAF-1 and PDX-1 was accompanied by improved insulin levels and reduced apoptosis. Concentrations of 10 µM and 20 µM for 12 and 24 h were more effective in achieving significant differences in the experimental and control groups. Propranolol reversed the effect of isoproterenol mostly at maximum concentrations and time periods.

Conclusions

A positive effect of a β-adrenergic agonist on RAF-1 and PDX-1, reduction in β-cell apoptosis and improved insulin contents can help to understand the pathogenesis of diabetes and to develop novel approaches for the β-cell dysfunction in diabetes.

Web URL: **https://www.ncbi.nlm.nih.gov/pmc/articles/PMC5332455/**

72. Safi, S. Z., Noreen, M., Imran, M., Waheed, Y., Shah, A. M. U. H., & Muhammad, N. (2017). Alteration in ocular blood flow and its effect on the progression of glaucoma. ***国际眼科杂志 (中文刊)*****, *17*(3), 394-398.**

ABSTRACT:

Glaucoma is a multifactorial neurodegenerative disease that can result in permanent vision loss by damaging optic nerves due to higher pressure in the eye. Although most of the fundamental pathophysiological mechanisms involved in glaucoma are undetermined but alteration in ocular blood flow (OBF) in tissues such as optic nerve, retina, choroid and iris is an important risk factor for glaucoma. Various factors such as limited knowledge of the factors causing optic nerve damage, confusion in the measurement assays and lack of therapies, make hindrances in the understanding of glaucoma. Researchers are continuously accumulating evidence to suggest that alterations in OBF play important role in the pathogenesis of glaucoma but most of the times they have diverse and contradictory conclusions regarding changes in the OBF and risk of glaucoma. In this article we have reviewed different aspects of glaucoma and the effect of OBF in the disease progression.

Web URL: **http://ies.ijo.cn/cn_publish/2017/3/201703002.pdf**

73. Waheed, Y., Najmi, M. H., Aziz, H., Waheed, H., Imran, M., & Safi, S. Z. (2017). Prevalence of hepatitis C in people who inject drugs in the cities of Rawalpindi and Islamabad, Pakistan. *Biomedical reports*, *7*(3), 263-266.

ABSTRACT:

Pakistan has the second highest burden of hepatitis C (HCV) in the world. The major route of HCV transmission is contaminated blood or needle sharing. Seventy percent of people who inject drugs (PWIDs) shared needles at some time in their addiction history. The aim of the present study was to estimate the prevalence of HCV in PWIDs in cities of Pakistan. We enrolled 100 PWIDs from the Rawalpindi and Islamabad cities of Pakistan. Blood samples were taken in collection tubes and were subjected to HCV screening by using three rapid HCV screening kits including one step anti-HCV test, onsite HCV Ab rapid test and advance quality rapid anti-HCV test. All 100 blood samples were also subjected to HCV detection by using Elecsys anti-HCV II performed on the Roche Cobas 601 platform based on the ECLIA principle. Seventy-two percent of PWIDs showed the presence of HCV antibodies using the Roche anti-HCV II ECLIA test. We also compared the performance of different rapid kits in comparison with the anti-HCV II by Roche. The sensitivity of CTK kit was 84.72%, which was almost equal to the sensitivity by the SD Bioline HCV and Advanced Quality Rapid HCV tests, which was 83.33%. All three kits showed 100% specificity and positive predictive values. The results showed that the three market competitors of HCV rapid test showed almost equal results. The prevalence of HCV is very high in PWIDs in the capital twin cities of Pakistan. There is dire need to initiate the administration of a hepatitis test and treatment program for both high-risk and the general HCV-positive population. This is the optimal way to achieve HCV control targets established by the United Nations Sustainable Development Goals and Global Health Sector Strategy by WHO.

Web URL: **https://www.spandidos-publications.com/br/7/3/263?text=fulltext**

74. Waheed, Y., Safi, S. Z., Najmi, M. H., Aziz, H., & Imran, M. (2017). Prediction of promiscuous T cell epitopes in RNA dependent RNA polymerase of Chikungunya virus. *Asian Pacific journal of tropical medicine*, *10*(8), 760-764.

ABSTRACT:

Objective

To explore RNA dependent RNA polymerase of Chikungunya virus (CHIKV) and develop T cell based epitopes with high antigenicity and good binding affinity for the human leukocyte antigen (HLA) classes as targets for epitopes based CHIKV vaccine.

Methods

In this study we downloaded 371 non-structural protein 4 protein sequences of CHIKV belonging to different regions of the world from the US National Institute of Allergy and Infectious Diseases (NIAID) virus pathogen resource database. All the sequences were aligned by using CLUSTALW software and a consensus sequence was developed by using Uni Pro U Gene Software version 1.2.1. Propred I and Propred software were used to predict HLA I and HLA II binding promiscuous epitopes from the consensus sequence of non-structural protein 4 protein. The predicted epitopes were analyzed to determine their antigenicity through Vaxijen server version 2.0. All the HLA I binding epitopes were scanned to determine their immunogenic potential through the Immune Epitope Database (IEDB). All the predicted epitopes of our study were fed to IEDB database to determine whether they had been tested earlier.

Results

Twenty two HLA class II epitopes and eight HLA class I epitopes were predicted. The promiscuous epitopes WMNMEVKII at position 486–494 and VRRLNAVLL at 331–339 were found to bind with 37 and 36 of the 51 HLA class II alleles respectively. Epitope MANRSRYQS at position 58–66 and epitopes YQSRKVENM at positions 64–72 were predicted to bind with 12 and 9 HLA II alleles with antigenicity scores of 0.754 9 and 1.013 0 respectively. Epitope YSPPINVRL was predicted to bind 18 HLA I alleles and its antigenicity score was 1.425 9 and immunogenicity score was 0.173 83. This epitope is very useful in the preparation of a universal vaccine against CHIKV infection.

Conclusions

Epitopes reported in this study showed promiscuity, antigenicity as well as good binding affinity for the HLA classes. These epitopes will provide the baseline for development of efficacious vaccine for CHIKV.

Web URL: **https://www.sciencedirect.com/science/article/pii/S1995764517305734**

75. Waheed, Y., Tahir, M., Waheed, H., & Safi, S. Z. (2017). Recent advances on Ebola virus. Asian Pacific Journal of Tropical Disease, 7(2), 65-67.

ABSTRACT:

The 2014–2015 Ebola epidemic in West Africa was the largest of its kind, with more than 11 000 deaths and 28 637 cases. The epidemic mobilized a coalition of countries from US to China, European Union, and African countries. The international community was not prepared to face this unprecedented epidemic. Numbers of research groups are working to find a potent vaccine against Ebola. Ebola virus has the ability to dodge the immune system either by blocking interferon production or by glycoprotein-based immune diversion. Individuals who survived from the Ebola virus are facing different health issues after the infection. The rate of miscarriage is also high in Ebola survivors while there are variable reports of the presence of Ebola virus in semen of Ebola survivors. There are many asymptomatic Ebola patients under consideration. West African countries lack the basic healthcare system, for which the actual number of deaths by the Ebola outbreak are much more than the deaths caused by the direct viral infection. The hospitals were empty due to fear and death of nurses and doctors. Millions of children missed the vaccine against measles. Hundreds of thousands of people could not get food. The Ebola epidemic also affected the mental health of people living in endemic countries. The families affected by Ebola are facing discrimination in the society. There is a dire need to adopt United Nations Sustainable Development Goal 3, which stresses to prepare ourselves to face any national or global health risk.

Web URL:

http://www.ingentaconnect.com/content/doaj/22221808/2017/00000007/00000002/art00001

76. Zeeshan, R., & Mutahir, Z. (2017). Cancer metastasis-tricks of the trade. *Bosnian journal of basic medical sciences*, *17*(3), 172.

ABSTRACT:

Decades of cancer research have unraveled genetic, epigenetic and molecular pathways leading to plausible therapeutic targets; many of which hold great promise in improving clinical outcomes. Metastatic tumors become evident early on and are one of the major causes of cancer-related fatalities worldwide. This review depicts the sequential events of cancer metastasis. Genetic and epigenetic heterogeneity influences local tumor cell invasion, intravasation, survival in circulation, extravasation and colonization to distant sites. Each sequential event is associated with heterogeneous tumor microenvironment, gain of competence, unique population of cancer stem cells (CSCs), circulatory pathway, compatible niche and immune system support. A tight regulation of metastasis-promoting mechanisms and, in parallel, evading inhibitory mechanisms contribute to the severity and site of metastasis. A comprehensive understanding of tumor cell fate as an individual entity, as well as in combination with different promoting factors and associated molecular mechanisms, is anticipated in the coming years. This will enable scientists to depict design strategies for targeted cancer therapies.

Web URL: **https://www.ncbi.nlm.nih.gov/pmc/articles/PMC5581965/**

77. Chen, J., Zeng, K., Lei, S., Wang, M., Asif, A., & Ge, X. (2017). The Molecular Imprinted Nanotrapper for Catalase: A Chemical-Free Inhibition Way to Trigger Tumor Cells Apoptosis. *Particle & Particle Systems Characterization*, *34*(2).

ABSTRACT:

A Novel catalase-imprinted nanoparticle is fabricated and used as the high-efficient intracellular catalase nanotrapper to induce the overproduction of H_2O_2 in cells, so as to trigger the cell apoptosis through a chemical-free inhibition way.

Web URL: **http://onlinelibrary.wiley.com/doi/10.1002/ppsc.201600260/full**

78. Wang, J., Rong, J., Fang, Z., Wang, M., Asif, A., Wu, Q., ... & Ge, X. (2017). Monodisperse Polypyrrole Nanoparticles Prepared via γ-Ray Radiolysis of Water: An Efficient Near-Infrared Photothermal Agent for Cancer Therapy. *Particle & Particle Systems Characterization*, *34*(3).

ABSTRACT:

Biosafe nanoparticles with strong near-infrared (NIR) light photothermal conversion effect can bring effective hyperthermia as one of the promising approaches in cancer therapy. In this work, a new facile and green preparation method of polypyrrole (PPy) nanoparticles based on ^{60}Co γ-ray radiation on a simple air-saturated strong acidic aqueous solution of pyrrole (pH ≤ 1) is studied. According to the MCAP-FACSIMILE simulation on the concentrations of the radiolysis products of water at the presence of H^+ and O_2, the main strong oxidative radiolysis products ·OH and H_2O_2 rapidly induce the polymerization of pyrrole. The size of the prepared PPy nanoparticles is about several tens of nanometers and can be controlled by the pH, the concentration of the stabilizer poly(vinyl alcohol), and the absorbed dose rate (the amount of energy absorbed per unit mass of the irradiated material within per unit of time). The PPy nanoparticles show rapid and remarkable NIR (808 nm) photothermal conversion efficiency up to 40.1% in water. Furthermore, the in vitro and in vivo experiments confirm that the prepared PPy nanoparticles exhibit enough strong NIR photothermal effect in tumor cells (4T1 and HeLa) and show a promising prospect as the NIR photothermal agent for the future cancer therapy.

Web URL: **http://onlinelibrary.wiley.com/doi/10.1002/ppsc.201600430/full**

79. Asif, M., & Asif, A. (2017). Effects of internal inductance on the Shafranov parameter by using the solution of equilibrium problem. *Modern Physics Letters B*, *31*(07), 1750078.

ABSTRACT:

In this work, the dependence of Shafranov parameter on plasma internal inductance has been studied by using the solution of Grad–Shafranov equation (GSE) for Hefei Tokamak-7. The Shafranov parameter was obtained from the solution of GSE, using the expansion of free functions, which is quadratic in flux function. Then, we can find the dependence of Shafranov parameter on plasma internal inductance.

Web URL:

http://www.worldscientific.com/doi/abs/10.1142/S0217984917500786?journalCode=mplb

80. Asif, M., & Asif, A. (2017). Theoretical calculation of electron density and temperature in the edge of tokamak. *Modern Physics Letters B*, *31*(17), 1750196.

ABSTRACT:

In this work, we use a method based on the concept of particle confinement time (τp)(τp) uniqueness to calculate the electron density and temperature in ohmically heated, edge plasma of the Hefei tokamak-7. Here, with the help of the data taken from Johnson and Hinnov's table, we have done an extensive work to find electron densities and temperatures that satisfy the τpτp uniqueness to evaluate the temporal evolution of electron density (ne)(ne) and temperature (Te)(Te). The results are in good agreement as measured from the Langmuir probe array in previous works.

Web URL:

http://www.worldscientific.com/doi/abs/10.1142/S0217984917501962?journalCode=mplb

81. Akhtar, M. A., Hayat, A., Iqbal, N., Marty, J. L., & Nawaz, M. H. (2017). Functionalized graphene oxide–polypyrrole–chitosan (fGO–PPy–CS) modified screen-printed electrodes for non-enzymatic hydrogen peroxide detection. *Journal of Nanoparticle Research*, *19*(10), 334.

ABSTRACT:

Functionalized graphene oxide (fGO) was synthesized and subsequently used for synthesis of nanocomposite with polypyrrole (PPy) and chitosan (CS) to give fGO–PPy–CS nanocomposites. Screen-printed carbon electrodes were then modified with these nanocomposites to construct an unprecedented hydrogen peroxide (H_2O_2) sensor. Cyclic voltammetry (CV) and amperometric response demonstrated that the composite materials hold potential for electrocataytic reduction towards H_2O_2. Under optimal experimental conditions, the amperometric response of the fGO–PPy–CS sensor was linearly proportional to H_2O_2 in the range of 2.5–200 µM with a detection limit of 1.95 µM ($S/N = 3$). The present study provides new opportunities for fGO–PPy–CS-modified electrodes to probe the improved non-

enzymatic detection of H_2O_2. It further broadens the applications of graphene-based conducting composites in the field of sensors and biosensors for diverse applications.

Web URL: **https://link.springer.com/article/10.1007/s11051-017-4029-x**

82. Jaafar, M. H., Safi, S. Z., Tan, M. P., Rampal, S., & Mahadeva, S. (2017). Efficacy of Rebamipide in Organic and Functional Dyspepsia: A Systematic Review and Meta-Analysis. *Digestive diseases and sciences*, 1-11.

ABSTRACT:

Objective

The role of gastritis in dyspepsia remains controversial. We aimed to examine the efficacy of rebamipide, a gastric mucosal protective agent, in both organic and functional dyspepsia.

Design

A systematic review and meta-analysis was performed. The following databases were searched using the keywords ("rebamipide" OR "gastroprotective agent*" OR "mucosta") AND ("dyspepsia" OR "indigestion" OR "gastrointestinal symptoms"): PubMed, Wed of Science, Embase, CINAHL, Cochrane Clinical Trials Register. The primary outcome was dyspepsia or upper GI symptom score improvement. Pooled analysis of the main outcome data were presented as risk ratio (RR) for dichotomous data and standardized mean difference (SMD) for continuous data.

Results

From an initial 248 records, 17 randomised controlled trial (RCT) publications involving 2170 subjects (1224 rebamipide, 946 placebo/control) were included in the final analysis. Twelve RCTs were conducted in subjects with organic dyspepsia (peptic ulcer disease, reflux esophagitis or NSAID-induced gastropathy) and five RCTs were conducted in patients with functional dyspepsia (FD). Overall, dyspepsia symptom improvement was significantly better with rebamipide compared to placebo/control drug (RR 0.77, 95% CI = 0.64–0.93; SMD −0.46,

95% CI = −0.83 to −0.09). Significant symptom improvement was observed both in pooled RR and SMD in subjects with organic dyspepsia (RR 0.72, 95% CI = 0.61–0.86; SMD −0.23, 95% CI = −0.4 to −0.07), while symptom improvement in FD was observed in pooled SMD but not RR (SMD −0.62, 95% CI = −1.16 to −0.08; RR 1.01, 95% CI = 0.71–1.45).

Conclusion

Rebamipide is effective in organic dyspepsia and may improve symptoms in functional dyspepsia.

Web URL: **https://link.springer.com/article/10.1007/s10620-017-4871-9**

DEPARTMENT OF STATISTICS

Journal Papers

1. Khan, S. A., Hussain, I., Hussain, T., Faisal, M., Muhammad, Y. S., & Mohamd Shoukry, A. (2017). Regional Frequency Analysis of Extremes Precipitation Using L-Moments and Partial L-Moments. *Advances in Meteorology*, *2017*.

ABSTRACT:

Extremes precipitation may cause a series of social, environmental, and ecological problems. Estimation of frequency of extreme precipitations and its magnitude is vital for making decisions about hydraulic structures such as dams, spillways, and dikes. In this study, we focus on regional frequency analysis of extreme precipitation based on monthly precipitation records (1999–2012) at 17 stations of Northern areas and Khyber Pakhtunkhwa, Pakistan. We develop regional frequency methods based on L-moment and partial L-moments (L- and PL-moments). The L- and PL-moments are derived for generalized extreme value (GEV), generalized logistic (GLO), generalized normal (GNO), and generalized Pareto (GPA) distributions. The Z-statistics and L- and PL-moments ratio diagrams of GNO, GEV, and GPA distributions were identified to represent the statistical properties of extreme precipitation in Northern areas and Khyber Pakhtunkhwa, Pakistan. We also perform a Monte Carlo simulation study to examine the sampling properties of L- and PL-moments. The results show that PL-moments perform better than L-moments for estimating large return period events.

Web URL: http://downloads.hindawi.com/journals/amete/2017/6954902.pdf

2. Ali, Z., Hussain, I., Faisal, M., Nazir, H. M., Abd-el Moemen, M., Hussain, T., & Shamsuddin, S. (2017). A novel multi-scalar drought index for monitoring drought: the standardized precipitation temperature index. *Water Resources Management*, *31*(15), 4957-4969.

ABSTRACT:

Nowadays human beings are facing many environmental challenges because of frequently occurring drought hazards. Several adverse impacts of drought hazard are continued in many parts of the world. Drought has a substantial influence on water resources and irrigation. It

may effect on the country's environment, communities, and industries. Therefore, it is important to improve drought monitoring system. In this paper, we proposed a novel method – Standardized Precipitation Temperature Index (SPTI) for drought monitoring that utilize the regional tempreature. We compared the performance of our proposed drought index – SPTI with commonly used drought indices (i.e., Standardized Precipitation Index (SPI) and Standardized Precipitation Evapotranspiration Index (SPEI)) for 17 meteorological stations of Khyber Pakhtunkhwa (KPK) province (Pakistan) that have both extreme (arid and humid) climatic environment. We found that SPTI is strongly correlated with SPI and performed better than SPEI in low temperature regions for drought monitoring. In summary, SPTI is recommended for detecting and monitoring the drought conditions over different time scales.

Web URL: ***https://link.springer.com/article/10.1007/s11269-017-1788-1***

3. Ali, Z., Hussain, I., Faisal, M., Nazir, H. M., Hussain, T., Shad, M. Y., ... & Hussain Gani, S. (2017). Forecasting Drought Using Multilayer Perceptron Artificial Neural Network Model. ***Advances in Meteorology*****,** ***2017*****.**

ABSTRACT:

These days human beings are facing many environmental challenges due to frequently occurring drought hazards. It may have an effect on the country's environment, the community, and industries. Several adverse impacts of drought hazard are continued in Pakistan, including other hazards. However, early measurement and detection of drought can provide guidance to water resources management for employing drought mitigation policies. In this paper, we used a multilayer perceptron neural network (MLPNN) algorithm for drought forecasting. We applied and tested MLPNN algorithm on monthly time series data of Standardized Precipitation Evapotranspiration Index (SPEI) for seventeen climatological stations located in Northern Area and KPK (Pakistan). We found that MLPNN has potential capability for SPEI drought forecasting based on performance measures (i.e., Mean Average Error (MAE), the coefficient of correlation (), and Root Mean Square Error (RMSE)). Water resources and management planner can take

necessary action in advance (e.g., in water scarcity areas) by using MLPNN model as part of their decision-making.

Web URL: ***http://downloads.hindawi.com/journals/amete/2017/5681308.pdf***

4. Ibrahim, K. A., Nawaz, A., Mumtaz, S., Iqbal, F. M., Khan, A., Zaman, S., ... & Shah, S. N. H. (2017). Formulation, Evaluation and release rate characteristics of medicated jelly of vitamin C. *Pakistan journal of pharmaceutical sciences*, *30*(2 (Suppl.)), 579-583.

ABSTRACT:

Medicated jelly formulations are patient friendly dosage form for pediatric, geriatric and dysphagic patients. These formulations offer rapid dissolution and absorption of drugs through oral mucosa therefore show the early onset of action. The objective of the study was to develop and evaluate oral jelly formulations of vitamin C. Slurry method was adopted using glucose 103gm, sugar 67gm, gelatin 10gm and sorbitol 6.56gm. Preformulation studies were performed including the organoleptic profile, pH, and solubility of both drugs. The medicated jelly of Vitamin C was prepared and evaluated for physical characteristics, weight variation, syneresis, pH, taste and palatability, drug content, release rate characteristics and stability studies. All the jellies were found to have patient welcoming taste and were palatable. All formulations showed more than 50% drug release within 15 minutes, while 93% drug was released in 30 minutes. The results of release kinetics showed that the formulation followed the zero order release kinetics. Thus the drug was released at constant rate independent of the drug concentration involved in the process. All the medicated jellies were found to remain stable stored for 60 days at different temperatures. The present study revealed that medicated jellies of vitamin C could be employed orally in an effective form as an alternative solid oral dosage form for special population such as pediatrics, geriatrics and patients with dysphagia.

Web URL: ***http://europepmc.org/abstract/med/28650324***

5. Abbas, S., Taqi, S. A., Mustafa, F., Murtaza, M., & Shahbaz, M. Q. (2017). Topp-Leone Inverse Weibull Distribution: Theory and Application. *European Journal of Pure and Applied Mathematics*, *10*(5), 1005-1022.

ABSTRACT:

In this article, the discussion has been carried out through the generalization of Inverse Weibull distribution. We introduce a new three parameter life model called the Topp-Leone Inverse Weibull distribution. We provide comperhensive result of the mathematical characteristic, including moments, quantile function, random number generator, survival function, hazard rate function, and mode. Distributional properties of order statistics are analyzed. The parameters of the proposed model are estimated by the method of maximum likelihood. Simulation study is performed to investigate the performance of the maximum likelihood estimators. To assess the flexibility, empirical results of new model are obtained by modeling two real data sets.

Web URL: http://ejpam.com/index.php/ejpam/article/viewFile/3084/567

6. Ismail, M. (2017). Combination of Ratio and Regression Estimator of Population Mean in Presence of Non–response. *Gazi University Journal of Science*, *30*(4), 634-642.

ABSTRACT:

Singh and Kumar [1] developed regression-cum-ratio estimator for population mean in the presence of non–response for two-phase sampling using information of two auxiliary variables x and z . In this paper simple generalized regression-cum-ratio estimator in the presence of non–response has been presented with three different situations. Empirical and theoretical study is carried out to compare the efficiency of the suggested estimators over the existing estimators.

Web URL: **http://dergipark.gov.tr/download/article-file/380224**

7. Sanaullah, A., Asghar, A. & Hanif, M. (2017). General class of exponential estimator for estimating finite population variance. *Journal of Reliability and Statistical Studies.* 10(2)

ABSTRACT:

In this article, we consider the problem of estimating an unknown population variance using two auxiliary variables. A generalized exponential estimator along with a class of estimators has been proposed for estimating population variance. The bias and the mean square error of the proposed estimator are obtained to the first order of approximations. It is shown that the

proposed generalized estimator is more efficient than the existing literature estimators. An empirical and a simulated study have also been carried out to demonstrate the efficiency of proposed estimator with the literature.

Web URL: **http://www.jrss.in.net/assets/01%20JRSS%20100201.pdf**

8. Not Found

ABSTRACT:

Web URL:

DEPARTMENT OF PHYSICS

Journal Papers

1. Akhtar, M. N., Khan, M. A., Ahmad, M., Nazir, M. S., Imran, M., Ali, A., ... & Murtaza, G. (2017). Evaluation of structural, morphological and magnetic properties of CuZnNi (CuxZn 0.5− x Ni 0.5 Fe 2 O 4) nanocrystalline ferrites for core, switching and MLCI's applications. *Journal of Magnetism and Magnetic Materials*, *421*, 260-268.

ABSTRACT:

The influence of Cu substitution on the structural and morphological characteristics of Ni–Zn nanocrystalline ferrites have been discussed in this work. The detailed and systematic magnetic characterizations were also done for Cu substituted Ni–Zn nanoferrites. The nanocrystalline ferrites of Cu substituted $Cu_xZn_{0.5-x}Ni_{0.5}Fe_2O_4$ferrites ($x$=0, 0.1, 0.2, 0.3, 0.4 and 0.5) were synthesized using sol gel self-combustion hybrid method. X-ray diffraction (XRD), Field emission scanning electron microscopy (FESEM), Transmission electron microscope (TEM) and Vibrating sample magnetometer (VSM) were used to investigate the properties of Cu substituted nanocrystalline ferrites. Single phase structure of Cu substituted in Ni–Zn nanocrystalline ferrites were investigated for all the samples. Crystallite size, lattice constant and volume of the cell were found to increase by increasing Cu contents in spinel structure. The better morphology with well-organized nanocrystals of Cu–Zn–Ni ferrites at x=0 and 0.5 were observed from both FESEM and TEM analysis. The average grain size was 35–46 nm for all prepared nanocrystalline samples. Magnetic properties such as coercivity, saturation, remanence, magnetic squareness, magneto crystalline anisotropy constant (K) and Bohr magneton were measured from the recorded M–H loops. The magnetic saturation and remanence were increased by the incorporation of Cu contents. However, coercivity follow the Stoner-Wolforth model except for x=0.3 which may be due to the site occupancy and replacement of Cu contents from octahedral site. The squareness ratio confirmed the super paramgnetic behaviour of the Cu substituted in Ni–Zn nanocrystalline ferrites. Furthermore, Cu substituted Ni–Zn nanocrystalline ferrites may be suitable for many industrial and domestic

applications such as components of transformers, core, switching, and MLCI's due to variety of the soft magnetic characteristics.

Web URL: **http://www.sciencedirect.com/science/article/pii/S0304885316317255**

2. Hussain, S., Liu, T., Javed, M. S., Aslam, N., & Zeng, W. (2017). Highly reactive 0D ZnS nanospheres and nanoparticles for formaldehyde gas-sensing properties. ***Sensors and Actuators B: Chemical*****,** ***239*****, 1243-1250.**

ABSTRACT:

Wurtzite zero dimensional ZnS nanospheres and random-shaped nanoparticles successfully synthesized via a low temperature hydrothermal route. The formation of nanostructures is attributed due to PVP and thiourea and discussed in details. The as-prepared nanostructures were characterized by XRD, EDS, SEM and HRTEM. Based on experimental results, a plausible growth mechanism is also proposed along with crystal structure of ZnS. The gas–sensing properties of as–prepared ZnS products are tested using efficient substrate sensors via an intelligent gas testing system. Both at room and 100–400 °C temperature, high response and selectivity towards formaldehyde than other gases is observed. Comparative studies of ZnS nanostructures for different concentrations of formaldehyde gas and definite sensor-stability for different gases is studied, as well.

Web URL: ***http://www.sciencedirect.com/science/article/pii/S0925400516315532***

3. Anjum, S., Hameed, S., Awan, M. S., Amed, E., & Sattar, A. (2017). Effect of strontium doped M-Type bariam hexa-ferrites on structural, magnetic and optical properties. ***Optik-International Journal for Light and Electron Optics*****,** ***131*****, 977-985.**

ABSTRACT:

The series of M-type $Ba_{1-x}Sr_xFe_{12}O_{19}$ (x = 0.0, 0.2, 0.4, 0.6, 0.8, 1) have been fabricated using powder metallurgy route. The effects of strontium ions have been systematically investigated. The samples are sintered at 1200 °C for 2 h. The structural properties and surface morphology is determined using X-ray diffraction technique, Fourier Infrared Spectroscopy and Field Emission Scanning Electron Microscope respectively. The magnetic and optical properties are

carried out using vibrating sample magnetometer and UV–vis spectroscopy. The XRD analysis revealed that these samples have hexagonal structure. FTIR analysis confirmed that bands in the range 430–590 cm^{-1} are due to the stretching vibration of oxygen atom and metal ions (M-O) that is Fe-O confirming the formation of hexa-ferrite. The average grain size is determined using FSEM i.e about 0.37–1.5 µm. The VSM analysis showed that saturation magnetization decreased with increasing concentration of Sr^{+2} ions and this decrease is due to the different site occupation of Sr^{+2} and Fe^{+3} ions. The band gap energy decreased with the increasing concentration of strontium ions. This is due to the vacancies of electrons in the valance band of Ba and Sr. The decrease in the distance between conduction and valance band causes the increase in conductivity due to which band gap energy decreases. The widest applications of these hard ferrites permanent magnets are in motors, speakers sensors and MRI systems.

Web URL: ***http://www.sciencedirect.com/science/article/pii/S0030402616315467***

4. Feroze, A., Idrees, M., Kim, D. K., Nadeem, M., Siddiqi, S. A., Shaukat, S. F., ... & Siddique, M. (2017). Low Temperature Synthesis and Properties of BiFeO3. ***Journal of Electronic Materials*****, 1-8.**

ABSTRACT:

Extensive efforts have been made to synthesize single phase and stoichiometric BiFeO3. Some modified techniques have been tried in synthesizing BiFeO3 as compared with the conventionally used co-precipitation method. Thermogravimetric Analysis/Differential Scanning Calorimetry and x-ray diffraction experiments were used exclusively to explore the effects of heat treatment temperature and time on crystallographic behavior of the prepared BiFeO3 powder. Field emission scanning electron microscopy was used to explore the microstructure of the synthesized BiFeO3. The appearance of different magnetic phases in 57Fe Mo¨ssbauer spectra and field dependent magnetization was confirmed on the basis of particle size distribution. In this research, an easy, low cost and high-yield method for the low temperature single phase and stoichiometric synthesis of BiFeO3 has been suggested.

Web URL: ***https://link.springer.com/content/pdf/10.1007/s11664-017-5463-3.pdf***

5. Asif, M. (2017). Effect of internal inductance on the Shafranoy parameter by using the solution of equilibrium problems. *Modern Physics Letter B*. 30(17).

ABSTRACT:

In this work, dependence of energy confinement time on plasma internal inductance has been studied by using the solution of Grad–Shafranov equation (GSE) for circular cross-section HT-7 tokamak. For this, the Shafranov parameter (asymmetry factor) and poloidal beta were obtained from solution of GSE. Then we can find the dependence of energy confinement time, on plasma internal inductance. It is observed that the maximum energy confinement time is related to the low values of internal inductance (0.7<li<0.9)(0.7<li<0.9).

Web URL: ***http://www.worldscientific.com/doi/abs/10.1142/S0217984916502110***

6. Rafique, M., Rafique, M. S., Butt, S. H., Kalsoom, U., Afzal, A., Anjum, S., & Usman, A. (2017). Dependence of the structural optical and thermo-physical properties of gold nano-particles synthesized by laser ablation method on the nature of laser. *Optik-International Journal for Light and Electron Optics*, *134*, 140-148.

ABSTRACT:

This current project is dedicated to a fast, easy and one step method for the synthesis of gold nano-particles. Gold (Au) nano-particles have been fabricated by laser ablation method in de-ionized water. The purpose was to explore the dependence of the various properties of the gold nano particles on the nature of laser. In order to prepare colloidal solutions, a low power continuous wave (CW) diode laser and a nanosecond pulsed Nd:YAG laser have been used to ablate the gold target. The structural, physical, optical and thermal characteristics of prepared nano-particles have been investigated by X-ray diffraction (XRD), atomic force microscopy (AFM), UV–vis spectroscopy and thermal conductivity of liquids and gases unit (TCLGU), respectively. The XRD analyses revealed the formation of polycrystalline gold nano-particles with (111), (200) and (220) plans in case of both the lasers. AFM micrographs showed that prepared nano-particles are spherical in dimensions. The size of nanoparticles synthesized by CW laser ranges from 5 to 20 nm whereas the size ranges from 12 to 49 nm in case of pulsed laser. UV–vis spectroscopy showed surface plasmon resonance (SPR) peak at 512 nm for CW

laser prepared nanoparticles as compared to pulsed laser at 525 nm which is also indicative of the smaller size in case of CW laser. The thermal conductivity of colloidal solution prepared by CW laser is 33% whereas in case of pulsed laser is 48% more as compared to the deionized water (base liquid).

Web URL: ***http://www.sciencedirect.com/science/article/pii/S0030402617300268***

7. Saleem, M., Ahmad, M. A., Fang, L., Raza, R., Akhtar, M. N., & Rehman, S. U. (2017). Solution-derived ZnO nanoflowers based photoelectrodes for dye-sensitized solar cells. ***Materials Research Bulletin*****.**

ABSTRACT:

Flower-like ZnO nanostructures, composed of hexagonal nanorods were manipulated, via a low temperature hydrothermal method from an aqueous solution using polyethyleneimine (PEI) as a surfactant in the seed sole. It was found that the PEI in the seed sole not only affected the geometrical shape of ZnO flowers but also changed the length and spacing of the petals. These flower-like nanostructures were used as photoelectrodes in dye-sensitized solar cells. Compared to rod-like flowers (sample X1), the blade-like flowers (sample X2) nanostructures demonstrate increased power conversion efficiency (η) of about 106%. Meanwhile, short-circuits current density (J_{SC}), open-circuit voltage (V_{OC}), and fill factor (FF) are all substantially improved. The enhancement of η, V_{OC} and FF in the blade-like-flower photoelectrodes were mainly ascribed to the enlargement of internal surface area between the blades for higher dye loading and the improved light harvesting from efficient light scattering. The band gap energies were 3.31 eV and 3.27 eV for rod-like flowers and blade-like flowers respectively. The decrease in the optical band gap with the increase of film roughness was due to decrease of lattice defects.

Web URL: ***http://www.sciencedirect.com/science/article/pii/S0025540816307656***

8. Amin, N., Afzal, R. M., Yousaf, M., & Javid, M. A. (2017). Comparison amongst pulse sequences for enhanced contrast to noise ratio in magnetic resonance imaging. ***JPMA. The Journal of the Pakistan Medical Association*****,** ***67*****(2), 225.**

ABSTRACT:

Objective: To provide optimised pulse sequence and imaging protocols for contrast-to-noise ratio and for tissues that have different signal intensities in magnetic resonance imaging.

Methods: A tissue equivalent material, ferrous benzoic xylenol orange gel, was prepared using gelatine, ferrous ammonium sulfate,sulfuric acid, xylenol orange tetrasodium salt and benzoic acid. The gel wasirradiated using 6MV photonsfrom a Varian Clinac 600C linear accelerator, with a dose of 5, 10, 15, 20 and 25 gray. Experimental variations in imaging parameters were performed in echo time and repetition time. The quantitative analysis consisted of contrast-to-noise ratio.

Results: Conventional spin echo and fast spin echo were equivalent for the tissues of comparable signal intensities and for entities moderate difference between signal intensities. Conventional spin echo provided remarkable contrast for tissues where signal intensity difference was extremely high in T1, T2-weighted study. An appropriate inversion time of fast fluid attenuated inversion recovery made it significant to measure contrast between tissues where signal intensity difference was the smallest and ordinary.

Conclusion: Choice of pulse sequence and parameters played a vital role in developing fine image contrast

Web URL: ***http://www.jpma.org.pk/PdfDownload/8082.pdf***

9. Ali, A., Grössinger, R., Imran, M., Khan, M. A., Elahi, A., Akhtar, M. N., ... & Ahmad, M. (2017). Magnetic and High-Frequency Dielectric Parameters of Divalent Ion-Substituted W-Type Hexagonal Ferrites. ***Journal of Electronic Materials*****,** ***46*****(2), 903-910.**

ABSTRACT:

Polycrystalline W-type hexagonal ferrites with chemical formulae Ba0.5Sr0.5 Co2xMexFe16O27 (x = 0, 0.5, Me = Mn, Mg, Zn, Ni) have been prepared using sol–gel autocombustion. It has been reported in our earlier published work that all the samples exhibit a single-phase W-type hexagonal structure which was confirmed by x-ray diffraction (XRD) analysis. The values of bulk density lie in the range of 4.64–4.78 g/cm3 for all the samples which are quite high as compared to those for other types of hexaferrites. It was also observed that Znsubstituted

ferrite reflects the highest (14.7 9 107 X-cm) whereas Mn-substituted ferrite has the lowest (11.3 9 107 X-cm) values of direct current (DC) electrical resistivity. The observed values of saturation magnetization (Ms) are found to be in the range of 62.01–68.7 emu/g depending upon the type of cation substitution into the hexagonal lattice. All the samples exhibit a typical soft magnetic character with low values of coercivity (Hc) that are in the range of 26–85 Oe. These ferrites may be promising materials for microwave absorbers due to their higher saturation magnetization and low coercivities. Both the dielectric constant and tangent loss decrease with increasing frequency in the lower frequency region and become constant in the higher frequency region. The much lower dielectric constant obtained in this study makes the investigated ferrites very useful for high-frequency applications, i.e. dielectric resonators and for camouflaging military targets such as ships, tanks and aircrafts, etc.

Web URL: **https://link.springer.com/content/pdf/10.1007/s11664-016-4883-9.pdf**

10. Ablikim, M., Achasov, M. N., Ahmed, S., Albrecht, M., Amoroso, A., An, F. F., ... & Ferroli, R. B. (2017). Study of J/ψ and ψ (3686) decay to Λ Λ¯ and Σ 0 Σ¯ 0 final states. ***Physical Review D*****, *95*(5), 052003.**

ABSTRACT:

Using 1310.6 × 106 J=ψ and 447.9 × 106 ψð3686Þ events collected with the BESIII detector at the BEPCII eþe− collider, the branching fractions and the angular distributions of J=ψ and ψð3686Þ decays to ΛΛ¯ and Σ0Σ¯ 0 final states are measured. The branching fractions are determined, with much improved precision, to be 19.43 0.03 0.33, 11.64 0.04 0.23, 3.97 0.02 0.12 and 2.44 0.03 0.11 for J=ψ → ΛΛ¯, J=ψ → Σ0Σ¯ 0, ψð3686Þ → ΛΛ¯ and ψð3686Þ → Σ0Σ¯ 0, respectively. The polar angular distributions of ψð3686Þ decays are measured for the first time, while those of J=ψ decays are measured with much improved precision. In addition, the ratios of branching fractions Bðψð3686Þ→ΛΛ¯Þ BðJ=ψ→ΛΛ¯Þ and Bðψð3686Þ→Σ0Σ¯ 0Þ Bð J=ψ→Σ0Σ¯ 0Þ are determined to test the “12% rule.” DOI: 10

Web URL: ***https://journals.aps.org/prd/pdf/10.1103/PhysRevD.95.052003***

11. Nisar, S. & BESIII Collaboration. (2017). Measurement of the absolute branching fraction for $\Lambda_c^+ \to \Lambda \mu^+ \nu_\mu$. *Physics Letters B*, *767*, 42-47.

ABSTRACT:

We report the first measurement of the absolute branching fraction for Λc+→Λμ+νμ. This measurement is based on a sample of e+e− annihilation data produced at a center-of-mass energy s=4.6 GeV, collected with the BESIII detector at the BEPCII storage rings. The sample corresponds to an integrated luminosity of 567 pb−1. The branching fraction is determined to be B(Λc+→Λμ+νμ)=(3.49±0.46(stat)±0.27(syst))%. In addition, we calculate the ratio B(Λc+→Λμ+νμ)/B(Λc+→Λe+νe) to be 0.96±0.16(stat)±0.04(syst).

Web URL: **http://www.sciencedirect.com/science/article/pii/S0370269317300655**

12. Not Found

ABSTRACT:

Web URL:

13. Ablikim, M., Achasov, M. N., Ahmed, S., Ai, X. C., Albayrak, O., Albrecht, M., ... & Bai, J. Z. (2017). Observation of Λ c+→ n K S 0 π+. ***Physical Review Letters*****,** ***118*****(11), 112001.**

ABSTRACT:

We report the first direct measurement of decays of the Λþ c baryon involving the neutron. The analysis is performed using 567 pb−1 of eþe− collision data collected at ffiffi s p ¼ 4.599 GeV with the BESIII detector at the BEPCII collider. We observe the decay Λþ c → nK0 Sπþ and measure the absolute branching fraction to be BðΛþ c → nK0 Sπþ¼½1.82 0.23ðstatÞ 0.11ðsystÞ%. A comparison to B½Λþ c → pðK¯ πÞ0 provides an important test of isospin symmetry and final state interactions.

Web URL: ***https://journals.aps.org/prl/pdf/10.1103/PhysRevLett.118.112001***

14. Ablikim, M., Achasov, M. N., Ahmed, S., Ai, X. C., Albayrak, O., Albrecht, M., ... & Bai, J. Z. (2017). Precise Measurement of the e+ e−→ π+ π− J/ψ Cross Section at Center-of-Mass Energies from 3.77 to 4.60 GeV. ***Physical review letters*****,** ***118*****(9), 092001.**

ABSTRACT:

The cross section for the process eþe− → πþπ−J=ψ is measured precisely at center-of-mass energies from 3.77 to 4.60 GeV using 9 fb−1 of data collected with the BESIII detector operating

at the BEPCII storage ring. Two resonant structures are observed in a fit to the cross section. The first resonance has a mass of ð4222.0 3.1 1.4Þ MeV=c2 and a width of ð44.1 4.3 2.0Þ MeV, while the second one has a mass of ð4320.0 10.4 7.0Þ MeV=c2 and a width of ð101.4þ25.3 −19.7 10.2Þ MeV, where the first errors are statistical and second ones are systematic. The first resonance agrees with the Yð4260Þ resonance reported by previous experiments. The precision of its resonant parameters is improved significantly. The second resonance is observed in eþe− → πþπ−J=ψ for the first time. The statistical significance of this resonance is estimated to be larger than 7.6σ. The mass and width of the second resonance agree with the Yð4360Þ resonance reported by the BABAR and Belle experiments within errors. Finally, the Yð4008Þ resonance previously observed by the Belle experiment is not confirmed in the description of the BESIII data.

Web URL: ***https://journals.aps.org/prl/pdf/10.1103/PhysRevLett.118.092001***

15. Ablikim, M., Achasov, M. N., Ahmed, S., Ai, X. C., Albayrak, O., Albrecht, M., ... & Bai, J. Z. (2017). Evidence of Two Resonant Structures in e + e − → π + π − h c. ***Physical review letters*****,** ***118*****(9)**

ABSTRACT:

The cross sections of e+e-→π+π-hc at center-of-mass energies from 3.896 to 4.600 GeV are measured using data samples collected with the BESIII detector operating at the Beijing Electron Positron Collider. The cross sections are found to be of the same order of magnitude as those of e+e-→π+π-J/ψ and e+e-→π+π-ψ(2S), but the line shape is inconsistent with the Y states observed in the latter two modes. Two structures are observed in the e+e-→π+π-hc cross sections around 4.22 and 4.39…

Web URL:

https://www.researchgate.net/publication/314162029_Evidence_of_Two_Resonant_Structures_in_e_e_-_p_p_-_h_c

16. Ablikim, M., Achasov, M. N., Ahmed, S., Ai, X. C., Albayrak, O., Albrecht, M., ... & Bai, J. Z. (2017). Amplitude analysis of the χc1→ηπ+π− decays. ***Physical review letters*****,** ***95.***

ABSTRACT:

Using 448.0 × 106 ψð3686Þ events collected with the BESIII detector, an amplitude analysis is performed for ψð3686Þ → γχc1, χc1 → ηπþπ− decays. The most dominant two-body structure observed is a0ð980Þπ∓; a0ð980Þ → ηπ. The a0ð980Þ line shape is modeled using a dispersion relation, and a significant nonzero a0ð980Þ coupling to the η0 π channel is measured. We observe χc1 → a2ð1700Þπ production for the first time, with a significance larger than 17σ. The production of mesons with exotic quantum numbers, JPC ¼ 1−þ, is investigated, and upper limits for the branching fractions χc1 → π1ð1400Þπ∓, χc1 → π1ð1600Þπ∓, and χc1 → π1ð2015Þπ∓, with subsequent π1ðXÞ → ηπ decay, are determined. DOI: 1

Web URL:

https://www.researchgate.net/publication/318584918_Amplitude_analysis_of_the_chc1_epp-_decays

17. Ablikim, M., Achasov, M. N., Ahmed, S., Ai, X. C., Albayrak, O., Albrecht, M., ... & Bai, J. Z. (2017). Determination of the number of J//ψ J//ψ events with inclusive J//ψ J//ψ. *Chinese Physics C*, *41*.

ABSTRACT:

A measurement of the number of J/ψ events collected with the BESIII detector in 2009 and 2012 is performed using inclusive decays of the J/ψ. The number of J/ψ events taken in 2009 is recalculated to be $(223.7 \pm 1.4) \times 10^6$, which is in good agreement with the previous measurement, but with significantly improved precision due to improvements in the BESIII software. The number of J/ψ events taken in 2012 is determined to be $(1086.9 \pm 6.0) \times 10^6$. In total, the number of J/ψ events collected with the BESIII detector is measured to be $(1310.6 \pm 7.0) \times 10^6$, where the uncertainty is dominated by systematic effects and the statistical uncertainty is negligible.

Web URL: ***http://iopscience.iop.org/article/10.1088/1674-1137/41/1/013001***

18. Ablikim, M. (2017). Amplitude analysis of the decays η′→ π+ π− π0 and η′→ π0π0π0. *Physical review letters*, *118*.

ABSTRACT:

Based on a sample of 1.31×109 J/ψ events collected with the BESIII detector, an amplitude analysis of the isospin-violating decays η′→π+π-π0 and η′→π0π0π0 is performed. A significant P-wave contribution from η′→ρ±π is observed for the first time in η′→π+π-π0. The branching fraction is determined to be B(η′→ρ±π)=(7.44±0.60±1.26±1.84)×10-4, where the first uncertainty is statistical, the second systematic, and the third model dependent. In addition to the nonresonant S-wave component, there is a significant σ meson component. The branching fractions of the combined S-wave components are determined to be B(η′→π+π-π0)S=(37.63±0.77±2.22±4.48)×10-4 and B(η′→π0π0π0)=(35.22±0.82±2.54)×10-4, respectively. The latter one is consistent with previous BESIII measurements.

Web URL: ***https://experts.umn.edu/en/publications/amplitude-analysis-of-the-decays-%CE%B7-%CF%80%CF%80-%CF%800-and-%CE%B7-%CF%800%CF%800%CF%800***

19. Xu, J., Yang, Q., Javed, M. S., Gong, Y., Aslam, M. K., & Chen, C. (2017). The effects of NaF concentration on electrochemical and corrosion behavior of AZ31B magnesium alloy in a composite electrolyte. *RSC Advances*, *7*(10), 5880-5887.

ABSTRACT:

Electrochemical and corrosion behavior of AZ31B magnesium alloy have been investigated using electrochemical methods in a composite solution of $MgSO_4$–$Mg(NO_3)_2$ (0.14 mol L^{-1} $MgSO_4$, 1.86 mol L^{-1} $Mg(NO_3)_2$) under different sodium fluoride (NaF) concentrations. The surface of the AZ31B magnesium alloy is characterized using scanning electron microscopy, Fourier transform infrared spectroscopy and X-ray photoelectron spectroscopy. The experimental results indicate that the magnesium electrode achieves a low corrosion rate and high reactivity in the selected composite solution. Furthermore, the effect of NaF on the AZ31B magnesium alloy in the composite electrolyte is investigated in detail and the results demonstrated that the inhibition efficiency increased up to 80% and the delay time was reduced by four times when the NaF concentration reaches 30 mmol L^{-1}. Thus, NaF could efficiently reduce corrosion rate and improve the discharge activity of the magnesium anode as it changes the composition of the surface film. We believe that the composite electrolyte of $MgSO_4$–$Mg(NO_3)_2$ with optimized concentration of NaF is a promising candidate for

improving the corrosion resistance and reducing the delayed action of AZ31B alloy in aqueous solution.

Web URL: **http://pubs.rsc.org/-/content/articlehtml/2017/ra/c6ra27263k**

20. Javed, M. S., Shaheen, N., Idrees, A., Hu, C., & Raza, R. (2017). Electrochemical investigations of cobalt-free perovskite cathode material for intermediate temperature solid oxide fuel cell. *International Journal of Hydrogen Energy*, *42*(15), 10416-10422.

ABSTRACT:

A novel cobalt-free perovskite zinc-doped lanthanum strontium iron oxide ($La_{0.8}Sr_{0.2}Zn_xFe_{1-x}O_{3-\delta}$, LSZF, x = 0.1–0.3) is synthesized and evaluated as cathode material for intermediate temperature solid oxide fuel cell (IT-SOFC) with samarium doped ceria (SDC) electrolyte. LSZF cathode at x = 0.2 composition demonstrates the remarkable electrochemical activity at intermediate temperature (550 °C): such as, high electrical conductivity (13.63 S cm^{-1}), excellent thermal stability with SDC electrolyte (12.10 μK^{-1}), high surface area (4.52 m^2 g^{-1}), extremely reduced area specific resistance (0.69 Ω cm^{-2}) and low activation energy (0.117 eV). Furthermore, single fuel cells are fabricated using LSZF as a cathode, which exhibits the excellent performance by achieving the high power density of 409 mW cm^{-2} under natural gas as a fuel and ambient air as an oxidant at 550 °C with good stability over 10 h. All experimental results indicate that the LSZF is a promising cathode material for natural gas based intermediate temperature fuel cell applications.

Web URL: ***http://www.sciencedirect.com/science/article/pii/S0360319917305141***

21. Zeba, I., Batool, M., Khan, A. A., Jamil, M., & Rozina, C. (2016). SNS potential with exchange field in quantum dusty plasmas. *Plasma Physics and Controlled Fusion*, *59*(2), 025008.

ABSTRACT:

The shielding potential of a static test charge is studied in quantum dusty plasmas. The plasma system consisting upon electrons, ions and negatively static charged dust species, is embedded in an ambient magnetic field. The modified equation of dispersion is derived using quantum

hydrodynamic model (QHD) for magnetized plasmas. The quantum effects are inculcated through Fermi degenerate pressure, tunneling effect and exchange-correlation effects. The study of shielding is important to know the existence of the silence zones in space and astrophysical objects as well as crystal formation. The graphical description of the normalized potential depict the significance of the exchange and correlation effects arising through spin and other variables on the shielding potential.

Web URL: ***http://iopscience.iop.org/article/10.1088/1361-6587/59/2/025008/meta***

22. Jamil, M., Rasheed, A., Amir, M., Abbas, G., & Jung, Y. D. (2017). Jeans-Alfvén instability in quantum dusty magnetoplasmas. ***Journal of Plasma Physics*****,** ***83*****(1).**

ABSTRACT:

The Jeans instability is examined in quantum dusty magnetoplasmas due to low-frequency magnetosonic perturbations. The fluid model consisting of the momentum balance equation for quantum plasmas, Poisson's equation for the gravitational potential and Maxwell's equations for electromagnetic magnetosonic perturbations is solved. The numerical analysis elaborates the significant contribution of magnetic field, electron number density and variable dust mass to the Jeans instability.

Web URL:

https://www.cambridge.org/core/journals/journal-of-plasma-physics/article/jeansalfven-instability-in-quantum-dusty-magnetoplasmas/2E9C7D73EE04BD2DE8AB55806E43F377

23. Mustafa, F., Aslam, S., Jamil, A., & Ahmad, M. A. (2017). Synthesis and characterization of wide band gap nickel oxide (NiO) powder via a facile route. ***Optik-International Journal for Light and Electron Optics*****,** ***140*****, 38-44.**

ABSTRACT:

Here we report facile synthesis of Nano sized nickel oxide (NiO) powder via wet chemical method. The structural and optical properties have been investigated via XRD, FTIR, UV–Vis, SEM and EDS as a function of temperature (200 °C–700 °C), which peculiarly dictates the phase transformation and densification of the NiO nanoparticles. A theoretical evaluation of average

particle size (APS) and the specific surface area (SSA) of the NiO nanoparticles was carried out based on the XRD data. The data confirms the purity of the crystalline index particularly beyond 400 °C.The SEM images identify cubic phase crystalline structures with grain boundaries clearly diffusing into each other as a result of agglomeration beyond 400 °C. Our proposed one-step method of synthesis promises high electrical, thermal and optical quality NiO nanoparticles for a wide range of optoelectronic applications.

Web URL: ***http://www.sciencedirect.com/science/article/pii/S0030402617304187***

24. Idrees, M., Razaq, A., Islam, A., Yasmeen, S., Sultana, K., Asif, M. H., & Nadeem, M. (2017). Morphology and Dielectric Properties of Directly Collected and Polyaniline Coated Lignocelluloses Fibers. *Synthetic Metals*, *232*, 138-143.

ABSTRACT:

In era of modern technology, light-weight, flexible, low-cost and environmentally safe substrates/electrodes are highly feasible for application in disposable electronics and energy storage devices. This study presents morphological and dielectric characteristics of naked and polyaniline (PANI) coated lignocelluloses fibers, directly collected from self-growing plant, Typha Angustifolia. Impedance spectroscopy measurements performed in frequency range from 0.1 Hz to 10 MHz revealed increase of six orders magnitude in conductive properties of lignocelluloses fibers coated with polyaniline. Dielectric constant of polyaniline coated lignocelluloses fibers also increased by three to five orders magnitude and revealed weak frequency dependence. Presented morphological and dielectric investigations of directly collected and PANI coated lignocelluloses fibers will open possibilities to develop facile, low-cost, flexible and environment friendly paper substrates for energy storage and disposable electronic applications.

Web URL: ***https://www.sciencedirect.com/science/article/pii/S0379677917302308***

25. Mumtaz, S., Ahmad, M. A., Raza, R., Arshad, M. S., Ahmed, B., Ashiq, M. N., & Abbas, G. (2017). Nano grained Sr and Zr co-doped BaCeO3 electrolytes for intermediate temperature solid oxide fuel cells. *Ceramics International*, *43*(16), 14354-14360.

ABSTRACT:

Electrolyte materials in solid oxide fuel cells play a vital role in the performance of the cell. In the present work we are going to report a nano grained perovskite materials used for intermediate temperature (450–650 °C) solid oxide fuel cell. Here electrolytes having composition $Ba_{1-x}Sr_xCe_{1-y}Zr_yO_{3-\delta}$ where x = 0.2, 0.3 and y = 0.2, 0.3 were synthesized by sol-gel method. Two prepared samples were named as BSCZ1 and BSCZ2 for x = y = 0.2&0.3, respectively. Structural analysis and surface morphology were performed using XRD and SEM, respectively. The particle size of BSCZ1 and BSCZ2 electrolyte materials calculated by Scherer's formula were found to be 25 nm and 28 nm, respectively. The protonic conductivities were determined by four probe method and maximum results of measurements were found to be 0.007 and 0.008 S/cm for BSCZ1 and BSCZ2, respectively at temperature of 650 °C. Electrical impedance spectroscopy results show ionic behavior which is suited for good electrolytes. It has been noted that the BSCZ2 electrolyte material executes maximum power density of 250 mW/cm^2 at 650 °C.

Web URL: ***https://www.sciencedirect.com/science/article/pii/S0272884217316395***

26. Rauf, S., Nawaz, M. A. H., Muhammad, N., Raza, R., Shahid, S. A., Marty, J. L., & Hayat, A. (2017). Protic ionic liquids as a versatile modulator and stabilizer in regulating artificial peroxidase activity of carbon materials for glucose colorimetric sensing. *Journal of Molecular Liquids*, *243*, 333-340.

ABSTRACT:

Herein, by utilizing ionic liquid, we have shown for the first time that activated carbon can be used as a cheap and recyclable peroxidase mimic in the construction of colorimetric sensors for biomedical applications. The purposed nanozyme catalyzed the oxidation of 3,3',5,5'-tetramethylbenzidine (TMB) in the presence of hydrogen peroxide (H_2O_2) to produce a blue colored product which can be monitored at 652 nm. H_2O_2 is the oxidative product of glucose in the presence of glucose oxidase. Therefore, the oxidation of glucose can be quantitatively related to the colorimetric response by combining these two reactions. Under the optimal experimental conditions, a linear response was observed for glucose concentrations ranging

from 12 to 550 µmol/L, with a detection limit of 3.5 µmol/L. Furthermore, the specificity of the proposed method was demonstrated against common interfering compounds including uric acid, ascorbic acid, lactose, sucrose and maltose. The applicability of the proposed method was demonstrated for glucose detection in human serum samples. The proposed methodology can serve as a general way to design ionic liquid based nanozyme mimetics for various catalytic reactions and colorimetric sensing applications.

Web URL: ***https://www.sciencedirect.com/science/article/pii/S0167732217325886***

27. Ullah, M., Rana, A. M., Ahmed, E., Raza, R., Shah, Z. A., & AHMAD, E. M. (2017). BORON-INCORPORATED DIAMOND TO ACT AS ELECTRODE MATERIAL IN LITHIUM ION BATTERIES. ***Journal of Ovonic Research*****,** ***13*****(4).**

ABSTRACT:

A crystalline electrode made up of 75% active material (boron-incorporated diamond, BID), 10% poly vinylidene fluoride + 1-methyl-2pyrrolidinone and 15% carbon black was synthesized using the combustion technique at 1173 K for one hour to make homogeneous distribution of sub-micron sized particles. Characterization of the electrode material has been performed through X-ray diffraction, Raman Spectroscopy and Scanning electron microscopy before using it in lithium-ion batteries. The amount of Li in the boron-doped diamond strongly affects its electrochemical performance as electrode. Electrochemical measurements have illustrated much better cycling stability in the –4.0 to 4.5V range at different rates of current. The successful electrochemical activity of boron-incorporated diamond electrode along with lithium electrode insertion in Li+ ion batteries has been reported and discussed here. The peak current shows an almost linear relationship with square root of the scan rate. In addition, effective electrode area was estimated to be 0.54 cm2 .Electronic properties of Li-containing electrodes were investigated using DFT approach which showed polaronic conducting behavior which seems advantageous for high power capability.

Web URL: ***http://www.chalcogen.ro/187_UllahM.pdf***

28. Wang, B., Cai, Y., Xia, C., Kim, J. S., Liu, Y., Dong, W., ... & Zhu, B. (2017). Semiconductor-ionic membrane of lasrcofe-oxide-doped ceria solid oxide fuel cells. *Electrochimica Acta*, *248*, 496-504.

ABSTRACT:

A novel semiconductor-ionic $La_{0.6}Sr_{0.4}Co_{0.2}Fe_{0.8}O_{3-\delta}$ (LSCF)-Sm/Ca co-doped CeO_2(SCDC) nanocomposite has been developed as a membrane, which is sandwiched between two layers of $Ni_{0.8}Co_{0.15}Al_{0.05}$Li-oxide (NCAL) to construct semiconductor-ion membrane fuel cell (SIMFC). Such a device presented an open circuit voltage (OCV) above 1.0 V and maximum power density of 814 mW cm^{-2} at 550 °C, which is much higher than 0.84 V and 300 mW cm^{-2} for the fuel cell using the SCDC membrane. Moreover, the SIMFC has a relatively promising long-term stability, the voltage can maintain at 0.966 V for 60 hours without degradation during the fuel cells operation and the open-circuit voltage (OCV) can return to 1.06 V after long-term fuel cell operation. The introduction of LSCF electronic conductor into the membrane did not cause any short circuit but brought significant enhancement of fuel cell performances. The Schottky junction is proposed to prevent the internal electrons passing thus avoiding the device short circuiting problem.

Web URL: **https://www.sciencedirect.com/science/article/pii/S0013468617315451**

29. Afzal, M., Madaan, S., Dong, W., Raza, R., Xia, C., & Zhu, B. (2017). Analysis of a perovskite-ceria functional layer-based solid oxide fuel cell. *International Journal of Hydrogen Energy*.

ABSTRACT:

A fuel cell based on a functional layer of perovskite $Ba_{0.5}Sr_{0.5}Co_{0.8}Fe_{0.2}O_{3-\delta}$ (BSCF) composited samarium doped ceria (SDC) has been developed. The device achieves a peak power density of 640.4 mW cm^{-2} with an open circuit voltage (OCV) of 1.04 V at 560 °C using hydrogen and air as the fuel and oxidant, respectively. A numerical model is applied to fit the experimental cell voltage. The kinetics of anodic and cathodic reactions are modeled based on the measurements obtained by electrochemical impedance spectroscopy (EIS). Modeling results are in well agreement with the experimental data. Mechanical stability of the cell is also examined by

using analysis with field emission scanning electron microscope (FESEM) associated with energy dispersive spectroscopy (EDS) after testing the cell performance.

Web URL: ***http://www.sciencedirect.com/science/article/pii/S0360319917318177***

30. Zhu, B., Wang, B., Wang, Y., Raza, R., Tan, W., Kim, J. S., ... & Lund, P. (2017). Charge separation and transport in La 0.6 Sr 0.4 Co 0.2 Fe 0.8 O 3-δ and ion-doping ceria heterostructure material for new generation fuel cell. *Nano Energy*, *37*, 195-202.

ABSTRACT:

Functionalities in heterostructure oxide material interfaces are an emerging subject resulting in extraordinary material properties such as great enhancement in the ionic conductivity in a heterostructure between a semiconductor $SrTiO_3$ and an ionic conductor YSZ (yttrium stabilized zirconia), which can be expected to have a profound effect in oxygen ion conductors and solid oxide fuel cells [1–4]. Hereby we report a semiconductor-ionic heterostructure $La_{0.6}Sr_{0.4}Co_{0.2}Fe_{0.8}O_{3-\delta}$ (LSCF) and Sm-Ca co-doped ceria (SCDC) material possessing unique properties for new generation fuel cells using semiconductor-ionic heterostructure composite materials. The LSCF-SCDC system contains both ionic and electronic conductivities, above 0.1 S/cm, but used as the electrolyte for the fuel cell it has displayed promising performance in terms of OCV (above 1.0 V) and enhanced power density (ca. 1000 mW/cm^2 at 550 °C). Such high electronic conduction in the electrolyte membrane does not cause any short-circuiting problem in the device, instead delivering enhanced power output. Thus, the study of the charge separation/transport and electron blocking mechanism is crucial and can play a vital role in understanding the resulting physical properties and physics of the materials and device. With atomic level resolution ARM 200CF microscope equipped with the electron energy-loss spectroscopy (EELS) analysis, we can characterize more accurately the buried interface between the LSCF and SCDC further reveal the properties and distribution of charge carriers in the heterostructures. This phenomenon constrains the carrier mobility and determines the charge separation and devices' fundamental working mechanism; continued exploration of this frontier can fulfill a next generation fuel cell based on the new concept of semiconductor-ionic fuel cells (SIFCs).

Web URL: **http://www.sciencedirect.com/science/article/pii/S2211285517302756**

31. Arshad, M. S., Mushtaq, N., Ahmad, M. A., Naseem, S., Atiq, S., Ahmed, Z., ... & Raza, R. (2017). Nickel foam anode-supported solid oxide fuel cells with composite electrolytes. *International Journal of Hydrogen Energy*, *42*(34), 22288-22293.

ABSTRACT:

In this paper, three composite electrolytes ($Ce_{0.8}Sm_{0.2}O_{1.9}/Na_2CO_3$) SDC, ($Ce_{0.8}Gd_{0.2}O_{1.9}/Na_2CO_3$) GDC and ($La_{0.8}Sr_{0.2}Ga_{0.8}Mg_{0.2}O_{3-\delta}/Na_2CO_3$) LSGM have been studied to review the effect of Na_2CO_3, present as second phase, and effect of Ni support, sintering and pressure for dry pressing for fuel cell performance. The electrolytes were prepared through a co-precipitation method. Different techniques were used to characterize the prepared electrolytes. The crystal structures were determined using x-ray diffraction (XRD) and structural morphologies were analyzed through scanning electron microscopy (SEM). The four-probe dc conductivity and two probe AC impedance analysis were carried out in open air. The fuel cell performance was determined with and without Ni support on anode side which resulted in a considerable difference in obtained peak power densities. It is suggested that prepared electrolytes can find potential applications in low temperatures Solid Oxide Fuel Cells (LT-SOFCs).

Web URL: ***https://www.sciencedirect.com/science/article/pii/S0360319917323029***

32. Abdikian, A., & Ehsan, Z. (2017). Propagation of electrostatic surface waves in a thin degenerate plasma film with electron exchange–correlation effects. *Physics Letters A*, *381*(35), 2939-2943.

ABSTRACT:

Propagation of an electrostatic surface wave in a thin degenerate Fermi plasma film in the presence of constant external magnetic field is studied here. Dispersion relations for the symmetric and anti-symmetric modes have been derived and studied quantitatively with the exchange–correlation effects. It has been studied that with the increase in the strength of magnetic field, phase velocity of the waves decreases. Also electron exchange–correlation effects significantly modify the behavior of the surface waves such as frequency of surface wave is found to be downshifted by these effects. Moreover it has been studied that the group velocity of the anti-symmetric mode is greater than the symmetric mode for the whole wave

numbers; however, these modes merge into a single mode with the increase of the wave number.

Web URL: ***https://www.sciencedirect.com/science/article/pii/S0375960117306849***

33. Ablikim, M., Achasov, M. N., Ahmed, S., Ai, X. C., Albayrak, O., Albrecht, M., ... & Bai, J. Z. (2017). Observation of the decay Λ+c→Σ−π+π+π0Λc+→Σ−π+π+π0. Physics Letters B.*772*

ABSTRACT:

We report the first observation of the decay Λc+→Σ−π+π+π0, based on data obtained in e+e− annihilations with an integrated luminosity of 567 pb^{-1} at s=4.6GeV. The data were collected with the BESIII detector at the BEPCII storage rings. The absolute branching fraction B(Λc+→Σ−π+π+π0) is determined to be (2.11±0.33(stat.)±0.14(syst.))%. In addition, an improved measurement of B(Λ+c→Σ−π+π+) is determined as (1.81±0.17(stat.)±0.09(syst.))%.

Web URL: ***https://www.sciencedirect.com/science/article/pii/S0370269317305415***

34. Ablikim, M., Achasov, M. N., Ahmed, S., Ai, X. C., Albayrak, O., Albrecht, M., ... & Bai, J. Z. (2017). Determination of the Spin and Parity of the Zc(3900). Phys. Rev. Lett. 119

ABSTRACT:

The spin and parity of the Zc(3900)± state are determined to be JP=1+ with a statistical significance larger than 7σ over other quantum numbers in a partial wave analysis of the process e+e−→π+π−J/ψ. We use a data sample of 1.92 fb−1 accumulated at s√=4.23 and 4.26 GeV with the BESIII experiment. When parameterizing the Zc(3900)± with a Flatte-like formula, we determine its pole mass Mpole=(3881.2±4.2stat±52.7syst)MeV/c2 and pole width Γpole=(51.8±4.6stat±36.0syst)MeV. We also measure cross sections for the process e+e−→Zc(3900)+π−+c.c.→J/ψπ+π− and determine an upper limit at the 90\% confidence level for the process e+e−→Zc(4020)+π−+c.c.→J/ψπ+π−.

Web URL: ***https://arxiv.org/abs/1706.04100***

35. Ablikim, M., Achasov, M. N., Ahmed, S., Ai, X. C., Albayrak, O., Albrecht, M., ... & Bai, J. Z. (2017). Observation of e+e−→ηhc at center-of-mass energies from 4.085 to 4.600 GeV. Physical Review D. 96

ABSTRACT:

We observe for the first time the process e+e-→ηhc with data collected by the BESIII experiment. Significant signals are observed at the center-of-mass energy s=4.226 GeV, and the Born cross section is measured to be (9.5-2.0+2.2±2.7) pb. Evidence for ηhc is observed at s=4.358 GeV with a Born cross section of (10.0-2.7+3.1±2.6) pb, and upper limits on the production cross section at other center-of-mass energies between 4.085 and 4.600 GeV are determined.

Web URL: ***https://experts.umn.edu/en/publications/observation-of-ee%CE%B7hc-at-center-of-mass-energies-from-4085-to-4600***

36. Not Found

ABSTRACT:

Web URL:

37. Ablikim, M., Achasov, M. N., Ahmed, S., Ai, X. C., Albayrak, O., Albrecht, M., ... & Bai, J. Z. (2017). Branching fraction measurements of ψ(3686)→γχcJ. Physical Review D. 96

ABSTRACT:

Using a sample of 106 million ψð3686Þ decays, the branching fractions of ψð3686Þ → γχc0, ψð3686Þ → γχc1, and ψð3686Þ → γχc2 are measured with improved precision to be ð9.389 0.014 0.332Þ%, ð9.905 0.011 0.353Þ%, and ð9.621 0.013 0.272Þ%, respectively, where the first uncertainties are statistical and the second ones are systematic. The product branching fractions of ψð3686Þ → γχc1; χc1 → γJ=ψ and ψð3686Þ → γχc2; χc2 → γJ=ψ and the branching fractions of χc1 → γJ=ψ and χc2 → γJ=ψ are also presented.

Web URL: **https://journals.aps.org/prd/pdf/10.1103/PhysRevD.96.032001**

38. Ablikim, M., Achasov, M. N., Ahmed, S., Ai, X. C., Albayrak, O., Albrecht, M., ... & Bai, J. Z. (2017). Search for the radiative leptonic decay D+→ γ e+ ν e. ***Physical Review D*****, *95*(7), 071102.**

ABSTRACT:

Using an electron-positron collision data sample of 2.93 fb−1 collected at a center-of-mass energy of ffiffi s p ¼ 3.773 GeV with the BESIII detector, we present the first search for the radiative leptonic decay Dþ → γeþve. The analysis is performed with a double-tag method. We do not observe a significant Dþ → γeþve signal, and obtain an upper limit on the branching fraction of Dþ → γeþve decay with the energy of radiative photon larger than 10 MeV of 3.0 × 10−5 at the 90% confidence level.

Web URL: ***https://journals.aps.org/prd/pdf/10.1103/PhysRevD.95.071102***

39. Ablikim, M., Achasov, M. N., Ahmed, S., Ai, X. C., Albayrak, O., Albrecht, M., ... & Bai, J. Z. (2017). Evidence for the singly-Cabibbo-suppressed decay $\Lambda_ {c}^{+}\to p\eta $ and search for $\Lambda_ {c}^{+}\to p\pi^{0} $. ***arXiv preprint arXiv:1702.05279*****.**

ABSTRACT:

We study the singly-Cabibbo-suppressed decays Λ+ c → pη and Λ+ c → pπ0 using Λ+ c Λ¯− c pairs produced by e +e − collisions at a center-of-mass energy of √ s = 4.6 GeV. The data sample was collected by the BESIII detector at the BEPCII collider and corresponds to an integrated luminosity of 567 pb−1 . We find the first evidence for the decay Λ+ c → pη with a statistical significance of 4.2σ and measure its branching fraction to be B(Λ+ c → pη) = (1.24 ± 0.28(stat.) ± 0.10(syst.)) × 10−3 . No significant Λ+ c → pπ0 signal is observed. We set an upper limit on its branching fraction B(Λ+ c → pπ0) < 2.7 × 10−4 at the 90% confidence level.

Web URL: **https://arxiv.org/pdf/1702.05279.pdf**

40. Ablikim, M., Achasov, M. N., Ahmed, S., Ai, X. C., Albayrak, O., Albrecht, M., ... & Bai, J. Z. (2017). Luminosity measurements for the R scan experiment at BESIII. ***arXiv preprint arXiv:1702.04977*****.**

ABSTRACT:

By analyzing the large-angle Bhabha scattering events e +e − → (γ)e +e − and diphoton events e +e − → γγ for the data sets collected at center-of-mass (c.m.) energies between 2.2324 and 4.5900 GeV (131 energy points in total) with the upgraded Beijing Spectrometer (BESIII) at the Beijing Electron-Positron Collider (BEPCII), the integrated luminosities have been measured at

the different c.m. energies, individually. The results are the important inputs for R value and J/ψ resonance parameter measurements.

Web URL: ***https://arxiv.org/pdf/1702.04977.pdf***

41. Ablikim, M., Achasov, M. N., Ahmed, S., Ai, X. C., Albayrak, O., Albrecht, M., ... & Bai, J. Z. (2017). Amplitude analysis of D0 → K− π + π + π −. ***Physical Review D*****, *95***

ABSTRACT:

We present an amplitude analysis of the decay D0 → K−πþπþπ− based on a data sample of 2.93 fb−1 acquired by the BESIII detector at the ψð3770Þ resonance. With a nearly background free sample of about 16000 events, we investigate the substructure of the decay and determine the relative fractions and the phases among the different intermediate processes. Our amplitude model includes the two-body decays D0 → K¯ 0ρ0, D0 → K−aþ 1 ð1260Þ and D0 → K− 1 ð1270ÞπþB, the three-body decays D0 → K¯ 0πþπ− and D0 → K−πþρ0, as well as the four-body nonresonant decay D0 → K−πþπþπ−. The dominant intermediate process is D0 → K−aþ 1 ð1260Þ, accounting for a fit fraction of 54.6%. D

Web URL: ***https://journals.aps.org/prd/pdf/10.1103/PhysRevD.95.072010***

42. Ablikim, M., Achasov, M. N., Ahmed, S., Ai, X. C., Albayrak, O., Albrecht, M., ... & Bai, J. Z. (2017). Observation of ψ(3686)→e+e−χcJ and χcJ→e+e−J/ψ. Phys.Rev.Lett. 118(22)

ABSTRACT:

Using 4.479×108 ψ(3686) events collected with the BESIII detector, we search for the decays ψ(3686)→e+e-χcJ and χcJ→e+e-J/ψ, where J=0, 1, 2. The decays ψ(3686)→e+e-χcJ and χcJ→e+e-J/ψ are observed for the first time. The measured branching fractions are B(ψ(3686)→e+e-χcJ)=(11.7±2.5±1.0)×10-4, (8.6±0.3±0.6)×10-4, (6.9±0.5±0.6)×10-4 for J=0, 1, 2, and B(χcJ→e+e-J/ψ)=(1.51±0.30±0.13)×10-4, (3.73±0.09±0.25)×10-3, (2.48±0.08±0.16)×10-3 for J=0, 1, 2, respectively. The ratios of the branching fractions B(ψ(3686)→e+e-χcJ)/B(ψ(3686)→γχcJ) and B(χcJ→e+e-J/ψ)/B(χcJ→γJ/ψ) are also reported. Also, the α values of helicity angular distributions of the e+e- pair are determined for ψ(3686)→e+e-χc1,2 and χc1,2→e+e-J/ψ.

Web URL: ***http://inspirehep.net/record/1509920/***

43. BESIII Collaboration. (2017). Measurements of cross section of at center-of-mass energies between 4.008 and 4.600 GeV. *Physics Letters B*, *771*, 45-51.

ABSTRACT:

Based on e+e− annihilation data samples collected with the BESIII detector at the BEPCII collider at 13 center-of-mass energies from 4.008 to 4.600 GeV, measurements of the Born cross section of $e^+e^-\to p\bar{p}\pi^0$ are performed. No significant resonant structure is observed in the measured energy dependence of the cross section. The upper limit on the Born cross section of $e^+e^-\to Y(4260)\to p\bar{p}\pi^0$ at the 90% C.L. is determined to be 0.01 pb. The upper limit on the ratio of the branching fractions $\mathcal{B}(Y(4260)\to p\bar{p}\pi^0)\mathcal{B}(Y(4260)\to\pi^+\pi^- J/\psi)$ at the 90% C.L. is determined to be 0.02%.

Web URL: ***http://www.sciencedirect.com/science/article/pii/S0370269317303969***

44. Rozina, C., Jamil, M., Khan, A. A., Zeba, I., & Saman, J. (2017). Low frequency waves in streaming quantum dusty plasmas. *Physics of Plasmas*, *24*(9), 093702.

ABSTRACT:

The influence of quantum effects on the excitation of two instabilities, namely quantum dust-acoustic and quantum dust-lower-hybrid waves due to the free streaming of ion/dust particles in uniformly magnetized dusty plasmas has been investigated using a quantum hydrodynamic model. We have obtained dispersion relations under some particular conditions applied on streaming ions and two contrastreaming dust particle beams at equilibrium and have analyzed the growth rates graphically. We have shown that with the increase of both the electron number density and the streaming speed of ion there is enhancement in the instability due to the fact that the dense plasma particle system with more energetic species having a high speed results in the increase of the growth rate in the electrostatic mode. The application of this work has been pointed out for laboratory as well as for space dusty plasmas.

Web URL: ***http://aip.scitation.org/doi/full/10.1063/1.4998618***

45. Naeem, H., Bing, G., Naeem, M. R., Aamir, M., & Javed, M. S. (2017). A new approach for image detection based on refined Bag of Words algorithm. *Optik-International Journal for Light and Electron Optics*, *140*, 823-832.

ABSTRACT:

This paper presents an efficient image retrieval approach based on enhanced Bag of Words (BOW). By keeping eyes on low classification efficiency and accuracy of existing image retrieval system based on traditional BOW, a new classification method combined features of scale invariant feature transform (SIFT) and GIST principle (CGSF) is proposed. This method use SIFT algorithm to extract the local feature vector and GIST algorithm to extract the global feature vector for images. The feature fusion scheme is applied to combine local with global features through weight which can enhance the classification accuracy with efficiency. At the end, VLFeat linear support vector machine (SVM) classifier is used to classify the visual dictionary and Osirix medical computed tomography (CT) image dataset is selected for experimental verification. Three experiments are carried out based on factors that contribute to performance and accuracy (dictionary size and λ co-efficient). The experimental results prove that our proposed technique is much robust and accurate than traditional algorithms in image retrieval. Furthermore, our method is matched with literature in classification accuracy and the outcomes indicate the noticeable benefits in medical, internet of things and many other domains.

Web URL: ***http://www.sciencedirect.com/science/article/pii/S0030402617305405***

46. Amjad, R. J., Santos, W., Jacinto, C., & Dousti, M. R. (2017). Luminescence dynamics in Eu3+ doped fluoroborate glasses. *Journal of Luminescence*, *192*, 827-831.

ABSTRACT:

Rare earth ions doped transparent glasses are among promising solid-state materials for various optical applications. In this report, Eu^{3+} ions doped new fluoroborate glasses were prepared by conventional melt-quenching technique and their optical properties were characterized by absorption and luminescence spectroscopy as well as excited state lifetime measurements. The absorption spectra revealed the characteristic transitions between

the $^7F_0$ ground state and $^7F_1$ first excited state to the upper-lying electronic states. The variation in the luminescence intensity of the radiative transitions occurring at 590 and 611 nm and the bi-exponential behavior of the fluorescence decay of the $^5D_0$ level, with different trend for the amplitude of the decays, are discussed in terms of low and high symmetry sites depending on the EuF_3 concentration and the possible energy transfer between ions at these sites.

Web URL: ***https://www.sciencedirect.com/science/article/pii/S0022231317303502***

47. Rajesh, D., Amjad, R. J., Dousti, M. R., & de Camargo, A. S. S. (2017). Enhanced VIS and NIR emissions of Pr 3+ ions in TZYN glasses containing silver ions and nanoparticles. ***Journal of Alloys and Compounds*****,** ***695*****, 607-612.**

ABSTRACT:

TeO_2-ZnO-YF_3-NaF glasses doped with Pr_2O_3 and containing $AgNO_3$ were prepared for the first time by single step melt quenching technique. Ag nanoparticles were grown by controlled heat treatment of the glasses during different periods of times (up to 10 h) at 300 °C, which is below the glass transition temperature. TEM images show the presence of Ag NPs with average diameter 10–46 nm and, in agreement, a broad absorption band, peaked around 492 nm, was observed and attributed to the surface plasmon resonance band (SPR) of the NPs in Pr^{3+} free glasses. UV–Vis absorption, and visible and near-infrared steady state and time-dependent fluorescence techniques were used to characterize the effect of the NPs on the emission properties of Pr^{3+}. The enhancement of Pr^{3+} Stokes luminescence with the increase in NPs concentration was observed for samples excited in resonance (480 nm) and off-resonance (440 and 470 nm) with the SPR band. An increase of the excited state lifetime value for Pr^{3+}:$^3P_0$ level was also observed in the presence of other Ag species (dimmers, trimmers, molecule-like and non plasmonic Ag particles) and NPs. Thus, the results show that besides the possible local field effect of the NPs, the enhancement of luminescence intensity is also likely to be due to energy transfer from the Ag species to Pr^{3+} ions. These new glasses show interesting properties that could become useful for photonic device applications.

Web URL: **http://www.sciencedirect.com/science/article/pii/S0925838816335253**

48. Dousti, M. R., & Amjad, R. J. (2017). Effect of silver nanoparticles on the upconversion and near-infrared emissions of Er 3+: Yb 3+ co-doped zinc tellurite glasses. *Measurement*, *105*, 114-119.

ABSTRACT:

The effect of the silver nanoparticles on the optical response of the Er^{3+}/Yb^{3+} co-doped zinc tellurite glasses was studied. The glasses were characterized by optical absorption spectroscopy, transmission electron microscopy and X-ray diffractometry. The characteristic radiative emissions of Er^{3+} ions at visible (upconversion) and near-infrared spectral regions were recorded by exciting the samples at 980 nm excitation wavelength. The intensities of upconversion and near-infrared emissions were enhanced up to 180% and 130%, respectively. The increase in luminescence intensity is attributed to the enhanced effective localized field induced by silver nanoparticles. Lifetime measurements were conducted to investigate the presence of energy transfer between Er^{3+} and silver.

Web URL: ***http://www.sciencedirect.com/science/article/pii/S0263224117302166***

49. Aboud, H., & Amjad, R. J. (2017). SnO2 nanoparticles concentration dependent structural and luminescence characteristics of Er+ 3 doped zinc-lead-phosphate glass. *Journal of Non-Crystalline Solids*, *471*, 1-5.

ABSTRACT:

We report the modifications in the structural and luminescence properties of erbium (Er^{+3}) doped Zinc-Lead-Phosphate (ZLP) glasses containing SnO_2 nanoparticles (SNPs). Glasses are prepared via melt quenching technique and characterized using high resolution scanning electron microscope (FE-SEM), differential thermal analyzer (DTA), Fourier transform infrared (FTIR), UV–Visible absorption and photoluminescence (PL) spectroscopy. The DTA results showed an enhancement in the thermal stability with the incorporation of SNPs. The FESEM micrograph revealed the occurrence of uniformly distributed SNPs with average diameter around 21 nm. FTIR spectra exhibited various bonding vibrations, where the IR transmission band intensities are increased accompanied by a shift with the increase of SNPs contents. The UV–Vis spectra displayed six significant absorption peaks centered around 1536, 979, 799, 650,

523, and 485 nm. Room temperature PL spectra showed three emission peaks centered at 502, 545 and 606 nm. The emission intensities are enhanced with increasing SNPs contents. Present glass composition may be useful for the development of solid state lasers and other photonic devices.

Web URL: **https://www.sciencedirect.com/science/article/pii/S0022309317301308**

50. Rajesh, D., Dousti, M. R., Amjad, R. J., & de Camargo, A. S. S. (2017). Enhancement of down-and upconversion intensities in Er3+/Yb3+ co-doped oxyfluoro tellurite glasses induced by Ag species and nanoparticles. ***Journal of Luminescence*****,** ***192*****, 250-255.**

ABSTRACT:

New oxyfluoro-tellurite glasses co-doped with Er^{3+}/Yb^{3+} and containing silver species and nano particles (NPs) were prepared using the conventional melt quenching technique. The X-ray diffraction patterns obtained in this work do not reveal any crystalline phase in the glass. Heat treatment at 290 °C, for about 6 h, of an Er^{3+}/Yb^{3+}co-doped oxyfluoro-tellurite glass containing 1.0 mol% $AgNO_3$ yielded well-dispersed, nearly spherical Ag NPs, as verified by transmission electron microscopy. The observed surface plasmon resonance (SPR) band was observed around 490 nm for heat treated glasses containing only silver. Upon off resonance (375 nm) and in resonance (486 nm) excitation of SPR band, the intense visible (520, 540 and 650 nm) and NIR (0.98 μm and 1.53 μm) downconversion emission bands were observed and further enhanced with the increase of Ag concentration and heat treatment duration up to 6 h. An intensity drop was observed by further heat treatment (up to 9 h). In addition, enhancement of upconversion emissions, in the green and red, as a function of Ag concentration and heat treatment time, has also been verified. The intensity was found to be enhanced by increasing the Ag concentration and heat treatment time up to 3 h. However, further increase in the heat treatment time duration (up to 9 h) resulted in reduced intensities. Enhancement in the luminescence intensity was discussed in terms of the surface plasmon resonance whereas the quenching was attributed to the intense absorption of photons, emitted from RE ions, by larger Ag NPs.

Web URL: ***https://www.sciencedirect.com/science/article/pii/S0022231317302922***

51. Rafique, M. Y., Pan, L., & Guo, Z. (2017). Switching behavior and novel stable states of magnetic hexagonal nanorings. *Journal of Magnetism and Magnetic Materials*, *432*, 1-9.

ABSTRACT:

Micromagnetic simulations for Cobalt hexagonal shape nanorings show onion (O) and vortex state (V) along with new state named “tri-domain state”. The tri-domain state is observed in sufficiently large width of ring. The magnetic reversible mechanism and transition of states are explained with help of vector field display. The transitions from one state to other occur by propagation of domain wall. The vertical parts of hexagonal rings play important role in developing the new “tri-domain” state. The behaviors of switching fields from onion to tri-domain (HO-Tr), tri-domain to vortex state (HTr--V) and vortex to onion state and “states size” are discussed in term of geometrical parameter of ring.

Web URL: ***http://www.sciencedirect.com/science/article/pii/S0304885316315803***

52. Ablikim, M., Achasov, M. N., Ahmed, S., Albrecht, M., Alekseev, M., Amoroso, A., ... & Bakina, O. (2017). Evidence for $ e^{+} e^{-}\to\gamma\eta_c (1S) $ at center-of-mass energies between 4.01 and 4.60 GeV. *arXiv preprint arXiv:1705.06853*.

ABSTRACT:

We present first evidence for the process e +e − → γηc(1S) at six center-of-mass energies between 4.01 and 4.60 GeV using data collected by the BESIII experiment operating at BEPCII. These data sets correspond to a total integrated luminosity of 4.6 fb−1 . We measure the Born cross section at each energy using a combination of twelve ηc(1S) decay channels. Because the significance of the signal is marginal at each energy (≤ 3.0σ), we also combine all six energies under various assumptions for the energy-dependence of the cross section. If the process is assumed to proceed via the Y (4260), we measure a peak Born cross section σpeak(e +e − → γηc(1S)) = 2.11 ± 0.49(stat.) ± 0.36(syst.) pb with a statistical significance of 4.2σ.

Web URL: ***https://arxiv.org/pdf/1705.06853.pdf***

53. Ablikim, M., Achasov, M. N., Ahmed, S., Ai, X. C., Albayrak, O., Albrecht, M., ... & Bai, J. Z. (2017). Measurement of $ e^{+} e^{-}\rightarrow\pi^{+}\pi^{-}\psi (3686) $ from 4.008 to

4.600~ GeV and observation of a charged structure in the $\pi^{\pm}\psi (3686) $ mass spectrum. *arXiv preprint arXiv:1703.08787*.

ABSTRACT:

We study the process e +e − → π +π −ψ(3686) using 5.1 fb−1 of data collected at 16 center-of-mass energy (√ s) points from 4.008 to 4.600 GeV by the BESIII detector operating at the BEPCII collider. The measured Born cross sections for e +e − → π +π −ψ(3686) are consistent with previous results, but with much improved precision. A fit to the cross section shows contributions from two structures: the first has M = 4209.5 ± 7.4 ± 1.4 MeV/c 2 and Γ = 80.1 ± 24.6 ± 2.9 MeV, and the second has M = 4383.8±4.2±0.8 MeV/c2 and Γ = 84.2±12.5±2.1 MeV, where the first errors are statistical and the second systematic. The lower-mass resonance is observed in the process e +e − → π +π −ψ(3686) for the first time with a statistical significance of 5.8σ. A charged charmonium-like structure is observed in the π ±ψ(3686) invariant mass spectrum for data at √ s = 4.416 GeV. A fit with an Swave Breit-Wigner function yields a mass M = 4032.1±2.4 MeV/c 2 , where the errors are statistical only. However, there are still unresolved discrepancies between the fit model and data. The width of the intermediate state varies in a wide range for different kinematic regions within the data set. Therefore no simple interpretation of the data has been found, and a future data sample with larger statistics and more theoretical input will be required to better understand this issue.

Web URL: ***https://arxiv.org/pdf/1703.08787.pdf***

54. Zafar, M., Naeem Awais, M., Asif, M., Razaq, A., & Amin, G. (2017). Fabrication and characterization of piezoelectric nanogenerator based on Al/ZnO/Au structure. *Microelectronics International*, *34*(1), 35-39.

ABSTRACT:

Purpose

The purpose of this research work is to harvest energy using the piezoelectric properties of ZnO nanowires (NW). Fabrication and characterization of the piezoelectric nanogenerator

(NG), based on Al/ZnO/Au structure without using hosting layer, were done to harvest energy. The proposed method has full potential to harvest the cost-effective energy.

Design/methodology/approach

ZnO NW were fabricated between the thin layers of Al- and Au-coated substrates for the development of piezoelectric NG. To grow ZnO NW, ZnO seed layer was prepared on the Al-coated substrate, and then ZnO NW were grown by aqueous chemical growth method. Finally, Au top electrode was used to conclude the Al/ZnO/Au NG structure. The Al and Au electrodes were used to establish the ohmic and Schottky contacts with ZnO NW, respectively.

Findings

Surface morphology of the fabricated device was done by using scanning electron microscopy, and electrical characterization of the sample was performed with digital oscilloscope, picoammeter and voltmeter. The energy harvesting experiment was performed to excite the presented device. The fabricated piezoelectric-sensitive device revealed the maximum open circuit voltage up to 5 V and maximum short circuit current up to 30 nA, with a maximum power of 150 nW. Consequently, it was also shown that the output of the fabricated device was increased by applying the stress. The presented work will help for the openings to capture the mechanical energy from the surroundings to power up the nano/micro-devices. This research work shows that NGs have the competency to build the self-powered nanosystems. It has potential applications in biosensing and personal electronics.

Originality/value

The fabrication of simple and cost-effective piezoelectric NG is done with a structure of Al/ZnO/Au without using hosting layer. The presented method elucidates an efficient and cost-effective approach to harvest the mechanical energy from the native environment.

Web URL: **http://www.emeraldinsight.com/doi/abs/10.1108/MI-11-2015-0092**

55. Khan, M. I., Imran, S., Saleem, M., & Rehman, S. U. (2018). Annealing effect on the structural, morphological and electrical properties of TiO2/ZnO bilayer thin films. *Results in Physics*, *8*, 249-252.

ABSTRACT:

The effect of annealing temperature on the structural, morphological and electrical properties of TiO_2/ZnO (TZ) thin films has been observed. Bilayer thin films of TiO_2/ZnO are deposited on FTO glass substrate by spray pyrolysis method. After deposition, these films are annealed at 573 K, 723 K and 873 K. XRD shows that $TiO_2$is present in anatase phase only and ZnO is present in hexagonal phase. No other phases of TiO_2 and ZnO are present. Also, there is no evidence of other compounds like Zn-Ti etc. It also shows that the average grain size of TiO_2/ZnO films is increased by increasing annealing temperature. AFM (Atomic force microscope) showed that the average roughness of TiO_2/ZnO films is decreased at temperature 573–723 K and then increased at 873 K. The calculated average sheet resistivity of thin films annealed at 573 K, 723 K and 873 K is 152.28×10^2, 75.29×10^2 and 63.34×10^2 ohm-m respectively. This decrease in sheet resistivity might be due to the increment of electron concentration with increasing thickness and the temperature of thin films.

Web URL: **https://www.sciencedirect.com/science/article/pii/S2211379717320077**

56. Rahman, S. S. U., Qureshi, M. T., Sultana, K., Rehman, W., Khan, M. Y., Asif, M. H., ... & Sultana, N. (2017). Single step growth of iron oxide nanoparticles and their use as glucose biosensor. *Results in physics*, *7*, 4451-4456.

ABSTRACT:

Iron-oxide nanoparticles are synthesized by the Green Chemistry method and using Gooseberry leaves extract as reducing agent. The characterization of the nanoparticles was carried by the common tools which include UV–Vis, SEM, EDX, XRD, FTIR and CV. UV–Vis confirms the formation of iron oxide nanoparticles. SEM verifies the spherical morphology of the nanoparticles. Elemental composition was determined by the EDX. XRD peaks details the spinal state crystal structure of the as-synthesized iron-oxide nanoparticles. CV results confirm the

electrochemical nature of the iron-oxide nanoparticles useful for biosensing. Finally Bioassay tests reveal that these nanoparticles can be potent candidate to be used as biosensors.

Web URL: https://www.sciencedirect.com/science/article/pii/S2211379717317497

57. Shah, H. U., Wang, F., Javed, M. S., Shaheen, N., Ye, Y., Wen, J., ... & He, K. (2017). Growth of hierarchical birnessite-type Cu0. 45Mn0. 55O2 nanosheets on flexible carbon textile for high-performance supercapacitors electrode. ***Journal of Alloys and Compounds*****,** ***725*****, 1223-1229.**

ABSTRACT:

The fabrication of high capacitance binder-free electrode materials with the advantages of having low costs and low toxicity has been attracting great attention for supercapacitors. In this study, we report the synthesis of hierarchical birnessite-type 3D $Cu_{0.45}Mn_{0.55}O_2$ (CMO) nanosheets (NS) directly grown on flexible carbon textile (CT) without any surfactant via a simple hydrothermal method. The CMO-NS supported on carbon textile were directly used as an integrated electrode for electrochemical measurments. The binder-free electrodes yielded high specific capacitance of 983 F g^{-1} in 1.0 M Na_2SO_4 aqueous electrolyte at a constant current density of 1.0 $mAcm^{-2}$. In addition, the CMO-NS electrode displayed outstanding cyclic stability by retaining 90% capacitance after 3000 cycles. Thus, the $Cu_{0.45}Mn_{0.55}O_2$ nanosheets combined with carbon textile form a promising electrode material for high-performance pseudocapacitors that have light weight and low cost.

Web URL: https://www.sciencedirect.com/science/article/pii/S0925838817316778

58. Not Found

ABSTRACT:

Web URL:

59. Lund, P. D., Zhu, B., Li, Y., Yun, S., Nasibulin, A. G., Raza, R., ... & Fan, L. (2017). Standardized Procedures Important for Improving Single-Component Ceramic Fuel Cell Technology. ***ACS Energy Letters*****,** ***2*****(12), 2752-2755.**

ABSTRACT:

The fuel cell is a promising clean energy technology for efficient conversion of fuel to power with no or low emissions.1 It utilizes electrochemical reactions and ion transport to generate electricity through redox-reactions (fuel oxidization, oxygen/air reduction). The main reaction product is water, sometimes also CO2 depending on the type of fuel used. Fuel cell applications range from small portable devices to medium-scale mobile and stationary uses.2

Web URL: **http://pubs.acs.org/doi/pdfplus/10.1021/acsenergylett.7b00997**

60. Mir, Z., Jamil, M., Rasheed, A., & Asif, M. (2017). Shear Alfvén Wave with Quantum Exchange-Correlation Effects in Plasmas. *Zeitschrift für Naturforschung A*, *72*(10), 891-898.

ABSTRACT:

The dust shear Alfvén wave is studied in three species dusty quantum plasmas. The quantum effects are incorporated through the Fermi degenerate pressure, tunneling potential, and in particular the exchange-correlation potential. The significance of exchange-correlation potential is pointed out by a graphical description of the dispersion relation, which shows that the exchange potential magnifies the phase speed. The low-frequency shear Alfvén wave is studied while considering many variables. The shear Alfvén wave gains higher phase speed at the range of small angles for the upper end of the wave vector spectrum. The increasing dust charge and the external magnetic field reflect the increasing tendency of phase speed. This study may explain many natural mechanisms associated with long wavelength radiations given in the summary.

Web URL: **https://www.degruyter.com/view/j/zna.2017.72.issue-10/zna-2017-0093/zna-2017-0093.xml**

61. Rasheed, A., Jamil, M., Jung, Y. D., Sahar, A., & Asif, M. (2017). The Exchange-Correlation Field Effect over the Magnetoacoustic-Gravitational Instability in Plasmas. *Zeitschrift für Naturforschung A*, *72*(10), 915-921.

ABSTRACT:

Jeans instability with magnetosonic perturbations is discussed in quantum dusty magnetoplasmas. The quantum and smaller thermal effects are associated only with electrons.

The quantum characteristics include exchange-correlation potential, recoil effect, and Fermi degenerate pressure. The multifluid model of plasmas is used for the analytical study of this problem. The significant contribution of electron exchange is noticed on the threshold value of wave vector and Jeans instability. The presence of electron exchange and correlation effects reduce the time to stabilise the phenomenon of self-gravitational collapse of massive species. The results of Jeans instability by magnetosonic perturbations at quantum scale help to disclose the details of the self-gravitating dusty magnetoplasma systems.

Web URL: **https://www.degruyter.com/view/j/zna.2017.72.issue-10/zna-2017-0164/zna-2017-0164.xml**

62. Jamil, A., Mustafa, F., Aslam, S., Arshad, U., & Ahmad, M. A. (2017). Structural and optical properties of thermally reduced graphene oxide for energy devices. *Chinese Physics B*, *26*(8), 086501.

ABSTRACT:

Natural intercalation of the graphite oxide, obtained as a product of Hummer's method, via ultra-sonication of water dispersed graphite oxide has been carried out to obtain graphene oxide (GO) and thermally reduced graphene oxide (RGO). Here we report the effect of metallic nitrate on the oxidation properties of graphite and then formation of metallic oxide (MO) composites with GO and RGO for the first time. We observed a change in the efficiency of the oxidation process as we replaced the conventionally used sodium nitrate with that of nickel nitrate Ni(NO $^{3)}_{2}$, cadmium nitrate Cd(NO $^{3)}_{2}$, and zinc nitrate Zn(NO $^{3)}_{2}$. The structural properties were investigated by x-ray diffraction and observed the successful formation of composite of *M*O–GO and *M*O–RGO ($M = \mathrm{Zn}$, Cd, Ni). We sought to study the effect on the oxidation process through optical characterization via UV-Vis spectroscopy and Fourier Transform Infrared (FTIR) spectroscopy. Moreover, Thermo Gravimetric Analysis (TGA) was carried out to confirm > 90% weight loss in each process thus proving the reliability of the oxidation cycles. We have found that the nature of the oxidation process of graphite powder and its optical and electrochemical characteristics can be tuned by replacing the sodium nitrate (NaNO $^{3)}$ by other metallic nitrates as Cd(NO $^{3)}_{2}$, Ni(NO $^{3)}_{2}$, and Zn(NO $^{3)}_{2}$. On the basis of

obtained results, the synthesized GO and RGO may be expected as a promising material in antibacterial activity and in electrodes fabrication for energy devices such as solar cell, fuel cell, and super capacitors.

Web URL: **http://cpb.iphy.ac.cn/article/2017/1899/cpb_26_8_086501.html**

63. Jamil, M., Rasheed, A., Hadi, F., Ali, G., & Ayub, M. (2017). Streaming Jeans-Alfvén Instability in Quantum Magnetoplasmas. *Zeitschrift für Naturforschung A*, *72*(11), 1003-1008.

ABSTRACT:

The physical mechanism of magnetosonic perturbations which modifies the Jeans instability in streaming quantum dusty magnetoplasmas is examined. These perturbations are low frequency and electromagnetic in nature that propagate with Alfvén speed. The fluid model consisting of momentum balance equations for quantum plasmas, Poisson's equation for gravitational potential, and Maxwell's equations for magnetosonic perturbations is used for the coupled solution. The numerical analysis of the dispersion relation elaborates the significant contribution of streaming speed of plasma species at equilibrium v_0, uniform external magnetic field B_0, electron number density at equilibrium n_{0e}, and variable dust mass m_d over the Jeans instability. This study helps to understand the possible mechanism responsible for the formation of astrophysical objects.

Web URL: **https://www.degruyter.com/view/j/zna.2017.72.issue-11/zna-2017-0244/zna-2017-0244.xml**

64. Javed, A., Rasheed, A., Jamil, M., Siddique, M., & Tsintsadze, N. L. (2017). Effect of magnetic quantization on ion acoustic waves ultra-relativistic dense plasma. *Physics of Plasmas*, *24*(11), 112301.

ABSTRACT:

In this paper, we have studied the influence of magnetic quantization of orbital motion of the electrons on the profile of linear and nonlinear ion-acoustic waves, which are propagating in the ultra-relativistic dense magneto quantum plasmas. We have employed both Thomas Fermi and Quantum Magneto Hydrodynamic models (along with the Poisson equation) of quantum

plasmas. To investigate the large amplitude nonlinear structure of the acoustic wave, Sagdeev-Pseudo-Potential approach has been adopted. The numerical analysis of the linear dispersion relation and the nonlinear acoustic waves has been presented by drawing their graphs that highlight the effects of plasma parameters on these waves in both the linear and the nonlinear regimes. It has been noticed that only supersonic ion acoustic solitary waves can be excited in the above mentioned quantum plasma even when the value of the critical Mach number is less than unity. Both width and depth of Sagdeev potential reduces on increasing the magnetic quantization parameter η. Whereas the amplitude of the ion acoustic soliton reduces on increasing η, its width appears to be directly proportional to η. The present work would be helpful to understand the excitation of nonlinear ion-acoustic waves in the dense astrophysical environments such as magnetars and in intense-laser plasma interactions.

Web URL: **http://aip.scitation.org/doi/full/10.1063/1.4996601**

65. Sumera, P., Rasheed, A., Jamil, M., Siddique, M., & Areeb, F. (2017). Landau quantization effects on hole-acoustic instability in semiconductor plasmas. *Physics of Plasmas*, *24*(12), 122107.

ABSTRACT:

The growth rate of the hole acoustic waves (HAWs) exciting in magnetized semiconductor quantum plasma pumped by the electron beam has been investigated. The instability of the waves contains quantum effects including the exchange and correlation potential, Bohm potential, Fermi-degenerate pressure, and the magnetic quantization of semiconductor plasma species. The effects of various plasma parameters, which include relative concentration of plasma particles, beam electron temperature, beam speed, plasma temperature (temperature of electrons/holes), and Landau electron orbital magnetic quantization parameter η, on the growth rate of HAWs, have been discussed. The numerical study of our model of acoustic waves has been applied, as an example, to the GaAs semiconductor exposed to electron beam in the magnetic field environment. An increment in either the concentration of the semiconductor electrons or the speed of beam electrons, in the presence of magnetic quantization of fermion orbital motion, enhances remarkably the growth rate of the HAWs. Although the growth rate of

the waves reduces with a rise in the thermal temperature of plasma species, at a particular temperature, we receive a higher instability due to the contribution of magnetic quantization of fermions to it.

Web URL: **http://aip.scitation.org/doi/full/10.1063/1.5002675**

66. Lee, M. J., Chung, K. S., Jamil, M., Rasheed, A., & Jung, Y. D. (2017). Janus modes of Hasegawa plasma waves in a streaming and tempestuous plasma pillar. *Physics of Plasmas*, *24*(12), 122111.

ABSTRACT:

Janus modes of the damping and growing of Hasegawa plasma waves are studied in a plasma pillar containing the dissipation and the beam energy deposition caused by tempestuous electrons and streaming ions. We find that the Janus modes split into the upper- and the lower-modes. For the upper-mode, the imaginary part of the wave frequency is negative for any parameters so that the corresponding Hasegawa space-charge plasma wave is always damped away. We found that the damping rate of the upper-mode decreases with a reduction of the pillar radius and a raising of the degree of the harmonic-roots. However, for the lower-mode, called lower-Janus mode, the wave can be either damped away or growing, depending on the wave number, streaming velocity, and geometric factor. The lower-Janus mode can be a pure growing wave with a reduction of the pillar radius. Interestingly, this growing mode turns to damping as the wave number decreases

Web URL: **https://www.youtube.com/watch?v=Co-_evFtlII**

67. Khan, A. A., Zeba, I., Jamil, M., & Asif, M. (2017). Oscillatory wake potential with exchange-correlation in plasmas. *Physics of Plasmas*, *24*(12), 123708.

ABSTRACT:

The oscillatory wake potential of a moving test charge is studied in quantum dusty plasmas. The plasma system consisting of electrons, ions and negatively charged dust species is embedded in an ambient magnetic field. The modified equation of dispersion is derived using a Quantum Hydrodynamic Model for magnetized plasmas. The quantum effects are inculcated through

Fermi degenerate pressure, the tunneling effect and exchange-correlation effects. The study of oscillatory wake is important to know the existence of silence zones in space and astrophysical objects as well as for crystal formation. The graphical description of the potential depicts the significance of the exchange and correlation effects arising through spin and other variables on the wake potential.

Web URL: **http://aip.scitation.org/doi/full/10.1063/1.4999462**

68. Ablikim, M., Achasov, M. N., Ahmed, S., Albrecht, M., Amoroso, A., An, F. F., ... & Ferroli, R. B. (2017). Study of J/ψ and ψ (3686) decays to π+ π− η′. *Physical Review D*, *96*(11), 112012.

ABSTRACT:

Using the data samples of 1.31 × 109 J=ψ events and 4.48 × 108 ψð3686Þ events collected with the BESIII detector, partial wave analyses on the decays J=ψ and ψð3686Þ → πþπ−η0 are performed with a relativistic covariant tensor amplitude approach. The dominant contribution is found to be J=ψ and ψð3686Þ decays to ρη0 . In the J=ψ decay, the branching fraction BðJ=ψ → ρη0 Þ is determined to be ð7.90 0.19ðstatÞ 0.49ðsysÞÞ × 10−5. Two solutions are found in the ψð3686Þ decay, and the corresponding branching fraction Bðψð3686Þ → ρη0 Þ is ð1.02 0.11ðstatÞ 0.24ðsysÞÞ × 10−5 for the case of destructive interference, and ð5.69 1.28ðstatÞ 2.36ðsysÞÞ × 10−6 for constructive interference. As a consequence, the ratios of branching fractions between ψð3686Þ and J=ψ decays to ρη0 are calculated to be ð12.9 1.4ðstatÞ 3.1ðsysÞÞ% and ð7.2 1.6ðstatÞ 3.0ðsysÞÞ%, respectively. We also determine the inclusive branching fractions of J=ψ and ψð3686Þ decays to πþπ−η0 to be ð1.36 0.02ðstatÞ 0.08ðsysÞÞ × 10−4 and ð1.51 0.14ðstatÞ 0.23ðsysÞÞ × 10−5, respectively.

Web URL: **https://journals.aps.org/prd/pdf/10.1103/PhysRevD.96.112012**

69. Ablikim, M., Achasov, M. N., Ahmed, S., Albrecht, M., Amoroso, A., An, F. F., ... & Ban, Y. (2017). Search for ψ (3686)→ γ η c (η (1405))→ γ π+ π− π 0. *Physical Review D*, *96*(11), 112008.

ABSTRACT:

Using a sample of 448.1 × 106 ψð3686Þ events collected with the BESIII detector, a search for the isospin violating decay ηc → πþπ−π0 via ψð3686Þ → γηc is presented. No signal is observed, and the upper limit on Bðψð3686Þ → γηcÞ × Bðηc → πþπ−π0Þ is determined to be 1.6 × 10−6 at the 90% confidence level. In addition, a search for ηð1405Þ → fðð980Þπ0 in ψð3686Þ radiative decays is performed. No signal is observed, and the branching fraction Bðψð3686Þ → γηð1405ÞÞ × Bðηð1405Þ → fðð980Þπ0Þ × Bðfðð980Þ → πþπ−Þ is calculated to be less than 5.0 × 10−7 at the 90% confidence level.

Web URL: **https://journals.aps.org/prd/pdf/10.1103/PhysRevD.96.112008**

70. Ablikim, M., Achasov, M. N., Ahmed, S., Albrecht, M., Amoroso, A., An, F. F., ... & Ferroli, R. B. (2017). Observation of χ c 2→ η′ η′ and χ c 0, 2→ η η′. ***Physical Review D*****,** ***96*****(11), 112006.**

ABSTRACT:

Using a sample of 448.1×106 ψ(3686) events collected with the BESIII detector in 2009 and 2012, we study the decays χc0,2→η′η′ and ηη′. The decays χc2→η′η′, χc0→ηη′ and χc2→ηη′ are observed for the first time with statistical significances of 9.6σ, 13.4σ and 7.5σ, respectively. The branching fractions are determined to be B(χc0→η′η′)=(2.19±0.03±0.14)×10−3, B(χc2→η′η′)=(4.76±0.56±0.38)×10−5, B(χc0→ηη′)=(8.92±0.84±0.65)×10−5 and B(χc2→ηη′)=(2.27±0.43±0.25)×10−5, where the first uncertainties are statistical and the second are systematic. The precision for the measurement of B(χc0→η′η′) is significantly improved compared to previous measurements. Based on the measured branching fractions, the role played by the doubly and singly Okubo-Zweig-Iizuka disconnected transition amplitudes for χc0,2 decays into pseudoscalar meson pairs can be clarified.

Web URL: http://link.aps.org/pdf/10.1103/PhysRevD.96.112006

71. Ablikim, M., Achasov, M. N., Ahmed, S., Ai, X. C., Albayrak, O., Albrecht, M., ... & Bai, J. Z. (2017). Observation of the helicity-selection-rule suppressed decay of the χ c 2 charmonium state. ***Physical Review D*****,** ***96*****(11), 111102.**

ABSTRACT:

The decays of χc2 → KþK−π0, KSKπ∓, and πþπ−π0 are studied with the ψð3686Þ data samples collected with the Beijing Spectrometer (BESIII). For the first time, the branching fractions of χc2 → KK¯ , χc2 → a 2 ð1320Þπ∓=a0 2ð1320Þπ0, and χc2 → ρð770Þπ∓ are measured. Here, KK¯ denotes both KK∓ and its isospin-conjugated process K0K¯ 0 þ c:c:, and K denotes the resonances Kð892Þ, K 2ð1430Þ, and K 3ð1780Þ. The observations indicate a strong violation of the helicity selection rule in χc2 decays into vector and pseudoscalar meson pairs. The measured branching fractions of χc2 → Kð892ÞK¯ are more than ten times larger than the upper limit of χc2 → ρð770Þπ∓, which is so far the first direct observation of a significant U-spin symmetry breaking effect in charmonium decays.

Web URL: https://journals.aps.org/prd/pdf/10.1103/PhysRevD.96.111102

72. Ablikim, M., Achasov, M. N., Ahmed, S., Albrecht, M., Amoroso, A., An, F. F., ... & Ban, Y. (2017). Search for the rare decays J/ψ→ D 0 e+ e−+ c. c. and ψ (3686)→ D 0 e+ e−+ c. c. *Physical Review D*, *96*(11), 111101.

ABSTRACT:

Using the data samples of ð1310.6 7.2Þ × 106 J=ψ events and ð448.1 2.9Þ × 106 ψð3686Þ events collected with the BESIII detector, we search for the rare decays J=ψ → D0eþe− þ c:c: and ψð3686Þ → D0eþe− þ c:c: No significant signals are observed and the corresponding upper limits on the branching fractions at the 90% confidence level are determined to be BðJ=ψ → D0eþe− þ c:c:Þ < 8.5 × 10−8 and Bðψð3686Þ → D0eþe− þ c:c:Þ < 1.4 × 10−7, respectively. Our limit on BðJ=ψ → D0eþe− þ c:c:Þ is more stringent by 2 orders of magnitude than the previous results, and Bðψð3686Þ → D0eþe− þ c:c:Þ is measured for the first time.

Web URL: https://journals.aps.org/prd/pdf/10.1103/PhysRevD.96.111101

73. Ablikim, M., Achasov, M. N., Ahmed, S., Albrecht, M., Alekseev, M., Amoroso, A., ... & Bakina, O. (2017). Branching fraction measurement of J/ψ→ K S K L and search for J/ψ→ K S K S. *Physical Review D*, *96*(11), 112001.

ABSTRACT:

Using a sample of 1.31 × 109 J=ψ events collected with the BESIII detector at the BEPCII collider, we study the decays of J=ψ → KSKL and KSKS. The branching fraction of J=ψ → KSKL is determined to be BðJ=ψ → KSKLÞ¼ð1.93 0.01ðstatÞ 0.05ðsystÞÞ × 10−4, which significantly improves on previous measurements. No clear signal is observed for the J=ψ → KSKS process, and the upper limit at the 95% confidence level for its branching fraction is determined to be BðJ=ψ → KSKSÞ < 1.4 × 10−8, which improves on the previous searches by 2 orders in magnitude and reaches the order of the Einstein-PodolskyRosen expectation.

Web URL: https://journals.aps.org/prd/pdf/10.1103/PhysRevD.96.112001

74. Ablikim, M., Achasov, M. N., Ahmed, S., Albrecht, M., Amoroso, A., An, F. F., ... & Ferroli, R. B. (2017). Improved measurements of two-photon widths of the χ c J states and helicity analysis for χ c 2→ γ γ. *Physical Review D*, *96*(9), 092007.

ABSTRACT:

Based on 448.1 × 106 ψð3686Þ events collected with the BESIII detector, the decays ψð3686Þ → γχcJ; χcJ → γγðJ ¼ 0; 1; 2Þ are studied. The decay branching fractions of χc0;2 → γγ are measured to be Bðχc0→γγÞ¼ð1.930.080.050.05Þ×10−4 andBðχc2→γγÞ¼ð3.100.090.070.11Þ×10−4, which correspond to two-photon decay widths of Γγγ ðχc0Þ ¼ 2.03 0.08 0.06 0.13 keV and Γγγ ðχc2Þ ¼ 0.60 0.02 0.01 0.04 keV with a ratio of R ¼ Γγγ ðχc2ÞÞ=Γγγ ðχc0Þ ¼ 0.295 0.014 0.007 0.027, where the uncertainties are statistical, systematic and associated with the uncertainties of Bðψð3686Þ → γχc0;2Þ and the total widths Γðχc0;2Þ, respectively. For the forbidden decay of χc1 → γγ, no signal is observed, and an upper limit on the two-photon width is obtained to be Γγγ ðχc1Þ < 5.3 eV at the 90% confidence level. The ratio of the two-photon widths between helicity-zero and helicity-two components in the decay χc2 → γγ is also measured to be f0=2 ¼ Γλ¼0 γγ ðχc2ÞÞ=Γλ¼2 γγ ðχc2Þ¼ð0.0 0.6 1.2Þ × 10−2, where the uncertainties are statistical and systematic, respectively.

Web URL: https://journals.aps.org/prd/pdf/10.1103/PhysRevD.96.092007

75. Ablikim, M., Achasov, M. N., Ahmed, S., Ai, X. C., Albayrak, O., Albrecht, M., ... & Bai, J. Z. (2017). Search for the rare decay D+→ D 0 e+ ν e. *Physical Review D*, *96*(9), 092002.

ABSTRACT:

Using a data set with an integrated luminosity of 2.93 fb−1 collected at ffiffi s p ¼ 3.773 GeV with the BESIII detector operating at the BEPCII storage rings, we search for the rare decay Dþ → D0eþve. No signal events are observed. We set the upper limit on the branching fraction for Dþ → D0eþve to be 1.0 × 10−4 at the 90% confidence level.

Web URL: https://journals.aps.org/prd/pdf/10.1103/PhysRevD.96.092002

76. Ablikim, M., Achasov, M. N., Ahmed, S., Albrecht, M., Alekseev, M., Amoroso, A., ... & Bakina, O. (2017). Measurement of branching fractions for ψ (3686)→ γ η′, γ η, and γ π 0. *Physical Review D*, *96*(5), 052003.

ABSTRACT:

Using a data sample of 448 × 106 ψð3686Þ events collected with the BESIII detector operating at the BEPCII storage ring, the decays ψð3686Þ → γη and ψð3686Þ → γπ0 are observed with a statistical significance of 7.3σ and 6.7σ, respectively. The branching fractions are measured to be Bðψð3686Þ → γηÞ ¼ ð0.85 0.18 0.05Þ × 10−6 and Bðψð3686Þ → γπ0Þ¼ð0.95 0.16 0.05Þ × 10−6. In addition, we measure the branching fraction of ψð3686Þ → γη0 to be Bðψð3686Þ→γη0 Þ¼ð125.12.26.2Þ×10−6, which represents an improvement of precision over previous results.

Web URL: https://journals.aps.org/prd/pdf/10.1103/PhysRevD.96.052003

77. Ablikim, M., Achasov, M. N., Ahmed, S., Ai, X. C., Albayrak, O., Albrecht, M., ... & Bai, J. Z. (2017). Observation of the doubly radiative decay η′→ γ γ π 0. *Physical Review D*, *96*(1), 012005.

ABSTRACT:

Based on a sample of 1.31 billion J=ψ events collected with the BESIII detector, we report the study of the doubly radiative decay η0 → γγπ0 for the first time, where the η0 meson is produced via the J=ψ → γη0 decay. The branching fraction of η0 → γγπ0 inclusive decay is measured to be Bðη0 → γγπ0ÞIncl ¼ ð3.20 0.07ðstatÞ 0.23ðsysÞÞ × 10−3, while the branching fractions of the dominant process η0 → γω and the nonresonant component are determined to

be Bðη0 → γωÞ × Bðω → γπ0Þ¼ð23.7 1.4ðstatÞ 1.8ðsysÞÞ × 10−4 and Bðη0 → γγπ0ÞNR ¼ ð6.16 0.64ðstatÞ 0.67ðsysÞÞ × 10−4, respectively. In addition, the M2 γγ -dependent partial widths of the inclusive decay are also presented.

Web URL: **https://journals.aps.org/prd/pdf/10.1103/PhysRevD.96.012005**

78. Ablikim, M., Achasov, M. N., Ahmed, S., Ai, X. C., Albayrak, O., Albrecht, M., ... & Bai, J. Z. (2017). Measurement of cross sections of the interactions e+ e−→ φφω and e+ e−→ φφφ at center-of-mass energies from 4.008 to 4.600 GeV. ***Physics Letters B*****, *774*, 78-86.**

ABSTRACT:

Using data samples collected with the BESIII detector at the BEPCII collider at six center-of-mass energies between 4.008 and 4.600 GeV, we observe the processes e+e−→φφω and e+e−→φφφ. The Born cross sections are measured and the ratio of the cross sections σ(e+e−→φφω)/σ(e+e−→φφφ) is estimated to be 1.75±0.22±0.19 averaged over six energy points, where the first uncertainty is statistical and the second is systematic. The results represent first measurements of these interactions.

Web URL: **https://www.sciencedirect.com/science/article/pii/S0370269317307190**

79. Ablikim, M., Achasov, M. N., Ai, X. C., Albayrak, O., Albrecht, M., Ambrose, D. J., ... & Ferroli, R. B. (2017). Dark photon search in the mass range between 1.5 and 3.4 GeV/c2. ***Physics Letters B*****, *774*, 252-257.**

ABSTRACT:

Using a data set of 2.93 fb^{-1} taken at a center-of-mass energy s=3.773 GeV with the BESIII detector at the BEPCII collider, we perform a search for an extra U(1) gauge boson, also denoted as a dark photon. We examine the initial state radiation reactions e+e−→e+e−γISR and e+e−→μ+μ−γISR for this search, where the dark photon would appear as an enhancement in the invariant mass distribution of the leptonic pairs. We observe no obvious enhancement in the mass range between 1.5 and 3.4 GeV/c^2 and set a 90% confidence level upper limit on the mixing strength of the dark photon and the Standard Model photon. We obtain a competitive limit in the tested mass range.

Web URL: **https://www.sciencedirect.com/science/article/pii/S0370269317307797**

80. Ablikim, M., Achasov, M. N., Ahmed, S., Albrecht, M., Amoroso, A., An, F. F., ... & Ferroli, R. B. (2017). Study of J/ψ and ψ (3686) decays to π+ π− η′. *Physical Review D*, *96*(11), 112012.

ABSTRACT:

Using the data samples of 1.31×109 J/ψ events and 4.48×108 ψ(3686) events collected with the BESIII detector, partial wave analyses on the decays J/ψ and ψ(3686)→π+π−η′ are performed with a relativistic covariant tensor amplitude approach. The dominant contribution is found to be J/ψ and ψ(3686) decays to ρη′. In the J/ψ decay, the branching fraction B(J/ψ→ρη′) is determined to be (7.90±0.19(stat)±0.49(sys))×10−5. Two solutions are found in the ψ(3686) decay, and the corresponding branching fraction B(ψ(3686)→ρη′) is (1.02±0.11(stat)±0.24(sys))×10−5 for the case of destructive interference, and (5.69±1.28(stat)±2.36(sys))×10−6 for constructive interference. As a consequence, the ratios of branching fractions between ψ(3686) and J/ψ decays to ρη′ are calculated to be (12.9±1.4(stat)±3.1(sys))% and (7.2±1.6(stat)±3.0(sys))%, respectively. We also determine the inclusive branching fractions of J/ψ and ψ(3686) decays to π+π−η′ to be (1.36±0.02(stat)±0.08(sys))×10−4 and (1.51±0.14(stat)±0.23(sys))×10−5, respectively.

Web URL: **https://journals.aps.org/prd/abstract/10.1103/PhysRevD.96.112012**

81. Zahid, M., Islam, M. U., Awan, M. S., Ashiq, M. N., Naseem, S., Ali, I., ... & Kamran, Z. (2017). Effect of dysprosium on structural and physical properties of Ba2NiCoFe12O22 Y-type hexaferrites. *Journal of the Australian Ceramic Society*, *53*(2), 875-882.

ABSTRACT:

A series of $Ba_2NiCoDy_xFe_{12-x}O_{22}$ (x = 0.00, 0.05, 0.01, 0.15, 0.20, 0.25) nano-structured Y-type hexaferrites were synthesized by the sol-gel auto-combustion technique. XRD analysis revealed Y-type hexagonal phase is formed. The increase in Dy content leads to the slight increase in the lattice parameter *c* indicating the distortion in the cell due to difference in atomic radii. SEM micrograph confirms the increase in grain size with the substitution of Dy. The irregular platelet-like particles were also observed in SEM profiles. Electrical permittivity

decreases with the increase of frequency due to interfacial polarization in accordance with Maxwell Wagner model. At high frequencies, grain boundaries were effective and at low frequencies, the permittivity decreases due to conducting grains. Magnetization and coercivity also decreases as the Dy doping increases. The decrease in magnetization may be attributed to segregation of Dy at grain boundaries. The decrease in coercivity is due to decrease in exchange coupling effect between neighboring domains.

Web URL: **https://link.springer.com/article/10.1007/s41779-017-0101-3**

82. Akhtar, M. N., Yousaf, M., Khan, S. N., Nazir, M. S., Ahmad, M., & Khan, M. A. (2017). Structural and electromagnetic evaluations of YIG rare earth doped (Gd, Pr, Ho, Yb) nanoferrites for high frequency applications. *Ceramics International*, *43*(18), 17032-17040.

ABSTRACT:

Multiple rare earth metal cations (Gd, Yb, Ho and Pr) were doped in yttrium iron garnet (YIG) nanocrystalline ferrites. Following five samples i.e. YIG ($Y_3Fe_5O_{12}$), Gd doped YIG ($Y_{2.8}Gd_{0.2}Fe_5O_{12}$), Pr doped YIG ($Y_{2.8}Pr_{0.2}Fe_5O_{12}$), Ho doped YIG ($Y_{2.8}Ho_{0.2}Fe_5O_{12}$) and Yb doped YIG ($Y_{2.8}Yb_{0.2}Fe_5O_{12}$) were prepared using sol-gel auto-combustion synthesis route. The samples were characterized via XRD, FTIR, SEM and VSM whereas VNA was also used to evaluate these samples for high frequency applications. XRD analysis confirms the peaks of garnet ferrites which show cubic phase structure for all YIG doped samples. The lattice constant in all the substituted garnet nanoferrites initially increased and then consequently decreased as the doping increased except for Pr-substituted YIG nanoferrites. This is due to the greater ionic radii of Pr as compared to other doped YIG nanoferrites. FTIR was used to find out the garnet phase in all the substituted YIG nanoferrites. The morphological features of the garnet nanoferrites were observed using the SEM images. High frequency measurements such as permittivity, permeability, dielectric losses, ac conductivity, electric modulus and Q factor of YIG and doped YIG nanoferrites were measured using VNA. Saturation magnetization, remanence, coercivity, squareness ratio, Bohr magneton and magneto crystalline anisotropy were measured from the magnetic hysteresis loops recorded by VSM. Pr-doped YIG show better dielectric and magnetic

properties with lower losses at higher frequency suggest the use of these garnet nanoferrites for microwave high frequency devices and applications.

Web URL: ***https://www.sciencedirect.com/science/article/pii/S0272884217320448***

83. Sohail, A., Arshad, S., & Ehsan, Z. (2017). Numerical analysis of plasma KdV equation: time-fractional approach. ***International Journal of Applied and Computational Mathematics*****, *3*(1), 1325-1336.**

ABSTRACT:

Numerical solution of the fractional order Modified Korteweg-de Vries equation governing the dynamics, is approximated using a novel space spectral time fractional finite difference tool. A spectral technique for space and a multi-step finite difference scheme for time are designed and implemented. The spatial spectral discretization error and the stability bounds are discussed. The nonlinear phenomena of plasma waves are well demonstrated with the aid of graphical analysis.

Web URL: **https://link.springer.com/article/10.1007/s40819-017-0420-7**

84. Aziz, M. H., Fatima, M., Atif,M., Noreen, Z., Ahmad, I., Shaheen, F., Ali, A., Ali, S. M., Ullah, H., Abbas, G. (2017). In Vitro Cytotoxicity of Magnetic Spinel Nanoferrites (CoMgFe2O4) against HepG2 Cells. Journal of Nanoelectronics and Optoelectronics 12:1–6

ABSTRACT:

Nanoscience and nanotechnology have fascinated new opportunities for the formation of advance materials for use in health as well as in medical applications. Due to unique chemical and physical properties, nanoparticles e.g., magnetic nanoferrites have been very useful and shown the potential application in nanomedicine. CoMgFe2O4 nanoparticles were synthesized by Sol–gel method. Morphological analysis of said nanoparticles (NPs) was confirmed by applying SEM and XRD. The exposure of spinel ferrites to Liver cancerous cells was examined by applying multidisciplinary techniques (MTT Assay and Inverted Microscopy). The exposure of CoMgFe2O4to liver carcinoma at 10–80 g/ml resulted in dose-dependent cellular viability loss and provoked cell death via apoptosis. In this study, experimental results have successfully demonstrated the translocation of magnetic ferrites nanoparticles in liver carcinoma (HepG2

cell model) and ensuring the significant toxicity. The study further proposed the forthcoming therapeutic use of these nanoferrites in the cancer study

Web URL:

https://www.researchgate.net/publication/322266087_In_Vitro_Cytotoxicity_of_Magnetic_Spinel_Nanoferrites_CoMgFe2O4_Against_HepG2_Cells

85. Aleem, A. R., Shahzadi, L., Alvi, F., Khan, A. F., Chaudhry, A. A., ur Rehman, I., & Yar, M. (2017). Thyroxin releasing chitosan/collagen based smart hydrogels to stimulate neovascularization. *Materials & Design*, *133*, 416-425.

ABSTRACT:

The development of new biomaterials with tailored properties is highly desired in tissue engineering field. The neovascularization is essential part of tissue regeneration which provides food and nutrients to cells. There is a real need for proangiogenic biomaterials to assist wound healing. The ideal dressing should be inexpensive and achieve rapid healing with minimal inconvenience to the patient. In this paper, new porous thyroxin containing pro-angiogenic hydrogels were generated via freeze gelation protocol. The chemical structural analysis of the synthesized hydrogels was investigated by Fourier Transform Infrared (FTIR) spectroscopy. The morphology and pore dimensions were studied by scanning electron microscopy (SEM). In swelling studies, 10 µg thyroxine loaded hydrogel (TLH-10) showed greater degree of swelling as compared to 1 µg loaded thyroxine material (TLH-1) and control. The degradation studies were tested in three different media, i.e. phosphate buffer saline (PBS), lysozyme and hydrogen peroxide and relatively higher degradation was seen in hydrogen peroxide. The synthesized materials were implanted on the chick chorioallantoic membrane to investigate their angiogenic potential. The TLH-1 hydrogel stimulated angiogenesis greater than the TLH-10; in this case blood vessels were attached and very much grown into the scaffold.

Web URL: https://www.sciencedirect.com/science/article/pii/S0264127517307219

86. Rafiq, M. Y., Iqbal, F., Aslam, F., Bilal, M., Munir, N., Sultana, I., ... & Razaq, A. (2017). Fabrication and characterization of ZnO/MnO2 and ZnO/TiO2 flexible nanocomposites for energy storage applications. *Journal of Alloys and Compounds*, *729*, 1072-1078.

ABSTRACT:

ZnO based nanostructure composites are attractive for high-tech applications of energy conversion and energy storage due to wide range in operating potential window. This study presents about fabrication of ZnO/MnO2 and ZnO/TiO2 composites via hydrothermal method in two consecutive steps. Furthermore lignocelluloses fiber directly collected form self-growing plant Monochoria Vagina, were incorporated in fabricated ZnO/MnO2 and ZnO/TiO2 composites for development of flexible and bulk paper composite electrode. The structural and morphological analysis were carried out using X-ray Diffraction (XRD), Scanning Electron Microscopy (SEM), respectively. XRD analysis confirm the crystalline structures for ZnO/MnO2 and ZnO/TiO2 samples with crystallite size ~62 nm and ~63 nm, respectively. SEM images shows the sheet-like and nanorods morphology for ZnO and MnO2 nanostructures, respectively. Fourier Transform Infrared (FTIR) Spectroscopy absorbance spectrum reveal the composite formation of ZnO/ MnO2/LC and ZnO/TiO2/LC as bulk paper electrodes whereas cyclic Voltammetry measurement showed the capacitive behavior of composite paper electrodes for the suitable applications in supercapacitors and batteries.

Web URL:

https://www.researchgate.net/profile/Faisal_Iqbal16/publication/320017841_Fabrication_and_characterization_of_ZnOMnO_2_and_ZnOTiO_2_flexible_nanocomposites_for_energy_storage_applications/links/59ef1611aca272c62d30064c/Fabrication-and-characterization-of-ZnO-MnO-2-and-ZnO-TiO-2-flexible-nanocomposites-for-energy-storage-applications.pdf

87. Javid, M. A., Mubeen, K., Md, M. W., Amin, N., & Mehmood, Z. (2017). Common clinical features of pediatric multiple sclerosis in Pakistan-A report of 15 cases. *JPMA. The Journal of the Pakistan Medical Association*, *67*(11), 1764-1766.

ABSTRACT:

The aim of this note is to assess the common clinical features of paediatric multiple sclerosis (PMS) in Pakistan. For this purpose, 150 MS patients with the age range of (1-72) years and mean age (34.2±11.09) years were studied during the period 2010 to 2015 from MRI centers of Pakistan. We found 15 paediatric MS cases which had clinical course relapsing-remitting MS

(11), secondary-progressive MS (3) and primary-progressive MS (1). Revised McDonald criteria 2010 of MRI was used to disseminate lesions in space and time. Sensory symptoms were found 27% in PMS patients and contributed brain area of corpus callosum, brain stem, periventricle, basal ganglia, white matter and cerebellum. Optic neuritis was the second clinical feature and its prevalence was reported 20% in paediatric patients. In conclusion, Paediatric multiple sclerosis is predicted 10 % with mean age 11.2 years in Pakistan. Sensory and optic neuritis are suggested the common clinical features of paediatric multiple sclerosis in Pakistan.

Web URL: **http://europepmc.org/abstract/med/29171579**

88. Not Found

ABSTRACT:

Web URL

89. Shaheen, F., Hammad Aziz, M., Fakhar-e-Alam, M., Atif, M., Fatima, M., Ahmad, R., ... & Ali, S. M. (2017). An In Vitro Study of the Photodynamic Effectiveness of GO-Ag Nanocomposites against Human Breast Cancer Cells. *Nanomaterials*, *7*(11), 401.

ABSTRACT:

Graphene-based materials have garnered significant attention because of their versatile bioapplications and extraordinary properties. Graphene oxide (GO) is an extremely oxidized form of graphene accompanied by the functional groups of oxygen on its surface. GO is an outstanding platform on which to pacify silver nanoparticles (Ag NPs), which gives rise to the graphene oxide-silver nanoparticle (GO-Ag) nanocomposite. In this experimental study, the toxicity of graphene oxide-silver (GO-Ag) nanocomposites was assessed in an in vitro human breast cancer model to optimize the parameters of photodynamic therapy. GO-Ag was prepared using the hydrothermal method, and characterization was done by X-ray diffraction, field-emission scanning electron microscope (FE-SEM), transmission Electron Microscopy (TEM), energy dispersive X-rays Analysis (EDAX), atomic force microscopy and ultraviolet-visible spectroscopy. The experiments were done both with laser exposure, as well as in darkness, to examine the phototoxicity and cytotoxicity of the nanocomposites.

The cytotoxicity of the GO-Ag was confirmed via a methyl-thiazole-tetrazolium (MTT) assay and intracellular reactive oxygen species production analysis. The phototoxic effect explored the dose-dependent decrease in the cell viability, as well as provoked cell death via apoptosis. An enormously significant escalation of $^1O_2$ in the samples when exposed to daylight was perceived. Statistical analysis was performed on the experimental results to confirm the worth and clarity of the results, with *p*-values < 0.05 selected as significant. These outcomes suggest that GO-Ag nanocomposites could serve as potential candidates for targeted breast cancer therapy.

Web URL: **http://www.mdpi.com/2079-4991/7/11/401/htm**

90. Ablikim, M., Achasov, M. N., Ai, X. C., Albayrak, O., Albrecht, M., Ambrose, D. J., ... & Ferroli, R. B. (2017). Improved measurements of branching fractions for η c→ φ φ and ω φ. *Physical Review D*, *95*(9), 092004.

ABSTRACT:

Using ð223.7 1.4Þ × 106 J=ψ events accumulated with the BESIII detector, we study ηc decays to φφ and ωφ final states. The branching fraction of ηc → φφ is measured to be Brðηc → φφÞ ¼ ð2.5 0.3þ0.3 −0.7 0.6Þ × 10−3, where the first uncertainty is statistical, the second is systematic, and the third is from the uncertainty of BrðJ=ψ → γηcÞ. No significant signal for the double Okubo-Zweig-Iizuka suppressed decay of ηc → ωφ is observed, and the upper limit on the branching fraction is determined to be Brðηc → ωφÞ < 2.5 × 10−4 at the 90% confidence level.

Web URL: ***https://journals.aps.org/prd/pdf/10.1103/PhysRevD.95.092004***

DEPARTMENT OF HUMANITIES

Journal Papers

1. Baig, M. M. Z. (2017). Sisterhood in Question: Rewriting a Life of Binaries in Margaret Atwood's The Penelopiad. *Journal of Research (Humanities).* LIII. 101-123

ABSTRACT:

In Atwood's The Penelopiad (2005), a feminist rewrite of Penelope's character from Homer's Odyssey, we find that a relationship among women as shown in the novella is dysfunctional and fractured. The subject position of a woman in the narrative has not been of great help to objectified women to the disadvantage of women and their rights. The narrative voice of a woman has not addressed the patriarchal and ideological world constructed on the binaries among women. The women, even in Atwood's writing, have been portrayed in the stereotypical fashion which disrupts sisterhood among female characters and exhibits differential power relations among them. Instead of writing back to the patriarchal canon, we read in the text about the Penelope-Helen rivalry, Penelope-Actoris mistress-slave relationship, EurycleiaAnticleia tug of war and their displacing Penelope as Odysseus's deputy in the house in his absence, and Penelope's narrative and maids' counter-narrative reflecting on how their uneven relationship capitalized on maids' horrendous slavish sufferings.

Web URL:

https://www.researchgate.net/profile/Mirza_Zubair_Baig/publication/315753465_Sisterhood_in_Question_Rewriting_a_Life_of_Binaries_in_Margaret_Atwood's_The_Penelopiad/links/58e22fb7aca272059ab2246f/Sisterhood-in-Question-Rewriting-a-Life-of-Binaries-in-Margaret-Atwoods-The-Penelopiad.pdf

2. Shah, Z. A., Ahmed, A. & Anjum, A.I. (2017). *ELF Annual Research Journal.* 18, 123-136.

ABSTRACT:

Exponential growth can be seen in language learning with the invention of smart phones. Portable, innovative and readily available technological devices such as smart-phones open a new horizon of opportunities for language learners to have their own computer tools in their

pockets anytime and anywhere. The present study investigates the effectiveness of smart phones for enhancing the listening skills of IELTS students. Twenty IELTS students were chosen from The Future Makers College, District Gujranwala. They were given a consent form to read and sign. After taking pre-test, they were taught for three weeks through smart phones. Data was statistically analyzed through SPSS version 18.Results proved that the students improved a lot in post-test. Paired samples T test was used to find out statistically significant difference in the performance of the students. Structured questionnaire was also administered to know their attitude and experience of using smart phones for enhancing listening skills. Significant increase in motivation of IELTS students was also found

Web URL: ***http://elf.salu.edu.pk/sites/default/files/journals/ELF-Vol-18-2016/07Paper.pdf***

3. Ashraf, R. (2017). Psychodynamics of Mother Daughter Relationship: Degrees of Deprivation, Oppression and Dispossession in Doris Lessing's Fiction. ***Khazar Journal of Humanities & Social Sciences*****,** ***20*****(1).**

ABSTRACT:

The aim of this study is to explore how Doris Lessing‟s works discloseín prominence the power dynamics of the conflicted and struggling relationship of mother and daughter, the paradigm of mother daughter relationship and its psychodynamics including explanations about the developmental stages of the relationship between the mother and the daughter, human behavior of the two in the context of relationship formation and maintenance, psychopathology where the daughter feels isolated and the psychoanalytic dimensions of treatment of this particular relationship, primarily in the world of psychoanalytic and feminist literary history. Resultantly, it has been unfolded that the phenomenon of mother daughter relation holds immense complexity and layers of intricacies in the feminist discourses where the presence of a mother figure has been deconstructed both thematically and stylistically as evident in Greek plays. Mother daughter relation has always enjoyed being of significance, at times appearing titled as „Electra Complex‟ after Sophocles‟ Electra while at others emerging out as the phenomenon of „Matrophobia‟ as titled by Sukenick and carried on further by second wave of feminists (Hallstein 8).

Web URL: ***http://jhss-khazar.org/wp-content/uploads/2016/11/2017..1.5._Rabia_Ashraf..pdf***

4. Musferah, M., (2017). Al-Sukākī's Classification of Metaphor and Qur'ānic Discourse, *Al-Idah* 34 (June). 108-122

ABSTRACT:

The present study is divided into two main sections; the first section will give a general overview about the figurative language and more focus on metaphor (istiᶜārah in Arabic) because the metaphor is considered as one of the most literary devices and the main category of the figurative language. So in this study has given various definitions of figurative language and metaphor according to Muslims and Non-Muslims linguists and along with this explained Al-sukākī's classification of metaphor which is little close to Al-Jurjānī's classification of metaphor and view respectably among Muslims and NonMuslims linguists. The second section of this study deals with metaphors given in Holy Qur'ān, which are denoted according to Al-sukākī's classification in this respect. In this reference the verses are presented with detailed tafsīrī literature so the reader could well comprehend the purposes and the classical aspect of metaphors in text and also could evaluate linguistic architecture of Holy Qur'ān.

Web URL: ***https://www.szic.pk/journal/jun2017/7.pdf***

5. Musferah, M., Ashraf, R., (2017). Lībās (Garment) Metaphor in Holy Qur'ān: A Conceptual Metaphorical Analysis. *Pakistan Journal of Islamic Research*. 18(1). 15-30

ABSTRACT:

The focus of this paper is the conceptual analysis of metaphors of Lībās extracted from Holy Qur'ān, keeping under consideration the cognitive and linguistic viewpoints of the study of metaphor. A semasiological approach and insight is applied to the data from the Qur'ānic corpus where the symbolic significance of lībās (garment) metaphor is singled out linking it with the very concept and semantic undertones of the lexeme. Using Cognitive Theory of Metaphor (CMT) as the theoretical framework (Lakoff & Johnson), the translations from selected verses of Qur'ān are examined analytically and contrasted with consideration of the historical, social and religious aspects. The tenets of this theory have been utilized for the study of Conceptual

Metaphorical Analysis (CMA) revealing how lībās (garment) metaphor has been used creatively and how it widely develops the understanding of the broader aspects of life. For this purpose, verses containing the Lībās metaphor are selected from Sūrah An-Nahl, Al- Arāf, Al- Hajj and Al Baqarah. The tenor and vehicle representation is taken after the concept of tenor, vehicle and ground of I.A Richards. The domain (source/ target) are also discussed to bring up a holistically semasiological view after the cognitive linguistic analysis of the metaphors.

Web URL: ***http://www.bzu.edu.pk/pjir.php***

6. Musferah, M., Ijaz, H. (2017). ELOQUENT HADITH – A CONCEPTUAL METAPHORICAL ANALYSIS. ***Al-Qalam. 22-38***

ABSTRACT:

Hadith (speech or saying of Holy Prophet صلى الله عليه وسلم (holds a great place and value as it is considered to be the first stepand foremost interpretation of the Holy Qur'ān. It presents a total picture of Islamic culture and values and is therefore, full of knowledge and philosophy. Many creative writings are being flourished by Islamic literary philosophers with the extractions of the Prophetic Traditions. This paper aims to highlight the eloquence and particularly function of metaphor in Hadiths in the theoretical framework put forward by Lakoff& Turner (1989) and developed later by Lakoff and Turner (1989), and others, e.g. Wreth (1994, 1999), which is known as the Cognitive Theory of Metaphor. It shows how the Hadith is structured around the idea of the variety of meaning of lexical items, and how every correspondence between the two domains of "literal" and "non-literal" can fit into it. This theory is very well known in the recent times. The structure of this paper is presented as follows. At first, introduction of the theoretical background and arguments of the study is discussed. Afterwards, underlining the significance of this study and its contribution to the field is mentioned. Further, the linguistic analysis of metaphor in the Hadith is discussed. Finally the article illustrates the rhetorical aspect of Hadiths.

Web URL: ***http://www.alqalamjournalpu.com/images/alqalam/june2017a1/2.Dr.-Musferah-MehfoozHuma-Ijaz.pdf***

7. Jibeen, T. (2017). Unconditional Self Acceptance and Self Esteem in Relation to Frustration Intolerance Beliefs and Psychological Distress. ***Journal of Rational-Emotive & Cognitive-Behavior Therapy*****,** ***35*****(2), 207-221.**

ABSTRACT:

The present study examines the moderating role of unconditional self acceptance and self esteem in relation to frustration intolerance beliefs and psychological distress. Participants were one hundred and fifty student (aged 18–25) studying at three universities (COMSATS Institute of Information Technology, University of Management Sciences, and University of Central Punjab) of Lahore, Pakistan. They completed a demographic information sheet, the Frustration Discomfort Scale (Harrington in Clin Psychol Psychother 12:374–387, 2005a), the Rosenberg Self-Esteem Scale (Rosenberg in Society and the adolescent self image. Princeton University Press, Princeton, 1965), the Unconditional Self Acceptance Questionnaire (Chamberlain and Haaga in J Ration Emotive Cogn Behav Ther 19:163–176, 2001a), and the General Health Questionnaire (Goldberg in Manual of the General Health Questionnaire. NFERNelson, Great Britain, 1972). The results demonstrated the moderating effects of unconditional self acceptance and self esteem in the relationship between frustration intolerance beliefs (entitlement, achievement, emotional intolerance, and discomfort intolerance) and psychological distress . The present findings highlight the importance unconditional self acceptance that reduces the emotional problems of students hindering their educational and personal growth.

Web URL: https://link.springer.com/article/10.1007/s10942-016-0251-1

8. Ashraf, F., & Najam, N. (2017). CO-MORBIDITY OF SPECIFIC LEARNING DISABILITIES AND DEPRESSIVE SYMPTOMS IN NON-CLINICAL SAMPLE OF ADOLESCENTS. ***Journal of Postgraduate Medical Institute (Peshawar-Pakistan)*****,** ***31*****(2).**

ABSTRACT:

Objective: To determine the comorbidity and relationship between specific learning disabilities and depressive symptoms in non-clinical sample of adolescents.

Methodology: A cross-sectional study was conducted at four government schools of Lahore from March to December 2014. The study comprised of 287 students selected through systematic random sampling technique, age ranges between 11 to 16 years. Demographic information questionnaire, learning disabilities checklist and children depression inventory were administered to obtain data. Descriptive Statistics, crosstab analysis and Pearson relationship were applied.

Results: The mean age of 287 participants was 12.98 ±1.22 years. Overall, 56 (19.51%) of adolescents were identified with mild, 83 (28.94%) with moderate and 40 (13.94%) with severe levels of comorbidity of depressive symptoms and specific learning disabilities. Significant relationships between depressive symptoms and specific learning disabilities were demonstrated (p value=.0001). These relationships were also found significant for sample of boys whereas for girls, only significant relationship was observed on subscale of ineffectiveness (p value=.036)

Conclusion: Significant comorbidity of depressive symptoms and specific learning disabilities was found. Comorbidity of severe level of depressive symptoms and specific learning disabilities was more prevalent for sample of boys.

Web URL: ***http://www.jpmi.org.pk/index.php/jpmi/article/download/2018/1849***

9. Chaudhry, K. A., Fida, W., Amjad, M, Anjum, N. & Imtiaz, S. (2017). Friendship Concepts among Female Medical Students: A Qualitative *Approach. Pakistan Journal of Madical & Health Sciences.* 11(1). 136-139

ABSTRACT:

This is a qualitative study which explained the concepts about reasoning of friendship among girls which they used to prefer while making somebody their companion. Aimed at this purpose, 8 medical students were conveniently sampled from a private medical college for a focus group discussion. Initially, a semi-structured questionnaire consisting of fifteen open-ended questions was designed. During a two-hour discussion, similarities and differences in opinion were noted down for further content analysis in order to generate themes and subthemes out of them. 5 main themes elicited were, definition of friendship; qualities to be

considered for making a friend; importance of a good friend in life; more loyal friend, a girl/boy; and ingredients of a genuine friendship. It was concluded that a genuine friendship depends on several psychological, social and emotional aspects of human behavior and gets strengthened by mutual understanding, support, and cooperation. This bonding as a friend plays the role of a therapist by sharing and managing stress as well as a motivator by boosting up their morale to achieve the set goals in life and as an entertainer by making they feel happy and satisfied.

Web URL: **http://www.pjmhsonline.com/2017/jan_march/pdf/136.pdf**

10. Fatima, S., Mehfooz, M., & Sharif, S. (2017). Role of Islamic religiosity in predicting academic motivation of university students. *Psychology of Religion and Spirituality*, *9*(4), 377.

ABSTRACT:

Previous research in the last 2 decades describes the connection between religiosity and academic outcomes, particularly in Christian samples. The present study was designed to find out the role of Islamic religious beliefs, practices, and positive religious coping in predicting academic motivation above and beyond the effects of demographic and academic-related factors among Muslim university students. Participants were 299 university students (mean age 19.35 years, SD 3.21, 68% males) registered under different undergraduate programs. They were assessed on the Islamic Beliefs, Islamic Religious Duty and Obligation, and Islamic Positive Religious Coping and Identification subscales as well as the Global Religiousness scale from the Psychological Measure of Islamic Religiosity. In addition, the Academic Motivation Scale was also administered to assess 3 intrinsic motivation outcomes, 3 extrinsic motivation outcomes, and amotivation. The results showed a significant incremental variance due to a differential contribution of religiosity factors over the demographic and academic factors in predicting type of academic motivation. Nevertheless, the number of siblings and current semester remained significant predictors of academic motivation even in the presence of other stronger predictors. However, moderation analysis showed an interaction effect of semester only in predicting intrinsic motivation to know and to accomplish things and extrinsic motivation of external regulation. It was worth noting that the religiosity level of students was more weakly correlated

with extrinsic motivation of external regulation than it was with other motivation constructs of intrinsic and extrinsic motivation.

Web URL: **http://www.ciitlahore.edu.pk/Papers/Abstracts/741-8586951164272442766.pdf**

11. Fatima, S., & Sharif, I. (2017). Executive functions, parental punishment, and aggression: Direct and moderated relations. *Social neuroscience*, *12*(6), 717-729.

ABSTRACT:

The main focus of the current study was to assess whether executive functions (EFs) moderate the effect of parental punishment on adolescent aggression. The sample were 370 participants (53% girls, 47% boys) enrolled at secondary and higher secondary levels and ranged in age between 13–19 years (M = 15.5, SD = 1.3). Participants were assessed on a self-report measure of aggression and two punishment measures, in addition to a demographic sheet. Then, they were individually assessed on four tests taken from the Delis–Kaplan Executive Functions System (D-KEFS) namely Trial Making Test (TMT), Design Fluency Test (DFT), Color Word Interference Test (CWIT), and Card Sorting Test (CST) to assess cognitive flexibility, nonverbal fluency, inhibition, and problem-solving ability, respectively. Correlation coefficients indicated that all four executive functioning measures and the two punishment measures were significantly correlated with aggression. Moderation analysis indicated that all EFs moderated the relationship between physical punishment and aggression, and only inhibition and problem-solving ability, but not cognitive flexibility and nonverbal fluency, moderated the relations between symbolic punishment and aggression. The findings support the hypothesis that EFs are protective personal factors that promote healthy adolescent adjustment in the presence of challenging environmental factors.

Web URL: **http://www.tandfonline.com/doi/full/10.1080/17470919.2016.1240710**

DEPARTMENT OF CHEMISTRY

1. Babar, A., Yar, M., Tarazi, H., Duarte, V., Alshammari, M. B., Gilani, M. A., ... & Khan, A. F. (2017). Molecular docking and glucosidase inhibition studies of novel N-arylthiazole-2-amines and Ethyl 2-[aryl (thiazol-2-yl) amino] acetates. *Medicinal Chemistry Research*, *26*(12), 3247-3261.

ABSTRACT:

This study describes an efficient synthesis of a series of novel ethyl 2-[aryl(thiazol-2-yl)amino]acetates (**4a–l**) from *N*-arylthiazole-2-amines (**3a–l**). The reaction conditions were optimized and the best results were obtained when ethyl chloroacetate was used as alkylating agent and NaH as base in THF. *α*-glucosidase and *β*-glucosidase inhibition activities of *N*-arylthiazole-2-amines (**3a–l**) and ethyl 2-[aryl(thiazol-2-yl)amino]acetates (**4a–l**) were determined, which revealed that most of the compounds showed high percentage inhibition towards the enzymes. Among the synthesized compounds, **4e** appeared to have the highest inhibition towards α-glucosidase having IC_{50} value of 150.4 ± 1.9 µM which was almost two folds as compared to acarbose (336.9 ± 9.0 µM) taken as standard. Molecular docking of the compounds **3g**, **3f**, **4a**, and **4e** was also performed which showed their bonding modes to the enzyme's active sites via amino and acetate groups, respectively.

Web URL: **https://link.springer.com/article/10.1007/s00044-017-2018-3**

2. Ilyas, A., Muhammad, N., Gilani, M. A., Ayub, K., Vankelecom, I. F., & Khan, A. L. (2017). Supported protic ionic liquid membrane based on 3-(trimethoxysilyl) propan-1-aminium acetate for the highly selective separation of CO2. *Journal of Membrane Science*, *543*, 301-309.

ABSTRACT:

The ability to tailor ionic liquids can result in very high separation efficiency for CO_2/CH_4 and CO_2/N_2. In this study, a new protic ionic liquid was synthesized with high CO_2 absorption capacity employing (3-aminopropyl) trimethoxysilane and acetic acid, both of these have been reported to exhibit high affinity for CO_2. The synthesized ionic liquid was characterized by FTIR and the supported ionic liquid membrane was tested to determine the separation of CO_2 from CH_4. Experiments were conducted at different temperatures and feed conditions, and pure and

mixed gas permeability/selectivity data were reported. This combination of silyl ether functionalized cation and acetate ion dramatically improved the membrane separation performance as the SILM displayed CO_2 permeance of 23 GPU combined with CO_2/CH_4 selectivity of 41. The synthesized SILM was stable upto 10 bar as no leaching of ionic liquid was observed and the permeance increased from 23 to 31 GPU as the temperature was raised from 25 °C to 65 °C, while the selectivity slightly decreased from 41 to 35 over the same temperature range. The exceptionally high selectivity of CO_2/CH_4 makes [APTMS][Ac] a promising room temperature ionic liquid for CO_2 separation without facilitated transport. A synergistic effect of methoxy groups from [APTMS] part of the ionic liquid caused the enhanced permeability of CO_2 as supported by theoretical calculations.

Web URL: **https://www.sciencedirect.com/science/article/pii/S0376738817314023**

3. Abid, S. M. A., Younus, H. A., Al-Rashida, M., Arshad, Z., Maryum, T., Gilani, M. A., ... & Iqbal, J. (2017). Sulfonyl hydrazones derived from 3-formylchromone as non-selective inhibitors of MAO-A and MAO-B: Synthesis, molecular modelling and in-silico ADME evaluation. *Bioorganic chemistry*, *75*, 291-302.

ABSTRACT:

A series of sulfonyl hydrazones derived from 3-formylchromone was synthesized and discovered to be effective, non-selective inhibitors of monoamine oxidases (MAO-A and MAO-B). The compounds are easily (synthetically) accessible in high yields, by simple condensation of 4-methylbenzenesulfonohydrazide with different (un)substituted 3-formylchromones. All compounds had IC_{50} values in lower micro-molar range (IC_{50} = 0.33–7.14 μM for MAO-A, and 1.12–3.56 μM for MAO-B). The most active MAO-B inhibitor was N′-[(E)-(6-fluoro-4-oxo-4H-chromen-3-yl)methylidene]-4-methylbenzenesulfonohydrazide (**3e**) with IC_{50} value of 1.12 ± 0.02 μM, and N′-[(E)-(6-chloro-4-oxo-4H-chromen-3-yl)methylidene]-4-methylbenzenesulfonohydrazide (**3f**) was the most active MAO-A inhibitor with IC_{50}value of 0.33 ± 0.01 μM. From enzyme kinetic studies, the mode of inhibition against MAO-B was found to be competitive, whereas against MAO-A, it was found to be non-competitive. Molecular docking studies indicated a new binding pocket for non-competitive MAO-A inhibitors. The

activity of these compounds is optimally combined with highly favorable ADME profile with predicted good oral bioavailability.

Web URL: **https://www.sciencedirect.com/science/article/pii/S004520681730617X**

4. Mustafa, G., Iqbal, M. J., Hassan, M., & Jamil, A. (2017). Bioinformatics Characterization of Growth Differentiation Factor 11 of Oryctolagus cuniculus. ***Journal of the Chemical Society of Pakistan*****,** ***39*****(6).**

ABSTRACT:

Growth differentiation factor 11 (GDF11) is a member of the transforming growth factor-β (TGF-β) superfamily and acts as a regulator for the aging of multiple tissues. The mature forms of human GDF11 and GDF8 show more than 90% sequence identity but the role of GDF11 is not well understood. For detail annotation of GDF11 from Oryctolagus cuniculus, the mature segment of GDF11 was analyzed using different bioinformatics online tools for its physicochemical properties and secondary structure predictions. Multiple tools for secondary structure prediction were used and the information about rabbit GDF11 given by these tools was compared. It was observed that all tools gave different information regarding properties of GDF11 secondary structure and concluded that no tool is perfect for prediction and multiple tools should be tried for protein secondary structure prediction. The final prediction should be manually selected which could be supported by tertiary structure prediction of protein. For phylogeny four closest homologous proteins of TGF-β superfamily were selected i.e. GDF11, GDF8, inhibin and Bone Morphogenetic Protein 7 (BMP7). Ten sequences of each protein from same mammals were retrieved from GenPept database and included in the phylogenetic analysis to show evolutionary relatedness among these proteins. All selected proteins were resolved in the tree and appeared in their respective clusters. It was confirmed from the phylogenetic tree that GDF11 and GDF8 are paralogs of each other as both proteins are appeared to be derived from a common ancestor in the tree. Findings of this study will help to understand the interactions of rabbit GDF11 with different ligands and molecular details of how these interactions could be reached.

Web URL:

https://www.researchgate.net/profile/Ghulam_Mustafa22/publication/321964392_Bioinformatics_Characterization_of_Growth_Differentiation_Factor_11_of_Oryctolagus_cuniculus/links/5a3b344da6fdcc7ffe641113/Bioinformatics-Characterization-of-Growth-Differentiation-Factor-11-of-Oryctolagus-cuniculus.pdf

5. Sohail, A., Ahmad, Z., Bég, O. A., Arshad, S., & Sherin, L. (2017). A review on hyperthermia via nanoparticle-mediated therapy. *Bulletin du Cancer*.

ABSTRACT:

Hyperthermia treatment, generated by magnetic nanoparticles (MNPs) is promising since it is tumour-focused, minimally invasive and uniform. The most unique feature of magnetic nanoparticles is their reaction to and manipulation by a magnetic force which is responsible for enabling their potential as heating mediators for cancer therapy. With magnetic nanoparticle hyperthermia, a tumour is preferentially loaded with systemically administered nanoparticles with high-absorption cross section for transduction of an extrinsic energy source to heat. To maximize the energy deposited in the tumour while limiting the exposure in healthy tissues, the heating is achieved by exposing the region of tissue containing magnetic nanoparticles to an alternating magnetic field. The magnetic nanoparticles dissipate heat from relaxation losses thereby heating localized tissue above normal physiological ranges. Besides thermal efficiency, the biocompatibility of magnetite nanoparticles assists in their deployment as efficient drug carriers for targeted therapeutic regimes. In the present article we provide a state-of-the-art review focused on progress in nanoparticle induced hyperthermia treatments which have several potential advantages over both global and local hyperthermia treatments achieved without nanoparticles. Green bio-nanotechnology has attracted substantial attention and has demonstrable abilities to improve cancer therapy. Furthermore we have listed the challenges associated with this treatment along with future opportunities in this field which it is envisaged will be of interest to biomedical engineers, bio-materials scientists, medical researchers and pharmacological research groups.

Web URL:

http://usir.salford.ac.uk/41346/1/E__USIR%20repository_2017_BULLETIN%20DU%20CANCER%20Hyper-thermia%20magnetic%20nanosystems%20ACCEPTED%20Feb%206th%202017.pdf

6. Fatima, M., Farooq, R., Lindström, R. W., & Saeed, M. (2017). A review on biocatalytic decomposition of azo dyes and electrons recovery. *Journal of Molecular Liquids*.

ABSTRACT:

Discharge of waste water from textile industry during coloring processes contains high concentrations of biologically difficult-to-degrade dye chemicals along with antifouling agents. Azo dyes considered to be the largest class of synthetic dyes used in the textile industries and are present in significant amounts in its effluents. These are highly stable because of its complex aromatic structure and covalent azo bonds. Traditional physico-chemical methods are not considered sufficient because of their high cost, partial degradation and more sludge production. The use of biocatalysts for decolorization is a gaining momentum due to having redox-active molecules. Current review explored techniques for the decomposition of textile dyes, their merits, limitations and recommended the emerging microbial fuel cell technology followed by aerobic treatment for complete degradation of dye intermediate metabolites.

Web URL: **https://www.sciencedirect.com/science/article/pii/S0167732217332245**

1. Ahmad, R., Islam, T., & Saleem, S. S. (2017). EMPLOYEE ENGAGEMENT, ORGANIZATIONAL COMMITMENT AND JOB SATISFACTION AS CONSEQUENT OF PERCEIVED CSR: A MEDIATION MODEL. *Journal of the Research Society of Pakistan*, *54*(1).

ABSTRACT:

Corporate Social Responsibility (CSR) has become as an important topic of research as it has ramifications for practitioners. Therefore, this study aims at examining organizational commitment and employee engagement as consequent of perceived CSR with the mediating role of job satisfaction. A questionnaire based survey was used to collect data from 736 faculty members of higher education institutions. Hypotheses were tested using structural equation modeling. Results reveal that, perceived CSR positively influence employees level of engagement and commitment towards their organization, whereas, this mechanism is partially supported considering job satisfaction as a mediating variable. This study is novel and has implications for the higher education institutions.

Web URL: **http://pu.edu.pk/images/journal/history/PDF-FILES/12a_54_1_17.pdf**

2. Saleem, S., Moosa, K., Imam, A., & Ahmed Khan, R. (2017). Service Quality and Student Satisfaction: The Moderating Role of University Culture, Reputation and Price in Education Sector of Pakistan. *Iranian Journal of Management Studies*, *10*(1), 237-258.

ABSTRACT:

Service quality is imperative for higher education institutes in order to remain competitive and growing. There is a need to ensure students' satisfaction with university. This study will help improve service quality of the institutes. Information and data are collected using a survey questionnaire from the higher education institutes of Pakistan using convenience sampling technique. Findings revealed that with the moderating effect of university culture, university reputation and price, higher education institutes can more significantly achieve the student satisfaction. University culture positively strengthens service quality to achieve and sustain student satisfaction, while price and university reputation strengthen the relationship in a negative direction. These moderators are the significant contributing factors.

Web URL: **https://ijms.ut.ac.ir/article_60913_07d3885063b9230934b3dd344f45553a.pdf**

3. Sulehri, I. G., Najmi, M. T., & Chaudhry, M. S. (2017). Research Productivity of LIS Professionals in Punjab, Pakistan. *Chinese Librarianship*, (44).

ABSTRACT:

The main objective of this study is to assess the research productivity of LIS professionals in Punjab, Pakistan. A quantitative research method, followed by a survey research design, was opted to complete the study. LIS professionals with an MPhil or PhD degree in library and information science from any HEC (Higher Education Commission, Pakistan) recognized universities from Punjab constituted the population of this study. The findings of the study show that research productivity of LIS professionals is increasing consistently.

Web URL: **http://www.iclc.us/cliej/cl44SNC.pdf**

4. Butt, G. S., Tariq, M., Shakil, M., & Ayub, M. (2017). IMPACT OF INTRODUCTION TO RESEARCH ON MEDICAL STUDENTS'LEARNING ABILITY. *Pak J Physiol*, *13*(2), 56-8.

ABSTRACT:

The significance of research cannot be neglected in medical science; it is very essential part of current medical education system especially in modular or Problem-Based Learning (PBL) when junk of information is available on internet. The purpose of this study was to analyze the impact of short session of introducing the research module among medical students.

Method: Using experimental research, quantitative research design was adopted. Before conducting a 3-hour short session with medical students an open-ended questionnaire was distributed among 80 students of 3rd year MBBS in order to know the extent of basic skills of doing research. Five open-ended questions were asked from students. The results were tabulated and analyzed on Microsoft Excel. Frequency and percentage were calculated for each item. Same questionnaire was distributed after the 3-hour lecture session.

Results: Mostly medical students did not know about the type of research being practiced in medicine in the world. They also did not know about the relevant databases, appropriate referencing styles and the databases provided through HEC digital library.

Conclusion: The course on information retrieval and management should be incorporated in the academic syllabi. Information literacy programmes should be conducted for all, especially the medical students

Web URL:

https://www.researchgate.net/profile/Tariq_Najmi/publication/321854160_IMPACT_OF_INTRODUCTION_TO_RESEARCH_ON_MEDICAL_STUDENTS%27_LEARNING_ABILITY/links/5a352dbb0f7e9b10d84507f3/IMPACT-OF-INTRODUCTION-TO-RESEARCH-ON-MEDICAL-STUDENTS-LEARNING-ABILITY.pdf

5. Ali, I., & Tariq, M. (2017). Use of University Library Web OP AC: A survey of Universities of Lahore. ***Pakistan Library & Information Science Journal*****,** ***48*****(2).**

ABSTRACT:

This study aim to explore the satisfaction level of research stndents from Web OPAC. It was also aimed to find out the purpose of using Web OPAC. Survey research method was used for this study. Population of the study was MS/M.phil and PhD students of those private and public sector universities recognized by HEC and have active Web OPAC. Convenient sampling method was used. For calculating sample size, formula by Yamane was used. Sample size was 357 MS/M.phil, PhD student of Eight Private and Public sector Universities of Lahore. SPSS was used for data analysis, Mean score and one sample t-test was applied for data analysis. The study showed that majority of students were moderately satisfied with Web OPAC and there is no significance difference between male, female and MS/M.phil, PhD students regarding satisfaction form Web OPAC. The study explored that vast majority of students used Web OPAC to know about library resources without visiting library, to know about number of documents available on particular subject and to know about the number of copies available on particular title. Title, author, and keyword/subject as a search field vast majority of research students showed their level of agreement and gave opinion that they use these fields as frequently.

Web URL:

http://web.a.ebscohost.com/abstract?direct=true&profile=ehost&scope=site&authtype=crawler&jrnl=00309956&AN=123906454&h=kcvrGlXjO9ftEosL3uK%2fA9Lk36R4rWh63D31Jln5SLKtA4HttnNl6R6okYtS8SQfkxBTGWW8%2ffCorfFM2pekvQ%3d%3d&crl=c&resultNs=AdminWe

bAuth&resultLocal=ErrCrlNotAuth&crlhashurl=login.aspx%3fdirect%3dtrue%26profile%3dehost%26scope%3dsite%26authtype%3dcrawler%26jrnl%3d00309956%26AN%3d123906454

6. Ali, I., & Tariq, M. (2017). Historical Development of Web OPAC in Pakistan. ***Pakistan Library & Information Science Journal*****, *48*(1).**

ABSTRACT:

Library catalogue is very important tool for searching the location of particular material within no time. Due to the global development of information technology and its implementation in libraries gave birth to Online Public Access Catalogue. OPAC has different feature. It is called an extension of card catalogue and OPAC acts as library Website home page like as portal. OPAC also used as promotional tool for library products. Current study intends to describe the history of Web OPAC especially in Pakistan. This study also describes the history of OP AC at international level and describes different generations of OP AC through ages. The study was theoretical in nature.

Web URL:

https://www.researchgate.net/profile/Tariq_Najmi/publication/320613680_Historical_Development_of_web_OPAC_in_Pakistan/links/59f0482daca272a250014605/Historical-Development-of-web-OPAC-in-Pakistan.pdf

AUTHOR INDEX

A

B

C

D

E

F

G

H

I

J

K

L

M

N

O

P

Q

R

S

T

U

V

W

X

Y

Z